PL-TR-93-3007
Vol. 1 of 2

PL-TR-93-3007
Vol. 1 of 2

2

SYNTHESIS AND STRUCTURAL CHARACTERIZATION OF NEW LIGHT MOLECULAR WEIGHT INORGANIC OXIDIZERS AND RELATED DERIVATIVES. VOLUME: I

Professor G.J. Schrobilgen

McMaster University
Department of Chemistry
Hamilton, Ontario L8S 4MI
Canada

1993

August 1993

Final Report

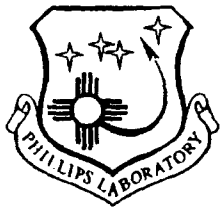

PHILLIPS LABORATORY
Propulsion Directorate
AIR FORCE MATERIEL COMMAND
EDWARDS AIR FORCE BASE CA 93524-7001

NOTICE

When U.S. Government drawings, specifications, or other data are used for any purpose other than a definitely related Government procurement operation, the fact that the Government may have formulated, furnished, or in any way supplied the said drawings, specifications, or other data, is not to be regarded by implication or otherwise, or in any way licensing the holder or any other person or corporation, or conveying any rights or permission to manufacture, use or sell any patented invention that may be related thereto.

FOREWORD

This report was prepared by Department of Chemistry, McMaster University, Hamilton–Ontario Canada, under contract F04611–91–K–0004, for Operating Location AC, Phillips Laboratory, Edwards AFB, CA. 93524–7001. Project Manager for Phillips Laboratory was Lt Robert Mantz.

This report has been reviewed and is approved for release and distribution in accordance with the distribution statement on the cover and on the SF Form 298.

ROBERT A. MANTZ, Capt, USAF
Project Manager

STEPHEN L. RODGERS
Chief, Emerging Technologies Branch

LEONARD C. BROLINE, Lt Col, USAF
Director,
Fundamental Technologies Division

RANNEY G. ADAMS
Public Affairs Director

REPORT DOCUMENTATION PAGE

Form Approved
OMB No. 0704-0188

1. AGENCY USE ONLY (Leave blank)	2. REPORT DATE	3. REPORT TYPE AND DATES COVERED
	February 1993	Final 1 May 1991 thru 30 April 1992

4. TITLE AND SUBTITLE
Synthesis and Structural Characterization of New Light Molecular Weight Inorganic Oxidizers and Relative Derivatives: Volume I

5. FUNDING NUMBERS
C: F04611-91-K-0004
PE: 62302F
PR: 5730
TA: 00N2

6. AUTHOR(S)
Schrobilgen, G. J. Prof

7. PERFORMING ORGANIZATION NAME(S) AND ADDRESS(ES)
McMaster University
Department of Chemistry
Hamilton, Ontario L8S 4MI
Canada

8. PERFORMING ORGANIZATION REPORT NUMBER

9. SPONSORING/MONITORING AGENCY NAME(S) AND ADDRESS(ES)
Phillips Laboratory
OLAC-PL/RKFE
Edwards AFB, California 93524-7680

10. SPONSORING/MONITORING AGENCY REPORT NUMBER
PL-TR-93-3007 Vol I

11. SUPPLEMENTARY NOTES
COSATI CODES: 07/02

12a. DISTRIBUTION/AVAILABILITY STATEMENT
Approved for Public Release; Distribution is Unlimited

12b. DISTRIBUTION CODE

13. ABSTRACT (Maximum 200 words)
The following annual report encompasses eleven areas of research. The basic philosophy underpinning this work has been to develop the technology for the synthesis, storage, and handling of new high-energy density materials. The importance of performing the "easier" heavy element chemistry as the ground work to synthesizing. The more challenging and potentially more useful lighter analogs has been stressed throughout much of this work. Where possible published or about to be published work is included in this report under each of the appropriate subheadings.

14. SUBJECT TERMS
Crystallography; NMR spectroscopy, synthesis, Raman spectroscopy; High-Valent Oxidents, Xe-N bonded species.

15. NUMBER OF PAGES

16. PRICE CODE

17. SECURITY CLASSIFICATION OF REPORT	18. SECURITY CLASSIFICATION OF THIS PAGE	19. SECURITY CLASSIFICATION OF ABSTRACT	20. LIMITATION OF ABSTRACT
Unclassified	Unclassified	Unclassified	SAR

NSN 7540-01-280-5500
Standard Form 298 (Rev. 2-89)
Prescribed by ANSI Std Z39-18
298-102

Table of Contents

List of Figures

Part IA

Part IB

Part III

List of Tables

Part IV

Part V

OVERVIEW OF THE REPORT

The following annual report encompasses eleven areas of research funded by the United States Air Force Phillips Laboratory, Edwards Air Force Base, California under Contract F04611-91-K-0004. Where possible published or about to be published work is included in this Report under each of the appropriate subheadings. The basic philosophy underpinning this work has been to develop the technology for the synthesis, storage and handling of new high-energy density materials. The importance of performing the "easier" heavy element chemistry as the ground work to synthesizing the more challenging and potentially more useful lighter analogs has been stressed throughout much of this work. The validity of this approach is been illustrated in a previous report (Technical Report, U.S. Department of the Air Force Contract No. F49620-87-C0049; February, 1992; Report No. PL-TR-91-3108; Phillips Laboratory, Propulsion Directorate, Air Force Systems Command, Edwards Air Force Base, CA; Vols. I - III) where the synthesis of $HC{\equiv}N\text{-}XeF^+$ is described. The synthesis of the xenon compound has made possible the realization of the lighter and more energetic krypton analog, $HC{\equiv}N\text{-}KrF^+$. The publication of these results in turn precipitated a total of four theoretical papers on $HC{\equiv}N\text{-}NgF^+$ (Ng = Ne, Ar, Kr, Xe). While the neon analog is forecast to be unstable, the argon analog, $HC{\equiv}N\text{-}ArF^+$ is predicted to be stable. The hope of binding ArF^+ (also presently unknown), potentially an oxidant of unprecedented strength, to a fuel moiety, $HC{\equiv}N$, is intriguing and the direct consequence of having done a thorough job delineating the chemistry of the heavier congeners.

Part I is concerned with the syntheses and characterization of noble-gas species in novel bonding situations, more specifically, the investigation of the interactions of the strong oxidant Lewis acid noble-gas centers neutral organic nitrogen bases. These recent findings represent a major extension of Group VIII (18) chemistry in that they (1) significantly extend the range of known Xe-N bonded species. Most importantly from the viewpoint of practical impact on the field of propellants and monopropellants, this aspect of our research has demonstrated that under the appropriate conditions, strongly oxidizing Lewis acid centers can be bound to fuel substrates containing a base center. Part I also describes the synthesis and characterization of the $XeOF_3^+$ cation. This strong oxidant cation has been characterized by X-ray crystallography and NMR spectroscopy.

The binding of lower molecular weight strong oxidizers to a Lewis base fuel follows from Part I. Part II describes evidence for the first interhalogen cation adduct with an organic base, namely,

$F_2Cl\text{-}N{\equiv}CCF_3^+$.

The work described in Part III, was prompted by our prevoius report on the Lewis base properties of $N{\equiv}SF_3$. Because of its resistance to oxidation (first adiabatic ionization potential, 12.50 eV), it was considered likely that $N{\equiv}SF_3$ would form adducts with the noble-gas cations XeF^+, $XeOTeF_5^+$ and $XeOSeF_5^+$ which would be stable to redox degradation. No estimates of electron affinity (EA) other than for XeF^+ (10.9 ev), KrF^+ (13.2 eV) and ArF^+ (13.6 eV) are available. However, the EA values of $XeOSeF_5^+$ and $XeOTeF_5^+$ are predicted to be less than that of XeF^+, and all xenon(II) cations are below the first ionization potential (IP) of $N{\equiv}SF_3$. Consequently, the xenon(II) cations were expected to form redox-stable adduct cations with $N{\equiv}SF_3$. The ligand, $N{\equiv}SF_3$, was studied in a variety of oxidatively resistant solvents deemed suitable for noble-gas compound syntheses, and adducted with the Lewis acid AsF_5 to assess the base character of the ligand. Aspects of this work were reported on in a previous report (Technical Report No. PL-TR-91-3108). The $F_5SeO\text{-}Xe\text{-}N{\equiv}SF_3^+$ and $F\text{-}Xe\text{-}N{\equiv}SF_3^+$ cations have been synthesized in BrF_5 solvent and fully characterized by ^{129}Xe, ^{14}N and ^{19}F NMR spectroscopy. The salt, $F\text{-}Xe\text{-}N{\equiv}SF_3^+AsF_6^-$, was also synthesized by the direct combination of $XeF^+AsF_6^-$ and $N{\equiv}SF_3$ at -20 °C and the vibrational spectrum was studied using low-temperature Raman spectroscopy. In addition, the solvolysis of $F\text{-}Xe\text{-}N{\equiv}SF_3^+$ has been studied in anhydrous HF and has lead to the novel $F_4S{=}N(H)\text{-}Xe\text{-}F^+$ cation. The latter cation has been characterized in solution by ^{129}Xe, ^{14}N and ^{19}F NMR spectroscopy. Based on the ^{19}F and ^{129}Xe NMR spectroscopic data, further solvolysis of this cation in HF gives rise to the $F_5S\text{-}N(H_2)\text{-}Xe\text{-}F^+$ cation, the first example of an sp^3-nitrogen bonded to a noble gas. Based on our understanding of Lewis acid-base adduct chemistry incorporating the strongly oxidizing noble-gas cations as acceptor centers, it should be possible to extend the range of bases coordinated to noble-gas cations and to other strong oxidizers such as chlorine fluoro-cations to include related bases having heats of formation that are more endothermic such as NH_2F ($\Delta H^\circ_{f(g)}$ = -9.1 kcal mol^{-1}, as a pure compound NH_2F is a violent detonator; cf., gas phase heats of formation for $HC{\equiv}N$, -31.2; NF_3, -31.9; NF_2H, -15.5; NH_3, -11.0 kcal mol^{-1}). Although the latter chemistry has not yet been achieved, much of the ground work has been laid by demonstrating that the higher molecular weight analogs exist. In the the previous study, it was shown that XeF^+ can be coordinated to the SF_5 analog, F_5SNH_2, and to $F_4S{=}NH$ in their respective novel cations $FXe\text{-}N(H_2)SF_5^+$ and $FXe\text{-}N(H){=}SF_4^+$. In the work presented in Part III the tellurium analog, $F_5TeN(H)Xe^+$, has been fully characterized in solution by multi-NMR

spectroscopy of the ^{15}N-enriched compound and shown to undergo an interesting mode of decomposition to give dinitrogen and hydrazinium cations.

The formation of novel xenon(IV) oxofluorides of the $OTeF_5$ group are described in Part IV. Preliminary evidence indicates that these derivatives may function as sources of singlet oxygen, $^1O_2$, in chemical syntheses.

Part V describes the application of XeF_6 as a synthetic reagent to the preparation of the novel oxofluoride, TcO_2F_3. The latter is the only Tc(VII) oxofluoride, other than TcO_3F, to have been characterized and is the first to have been characterized by X-ray crystallography. The *cis*-$TcO_2F_4^-$ anion has also been prepared and characterized.

Parts VI, VII and VIII describe the preparation and detailed characterization of the hypervalent, seven-coordinate, high-oxidation state anions IF_6O^- and F_6TeCN^- and the neutral precursor of TeF_6CN^-, F_5TeCN, and the PF_4^- anion and their associated chemistry in anhydrous $CH_3C{\equiv}N$.

Aspects of the work described in Parts VI and VII were carried out in collaboration with Drs. K.O. Christe and W.W. Wilson, Rocketdyne Division, Rockwell International, Canoga Park, California. Hypervalent fluoro- and oxofluoro-anions are known to offer the best possibility for stabilizing high oxidation states of the elements. These species are of particular importance as they serve to extend our knowledge of the interrelation of valence electron lone pair stereochemical activity and coordination number in strong oxidizer fluorides.

Part IX describes the structural characterization of the most weakly coordinating (least basic) anions known, $As(OTeF_5)_6^-$, $Sb(OTeF_5)_6^-$ and $Bi(OTeF_5)_6^-$. Although of high molecular weight, they are of interest to the program as they could allow the stabilization of energetic cationic species in the solid state that have only been observed in the gas phase, e.g., XeH^+ and hydrogen cluster ions.

The enhanced oxidant stregth of F_2 in the presence of Lewis acid (fluoride acceptors) has been known for some time. In Part X, ^{18}F radiotracer experiments have been used to deduce the nature of the activated complex responsible for enhancement of the low temperature fluorinating properties of F_2.

Part XI describes the design of a microwave discharge device capable of exciting a discharge under liquid nitrogen. We have since achieved such discharges in gaseous fluorine at pressures as high as 100 Torr in the presence and in the absence of krypton. Thus far the mixed gas discharges have

failed to produce KrF_2, which is deemed to be a satisfactory test of the viability of the technique for producing high fluxes of fluorine atoms of use in low-temperature synthetic applications. Our failure thus far is attributed to the fact that the fluorine atoms produced by this approach are excited and have not been allowed to relax. We have now designed a quartz discharge cell which will provide the added surfaces and path length needed for more efficient relaxation of the discharge medium.

PART IA

COORDINATION OF ORGANIC NITROGEN BASES TO HIGH-VALENT OXIDANTS

The syntheses and characterization of a large number of new xenon compounds that had been prepared by the interaction of the strong oxidant Lewis acid cation XeF^+ with a number of organic nitrogen bases are summarized in our Technical Report, U.S. Department of the Air Force Contract No. F49620-87-C0049; February, 1992; Report No. PL-TR-91-3108; Phillips Laboratory, Propulsion Directorate, Air Force Systems Command, Edwards Air Force Base, CA; Vols. I - III. The majority of the bases that had been selected for study were oxidatively resistant perfluoro-organic nitrogen bases with first ionization potentials exceeding 10-11 eV. These findings represent a major extension of Group VIII (18) chemistry in that they (1) significantly extend the range of known Xe-N bonded species, (2) demonstrate that a large range of fluoro-organic ligands are capable of stabilizing Xe(II), (3) produce several examples of the first compounds in which a noble-gas atom serves as an aromatic substituent; (4) provide new series of model compounds which may aid in developing synthetic approaches to the formation of new xenon-carbon and krypton-oxygen bonds; (5) provide the first examples of Kr-N bonded species, which, in turn provided the impetus for us to successfully attempt the synthesis of the first compound containing a Kr-O bond. Most importantly from the viewpoint of practical impact on the field of propellants and monopropellants, this aspect of our research has demonstrated that under the appropriate conditions, strongly oxidizing Lewis acid cations can be bound to fuel substrates containing a base center. The best illustration which we have discovered in the course of the previous contract work has been the $F\text{-}Kr\text{-}N{\equiv}CH^+$ cation, where KrF^+ represents the most potent chemical oxidant known and is bound to a fuel.

Based on our understanding of Lewis acid-base adduct chemistry incorporating the strongly oxidizing Xe(II) and Kr(II) cations as acceptor centers, we have proposed in the present contract that it should be possible to extend the range of bases coordinated to noble-gas cations and to other strong oxidizers such as chlorine fluoro-cations to include related bases having heats of formation that are more endothermic such as NH_2F ($\Delta H^\circ_{f(g)}$ = -9.1 kcal mol^{-1}, as a pure compound NH_2F is a violent detonator; cf., gas phase heats of formation for $HC{\equiv}N$, -31.2; NF_3, -31.9; NF_2H, -15.5; NH_3, -11.0 kcal mol^{-1}). Although the latter chemistry has not yet been achieved, much of the ground work has been laid by demonstrating that the higher molecular weight analogs exist. In this instance that XeF^+ can be coordinated to the SF_5 analog, F_5SNH_2, and to $F_4S{=}NH$ in their respective novel cations $FXe\text{-}N(H_2)SF_5^+$ and $FXe\text{-}N(H){=}SF_4^+$ (see Technical Report PL-TR-91-3108, February, 1992). We have also recently synthesized $FXe\text{-}N(H_2)TeF_5^+$ as the 99% ^{15}N-enriched salt. This experiment is significant as

it will provide us with direct proof through observation of $^{1}J(^{129}Xe\text{-}^{15}N)$ in the ^{129}Xe and ^{15}N NMR spectra that this cation and its sulfur analog contain Xe directly bonded to nitrogen, and are novel examples of a strongly oxidizing species bonded to hydrogen-rich nitrogen having a formal sp^3 hybridization. Having established the existence of the sp^3-hybridized nitrogen cation, substitution of the TeF_5 and SF_5 groups with F will allow us to prepare lower molecular weight NH_2F derivatives.

The coordination of oxidizers to base centers that result in neutral adducts is highly desirable as it would eliminate the need for high molecular weight, weakly oxidizing anions such as the AsF_6^- anion, that are required to stabilize the adduct cations discussed above. This approach would permit the coordination of the oxidizer species to the base center of a fuel without the need for a counter ion. In recent attempts to prepare the $OTeF_5$ and mixed $F/OTeF_5$ analogs of XeF_5^+ (see Technical Report PL-TR-91-3108, February, 1992), $XeF_{5-n}(OTeF_5)_n^+$, we have discovered that instead of the anticipated products, the $O_3Xe\text{-}N{\equiv}CCH_3$, $O_2F_2Xe\text{-}N{\equiv}CCH_3$ and $OF_4Xe\text{-}N{\equiv}CCH_3$ adducts were formed. These adducts represent the first examples of high-valent xenon bonded to nitrogen and, moreover, despite the strong oxidant characters of the xenon(VI) oxofluorides and XeO_3, it has nevertheless proven possible to coordinate these Lewis acids to the base center of a fuel. The geometries of these adducts are also of considerable interest. The VSEPR approach predicts the following geometries: $O_3Xe\text{-}N{\equiv}CCH_3$, AX_4E, trigonal bipyramid with the lone pair and $CH_3C{\equiv}N$ axial; $O_2F_2Xe\text{-}N{\equiv}CCH_3$, AX_5E, square pyramid with one O and the lone pair in axial positions and $OF_4Xe\text{-}N{\equiv}CCH_3$, AX_6E, pentagonal bipyramid with O and the lone pair in axial positions.

Experiments have been carried out in which the adducts have been derived from a doubly enriched sample of $O{=}Xe(OTeF_5)_4$; i.e., the oxygen doubly bonded to Xe is also $^{17/18}O$ and enriched. The isotopic splitting pattern in the ^{129}Xe NMR spectrum will serve to confirm the oxygen : xenon ratio in each adduct. In addition, the direct synthesis of the $^{17/18}O$-enriched $O{=}XeF_4$ adduct has carried out in Freon-114 and a white crystalline adduct has been isolated which is awaiting full characterization. We have undertaken experiments in which the $O_3Xe\text{-}N{\equiv}CCH_3$ (AX_4E, trigonal bipyramid with the lone pair and $CH_3C{\equiv}N$ axial) $O_2F_2Xe\text{-}N{\equiv}CCH_3$ (AX_5E, square pyramid with one O and the lone pair in axial positions) and ($OF_4Xe\text{-}N{\equiv}CCH_3$ (AX_6E, pentagonal bipyramidal or distorted octahedral structure; also see $XeOF_3^+$ structure) (Figure 1) have been derived from a doubly enriched sample of $O{=}Xe(OTeF_5)_4$; i.e., the oxygen in the $OTeF_5$ groups is also $^{17/18}O$-enriched (equations (4) and (5)). The secondary isotopic splitting patterns in the ^{129}Xe NMR spectra serve to

confirm the oxygen: xenon ratio in each adduct (Tables 2 and 3 and Figures 3 - 6). In addition, the direct synthesis of the $^{17/18}$O-enriched $O{=}XeF_4$ adduct has succeeded in Freon-114 solvent

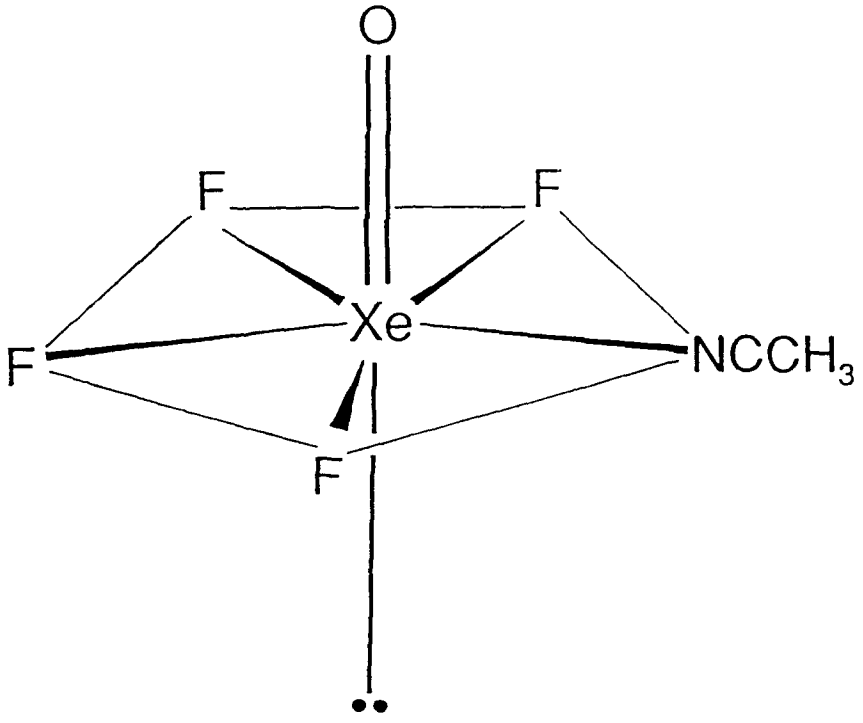

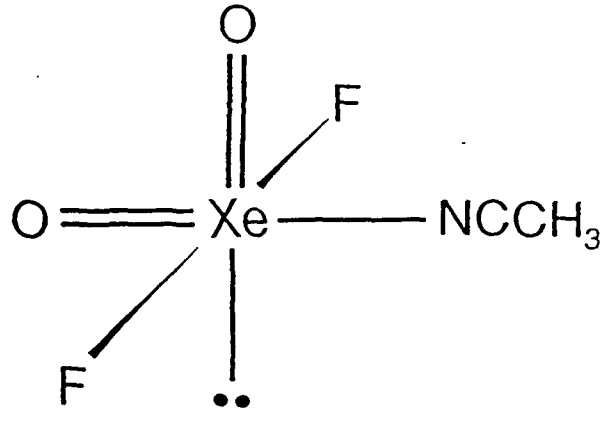

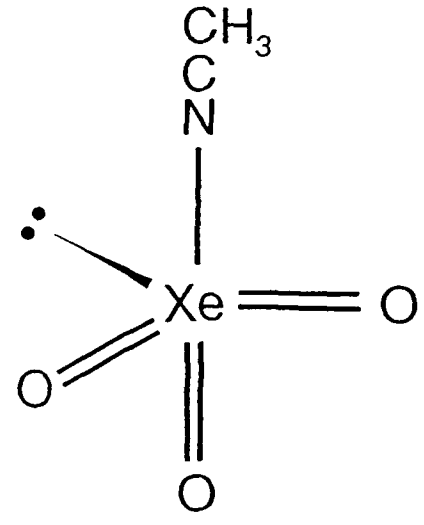

Figure 1.

Table 2. NMR Data for $XeOF_4$, XeO_2F_2 and XeO_3 in Various Solvents

Species	$\delta(^{129}Xe)$	$\delta(^{19}F)$	$^1J(^{129}Xe\text{-}^{19}F)$, Hz	Solvent	T, °C
$XeOF_4$	0.0	100.3	1128	neat	25
	23.7	-	1146	HF	-50
	-29.9	101.6	1131	$CFCl_3$	24
	164.7	93.3	1540	CH_3CN	-40
XeO_2F_2	171.0	105.1	1213	HF	-50
	263.0	86.5	1425	CH_3CN	-40
XeO_3	217.0	-	-	H_2O	25
	218.1	-	-	CH_3CN	-40

Table 3. Oxygen Isotopomer Distribution in $XeOF_4$, XeO_2F_2 and XeO_3 Acetonitrile Adducts

Isotopomer	Theoretical Ratio	Experimental Ratio
$CH_3C{\equiv}N\text{-}Xe^{16}OF_4$	1	1
$CH_3C{\equiv}N\text{-}Xe^{18}OF_4$	1.28	1.21
$CH_3C{\equiv}N\text{-}Xe^{16}O_2F_2$	1	1
$CH_3C{\equiv}N\text{-}Xe^{16}O^{18}OF_2$	2.09	2.42
$CH_3C{\equiv}N\text{-}Xe^{18}O_2F_2$	1.22	1.46
$CH_3C{\equiv}N\text{-}Xe^{16}O_3$	1	1
$CH_3C{\equiv}N\text{-}Xe^{16}O_2{}^{18}O$	3.6	3.6
$CH_3C{\equiv}N\text{-}Xe^{16}O^{18}O_2$	4.4	4.3
$CH_3C{\equiv}N\text{-}Xe^{18}O_3$	1.8	1.8

Isotopic abundances: ^{16}O 35.4 %, ^{17}O 21.9 %, ^{18}O 42.7 %.

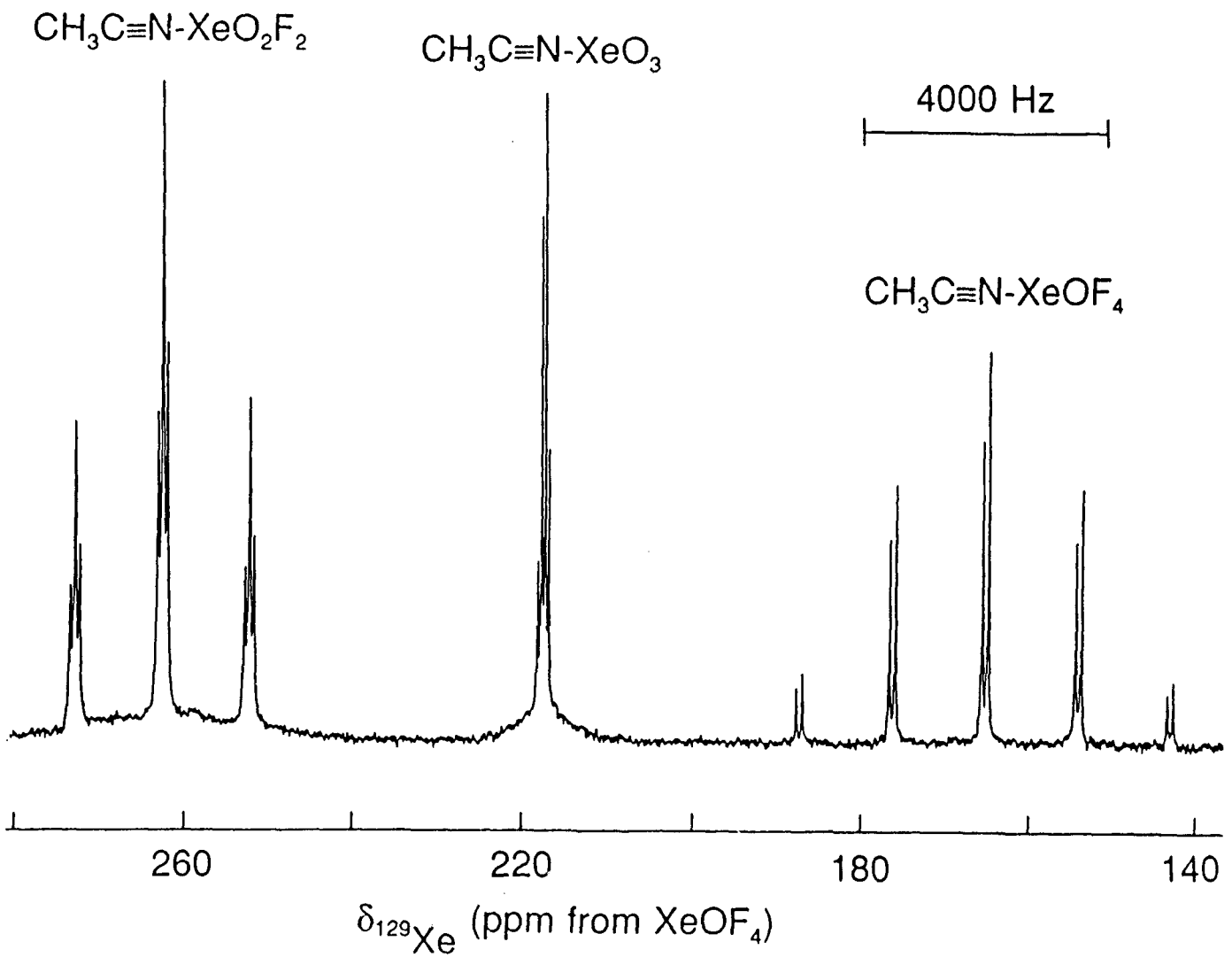

Figure 2. The ^{129}Xe NMR spectrum (139.051 MHz) at -40 °C showing the reaction products of doubly $^{17,18}O$-enriched $O{=}Xe(OTeF_5)_4$ with $2N(CH_3)_4^+F^-$ in CH_3CN.

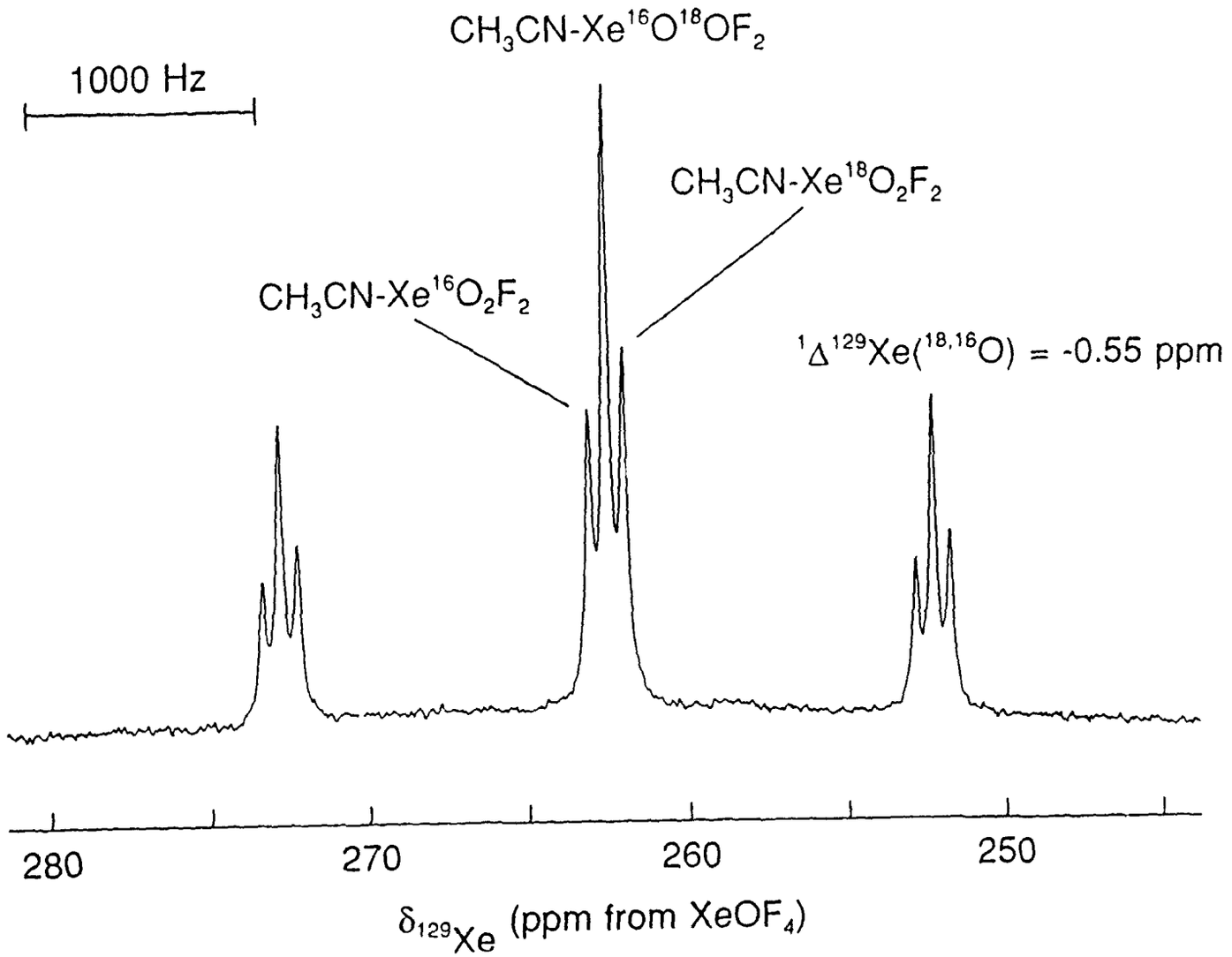

Figure 3. The ^{129}Xe NMR spectrum (139.051 MHz) at -40 °C showing the reaction products of doubly $^{17,18}O$-enriched $O{=}Xe(OTeF_5)_4$ with $2N(CH_3)_4^+F^-$ in CH_3CN. Expansion of CH_3CN-XeO_2F_2 multiplet.

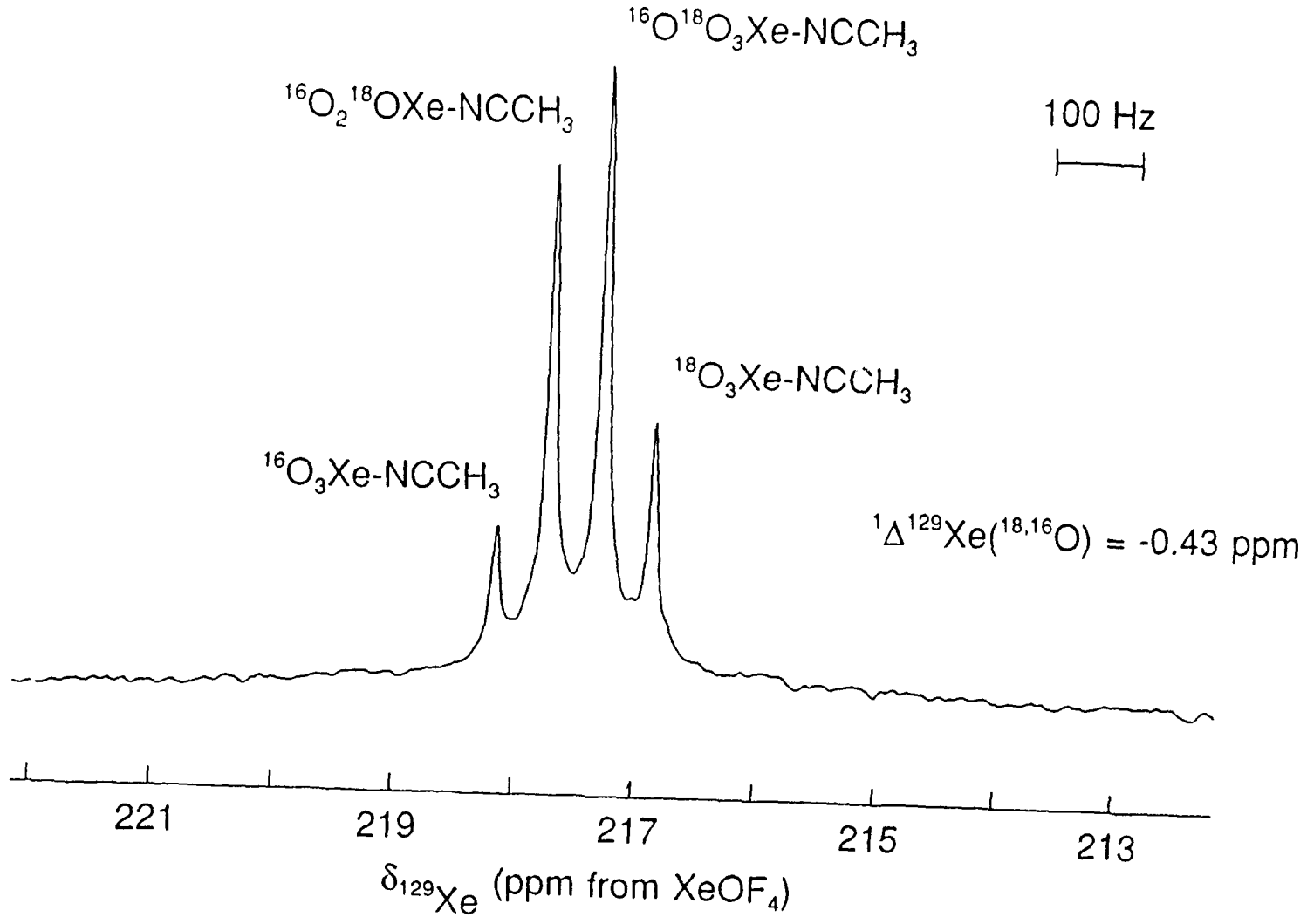

Figure 4. The ^{129}Xe NMR spectrum (139.051 MHz) at -40 °C showing the ion products of doubly ^{17,18}O-enriched O=Xe(OTeF$_5$)$_4$ with 2N(CH$_3$)$_4^+$F$^-$ in CH$_3$CN. Expansion of CH$_3$CN-XeO$_3$ resonance.

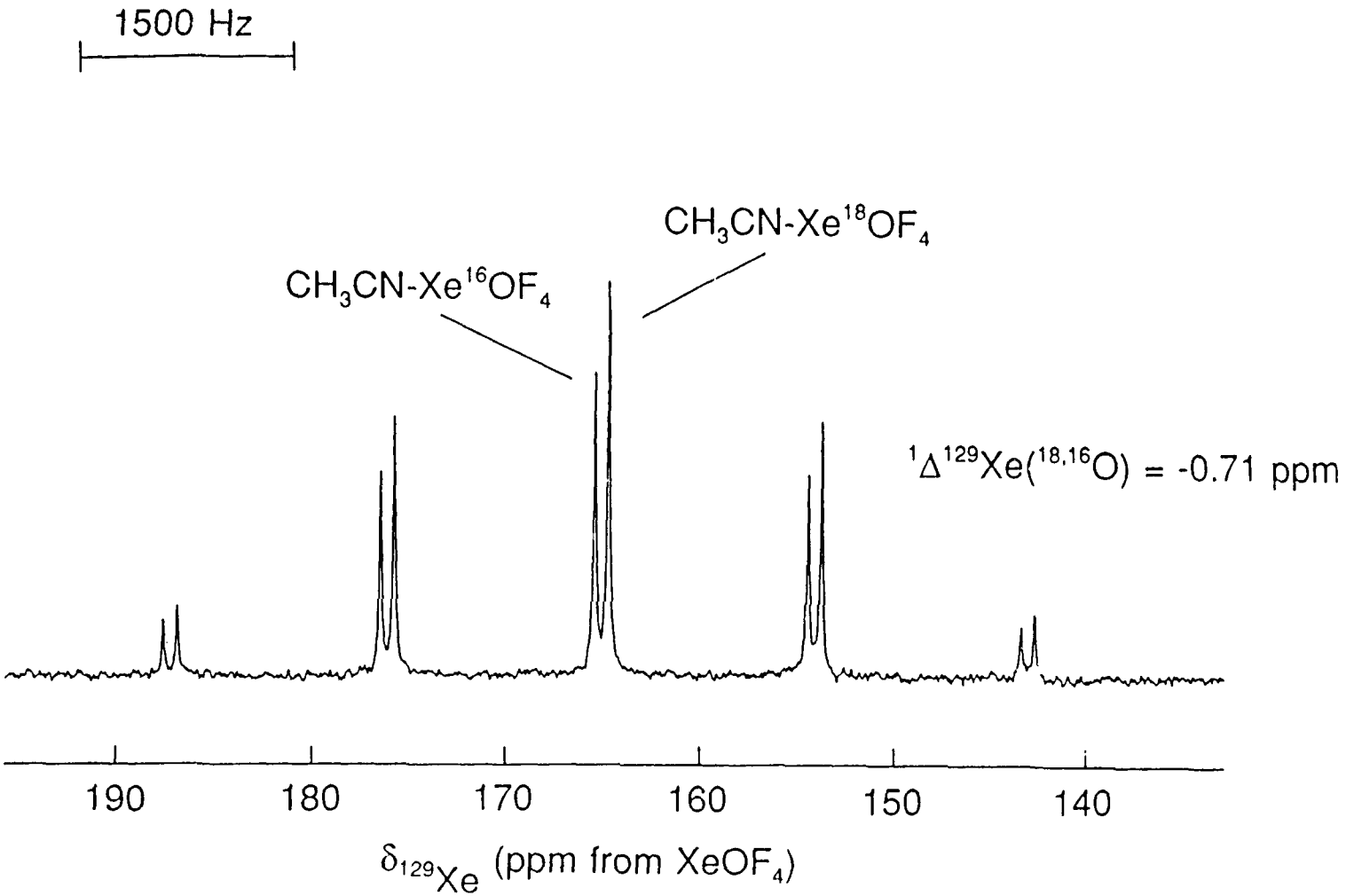

Figure 5. The ^{129}Xe NMR spectrum (139.051 MHz) at -40 °C showing the reaction products of doubly $^{17,18}O$-enriched $O{=}Xe(OTeF_5)_4$ with $2N(CH_3)_4^+F^-$ in CH_3CN. Expansion of CH_3CN-$XeOF_4$ multiplet.

(equation (6)), providing the first isolated example of a high-valent xenon-nitrogen bond. Crystalline material has been isolated and we hope to obtain the single crystal X-ray structure of the adduct which is anticipated to be based on a pentagonal bipyramid or a distorted octahedral geometry.

$$^{*}O{=}XeF_4 + 4/3\ B(^{*}OTeF_5)_3 \xrightarrow[20\ ^{\circ}C]{\text{Freon 114}} {}^{*}O{=}Xe(^{*}OTeF_5)_4 + 4/3BF_3 \qquad (4)$$

$$O{=}Xe(OTeF_5)_4 + nF^{-} \xrightarrow[-40\ ^{\circ}C]{CH_3CN} O{=}XeF_4 + O_2XeF_x(OTeF_5)_{2-x} + XeO_3 + TeF_6 + F_5TeOTeF_5 + OTeF_5^{-} \qquad (5)$$

$$XeOF_4 + CH_3CN \xrightarrow[-40\ ^{\circ}C]{\text{Freon 114}} CH_3C{\equiv}N\text{-}XeOF_4 \qquad (6)$$

PART IB

THE CRYSTAL STRUCTURE OF $XeOF_3^+SbF_6^-$

Contribution from the Department of Chemistry

McMaster University

Hamilton, Ontario L8S 4M1, Canada

The Oxotrifluoroxenon(VI) Cation; the X-Ray Crystal Structure of $XeOF_3^+SbF_6^-$ and a Solution ^{17}O and ^{129}Xe Nuclear Magnetic Resonance Study of the $^{17,18}O$-Enriched $XeOF_3^+$ Cation

Hélène P. Mercier, Jeremy C.P. Sanders, Gary J. Schrobilgen* and Scott S.-W. Tsai

Abstract. The crystal structure of $XeOF_3^+SbF_6^-$ has been determined. The compound crystallized in the triclinic system with a = 8.568(2) Å, b = 9.760(2) Å, c = 10.104(2) Å, α = 109.68(2)°, β = 92.58(2)°, γ = 104.27(2)°, V = 763.4 Å^3, D_{calc} = 3.829 g cm^{-3} for Z = 4. The structure has been refined in the space group $P\bar{1}$ to a final conventional R-factor of 0.045 for 1782 independent reflections with $I \geq 2.5\ \sigma(I)$. The structure consists of $XeOF_3^+SbF_6^-$ units with two close contacts between the Xe atom of the cation and F atoms of two SbF_6^- anions. The isolated $XeOF_3^+$ cation is shown to be consistent with the VSEPR rules and to possess an AX_4E arrangement of the four bond pair domains and the lone pair domain which give rise to a disphenoid-shaped cation having two longer axial Xe-F_{ax} bonds and an Xe-O bond which is coplanar with the shorter equatorial Xe-F_{eq} bond and xenon. Oxygen-17 and -18 enrichment of the $XeOF_3^+$ cation in HF and SbF_5 solvents has allowed the determination of the ^{17}O chemical shift and $^1J(^{129}Xe\text{-}^{17}O)$, as well as the $^{16,18}O$ induced secondary isotopic shift in the ^{129}Xe NMR spectrum for the first time.

INTRODUCTION

Xenon oxotetrafluoride was shown by Selig[1] to form the adduct $XeOF_4.2SbF_5$, but its structure was not investigated at that time. The structural characterization of the adducts $XeOF_4.2SbF_5$ and $XeOF_4.SbF_5$ was first reported from this laboratory[2-4] and it was shown by ^{19}F NMR and Raman spectroscopy that the adducts were the salts $XeOF_3^+SbF_6^-$ and $XeOF_3^+Sb_2F_{11}^-$. The geometry of the $XeOF_3^+$ cation was in accord with the disphenoidal AX_4E geometry predicted by the VSEPR model. A synthetic and Raman spectroscopic study of $XeOF_3^+$ salts by Bartlett and coworkers[5] upheld these findings. Subsequently, the ^{129}Xe NMR spectrum of $XeOF_3^+$ was obtained in SbF_5 solvent using natural isotopic abundances.[6]

With the exception of XeF_3^+, XeF_5^+ and $F_5Xe...F...XeF_5^+$,[7] no X-ray crystal structures had been determined for the high-valent xenon cations and for the oxofluoro-cations $XeOF_3^+$, XeO_2F^+[2-4,8] and $O_2FXe...F...XeO_2F^+$.[8] The present study reports the X-ray crystal structure of $XeOF_3^+SbF_6^-$. Although the ^{129}Xe and ^{19}F NMR spectra of the $XeOF_3^+$ cation have been obtained previously on natural abundance samples,[2,3,6] no ^{17}O NMR data had been recorded. In view of this and the general paucity of ^{17}O NMR data for oxo-xenon species, the preparation of $XeOF_3^+SbF_6^-$ enriched in ^{17}O and ^{18}O was undertaken in order to obtain the ^{17}O NMR spectrum and to observe the $^{16,18}O$ induced secondary isotope shift in the ^{129}Xe NMR spectrum.

RESULTS AND DISCUSSION

X-Ray Crystal Structure of $XeOF_3^+SbF_6^-$

Important bond lengths, angles and significant long contact distances for the $XeOF_3^+$ cations, together with bond lengths and angles for the SbF_6^- anions of the two molecules, which had to be defined in the $P\bar{1}$ space group, are listed in Table 1. Details of the data collection parameters and other crystallographic information for the $P\bar{1}$ space group are given in Table 2. The final atomic coordinates and the equivalent isotropic thermal parameters are summarized in Table 3. Figures 1 and 2 show the asymmetric unit of the crystal structure and the local environment around Xe1, respectively.

The free $XeOF_3^+$ cation is predicted by the VSEPR model[12] to be a disphenoid with the oxygen atom, a fluorine atom and the non-bonding electron pair in the equatorial plane and may be classed as an AX_4E arrangement of bond pairs (X) and a lone pair (E). The crystal structure shows essentially the geometry corresponding to this arrangement when the cation is considered in isolation from the anion. The location of the lone pair in the (Xe, O, F_{eq}) plane of the free cation may be inferred from the F_{ax}-Xe-F_{ax} bond angles F5-Xe1-F1 and F11-Xe2-F12 of 161.4(5)° and 163.9(5)°, respectively, and the F_{eq}-Xe-O bond angles O1-Xe1-F2 and O2-Xe2-F13 of 99.9(6) and 100.9(6)°, respectively. The latter angles are significantly less than the ideal angles (180 and 120°) expected in a trigonal bipyramid owing to axial fluorine - lone pair, and oxygen and equatorial fluorine bond pair - lone pair repulsions.

The structure of the $XeOF_3^+$ cation is similar to that of the isovalent $ClOF_3$ molecule.[13]

As in $XeOF_3^+$, the equatorial F and O ligands in $ClOF_3$ are bent towards each other with a F_{eq}-Cl-O bond angle of 108.9° and the axial ligands are bent back due to bond pair-lone pair repulsions to give an F_{ax}-Cl-F_{ax} bond angle of 170(5)°. The structure of the $XeOF_3^+$ cation is also related to that of the XeF_3^+ cation[14,15] and can be described by replacement of one of the equatorial lone pairs by the oxygen atom. The F_{ax}-Xe-F_{ax} angle of XeF_3^+ is 160.9(5) (SbF_6^- salt)[14] and 161.9(5)° ($Sb_2F_{11}^-$ salt)[15] and is very similar to that of $XeOF_3^+SbF_6^-$ (161.4(5) and 163.9(5)°).

Table 4 lists the Xe-F and Xe-O bond lengths of a number of xenon fluorides and oxofluorides to allow comparison with the bond lengths found for $XeOF_3^+$. The Xe-O bond lengths for all of the species listed are similar, ranging from 1.682(15) - 1.77(1) Å. The average Xe-F bond length in $XeOF_3^+$ is shorter (1.860(12) Å) than that found in $XeOF_4$ (1.900(5) Å).[17] This is consistent with the trend found for XeF_3^+ (1.883(13) Å[14]; 1.87(1) Å[15]) and XeF_4 (1.953(2) Å)[21] and is attributed to the decreased bond polarity resulting from the increased effective electronegativity of xenon as a result of its formal positive charge.[14] The Xe-F_{ax} bond lengths are longer than the Xe-F_{eq} bond lengths. This relates well with the data observed from the NMR study described below and can be explained in terms of bond order arguments. The bonding in the F_{ax}-Xe-F_{ax} unit can be regarded as a 3-center 4-electron system with each Xe-F_{ax} bond having a bond order of ½, whereas the Xe-F_{eq} bond is a 2-center-2-electron bond with a bond order of one. Thus the Xe-F_{eq} bond is stronger and shorter. The VSEPR model, which also predicts the Xe-F_{ax} bonds to be longer than the Xe-F_{eq} bond, does so without making any assumptions regarding the molecular orbitals used in bonding. By taking into account that the angle between the Xe,O,F_{eq} plane and the Xe-F_{ax} bond is less than the ideal angle of 90 ° and that the angle between the electron lone pair and the oxygen and fluorine equatorial ligands is considerably less

than 120°, it is inferred that these distortions arise from lone pair - bond pair repulsions which are minimized by elongation of the Xe-F_{ax} bonds.

The crystal structure of $XeOF_3^+SbF_6^-$ also shows two non-equivalent long fluorine-bridge contacts from two different SbF_6^- anions to each $XeOF_3^+$ cation (Figures 1 and 2), giving distorted octahedral coordination around the xenon atom as in monomeric XeF_6.[16,23-25] A direct consequence of the two fluorine bridge interactions is a two-dimensional layer structure in which there are no close contacts between parallel layers (Figure 3). The long contact distances are 2.535(13) Å for Xe1-F3, 2.449(10) Å for Xe1-F4, 2.589(10) Å for Xe2-F9 and 2.541(14) Å for Xe2-F14. These contact distances are significantly less than the sum of the Xe and F van der Waals radii (3.50 Å),[26] and indicate that there is substantial covalent character in these interactions. The bond valences for individual bonds as defined by Brown[9-11] are included in Table 1. Taking into account the two fluorine bridge contacts, the total bond valences for the Xe1 and Xe2 atoms are 5.85 and 5.66, respectively, and for the Sb1 and Sb2 atoms they are 4.89 and 5.01, respectively. The oxygen atoms O1 and O2 have bond valences values of 2.18 and 2.07, respectively, and the terminal fluorines have values of 0.98, 1.02 (F_{ax} on Xe); 1.05 - 1.22 (F_{eq} on Xe) and 0.81 - 0.92 (Sb). The bridge fluorine values range from 0.15 to 0.22 for the Xe contacts and 0.80 to 0.68 for the Sb contacts giving total bridge fluorine bond valences of 0.95 - 0.90. The total bond valences of xenon and the bond valences of the bridging fluorine confirm that only two significant long contacts between the cation and the anion need to be taken into account.

Table 5 gives the equation for the least-squares planes containing the equatorial ligands O and F_{eq} and the Xe atom. The long fluorine bridge contacts with the SbF_6^- anion approach the Xe atoms from above the plane of the equatorial ligands. For both Xe1 and Xe2, it is evident that

the shorter of the two long F---Xe contacts subtends the greater angle with the F_{eq}-Xe-O plane, i.e., F4 (F14) subtends an angle of 24.13(1)° (23.79(1)°) to the F2-Xe-O2 (F13-Xe2-O2) plane while F3 (F9) subtends an angle of 4.66(1)° (13.36(1)°) to the F2-Xe-O2 (F13-Xe2-O2) plane. The approaches of the bridging fluorines on the same side of the equatorial plane suggests that the non-bonding electron pair is displaced from the ideal equatorial (Xe, O, F_{eq}) plane of the AX_4E arrangement towards the least crowded triangular face of the resulting pseudo-octahedron, that is, the face comprised of the two bridging fluorines and what is the equatorial fluorine in the AX_4E description of the isolated $XeOF_3^+$ cation. The lone pair avoids occupying a face containing oxygen as that would result in a more crowded environment for the lone electron pair domain. The triangular face containing the oxygen atom, in fact, is compressed as a result of the splaying open of the opposite face resulting from lone pair - bond pair repulsions in the pseudo-trigonal face defined by the two long fluorine contacts and an axial fluorine (see Table 1 for relevant bond angles). Figure 4 shows a view down the axis passing through the triangular faces of the distorted octahedron, and is consistent with displacement of the lone pair domain towards the triangular face, directly below the xenon atom. Repulsion between the non-bonding electron pair and the bonding electron pairs causes the F1-F3-F4 and F9-F12-F14 triads to splay outwards. When the two long contacts are taken into account, the arrangement of bond pair domains and the lone pair domain resembles an AX_6E (distorted octahedral) arrangement akin to that of XeF_6 in the gas phase[23-25] except that the lone pair of $XeOF_3^+$ is not expected to be centered on the triangular face, but is expected to be displaced toward the lines of approach of the long Xe...F contacts.

One important difference between the structures of $XeOF_3^+SbF_6^-$ and $XeF_3^+SbF_6^-$[14] is the

direction of the secondary bonding interactions (fluorine bridges) between the cation and the anion. The directions of approach of these incoming electron pair(s) are dictated by their tendency to avoid the other electron pair(s) in the valence shell of xenon. Assuming that the arrangement of electron pairs around xenon in XeF_3^+ is a regular trigonal bipyramid, it was found that the directions of the secondary contacts in $XeF_3^+SbF_6^-$ were in agreement with the direction expected, i.e., they approach above and below the equatorial lone pairs in the centers of the triangular faces defined by the axial fluorines and the lone pairs, passing through two triangular faces of the trigonal bipyramidal AX_3E_2 arrangement of the free cation to give an arrangement in which the Xe atom and five F atoms are coplanar.[14] Thus, the XeF_3^+ cation and its fluorine bridge contacts approximate an AX_5E_2 arrangement that is closely related to the regular pentagonal planar AX_5E_2 geometry of XeF_5^-.[28]

The SbF_6^- anions of $XeOF_3^+SbF_6^-$ have the usual octahedral geometry and expected Sb-F bond lengths ranging from 1.827(12) to 1.940(9) Å. The Sb-F bond length differences are attributed to fluorine bridge formation, so that the two unique pairs of fluorines involved in bridging (F4, F9; F3, F14) have slightly elongated Sb-F bonds (Table 1) and the Sb-F bonds *trans* to the bridge bonds are slightly contracted, i.e., Sb1-F10, 1.839(11) and Sb1-F8, 1.847(15); Sb2-F18, 1.827(12), Sb2-F15, 1.842(13) Å.

The vibrational spectrum of $XeOF_3^+SbF_6^-$ has been reported previously.[4] In view of the present crystal structure, a factor-group analysis of the vibrational modes of the $XeOF_3^+SbF_6^-$ unit cell was carried out by use of the correlation chart method.[29] The free cation symmetry (C_s) was correlated to the site symmetry of the cation (C_1), which, in turn, was correlated to the crystal symmetry (C_i). Assuming complete vibrational coupling occurs in the unit cell of $XeOF_3^+SbF_6^-$,

18 modes having A_g symmetry are predicted to be active in the Raman spectrum and 18 modes having A_u symmetry are predicted to be active in the infrared spectrum. Thus, each vibrational band of the free cation is predicted to be split in the Raman and infrared spectra. Such splittings have been noted in the previously published Raman spectra of $XeOF_3^+SbF_6^-$[4,5] and can now be attributed to vibrational coupling within the unit cell. The totally symmetric Xe-F stretching modes all exhibited splitting. Although no splitting was resolved for the Xe-O stretching mode, re-examination of the Raman spectrum of $XeOF_3^+SbF_6^-$ under higher resolution conditions in the present study reveals a low-frequency shoulder 2.8 cm^{-1} to low frequency of the main band.

Solution ^{129}Xe and ^{17}O NMR Study of the $XeOF_3^+$ Cation

The ^{17}O-enriched salt $XeOF_3^+SbF_6^-$ was prepared from ^{17}O-enriched $XeOF_4$ (oxygen composition: ^{16}O, 36.5%; ^{17}O, 26.5%; ^{18}O, 37.0%) according to equation (1).

$$XeOF_4 + SbF_5 \xrightarrow{HF} XeOF_3^+SbF_6^- \qquad (1)$$

The $XeOF_3^+$ cation is expected to act as a strong acceptor towards F^- donor solvents such as HF resulting in loss of the one-bond Xe-F couplings in the ^{129}Xe and ^{19}F NMR spectra due to rapid fluorine ligand exchange.[6] However, the Xe=O bond is not labile and HF is a good solvent in which to observe the ^{17}O NMR spectrum, because its low viscosity helps to minimize the quadrupolar relaxation of the ^{17}O nucleus.[30] In order to observe the Xe-F couplings in $XeOF_3^+$, it is necessary to dissolve $XeOF_3^+SbF_6^-$ in the very strong fluoro-acid SbF_5. It has previously been demonstrated that the addition of XeF_2 to the SbF_5 not only enhances the solubility of $XeOF_3^+SbF_6^-$ in this medium due to the increased ionizing power of the solvent in the presence

of XeF^+ and $Sb_nF_{5n+1}^-$ ions, but also reduces its viscosity considerably, thereby allowing the observation of high-resolution spectra.[3]

The ^{129}Xe NMR spectrum at 30 °C of $XeOF_3^+SbF_6^-$ dissolved in HF and acidified with a fivefold molar excess of AsF_5 is depicted in Figure 5a. The AsF_5 was added in an effort to slow the intermolecular fluoride exchange and allow the observation of the one-bond Xe-F couplings. This method has previously been used to slow the fluorine ligand exchange in the IF_6^+ and TeF_3^+ cations so that $^1J(^{19}F\text{-}^{127}I)$ and $^1J(^{19}F\text{-}^{125}Te)$ could be observed.[31,32] The ^{129}Xe spectrum displays two singlets of similar intensity at 200.8 and 200.1 ppm attributable to the $Xe^{16}OF_3^+$ and $Xe^{18}OF_3^+$ isotopomers, respectively. The difference in chemical shift between the two isotopomers [$^1\Delta^{129}Xe(^{18,16}O)$, -0.69 ppm] represents the first observation of a secondary isotope shift in a xenon oxofluoro-cation. At high gain (Figure 5b) the broad equal-intensity sextet of the $Xe^{17}OF_3^+$ isotopomer can be seen. The multiplet arises from the coupling of ^{129}Xe to the ^{17}O (I = 5/2) and shows the expected variation in component linewidths for a quadrupolar nucleus undergoing modestly slow relaxation. The average $^{129}Xe\text{-}^{17}O$ coupling constant measured from this spectrum was 545 Hz; no coupling between Xe and the F ligands was observed indicating that intermolecular fluorine exchange is still rapid even in the presence of an excess of the strong fluoro-acid AsF_5. The ^{17}O NMR spectrum of the same sample (Figure 6) shows a singlet ($\Delta\nu_{1/2}$, 132 Hz) at 333.7 ppm with flanking ^{129}Xe satellites [$^1J(^{17}O\text{-}^{129}Xe)$, 619 Hz] attributable to the $Xe^{17}OF_3^+$ cation. The smaller value of $^1J(^{17}O\text{-}^{129}Xe)$ measured in the ^{129}Xe NMR spectrum as compared with that measured in the ^{17}O NMR spectrum is attributable to the partial quadrupole collapse of the equal-intensity sextet in the ^{129}Xe spectrum, which results in a symmetrical variation in the spacings between the components of the sextet.[30] This means that an accurate

value of the ^{129}Xe-^{17}O coupling cannot be measured from this spectrum without computer simulation.[30] However, the $^{1}J(^{17}O$-$^{129}Xe)$ value obtained from the ^{17}O NMR spectrum is reliable, since the separation between the ^{129}Xe satellites is independent of the different lifetimes of the ^{17}O spin states.[33] The ^{129}Xe NMR spectrum of a mixture of $XeOF_3^+SbF_6^-$ and XeF_2 (1:5.3 mole ratio) in neat SbF_5 is depicted in Figure 7a. The spectrum displays two broad partly overlapping doublets of triplets ascribed to the $Xe^{16}OF_3^+$ and $Xe^{18}OF_3^+$ isotopomers at 237.4 and 238.0 ppm, respectively. When the spectrum is resolution enhanced by Gaussian multiplication of the FID, the two multiplets corresponding to the two isotopomers are clearly distinguished (Figure 7b). The secondary isotope shift, $^{1}\Delta^{129}Xe(^{18,16}O)$, was measured as -0.59 ppm. The multiplet pattern arises from the coupling of the ^{129}Xe to the unique equatorial fluorine ligand [$^{1}J(^{129}Xe$-$^{19}F_{eq})$, 1012 Hz] and the two axial fluorine ligands [$^{1}J(^{129}Xe$-$^{19}F_{ax})$, 464 Hz]. These values are in reasonable agreement with those previously obtained on natural abundance samples of $XeOF_3^+SbF_6^-$.[3,6] The larger magnitude of $^{1}J(^{129}Xe$-$^{19}F_{eq})$ as compared with $^{1}J(^{129}Xe$-$^{19}F_{ax})$ is in good agreement with the prediction, based on simple MO ideas, that the Xe-F_{eq} bond will be stronger (bond order 1) than the Xe-F_{ax} bonds (bond order ½) and fits in well with the shorter Xe-F_{eq} bond length obtained from the crystal structure determination (see earlier discussion). A resonance attributable to the $Xe^{17}OF_3^+$ isotopomer was not observed presumably owing to the much faster quadrupolar relaxation of the ^{17}O nucleus in the more viscous SbF_5 solution, which would result in the resonance being collapsed into the baseline. Accordingly, the ^{17}O NMR spectrum of the sample shows a very broad ($\Delta\nu_{½}$, 5370 Hz) singlet at 342 ppm with no resolved ^{129}Xe satellites.

The values of $^{1}\Delta^{129}Xe(^{18,16}O)$ obtained for the $XeOF_3^+$ cation are of the same magnitude as those measured for $XeOF_4$ [$^{1}\Delta^{129}Xe(^{18,16}O)$, -0.58 ppm][34] and XeO_2F_2 [$^{1}\Delta^{129}Xe(^{18,16}O)$, -0.52

ppm].[34] The ^{17}O chemical shift of the $XeOF_3^+$ in HF is deshielded relative to that of $XeOF_4$ [$\delta(^{17}O)$, 316.3 ppm], in accord with the increased positive charge on the cation.[35] Interestingly, the ^{129}Xe-^{17}O coupling in $XeOF_3^+$ is significantly smaller than the corresponding coupling in $XeOF_4$ [$^1J(^{129}Xe$-$^{17}O)$, 704 Hz] which, if it is assumed that the Fermi-contact coupling mechanism provides the dominant contribution to the coupling constant, indicates a lower s-character in the Xe=O bond of the cation. However, this interpretation may not be justified in the light of recent experimental results which suggest that the non-contact contributions to the coupling constant, namely, the spin-orbital and spin-dipolar terms, can provide an important contribution to coupling constants involving heavy nuclei.[36] This is especially likely to be the case where a multiple bond exists between the two coupled nuclei, such as in the Xe=O bond.[37,38] Unfortunately, there is insufficient data at present to allow unequivocal interpretation of the trends observed in the coupling constants of such systems.

EXPERIMENTAL SECTION

Apparatus and Materials. All manipulations were performed under strictly anhydrous conditions in a nitrogen-filled dry box (Vacuum Atmospheres Model DLX) or on a vacuum line constructed from 316 stainless steel, nickel, Teflon and FEP. Preparative work was carried out in ¼-in.-o.d. lengths of FEP tubing which were heat-sealed at one end and connected through 45° SAE flares to Kel-F valves.

Xenon oxotetrafluoride enriched in ^{17}O and ^{18}O was prepared as previously described [34] using enriched water (ORIS, Saclay, France) with the following oxygen composition: ^{16}O, 36.5%,

^{17}O, 26.5% and ^{18}O, 37.0%.

Arsenic pentafluoride was prepared by the fluorination of AsF_3[39] in a nickel can. The AsF_3 (35.61 g, 0.2699 mol) was distilled *in vacuo* into a 1L nickel can equipped with a stainless steel Autoclave Engineers valve. Fluorine (0.4064 mol, 50% excess) was condensed into the can at -196 °C. The can was allowed to warm to room temperature and then heated to 163 °C overnight. The product was cooled to -196 °C and the excess fluorine pumped away through a soda lime trap. The AsF_5 was distilled into a nickel storage cylinder from which it was used without further purification.

The method used for the preparation of xenon difluoride was similar to that used by Malm and Chernick[40] for the preparation of XeF_4. In a typcal preparation, xenon (0.236 mol) and fluorine (0.118 mol) were condensed into a nickel can (249 mL) at -196 °C. The can and contents were then allowed to warm to room temperature. At room temperature, the total pressure was estimated to be 34 atm. An electric furnace, preheated to 400 °C was placed around the nickel can and maintained at this temperature for 7 hrs. The initial autogeneous pressure in the can at 400 °C was estimated to be 78 atm. After the specified time period, the furnace was removed and the nickel vessel and contents were rapidly quenched to room temperature in water. The can was cooled to -78 °C and excess xenon was condensed into a storage cylinder at -196 °C. The XeF_2 was collected by pumping the contents of the nickel reaction vessel through a cold trap at -78 °C. The yield of XeF_2 was 19.86 g. (99.3%). The purity of the product was checked by recording the Raman spectrum in the range 450 to 600 cm^{-1}. Xenon difluoride has a strong line at 496 cm^{-1} whereas the most likely impurity, XeF_4, has two strong lines at 502 and 543 cm^{-1}. The amount of XeF_4 found in any of the preparations was generally estimated to be less than 0.5%.

Literature methods were used for the synthesis or purification of HF (Harshaw Chemical Co.)[41] and SbF_5 (Ozark-Mahoning Co.).[42]

Synthesis of $Xe^{16,17,18}OF_3^+SbF_6^-$. Antimony pentafluoride (0.5162 g, 2.382 mmol) was syringed into a prefluorinated ¼-in.-o.d. FEP tube in a dry nitrogen glove bag. The tube was fitted with a Kel-F valve and anhydrous HF (*ca.* 0.7 mL) distilled on to the SbF_5 at -196 °C. The HF and SbF_5 were mixed thoroughly at room temperature. The resulting solution was frozen to -196 °C and a slight excess of $Xe^{16,17,18}OF_4$ (0.55188 g, 2.4607 mmol) distilled into the tube. The sample was allowed to warm to room temperature to give a clear colorless solution. The volatile materials were pumped off at -40 °C. The product was pumped for several hours at 0 °C to yield $Xe^{16,17,18}OF_3^+SbF_6^-$ as a fine white, crystalline solid (1.0442 g, 99.4%).

NMR Sample of $Xe^{16,17,18}OF_3^+SbF_6^-$ in HF Acidified with AsF_5. A 9-mm o.d. FEP tube was loaded with $Xe^{16,17,18}OF_3^+SbF_6^-$ (0.3391 g, 0.7689 mmol) in the dry box. The tube was attached to the metal vacuum line and anhydrous HF (*ca.* 1.5 mL), followed by AsF_5 (4 mmol), distilled in at -196 °C. The tube was heat-sealed at -196 °C and stored in liquid nitrogen until the NMR spectra could be run.

NMR Sample of $Xe^{16,17,18}OF_3^+SbF_6^-/XeF_2$ in Neat SbF_5. Antimony pentafluoride (*ca.* 2 mL) was syringed into a 9-mm FEP tube in a dry nitrogen glove bag. The tube was taken into the dry box and cooled to -196 °C in order to freeze the SbF_5. The $Xe^{16,17,18}OF_3^+SbF_6^-$ (0.2889 g, 0.6551 mmol) was added on top of the solid SbF_5. The sample was allowed to warm to room

temperature to give a viscous suspension. Xenon difluoride (0.5937 g, 3.507 mmol) was added to the mixture and slowly dissolved with agitation over a period of 2 h. A clear yellow, mobile solution resulted. The tube was heat-sealed at -196 °C and stored in liquid nitrogen until the NMR spectra could be run.

Crystal Structure Determination of $XeOF_3^+SbF_6^-$

Crystal Growing. Approximately 100 mg. of $XeOF_3^+SbF_6^-$ was transferred to an 8-mm glass tube equipped with a brass bellows valve, evacuated and the bottom of the tube immersed in 40 °C water inside a glass dewar. The compound sublimed over a period of several hours, resulting in deposits of crystalline material on the tube walls above the water level. The tube was then transferred to a dry box equipped with a microscope and the crystals were removed by cutting open the glass tube and prying them off the walls with an iridium stylus. The crystals were colorless thick plates and were sealed in 0.1, 0.2 and 0.3-mm Lindemann glass capillaries and stored at -10 °C prior to mounting on the diffractometer. A preliminary observation of the sealed crystals under a polarized microscope revealed that some of them were twined. The crystal used in this study was a plate with dimensions 0.2 x 0.3 x 0.05 mm.

Collection and Reduction of X-Ray Data. The crystal was centered on a Syntex $P2_1$ diffractometer. Accurate cell dimensions were determined at T = -89 °C from a least-squares refinement of the setting angles (χ, ϕ and 2θ) obtained from 21 accurately centered reflections (with $16.82° \leq 2\theta \leq 29.21°$) chosen from a variety of points in reciprocal space. The examination

of the peak profiles revealed single but slightly broadened peaks. Integrated diffraction intensities were collected using a θ - 2θ scan technique with scan rates varying from 1.5 to 14.65 °/min (in 2θ) so that the weaker reflections were examined most slowly to minimize counting errors. The data were collected with $0 \leq h \leq 11$, $-12 \leq k \leq 12$ and $-13 \leq l \leq 13$ and with $5 \leq 2\theta \leq 40°$, using silver radiation monochromatized with a graphite crystal ($\lambda = 0.56087$ Å). During data collection the intensities of three standard reflections were monitored every 97 reflections to check for crystal stability and alignment. A total of 3219 reflections were collected out of which 102 were standard reflections. A total of 2911 unique reflections remained after averaging of equivalent reflections. A total of 1782 reflections, satisfying the condition $I \geq 2.5\ \sigma(I)$, were used for structure solution. The intensities of the standards dropped regularly to about 90% of their original values during the course of the data collection; this decomposition was later corrected by scaling the data linearly between each set of standards. Corrections were made for Lorentz and polarization effects. Absorption corrections were applied by using the program DIFABS which also corrected for the crystal decay.

Crystal Data. The compound, F_9OSbXe ($f_w = 440.03$ g mol^{-1}), crystallizes in the triclinic system, space group $P\bar{1}$ with the following crystal data at T = -89° C: $a = 8.569(2)$ Å, $b = 9.760(2)$ Å, $c = 10.104(3)$ Å, $\alpha = 109.68(2)°$, $\beta = 92.58(2)°$, $\gamma = 104.27(2)°$, V = 770 Å^3, $D_{calc} = 3.83$ g cm^{-3} for Z = 4. Ag(Kα) radiation ($\lambda = 0.56087$ Å, μ(Ag Kα) = 42.8 cm^{-1}) was used.

Solution and Refinement of the Structure. The XPREP program[43] was used for determining the correct cell and space group. It first confirmed the original cell and that the lattice was triclinic

primitive. The structure was shown to be centrosymmetric by an examination of the E-statistics (calc., 0.969, theor., 0.968), and consequently the structure was solved in the space group $P\bar{1}$. The choice of the space group $P\bar{1}$ was confirmed later on by using the program MISSYM[43] which did not find any other symmetry.

A first solution was obtained without absorption corrections and it was achieved by conventional heavy-atom Patterson methods, which located the positions of the heavy atoms. The four atoms were assigned antimony scattering factors. The full-matrix least-squares refinement of the antimony atom positions and isotropic thermal parameters gave a conventional agreement index R ($=\sum||F_o| - |F_c||/\sum|F_o|$) of 0.20. Resulting differences in the stereochemistry about the four heavy atoms clearly indicated the nature of each atom. A difference Fourier synthesis revealed the remaining fluorine and oxygen atoms and confirmed the choice of the antimony and xenon atoms. Refinement of positional and isotropic temperature parameters for all atoms (the oxygen atom being assigned a fluorine scattering factor) converged at R = 0.13.

At this stage, it was possible to distinguish in each xenon environment, one bond length which was significantly shorter than the other ones, indicating the existence of a Xe-O bond. A significant improvement of the structure was achieved by introducing anisotropic thermal parameters for the four heavy atoms (Xe and Sb) and isotropic thermal parameters for the O and F atoms; the R factor dropped to R = 0.084. At that point, the examination of the F_o and F_c values revealed that, in general, the F_o values were smaller than the F_c values, indicating that isotropic corrections for secondary extinction needed to be included in the refinement. The introduction of a weighting factor ($w = 1 / \sigma^2(F) + 0.006617\ F^2$) gave a final solution with R = 0.053 (R_w = 0.055).

The structure was solved a second time using data that had been corrected for absorption. The initial model used the atomic coordinates and isotropic thermal parameters defined previously for the Xe, Sb, F and O atoms. The solution obtained (R = 0.053) indicated a significant improvement over that obtained without absorption corrections (R = 0.082). The structure was slightly improved by introducing anisotropic thermal parameters for the Xe and Sb atoms (R = 0.048). The F and O atoms could also be refined with anisotropic thermal parameters (R = 0.045). The final refinement was obtained by introducing a weight factor ($w = 1 / \sigma^2(F) + 0.004295\ F^2$) and an isotropic correction for secondary extinction, and gave rise to a residual, R, of 0.045 (R_w = 0.049). In the final difference Fourier map, the maximum and the minimum electron densities were 1.8 and -1.3 $Å^3$.

All calculations were performed on a 486 computer using the SHELXTL PLUS™ (Sheldrick, 1990)[43] determination package for structure solution and refinement as well as structure determination molecular graphics.

Nuclear Magnetic Resonance Spectroscopy

All spectra were recorded unlocked (field drift < 0.1 Hz h^{-1}) on a Bruker AM-500 spectrometer equipped with an 11.744-T cryomagnet and an Aspect 3000 computer. The spectra were obtained using a 10-mm broad-band VSP probe (tunable over the range 23 - 202 MHz) which was tuned to 67.801 and 139.051 MHz to observe ^{17}O and ^{129}Xe, respectively. Free induction decays for ^{17}O were accumulated in an 8K memory with a spectral width setting of 15 kHz, yielding an acquisition time of 0.270 s and a data point resolution of 3.70 Hz/data point.

Free induction decays for ^{129}Xe were accumulated in 8 and 16K memories with spectral width settings of 15 and 30 Khz, respectively. These yielded acquisition times of 0.270 and 0.278 s and data point resolutions of 3.70 and 3.59 Hz/data point, respectively. No relaxation delays were applied. Typically, 9000 - 15 000 transients were accumulated. The pulse widths corresponding to a bulk magnetization tip angle, θ, of approximately 90° were 6.4 μs (^{17}O) and 18 μs (^{129}Xe). Line broadening parameters used in the exponential multiplication of the free induction decays were set equal to the data point resolution of the spectrum.

The ^{17}O and ^{129}Xe NMR spectra were referenced to neat external samples of H_2O and $XeOF_4$, respectively, at ambient temperature (30 °C). The chemical shift convention used is that a positive (negative) sign indicates a chemical shift to high (low) frequency of the reference compound.

The NMR samples were prepared in 25-cm lengths of 3/8-in.-o.d., 1/32-in. wall FEP plastic tubing that had been reduced to 9-mm o.d. by squeezing in a heated precision brass mold. The FEP tubing was heat-sealed at one end with the open end flared (45° SAE) and joined, by means of compression fittings, to a Kel-F valve. The FEP tubes were heat-sealed under dynamic vacuum with their contents frozen at -196 °C. The sealed FEP sample tubes were inserted into thin-walled glass precision NMR tubes (Wilmad) in order to obtain the spectra.

Acknowledgments. We thank the U.S. Air Force Phillips Laboratory, Edwards Air Force Base, California for support of this work under Contract F04611-91-K-0004 and the Natural Sciences and Engineering Research Council of Canada for support in the form of an operating grant.

Supplementary Material. A structure determination summary (Table 6, 3 pages); tables of anisotropic thermal parameters (Table 7, 1 page); tabulation of calculated and observed structure factor amplitudes (Table 8, 7 pages); stereoview ORTEP of the packing in the unit cell and an ORTEP of the unit cell showing the two-dimensional layer structure (2 pages). Ordering information is given on any current masthead page.

REFERENCES

1. Selig, H. Inorg. Chem. 1966, 5, 183.
2. Gillespie, R.J.; Landa, B.; Schrobilgen, G.J. J. Chem. Soc. Chem. Commun. 1972, 607.
3. Gillespie, R.J.; Schrobilgen, G.J. Inorg. Chem. 1974, 13, 2370.
4. Gillespie, R.J.; Landa, B.; Schrobilgen, G.J. Inorg. Chem. 1976, 15, 1256.
5. McKee, D.E.; Adams, C.J.; Bartlett, N. Inorg. Chem. 1973, 12, 1722.
6. Schrobilgen, G.J.; Holloway, J.H.; Granger, P.; Brevard, C. Inorg. Chem. 1978, 17, 980.
7. Selig, H.; Holloway, J.H. Top. Curr. Chem. 1984, 124, 33.
8. Christe, K.O.; Wilson, W.W. Inorg. Chem. 1988, 27, 2714.
9. Brown, I.D. J. Solid State Chem. 1974, 11, 214.
10. Brown, I.D., in "Structure and Bonding in Crystals", eds. M. O'Keefe and A. Navrotsky, Academic Press, London, 1981, vol. 2, p 1.
11. Brown, I.D.; Altermatt, D. Acta Cryst. 1985, B41, 244.
12. Gillespie, R.J.; Hargittai, I., "The VSEPR Model of Molecular Geometry", Allyn and Bacon, Boston, 1991.
13. Oberhammer, H.; Christe, K.O. Inorg. Chem. 1982, 21, 273.
14. Boldrini, P.; Gillespie, R.J.; Ireland, P.R.; Schrobilgen, G.J. Inorg. Chem. 1974, 13, 1690.
15. McKee, D.E.; Zalkin, A.; Bartlett, N. Inorg. Chem. 1973, 12, 1713.
16. Gavin Jr, R.M.; Bartell, L.S. J. Chem. Phys. 1968, 48, 2460; J. Chem. Phys. 1968, 48, 2466.
17. Martins, J.; Wilson Jr., E.B. J. Mol. Spectrosc. 1968, 26, 410.
18. Holloway, J.H.; Kaučič V.; Martin-Rovet, D.; Russel, D.R.; Schrobilgen, G.J.; Selig, H.

1985, 24, 678.

19. Peterson, S.W.; Willet, R.D.; Huston, J.L. J. Chem. Phys. 1973, 59, 453.

20. Templeton, D.H.; Zalkin, A.; Forester, J.D.; Williamson, S.M., in "Noble Gas Compounds", H.H. Hyman (ed.), University of Chicago Press, Chicago, 1963, 221.

21. Burns, J.H.; Agron, P.A.; Levy. H.A.. in "Noble Gas Compounds", H.H. Hyman (ed.), University of Chicago Press, Chicago, 1963, 211.

22. Levy, H.A.; Agron, P.A., in "Noble Gas Compounds", H.H. Hyman (ed.), University of Chicago Press, Chicago, 1963, 221.

23. Cutler, J.N.; Bancroft, G.M.; Bozek, J.D.; Tan, K.H.; Schrobilgen, G.J. J. Am. Chem. Soc. 1991, 113, 9125.

24. Rothman, M.J.; Bartell, L.S.; Ewig, C.S.; van Wazer J.R. J. Chem. Phys. 1980, 73, 375.

25. Pitzer, K.S.; Bernstein, L.S. J. Chem. Phys. 1975, 63, 3849 and references therein.

26. Bondi, A. J. Phys. Chem. 1964, 68, 441.

27. The NRCVAX Crystal Structure System, Larson, A.C.; Lee, F.L.; LePage, Y; Webster, M.; Charland, J.P.; Gabe, E.J., Chemistry Division, NRC, Ottawa; PC version: White, P.S., Dpt of Chemistry, University of North Carolina, Chapel Hill, N.C.

28. Christe, K.O.; Curtis, E.C.; Dixon, D.A.; Mercier, H.P.; Sanders, J.C.P.; Schrobilgen, G.J. 1991, 113, 3351.

29. Carter, R.L. J. Chem. Educ. 1971, 48, 297 and references therein.

30. Sanders, J.C.P.; Schrobilgen, G.J. in "Multinuclear Magnetic Resonance in Liquids and Solids - Chemical Applications"; Granger, P., Harris, R.K., Eds.; NATO ASI Series C, Kluwer Academic Publishers: Boston, 1990; p 157.

31. Brownstein, M.; Selig, H. Inorg. Chem. 1972, 11, 656.

32. Collins, M.J.; Schrobilgen, G.J. Inorg. Chem. 1985, 24, 2608.

33. Bacon, J.; Gillespie, R.J.; Hartman, J.S.; Rao, U.K.K. Mol. Phys. 1970, 18, 561.

34. Schumacher, G.A.; Schrobilgen, G.J. Inorg. Chem., 1984, 23, 2923.

35. Jameson, C.J.; Mason, J. in "Multinuclear NMR"; Mason, J., Ed.; Plenum Press: New York, 1987; Chapter 3, p 66.

36. Power, W.P.; Lumsden, M.D.; Wasylishen, R.E. J. Am. Chem. Soc. 1991, 113, 8257 and references therein.

37. Jameson, C.J. in "Multinuclear NMR"; Mason, J., Ed.; Plenum Press: New York, 1987; Chapter 4, p 116.

38. Cogne, A.; Grand, A.; Laugier, J.; Robert, J.B.; Wiesenfeld, L. J. Am. Chem. Soc. 1980, 102, 2238.

39. Hoffman, C.J. Inorg. Synth. 1953, 4, 150.

40. Malm, J.G.; Chernick, C.L. Inorg. Synth., 1966, 8, 254.

41. Emara, A.A.A.; Schrobilgen, G.J. Inorg. Chem., 1992, 31, 1323.

42. Gillespie, R.J.; Netzer, A.; Schrobilgen, G.J. Inorg. Chem., 1974, 13, 1455.

43. Sheldrick, G.M. (1990); SHELXTL PLUS™ Release 4.21/V. Siemens Analytical X-Ray Instruments, Inc., Madison, WI.

Table 1. Bond distances (Å), Bond Angles (°) and Bond Valences in $XeOF_3^+SbF_6^-$

Bond Lengths (Å) and Corresponding Bond Valences (v.u.)[a]

Xe(1)	F(1)	F(2)	F(5)	F(3)[b]	F(4)[b]	O(1)
Bond valence	0.98	1.22	1.07	0.18	0.22	2.18
Bond length	1.896(11)	1.818(11)	1.864(12)	2.535(13)	2.449(10)	1.682(15)

Total bond valence: 5.85

Xe(2)	F(12)	F(13)	F(11)	F(9)[b]	F(14)[b]	O(2)
Bond valence	1.02	1.20	1.05	0.15	0.17	2.07
Bond length	1.885(12)	1.824(12)	1.871(12)	2.589(10)	2.541(14)	1.701(12)

Total bond valence: 5.66

Sb(1)	F(4)	F(6)	F(7)	F(8)	F(9)	F(10)
Bond valence	0.68	0.84	0.81	0.87	0.80	0.89
Bond length	1.940(9)	1.863(14)	1.877(14)	1.847(15)	1.881(11)	1.839(11)

Total bond valence: 4.89

Continued...

Table 1. (continued)

Sb(2)	F(14)	F(16)	F(18)	F(15)	F(17)	F(3)
Bond valence	0.76	0.87	0.92	0.89	0.84	0.73
Bond length	1.899(12)	1.850(11)	1.827(12)	1.842(13)	1.863(12)	1.912(12)

Total bond valence: 5.01

F(3)	Xe(1)	Sb(2)
Bond valence	0.18	0.73
Bond length	2.535(13)	1.912(12)

Total bond valence: 0.91

F(14)	Xe(2)	Sb(2)
Bond valence	0.17	0.76
Bond length	2.541(14)	1.899(12)

Total bond valence: 0.93

F(4)	Xe(1)	Sb(1)
Bond valence	0.22	0.68
Bond length	2.449(10)	1.940(9)

Total bond valence: 0.90

F(9)	Xe(2)	Sb(1)
Bond valence	0.15	0.80
Bond length	2.589(10)	1.881(11)

Total bond valence: 0.95

Continued...

Table 1. (continued)

Bond angles (°)

O(1)-Xe(1)-F(2)	99.9(6)	O(1)-Xe(1)-F(1)	95.2(6)	F(1)-Xe(1)-F(3)	88.4(5)
F(3)-Xe(1)-F(4)	100.7(4)	O(1)-Xe(1)-F(5)	92.5(7)	F(3)-Xe(1)-F(5)	81.8(5)
O(1)-Xe(1)-F(4)	84.2(5)	F(1)-Xe(1)-F(2)	81.0(5)	F(1)-Xe(1)-F(4)	122.9(4)
F(2)-Xe(1)-F(3)	72.7(4)	F(2)-Xe(1)-F(5)	81.0(5)	F(5)-Xe(1)-F(4)	74.7(4)
F(5)-Xe(1)-F(1)	161.4(5)				
O(2)-Xe(2)-F(13)	100.9(6)	O(2)-Xe(2)-F(11)	92.0(6)	F(9)-Xe(2)-F(11)	74.1(4)
F(9)-Xe(2)-F(14)	91.6(4)	O(2)-Xe(2)-F(12)	92.1(6)	F(9)-Xe(2)-F(12)	100.5(4)
O(2)-Xe(2)-F(14)	87.3(6)	F(11)-Xe(2)-F(13)	82.3(5)	F(11)-Xe(2)-F(14)	73.7(5)
F(9)-Xe(2)-F(13)	74.6(5)	F(12)-Xe(2)-F(13)	81.7(5)	F(12)-Xe(2)-F(14)	122.0(5)
F(11)-Xe(2)-F(12)	163.9(5)				

[a]Bond valence units (v.u.) are defined in ref.(9 - 11). [b]Anionic fluorine atom bridge to a cationic xenon atom, only Xe-F contacts up to 3.55 Å were included.

Table 2. Summary of Crystal Data and Refinement Results for $XeOF_3^+SbF_6^-$

space group	$P\bar{1}$
a (Å)	8.568(2)
b (Å)	9.760(2)
c (Å)	10.104(2)
α (°)	109.68(3)
β (°)	92.58(3)
γ (°)	104.27(3)
V (Å^3)	763.4(4)
molecules/unit cell	4
molecular wt (g mol^{-1})	440.0
calcd density (g cm^{-3})	3.829
T (°C)	-89
color	colorless
crystal decay (%)	no decay
μ (mm^{-1})	8.098
wavelength (Å) used for data collection	0.56086
sin θ/λ limit (Å^{-1})	0.6823
total no.of reflections measured	3117
no. of independent reflections	2911
no. of reflections used in struct. anal. $I > 2.5\sigma(I)$	1782

Table 2. (continued)

no. of variable parameters	218
final agreement factors	R = 0.0452
	wR = 0.0632

Table 3. Atomic Coordinates ($x10^4$) and Equivalent Isotropic Displacement Coefficients ($Å^2 \times 10^3$) for $XeOF_3^+SbF_6^-$

	x	y	z	U(eq)[a]
Xe(1)	4470(1)	-2246(1)	1293(1)	19(1)
O(1)	2941(15)	-2029(16)	350(13)	33(6)
F(1)	3286(13)	-4141(11)	1341(12)	30(4)
F(2)	5251(13)	-3484(12)	-138(10)	30(4)
F(3)	6997(13)	-2603(15)	2378(12)	37(5)
F(5)	6018(14)	-778(13)	894(12)	36(5)
Sb(1)	5589(1)	2265(1)	4114(1)	19(1)
F(4)	4387(13)	179(11)	3038(12)	33(4)
F(6)	5282(14)	1917(15)	5800(12)	38(5)
F(7)	7479(14)	1610(14)	4007(12)	37(5)
F(8)	5719(14)	2533(16)	2394(13)	42(6)
F(9)	3557(12)	2679(12)	4129(11)	29(4)
F(10)	6672(16)	4264(14)	5111(15)	52(6)
Xe(2)	710(1)	2118(1)	2754(1)	21(1)
O(2)	-962(15)	1497(16)	1511(13)	29(5)
F(11)	1714(14)	758(13)	1581(12)	38(5)
F(12)	121(15)	3878(12)	3781(12)	37(5)
F(13)	2074(13)	3450(13)	2129(11)	34(5)
Sb(2)	-738(1)	-2488(1)	2533(1)	21(1)
F(14)	-293(15)	-346(13)	3194(12)	38(5)
F(15)	-779(15)	-2474(15)	714(12)	43(5)
F(16)	1483(13)	-2226(15)	2759(12)	40(5)
F(17)	-820(13)	-2359(14)	4409(11)	34(5)
F(18)	-1231(16)	-4554(14)	1866(14)	47(5)

[a] Equivalent isotropic U defined as one third of the trace of the orthogonalized U_{ij} tensor.

Table 4. Xe-F and Xe-O Bond Lengths of Some Xenon Fluorides and Oxofluorides.

	Xe-F (Å)	Xe-O (Å)	Ref.
XeF_6	1.890(5)		16
$XeOF_4$	1.900(5)	1.703(2)	17
$XeOF_3^+SbF_6^-$	ax 1.879(12)	1.692(13)	a
	eq 1.821(12)		
$Cs^+(XeOF_4)_3F^-$	1.90(3)[b]	1.70(5)	18
XeO_2F_2	1.899(3)	1.714(4)	19
$K^+XeO_3F^-$	2.42(1)[c]	1.77(1)[d]	20
XeF_4	1.953(2)		21
$XeF_3^+SbF_6^-$	ax 1.906(14)[b]		14
	eq 1.835(10)		
$XeF_3^+SbF_6^-$	ax 1.89(1)		15
	eq 1.83(1)		
XeF_2	2.00(1)		22

[a]This work.

[b]Average value for the Xe-F bonds

[c]Average value for a Xe-F bond in which the F acts as a bridge between two xenon atoms

[d]Average value for the Xe-O bonds

Table 5. Equations for the Equatorial Least-Squares Planes of $XeOF_3^+$[a]

Atoms in the plane	A	B	C	D	σ(A)		d(Å)[b]	Angle /[c]	Angle ⊥[d]
Xe1, O1, F2	3.741X + 7.407Y - 4.373Z = 0.961				0.013	F1	-1.868		9.70
						F5	1.840		8.93
						F3	0.206	4.66	
						F4	1.001	24.13	
Xe2, O2, F13	-5.124X + 6.868Y + 3.459Z = 7.207				0.014	F12	1.865		8.31
						F11	-1.854		7.71
						F9	-0.598	13.36	
						F14	-1.025	23.79	

[a]Equations defined by AX + BY + CZ = D in the direct crystal coordinate system; calculated by the program BESPLN from the NRCVAX package.[27] σ is the standard deviation.

[b]Distances (Å) to the plane from the atoms out of the plane.

[c]Angle (deg) with the plane.

[d]Angle (deg) with the perpendicular to the plane.

FIGURE CAPTIONS

Figure 1. Asymmetric unit of the crystal structure of $XeOF_3^+SbF_6^-$; the long fluorine-bridge contacts are represented by dotted lines; thermal ellipsoids are shown at the 50% probability level.

Figure 2. Local environment around xenon in $XeOF_3^+SbF_6^-$; only the Xe1 environment is depicted.

Figure 3. The unit cell of $XeOF_3^+SbF_6^-$ showing the two-dimensional layer structure.

Figure 4. View down the axis passing through Xe1 and the triangular faces F2-F5-O1 and F1-F3-F4 in the $XeOF_3^+$ cation; a very similar arrangement is observed for Xe2.

Figure 5. ^{129}Xe NMR spectrum (139.051 MHz) at 30 °C of the ^{17}O- (26.5%) and ^{18}O- (37.0%) enriched $XeOF_3^+$ cation: a) $Xe^{16,17,18}OF_3^+SbF_6^-$ (*ca.* 0.5 M) in HF solvent acidified with AsF_5 (2.7 M); b) vertical expansion (x 32) showing the coupling of ^{129}Xe to ^{17}O (denoted with asterisks (*)) in the $Xe^{17}OF_3^+$ isotopomer.

Figure 6. ^{17}O NMR spectrum (67.801 MHz) at 30 °C of ^{17}O- (26.5%) and ^{18}O- (37.0%) enriched $XeOF_3^+SbF_6^-$ (*ca.* 0.5 M) in HF solution acidified with AsF_5 (2.7 M). Asterisks (*) denote ^{129}Xe satellites.

Figure 7. ^{129}Xe NMR spectrum (139.051 MHz) at 30 °C of ^{17}O- (26.5%) and ^{18}O- (37.0%) enriched $XeOF_3^+SbF_6^-$ (0.33 M) and XeF_2 (1.7 M) dissolved in SbF_5 solvent: a) spectrum obtained by Fourier transformation of the free induction decay using a Lorentzian fit; b) resolution enhanced spectrum obtained by Fourier transformation of the free induction decay using a Gaussian fit.

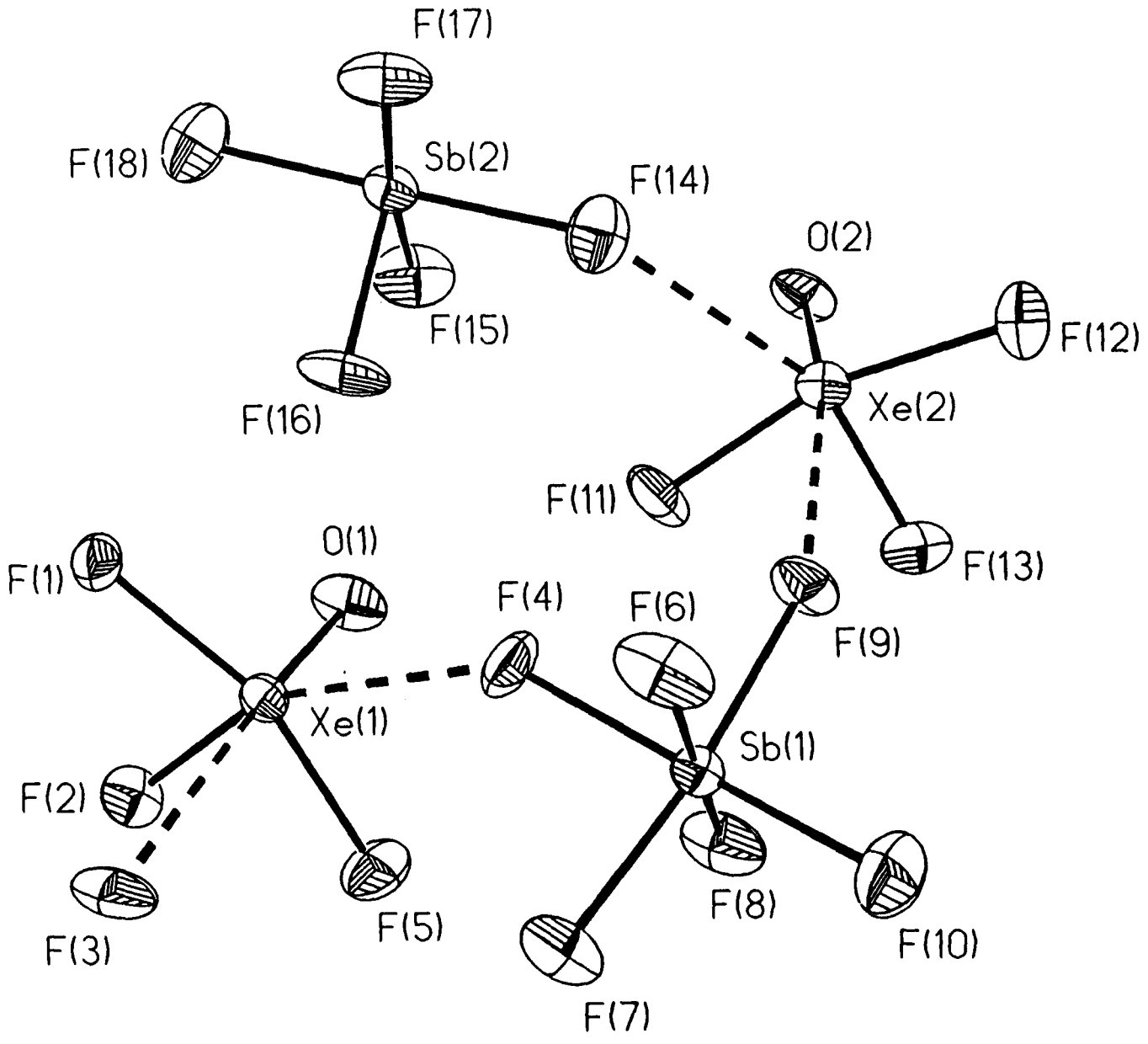
F(17)
F(18)
Sb(2)
F(14)
O(2)
F(15)
F(12)
F(16)
Xe(2)
F(11)
F(13)
O(1)
F(1)
F(4)
F(6)
F(9)
Xe(1)
Sb(1)
F(2)
F(8)
F(5)
F(10)
F(3)
F(7)

Figure 1

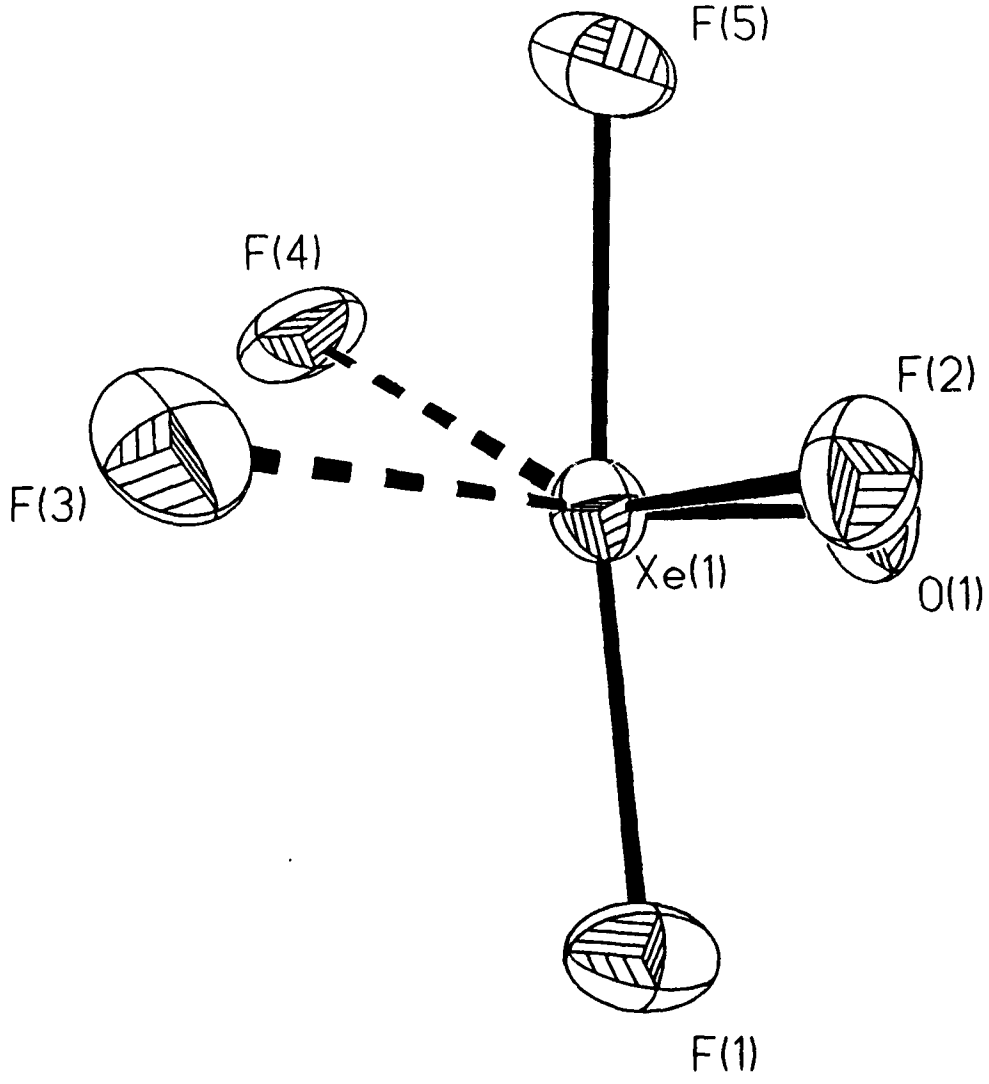

Figure 2

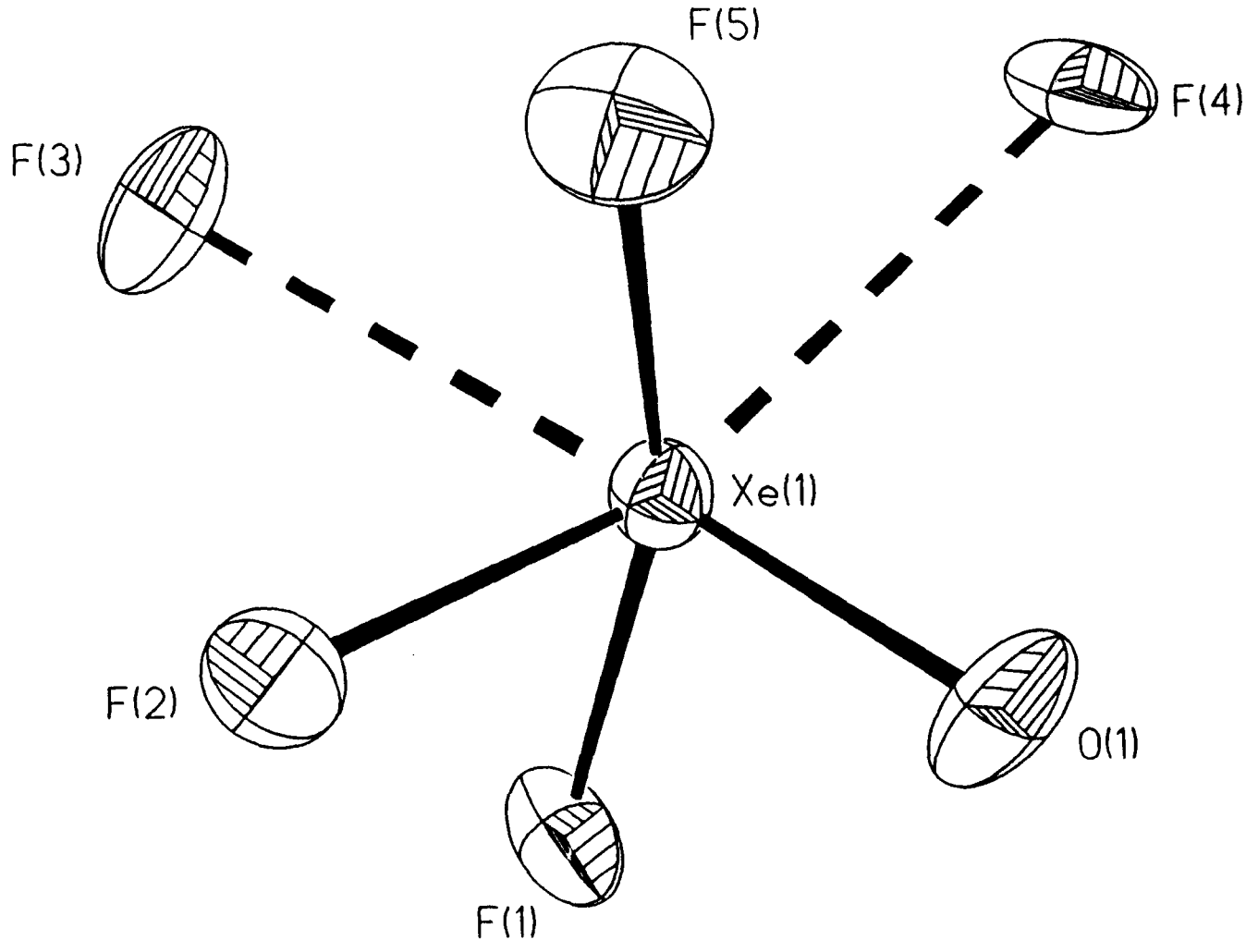

Figure 3

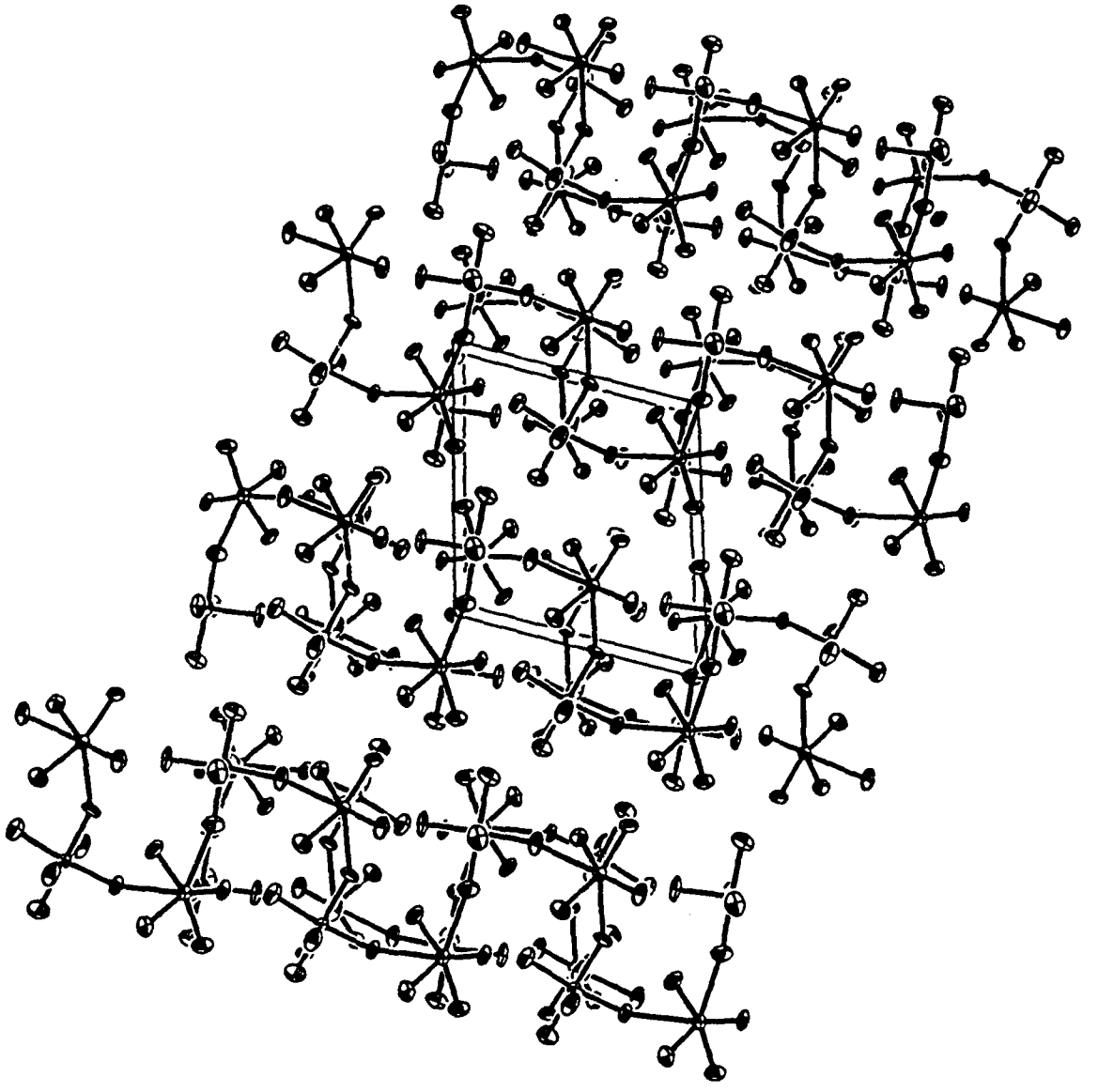

Figure 4

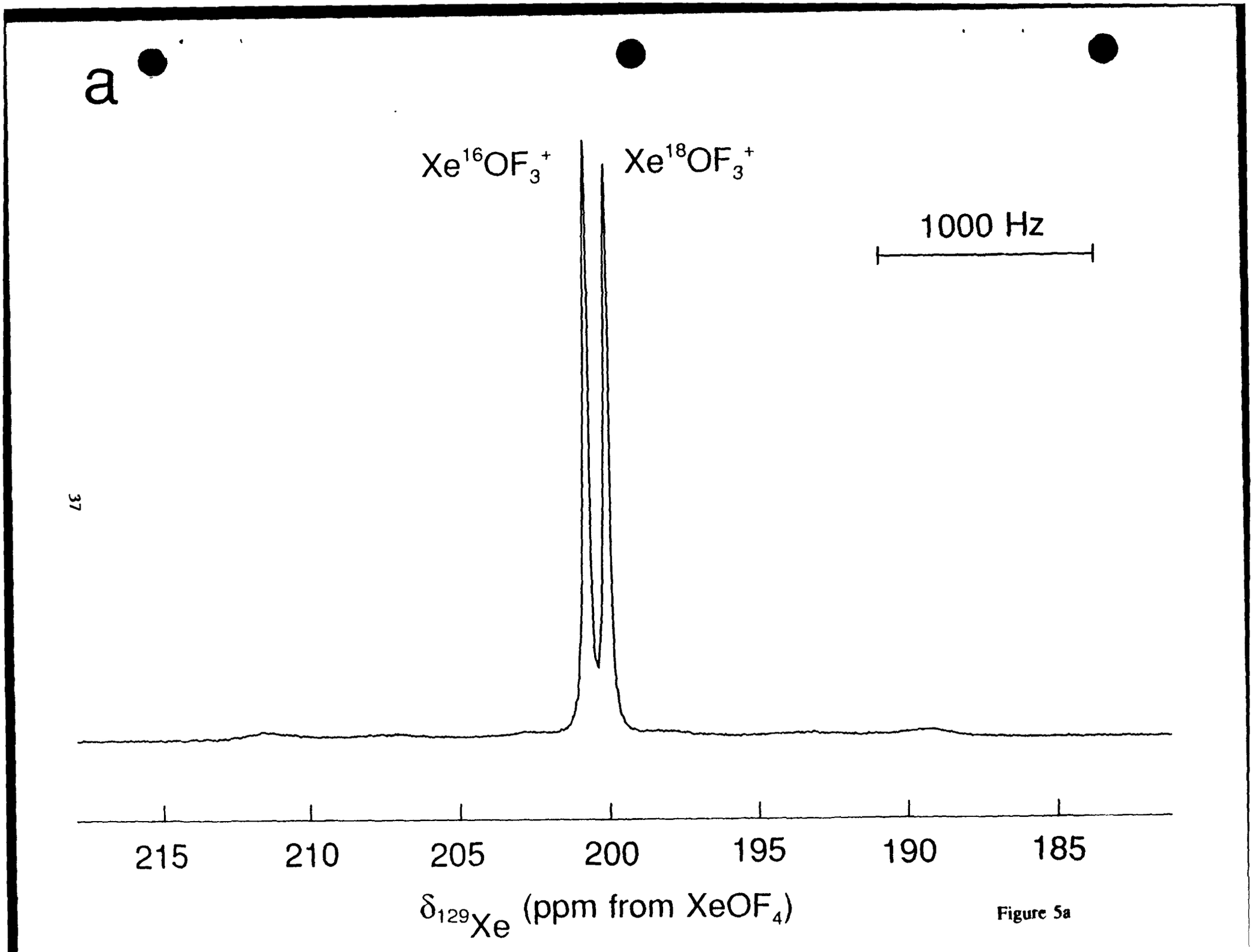
a
$Xe^{16}OF_3^+$
$Xe^{18}OF_3^+$
1000 Hz
215
210
205
200
195
190
185
$\delta_{129}Xe$ (ppm from $XeOF_4$)

Figure 5a

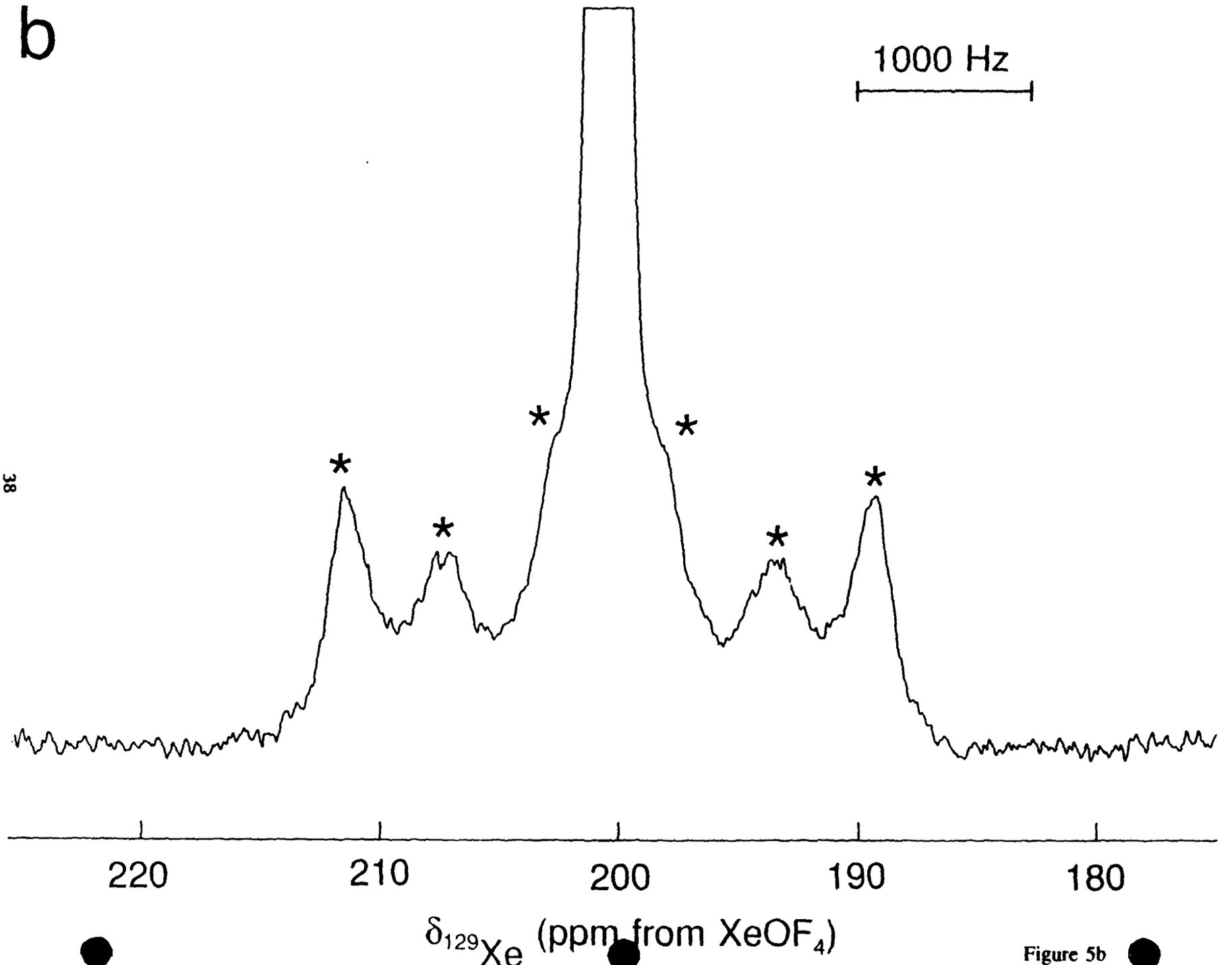

Figure 5b

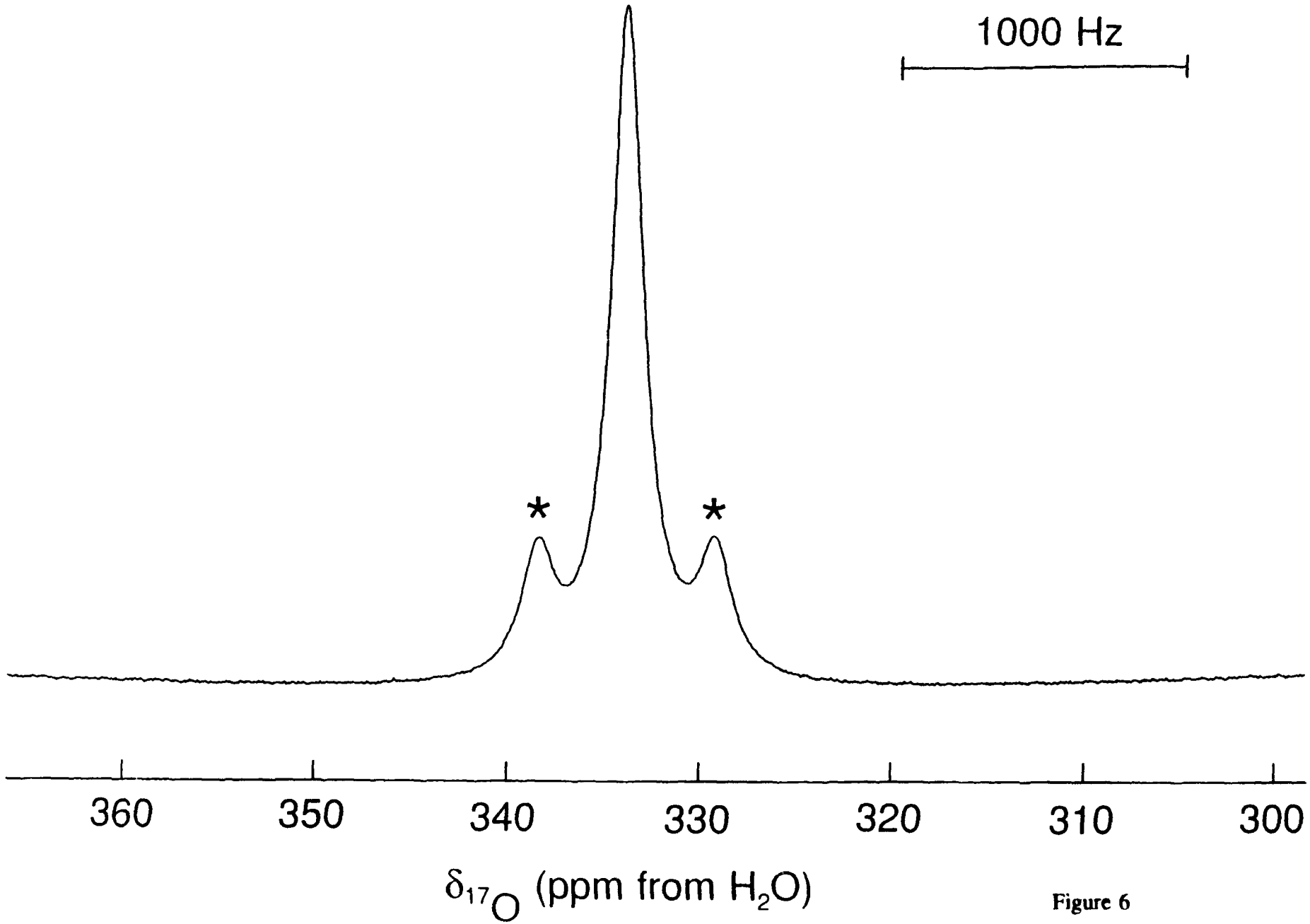

Figure 6

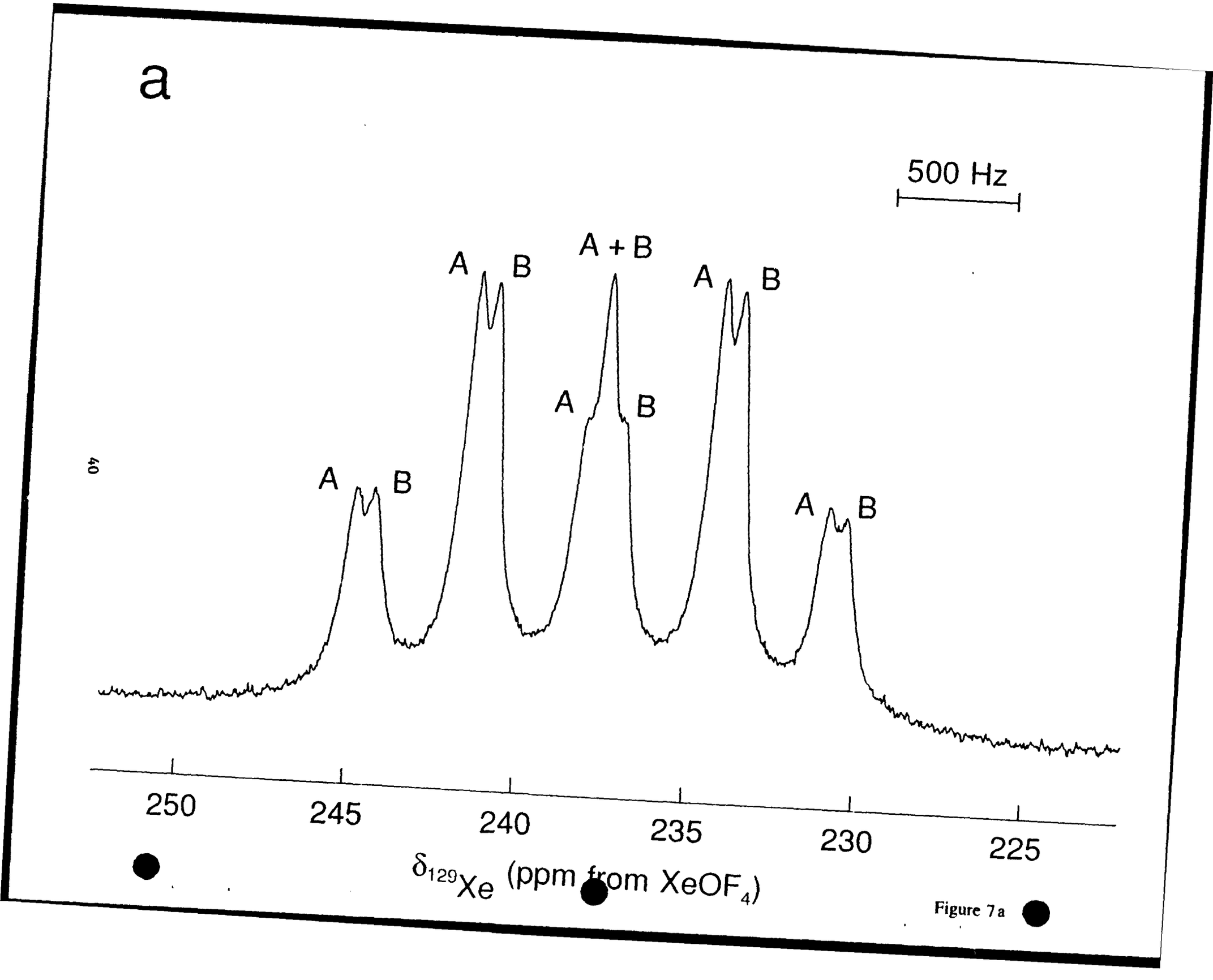
a
500 Hz
A
B
A + B
A
B
A
B
A
B
A
B
40
250
245
240
235
230
225
δ_{129}Xe (ppm from $XeOF_4$)

Figure 7a

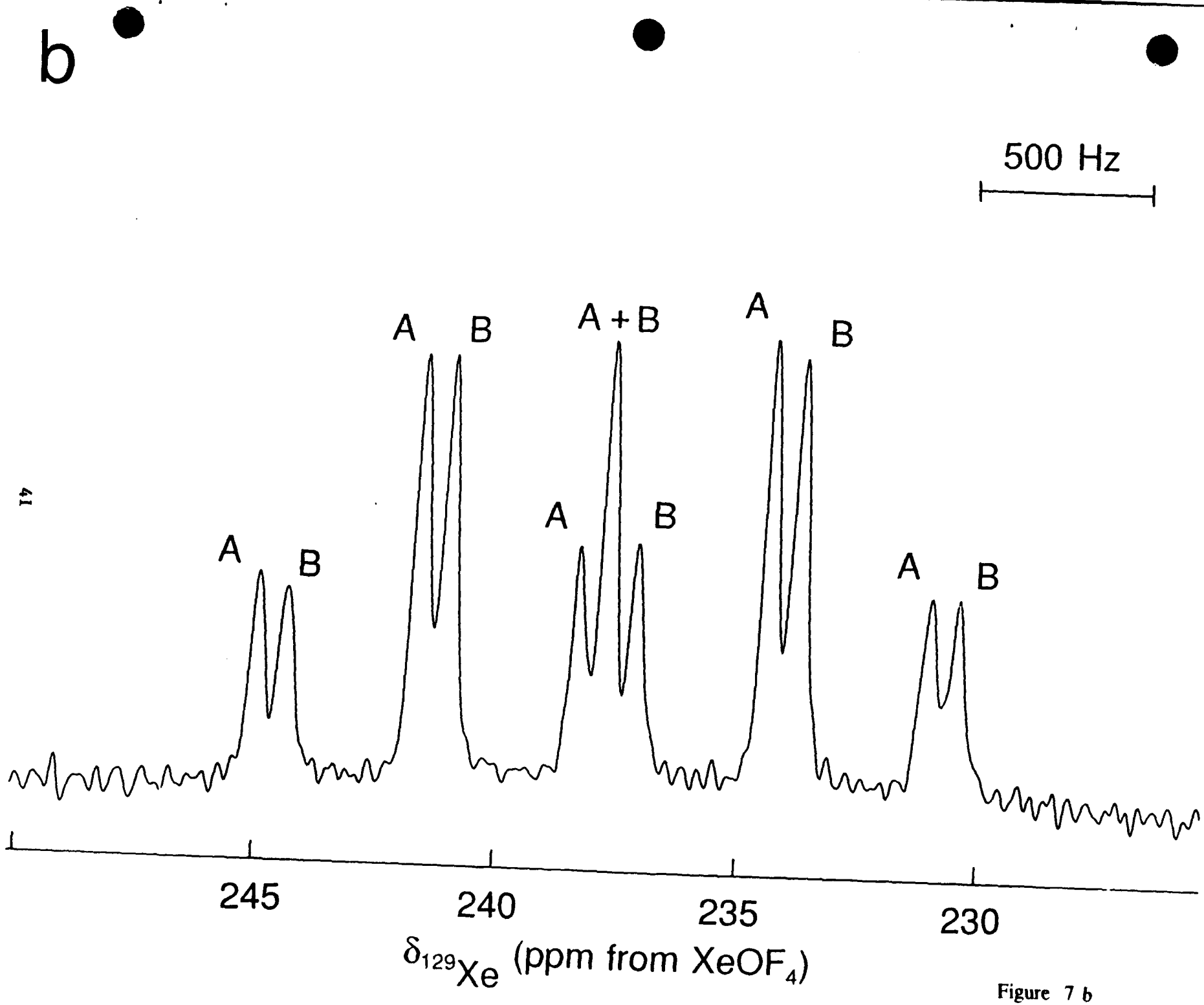
b
500 Hz
A
B
A + B
A
B
A
B
A
B
245
240
235
230
δ_{129}Xe (ppm from $XeOF_4$)

Figure 7 *b*

PART II

THE $F_2Cl\text{-}N{\equiv}CCF_3^+$ AND $F_2Cl\text{-}N{\equiv}CH^+$ CATIONS

AND ATTEMPTS TO FORM $FCl\text{-}N{\equiv}CH$

By taking advantage of the Lewis acid properties of the XeF^+ and KrF^+ cations, we have previously shown that a diverse range of noble-gas adduct cations exists; $F\text{-}Xe\text{-}L^+$, $F\text{-}Kr\text{-}N{\equiv}CH^+$ and $F\text{-}Kr\text{-}N{\equiv}CR_F^+$ (L = $HC{\equiv}N$, $RC{\equiv}N$, $R_FC{\equiv}N$, C_5F_5N, s-$C_3F_3N_3$). We have recently studied the Lewis acid properties of the strong oxidizer cation, ClF_2^+, by low temperature ^{19}F NMR spectroscopy and have shown that the cation is capable of binding to nitrogen base centers. Although $HC{\equiv}N$ adducts would provide more favorable monopropellants, we have elected to investigate the adduct formation of ClF_2^+ and ClF with $CF_3C{\equiv}N$ first and then to conduct parallel studies with $HC{\equiv}N$ because $CF_3C{\equiv}N$ (1st IP, 13.9 eV) is perhaps marginally oxidatively more resistant than $HC{\equiv}N$ (1st IP, 13.80 eV) and because our experience with related KrF= adducts has shown that the $FKr\text{-}N{\equiv}CH^+$ is kinetically less stable than $FKr\text{-}N{\equiv}CF_3^+$. Moreover, adduct formation can be more readily determined in the ^{19}F spectrum if both the Lewis acid and the Lewis base give rise to ^{19}F resonances. This approach has proven practical, allowing us to establish the correct synthetic conditions and procedures under less hazardous conditions.

The Lewis acid properties of the strong oxidizer cation ClF_2^+, as its AsF_6^-, salt have been studied in BrF_5 solvent at -58 °C by ^{19}F NMR spectroscopy. The interaction of 1 : 1 molar ratios of $ClF_2^+AsF_6^-$ and $CF_3C{\equiv}N$ leads to adduct formation

$$ClF_2^+AsF_6^- + CF_3C{\equiv}N \longrightarrow F_2Cl\text{-}N{\equiv}CCF_3^+AsF_6^- \qquad (1)$$

Two fluorine resonances corresponding to the adduct were observed; the fluorines on chlorine occur at -13.3 ppm and the resonance of the CF_3 group occurs at -55.8 ppm with relative integrated intensities of 2 : 3, respectively. The adduct has also been prepared in the presence of excess $CF_3C{\equiv}N$ so that the CF_3 resonances of free and complexed $CF_3C{\equiv}N$ were simultaneously

observed.

The adduct represents a new class of Cl-N bonded compound and is of particular interest because ClF_2^+ is a stronger oxidant than ClF_3 and has been chemically bound to an oxidizable center. Moreover, the ClF_2^+ derivatives are of lower molecular weight than their KrF^+ and XeF^+ analogs, making the adducts more attractive as monopropellants. Alternatives with lighter base centers are currently under investigation. At present, the reaction

$$ClF_2^+AsF_6^- + HC{\equiv}N \longrightarrow F_2Cl\text{-}N{\equiv}CH^+AsF_6^- \qquad (2)$$

is being studied. Thus far we have not been able to provide a full interpretation of the ^{19}F NMR spectra without complementary ^1H, ^{15}N and ^{13}C NMR studies.

Theoretical calculations indicate that the adduct cation of the presently unknown ArF^+ cation, $F\text{-}Ar\text{-}N{\equiv}CH^+$, will be stable with respect to dissociation and marginally stable with respect to redox degradation. We have attempted to prepare the isoelectronic neutral adduct $F\text{-}Cl\text{-}N{\equiv}CCF_3$, but have not had an opportunity to investigate the formation of $F\text{-}Cl\text{-}N{\equiv}CH$. The ^{19}F NMR spectra of $ClF/CF_3C{\equiv}N$ systems have been studied in SO_2ClF solvent owing to the chemical inertness of this solvent towards ClF. This has been verified by recording the spectrum of ClF in SO_2ClF at -91 °C, which consists of a broadened singlet at -406.9 ppm corresponding to ClF. The ^{19}F NMR spectra of the $ClF/CF_3C{\equiv}N$ system suggest that a new fluorine on chlorine environment results (-101.9 ppm) which is shifted to high frequency relative to that of ClF. However, the CF_3 resonance appears to be undergoing chemical exchange with the CF_3 resonance of uncomplexed $CF_3C{\equiv}N$, indicating that the adduct is partially dissociated, allowing the bound

and free base to exchange according to equilibrium (3).

$$ClF + CF_3C{\equiv}N \rightleftharpoons FCl\text{-}N{\equiv}CCF_3 \qquad (3)$$

PART III

COORDINATION OF INORGANIC NITROGEN BASES TO HIGH-VALENT OXIDANTS

INTRODUCTION

General Background. Since the discovery of the noble gases many attempts were made to prepare compounds incorporating the elements of Group VIII. The failure to isolate compounds of fluorine with argon by Moissan[1], and fluorine with xenon by Yost and Kaye[2] contributed to the belief in the inertness of these elements. The electronic theories of valence of Lewis[3] and Kossel[4] rationalized their apparent inertness in terms of their valence octet of electrons, to which the majority of the elements tended in their reactivity. It was unexpected by the scientific community when Bartlett and Lohmann isolated the salt, $Xe^{+}PtF_6^{-}$.[5,6] Shortly after the isolation of this salt, the first covalent derivatives of xenon were isolated and characterized, namely XeF_2,[7] XeF_4[8] and XeF_6.[9] There are several synthetic routes to oxides and oxofluorides of xenon. Examples are XeO_3[10] (Xe (VI)), $XeOF_4$[11] and XeO_2F_2[12] (Xe(VI)), and $XeOF_2$ (Xe(IV)).[13] No Xenon(II) oxides have been isolated and characterized. Several excellent reviews detail the early developments in the chemistry of the noble gases.[14,15,16] There is also a comprehensive review on the cation and anion derivatives of the xenon fluoride and oxofluorides.[17]

The bulk of synthetic xenon chemistry to date involves xenon in the 2^{+} oxidation state.

Lewis Acidity of the XeF^{+} Cation. Xenon difluoride behaves as a fluoride ion donor towards many Lewis acids, yielding compounds of the form $XeF_2 \cdot xMF_5$ (x = 1/2, 1, or 2; M = Lewis acid).[17] The compounds cannot be given a purely ionic formulation (i.e., $XeF^{+}M_xF_{5x+1}^{-}$); fluorine bridges between Xe and a fluorine of the "anion" indicate covalent character in the bonding. Single crystal X-ray diffraction of these adducts reveal that the Xe··F bridging bond lengths increase with decreasing lengths of terminal Xe-F bonds, which is interpreted as increased ionic character. For example, in $XeF_2 \cdot RuF_5$, the terminal Xe-F and bridging Xe--F bond lengths

are 1.87(2) and 2.18(2) Å, respectively.[18] The corresponding bond lengths in $XeF_2 \cdot 2SbF_5$ are 1.84 and 2.35 Å.[19,20]

The Raman and infrared spectra of solid adducts of XeF_2 with Lewis acids also corroborate the crystal data. They are best interpreted in terms of ionic formulations $XeF^+MF_6^-$ and $XeF^+M_2F_{11}^-$, but modes associated with Xe···F and M···F bridge stretching and F-Xe···F bending confirm the presence of fluorine bridges.[17]

Fluorine bridging of the cation XeF^+ to a fluorine of the anion indicates that XeF^+ has substantial Lewis acid character.

Synthetic Strategies and Criteria for the Formation of Stable Xe(II)-O and Xe(II)-N Bonds. Considerable effort has been spent in the isolation and characterization of compounds containing xenon(II) covalently bonded to a second row element other than fluorine; most examples contain bonds to oxygen or nitrogen.

There are two general classes of ligands which are suitable for stabilizing the positive oxidation states of the noble gases, those derived from moderate to strong protic acids which, as a result, form stable anions, and neutral oxidatively resistant Lewis base species, which exploit the Lewis acid character of XeF^+.

Suitable "anion-type" ligands must possess properties which render them resistant to oxidation if they are to withstand the high electron affinity of the noble gas in a formal positive oxidation state. The following are criteria for such ligands. A ligand of this class

1. must have a high effective group electronegativity,
2. usually exists as a moderate to strong protic acid,
3. should exist as a stable anion in alkali metal salts,

4. should form a positive chlorine derivative.

For example, in $FXeN(SO_2F)_2$ and $Xe[N(SO_2F)_2]_2$, the precursor acid $HN(SO_2F)_2$, the chlorine derivative $ClN(SO_2F)_2$, and stable alkali metal salts $M^+N(SO_2F)_2^-$ are known.

Neutral Lewis base-type ligands must meet somewhat modified requirements in order to serve as suitable noble-gas ligands. The adducts resulting between neutral Lewis base-type ligands and the XeF^+ cation can be thought of in terms of a partial electron transfer. The wave function Ψ_{AB} for a 1:1 adduct may be represented as in equation (1).

$$\Psi_{AB} = a\Psi(A,B) + b\Psi(A^-B^+) \qquad (1)$$

where $\Psi(A,B)$ is the "no-bond" wave function accounting for all electrostatic interactions between A and B, such as ionic, permanent dipole and induced dipole interactions. No electron transfer has taken place in this state. The term $\Psi(A^-B^+)$ is the wave function of the system after complete electron transfer of one electron from B, the base, to A, the acid. In an adduct, the degree of electron transfer is intermediate between these two states. In order for a base to form a stable adduct with the XeF^+ cation, its first ionisation potential must be of the same order as the electron affinity of XeF^+ (estimated value, 10.90 eV).[48] If it is significantly smaller than electron affinity of the cation, electron transfer is expected to dominate, resulting in oxidative degradation of the base. A first ionization potential for the base that is too high will result in a non-bonding situation.

Compounds Containing Xe(II)-O Bonds. The first examples of Xe(II)-O bonds were isolated using strong oxoacids whose anions were resistant to oxidative degradation. The mono- and bis-fluorosulphate derivatives of xenon (II) were synthesized[21,22] as shown in equations (2) and (3).

$$XeF_2 + HSO_3F \xrightarrow{-75\,^\circ C} FXeOSO_2F + HF \quad (2)$$

$$XeF_2 + 2\,HSO_3F \xrightarrow{-75\,^\circ C} Xe(OSO_2F)_2 + HF \quad (3)$$

Other strong oxo-acids which have yielded covalent derivatives of xenon (II) are HNO_3,[23] $HClO_4$,[21,22] HSO_3CF_3[22] and $HOC(O)CF_3$.[24] Xenon (II) derivatives containing the ligands $-OIOF_4$[25] and $-OPOF_2$[26] are not isolated by reactions of XeF_2 with the parent acids. The mono- and bis- derivatives are formed according tc equations (4) and (5).

$$XeF_2 + x\,P_2O_3F_4 \xrightarrow[-22\,^\circ C]{CFCl_3} x\,P(O)F_3 + F_{2-x}Xe(OPOF_2)_x \quad (4)$$

(x = 1 or 2)

$$XeF_2 + I_2O_4F_6 \xrightarrow[\text{or } CFCl_3]{SO_2ClF} F_{2-x}Xe(OIOF_4)_x + IOF_3 + x/2\,O_2 \quad (5)$$

(x = 1 or 2)

Mono- and bis- xenon (II) derivatives of the ligands $-OSeF_5$[27,28] and $-OTeF_5$[29-36] have been studied extensively. The $-OTeF_5$ group is exceeded only by fluorine and oxygen in its proven ability to stabilise the various oxidation states of xenon. This is attributed to its high effective group electronegativity resulting from the inductive effect of five fluorines on tellurium.[37] This is demonstrated by the existence of moderately stable $-OTeF_5$ analogues of XeF_4,[35] $XeOF_4$[38] and XeF_6.[38] All ligands discussed above can be classified as oxidatively resistant "anion-type" ligands.

Minkwitz[39] has published the only example in the scientific literature of a xenon-oxygen bond resulting from the interaction of a neutral Lewis base-type ligand, $(CF_3)_2S{=}O$ and a noble-gas cation XeF^+ according to equation (6).

$$(CF_3)_2S{=}O + XeF^+SbF_6^- \xrightarrow[12\ h,\ -65\ ^\circ C]{HF} (CF_3)_2S{=}O\text{-}XeF^+SbF_6^- \qquad (6)$$

An excess of the sulfurane is added and the solvent and unreacted sulfurane are pumped off under vacuum at -78 °C, leaving a shock sensitive salt, which degrades even at -78 °C in an FEP vessel.

Compounds Containing Xe(II)-N Bonds. Compounds with xenon-nitrogen bonds exist only for xenon in the 2^+ oxidation state. The first Xe-N bonded species[40] was synthesized and partially characterized in 1974 by LeBlond and DesMarteau, who isolated fluoro[imidobis(sulphurylfluoride)]xenon, $FXeN(SO_2F)_2$. Complete characterization by Schrobilgen followed.[41] Since then the bis- compound $Xe[N(SO_2F)_2]_2$,[42,43] the trifluoromethyl analogue $Xe[N(SO_2CF_3)_2]_2$,[44] and the cations $XeN(SO_2F)_2^+$ [43,45] and $F[XeN(SO_2F)_2]_2^+$ [42,43,45,47] have been characterized. The utility of the $-N(SO_2F)_2$ ligand to form stable bonds to xenon arises from the highly electron withdrawing groups bound to nitrogen making it acidic and the ligand is in general resistant to oxidative fluorination. The acidic character of the ligand intimated a general synthesis involving HF elimination as in the case of the xenon-oxygen bonded derivatives in which the ligand precursors were "anion-type" oxo-acid ligands. As a result $FXeN(SO_2F)_2$ and $Xe[N(SO_2CF_3)_2]_2$ were synthesised according to equation (7).

$$x\ HN(SO_2F)_2 + XeF_2 \xrightarrow[0\ ^\circ C]{CF_2Cl_2} x\ HF + F_{(2-x)}Xe[N(SO_2F)_2]_x \qquad (7)$$

$$(x = 1 \text{ or } 2)$$

A ligand transfer reagent (prepared as in equation (8)) uses the formation of Me_3SiF as the driving force for reaction (9) to isolate $Xe[N(SO_2CF_3)_2]_2$ in high yield.[44]

$$Me_3SiH + (CF_3SO_2)_2NH \xrightarrow{\text{-196 to 22 °C}} (CH_3)_3SiN(SO_2CF_3)_2 + H_2 \quad (8)$$

$$2\ Me_3SiN(SO_2CF_3)_2 + XeF_2 \xrightarrow[CF_2Cl_2]{\text{-22 to 10 °C}} Xe[N(SO_2CF_3)_2]_2 + 2\ Me_3SiF \quad (9)$$

Equation (9) represents the only method, apart from HF displacement, where a metathesis reaction is used to form a xenon-nitrogen bond. The first reported xenon-nitrogen adduct with a Lewis acid reported possessed the stoichiometry $2FXeN(SO_2F)_2 \cdot AsF_5$ and was postulated to have the ionic formulation $F[XeN(SO_2F)_2]_2^+AsF_6^-$ (see equation (10)).

$$FXeN(SO_2F)_2 + AsF_5 \xrightarrow{\text{-78 °C}} XeN(SO_2F)_2^+AsF_6^- \quad (10)$$

Subjecting the salt to dynamic vacuum at room temperature resulted in the isolation of the bridging cation $F[XeN(SO_2F)_2]_2^+$ [43] according to equation (11).

$$2\ XeN(SO_2F)_2^+AsF_6^- \xrightarrow[\text{vacuum}]{\text{23 °C}} F[XeN(SO_2F)_2]_2^+AsF_6^- + AsF_5 \quad (11)$$

The unbridged cation can be isolated by changing the anion[45] with the stronger fluoride ion acceptor SbF_5 as in equation (12).

$$F[XeN(SO_2F)_2]_2^+AsF_6^- + 3\ SbF_5 \xrightarrow[0\ °C]{SbF_5} 2\ XeN(SO_2F)_2^+Sb_3F_{16}^- \quad (12)$$

More recently, compounds containing xenon-nitrogen bonds have been synthesized by combining Lewis base-type ligands with the Lewis acid XeF^+.[46] The electron affinity of XeF^+ has been estimated to be 10.90 eV using thermochemical data.[48] Table 1 provides a list of potentially suitable nitrogen bases and their first ionization potentials.[48]

Table 1. Ionization Potentials of Some Organic and Inorganic Nitrogen Bases (eV)

Compound	1st Ionization Potential
$CF_3C{\equiv}N$	13.90
$N{\equiv}C\text{-}C{\equiv}N$	13.80 ± 0.02
$HC{\equiv}N$	13.80
trans-N_2F_2	13.10 ± 0.1
$CH_2FC{\equiv}N$	13.00 ± 0.1
$CHCl_2C{\equiv}N$	12.90 ± 0.3
$CH_2ClC{\equiv}N$	12.20 ± 0.1
$CF_3N{\equiv}C$	12.60
$N{\equiv}SF_3$	12.50
$ClC{\equiv}N$	12.49 ± 0.04
$CHF_2C{\equiv}N$	12.40
$CD_3C{\equiv}N$	12.235 ± 0.005
$CH_3C{\equiv}N$	12.194 ± 0.005
N_2F_4	12.04 ± 0.1
$BrC{\equiv}N$	11.95 ± 0.08
$C_2H_5C{\equiv}N$	11.85
$N{\equiv}SF$	11.82
n-$C_3H_7C{\equiv}N$	11.67
ND_3	11.52
s-$C_3F_3N_3$	11.50
$(CH_3)_2CHC{\equiv}N$	11.49
ND_2H	11.47 ± 0.02
$N{\equiv}C\text{-}C{\equiv}C\text{-}C{\equiv}N$	11.40 ± 0.2

Compound	1st Ionization Potential
$N\equiv C\text{-}C\equiv C\text{-}C\equiv C\text{-}C\equiv N$	11.40 ± 0.2
$S(C\equiv N)_2$	11.32
$CH_3N\equiv C$	11.32
$CH_3C\equiv C\text{-}H$	11.24
$(CH_3)_3CC\equiv N$	11.11
$IC\equiv N$	10.98 ± 0.05
B-$B_3F_3N_3$	10.79
$H_2NC\equiv N$	10.76
NH_3	10.34 ± 0.07
C_5F_5N	10.085 ± 0.05
s-$C_3H_3N_3$	10.07 ± 0.05
C_6F_5I	10.00
$CF_3\cdot$	9.25

The first example of a nitrogen base to form an adduct with XeF^+ was HC≡N, whose first adiabatic ionization potential has been determined to be 13.80 eV on the basis of photoionization studies.[49] A series of nitriles RC≡N forms adducts $RC{\equiv}N\text{-}XeF^+AsF_6^-$ which have been characterized in solution (R = H, CH_3, CH_2F, C_2H_5, C_2F_5, C_3F_7 and C_6F_5) and in the solid state (R = H, Me).[50,51] A detailed study which expands the ligand series has been carried out.[48] The general synthesis for these adducts involves the reaction of $XeF^+AsF_6^-$ or $Xe_2F_3^+AsF_6^-$ with the appropriate nitrile as shown in equations (13) and (14).

$$XeF^+AsF_6^- + RC{\equiv}N: \xrightarrow[-20 \text{ to } -10\ ^\circ C]{HF} RC{\equiv}N\text{-}XeF^+AsF_6^- \qquad (13)$$

$$Xe_2F_3^+AsF_6^- + RC{\equiv}N: \xrightarrow[-20 \text{ to } -10\ ^\circ C]{HF} RC{\equiv}N\text{-}XeF^+AsF_6^- + XeF_2 \qquad (14)$$

For R = H, the reaction was also carried out in SO_2ClF. These are the first examples of xenon bonded to an sp hybridized nitrogen.

The fluoro(perfluoropyridine)xenon(II) cations, $4\text{-}RC_5F_4N\text{-}XeF^+$ (R = F or CF_3)[52] have been formed in HF solvent according to equation (15) and equilibria (16) and (17) at -30 to -20 °C.

$$4\text{-}RC_5F_4N \xrightarrow{HF} 4\text{-}RC_5F_4NH^+(HF)_n^- \qquad (15)$$

$$4\text{-}RC_5F_4NH^+(HF)_n^- + XeF^+AsF_6^- \rightleftharpoons RC_5F_4NH^+AsF_6^- + XeF_2 + n\ HF \qquad (16)$$

$$4\text{-}RC_5F_4NH^+AsF_6^- + XeF_2 \rightleftharpoons 4\text{-}RC_5F_4N\text{-}XeF^+AsF_6^- + HF \qquad (17)$$

An alternative synthesis is the reaction of $4\text{-}RC_5F_4NH^+AsF_6^-$ with XeF_2 in BrF_5 and HF solvents at -30 °C as in equation (17). As expected the equilibrium favors a larger proportion of the

xenon(II) cation in BrF_5 solvent, enabling the salts to be isolated by pumping the BrF_5 solvent off at -30 °C. The first adiabatic ionization potential of C_5F_5N (10.08 ± 0.05 eV)[53] is approximately the same as that of the electron affinity of XeF^+, in accordance with the criterion for a stable adduct. The first ionization potential (11.50 eV)[53] of *s*-trifluorotriazine, *s*-$C_3F_3N_3$ and the existence of C_5F_5N-$XeF^+AsF_6^-$ suggested that the adduct *s*-$C_3F_3N_2N$-XeF^+ should also exist. This compound has been has made according to equation (18) by the reaction of $XeF^+AsF_6^-$ with excess *s*-trifluorotriazine at room temperature for three hours followed by removal of excess *s*-$C_3F_3N_3$ *in vacuo*.[52]

$$XeF^+AsF_6^- + s\text{-}C_3F_3N_3 \longrightarrow s\text{-}C_3F_3N_2N\text{-}XeF^+AsF_6^- \qquad (18)$$

The resulting white powder is stable indefinitely at room temperature.

The ligand $F_3S{\equiv}N$ (1st IP, 12.50 eV)[54] was also allowed to react with $XeF^+AsF_6^-$ in BrF_5 solvent at -60 °C giving the adduct $F_3S{\equiv}N$-XeF^+,[55] which is characterized by ^{19}F and ^{129}Xe NMR spectroscopy at -60 °C (see equation (19)).

$$F_3S{\equiv}N + XeF^+AsF_6^- \xrightarrow[-60\ ^\circ C]{BrF_5} F_3S{\equiv}N\text{-}XeF^+AsF_6^- \qquad (19)$$

Anhydrous HF solvent was distilled onto the salt isolated by the reaction of $F_3S{\equiv}N$ and $XeF^+AsF_6^-$ in BrF_5 at -60 °C and subsequent pumping under vacuum at -15 °C to remove the BrF_5 solvent. Solvolysis of the sample occurs at -20 °C, resulting in HF addition as in equations (20) and (21) as monitored by ^{19}F and ^{129}Xe NMR spectroscopy.

$$F_3S{\equiv}N\text{-}XeF^+ + HF \longrightarrow [F_4S{=}N(H)\text{-}Xe\text{-}F^+] \xrightarrow{-\ HF} F_4S{=}N\text{-}Xe^+ \qquad (20)$$

$$F_4S{=}N\text{-}Xe^+ + HF \longrightarrow F_5S\text{-}N(H)\text{-}Xe^+ \qquad (21)$$

The expected intermediate cation $F_4S{=}N(H)\text{-}Xe\text{-}F^+$ resulting from HF addition to $F_3S{\equiv}N\text{-}XeF^+$ is not observed by ^{19}F and ^{129}Xe NMR spectroscopy. This cation is assumed to eliminate HF to give $F_4S{=}N\text{-}Xe^+$. This is extraordinary considering that HF is in excess as the solvent. In the final cation the xenon-nitrogen bond can no longer be considered as dative. Further HF addition results in the cation $F_5S\text{-}N(H)\text{-}Xe^+$, which is the first example of an sp^3 hybridized nitrogen bonded to xenon.

EXPERIMENTAL

Vacuum Line Apparatus

The air- and moisture-sensitive nature of the precursors and products required that all manipulations be performed under strictly anhydrous conditions. Air-sensitive samples of low volatility were transferred in a dry nitrogen-filled glove bag or dry box. The dry box (Vacuum Atmospheres Model DLX) was equipped with a cryogenic well in order to manipulate materials which were thermally unstable under anhydrous conditions. Volatile materials were transferred using metal or glass vacuum lines. The metal line used was constructed from 316 stainless steel, nickel, Teflon, FEP and Kel-F. Pressures were monitored at ambient temperature using pressure transducers having inert, wetted surfaces of Inconel in conjunction with an MKS Model PDR-5B power supply and digital readout. The dynamic ranges of the pressure transducers were 0 to 1000 Torr and 0 to 1 Torr. The pressures were accurate to ± 0.5 % of scale. The glass vacuum system was equipped with grease-free Teflon stopcocks (J. Young) and pressures were monitored using a mercury manometer. Details of the apparatus are decribed elsewhere.[48]

Preparation and/or Purification of Starting Materials

Solvents. Bromine pentafluoride (Ozark Mahoning Co.) was distilled into a ¾-in. Kel-F tube fitted with a Kel-F valve containing anhydrous KF and purified by maintaining F_2 gas (ca. 2 atm) above the liquid for 5 - 7 days or until all the BrF_3 and Br_2 had reacted, giving a colorless liquid (see ref. 48). When required, BrF_5 was vacuum distilled into the appropriate vessel through a Kel-F Y-piece.

Hydrogen fluoride (Harshaw Chemical Co.) was purified by treatment with 5 atm. F_2 gas

in a nickel can for a period of one month converting any water present to HF and O_2 gas. The HF was subsequently distilled into a dry Kel-F storage vessel equipped with a Kel-F valve for storage at room temperature. When required, HF was vacuum distilled into the appropriate vessel through a Kel-F Y-piece.[48]

Chloroform, $CHCl_3$ containing 0.75 % ethanol as stabilizer (Caledon Laboratories, Ltd.) was dried over molecular sieves (3 Å). The sieves were poured into a cylindrical glass vessel with a Teflon stopcock (J. Young). The sieves were heated (220 °C) under dynamic vacuum for 24 h to activate. In a glove bag, the $CHCl_3$ was poured into the vessel and the solvent was degassed on a glass vacuum line. The solvent was allowed to sit over the molecular sieves for 2 days prior to use.

Freon-114 (1,2-dichlorotetrafluoroethane, Aldrich) was condensed from its lecture bottle to a glass bulb (ca. 120 mL volume) containing P_2O_5 and allowed to sit for several days. This was followed by distillation into another glass bulb for storage prior to use. All transfers of the solvent were then performed by vacuum distillation from this bulb.

Reagents. A high temperature, high pressure method was used for the synthesis of XeF_2, similar to that used by Malm and Chernick[56] for the preparaton of XeF_4. In a typical experiment, xenon (440 mmol) and fluorine (170 mmol) were condensed into a 834 mL nickel can (1/4-in. walls) at -196 °C. The can was placed into an electric furnace (preheated to 410 °C) and heated for 9 hours. The can was then quenched in cold water. The can was then cooled to -196 °C and any unreacted fluorine was pumped off. Unreacted xenon was condensed into another nickel storage can after warming the reaction can to -78 °C. The XeF_2 was collected by pumping the contents of the reaction can, warmed to 50 °C, through a 3/4-in. o.d. FEP U-tube cooled to -78

°C. The recovered sample was checked for the obvious impurity, XeF_4, by recording the Raman spectrum in the range 450 - 600cm^{-1}. Xenon difluoride has a strong line at 496 cm^{-1} whereas XeF_2 has two strong bands at 502 and 543 cm^{-1}. No XeF_4 could be detected in the Raman spectrum, indicating << 0.5% XeF_4 impurity. The product was stored under nitrogen in a 3/4-in. Kel-F vessel at room temperature in a dry box. All XeF_2 transfers were made as a solid in the dry box.

The adduct $XeF^+AsF_6^-$ was prepared according to equation (22) in anhydrous HF solvent. Full details of the synthesis are described in reference (48).

$$XeF_2 + AsF_5 \xrightarrow[RT]{HF} XeF^+AsF_6^- \qquad (22)$$

Arsenic trifluoride (AsF_3) was prepared according to the method of Hoffman[57] as shown in equation (23).

$$As_2O_3 + 3\ CaF_2 + 3\ H_2SO_4 \longrightarrow 2\ AsF_3 + 3\ CaSO_4 + 3\ H_2O \qquad (23)$$

The product was purified by distillation in an all-glass system using a column of glass helices, followed by storage over dry sodium fluoride. Arsenic (III) fluoride was then reacted with an excess of fluorine gas, giving arsenic pentafluoride. Details of the reaction conditions and purification are reported elsewhere.[47]

Tellurium hexafluoride was prepared according to equation (24) by reaction of tellurium powder and fluorine gas in a Monel can.[55]

$$Te + 3\ F_2 \longrightarrow TeF_6 \qquad (24)$$

Tellurium hexafluoride was also prepared by the reaction of TeF_4 and F_2[55] (Equation (25)).

$$TeF_4 + F_2 \longrightarrow TeF_6 \qquad (25)$$

Chlorotrimethylsilane (Aldrich Chemical Company, Inc.) was transferred in a glove bag into a glass cylindrical vessel with Teflon stopcock (J. Young) and distilled *in vacuo* via a glass Y-piece to an identical glass vessel. The reagent was used without further purification and all subsequent transfers were performed by vacuum distillation.

Preparation of $CF_3C(OH)NH_2^+AsF_6^-$. The compound 2,2,2-trifluoroacetamide (Aldrich) was recrystallised from dry $CHCl_3$. In a typical experiment, 1.2860 g (11.380 mmol) of solid 2,2,2-trifluoroacetamide was loaded into a 100 mL bulb attached to a glass H-vessel (Figure (1)) in the dry box. Dry $CHCl_3$ was vacuum distilled onto the 2,2,2-trifluoroacetamide by cooling the bulb (A) to -196 °C. Dissolution occurred with stirring at 50 °C to give a clear colorless solution. The solution was filtered warm through the medium porosity glass frit (B) into the adjacent bulb (C) and then cooled to 23 °C. Solvent was statically distilled off slowly by cooling the empty bulb to 18 °C overnight, yielding white rod-like crystals. After pumping the crystals under hard vacuum for 12 hours at room temperature to completely remove the solvent, the yield was 48.6 %. This process reduced the crystals to a powder.

Protonation of 2,2,2-trifluoroacetamide with AsF_5 / HF. In the dry box, purified 2,2,2-trifluoroacetamide (1.2708 g, 11.242 mmol) was loaded into a ½-in. o.d. FEP tube with a stainless steel valve assembly (Whitey) with ¼-in. connector tube attached (Figure (2)). Dry HF (4 mL) was vacuum distilled into the vessel (-196 °C). A pale orange color formed at the interface of the 2,2,2-trifluoroacetamide and the HF. Warming to -78 °C resulted in a yellow solution. Using the metal vacuum line, AsF_5 (2.5086 g, 14.76 mmol) was added to an evacuated, preweighed,

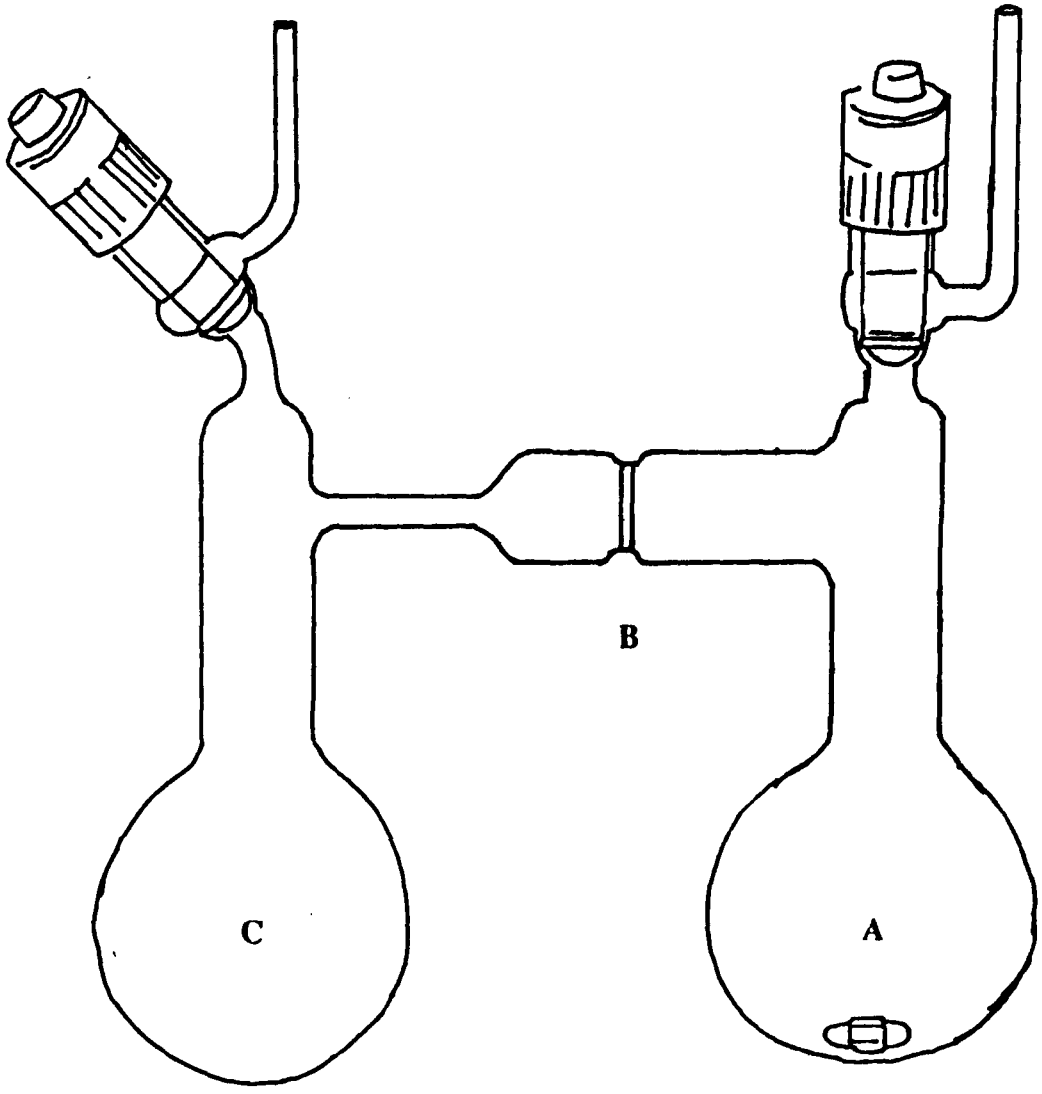

Figure 1. Glass H-vessel; (A) and (C), 10[illegible]mL bulbs, (B), medium porosity sintered-glass frit.

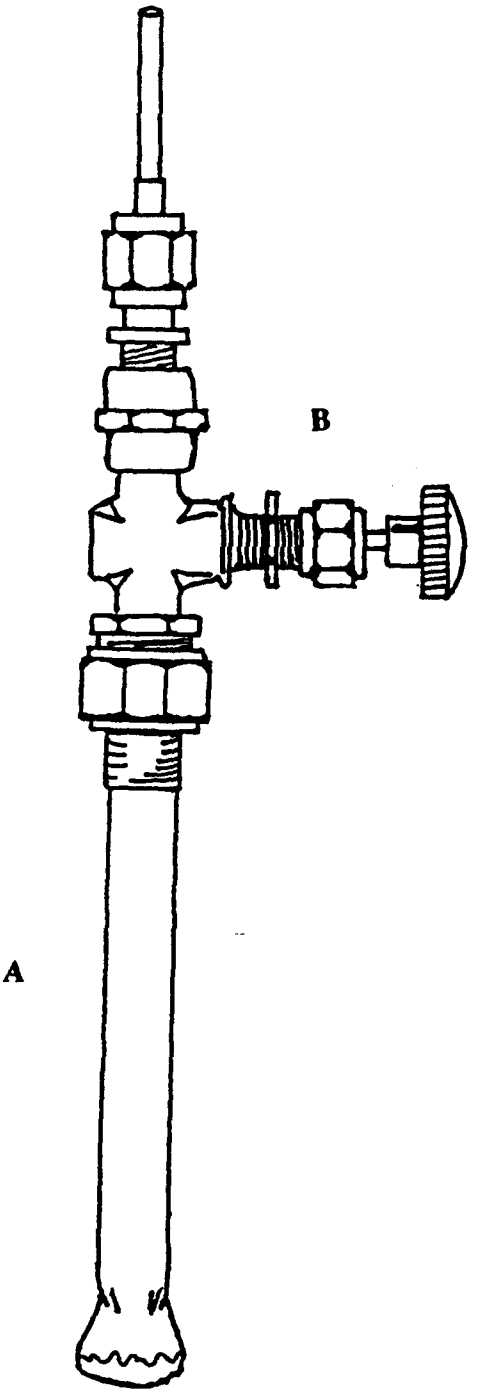

Figure 2. Stainless steel valve and FEP tube assembly; (A), ½-in. FEP tubing heat-sealed at one end, (B), Whitey ORM-2 stainless steel valve assembly.

calibrated glass bulb at room temperature from the nickel storage can. After weighing, the AsF_5 was condensed into the FEP tube at -196 °C. Warming with agitation to -78 °C resulted in a dark orange precipitate on the bottom of a yellow solution which dissolved upon warming to -50 °C to give a colorless solution. A white solid appearing to be free of HF and exhibiting no vapor pressure above the sample resulted after pumping with rough vacuum for 0.5 hours (3.382 g, 99.3 %). The salt decomposed over several months at room temperature thus storage at -78 °C under 1.5 atm. of dry nitrogen gas was necessary.

Preparation of Natural Abundance and 99% ^{15}N Enriched F_5TeNH_2. Aminotellurium pentafluoride was prepared using a modified version of the previously reported synthesis (equations (26) to (28)).[58]

$$\text{xs } NH_3 + (CH_3)_3SiCl \xrightarrow[\text{reflux, 6 hrs.}]{(CH_3CH_2)_2O} ((CH_3)_3Si)_2NH + NH_4Cl\ (s) \qquad (26)$$

$$((CH_3)_3Si)_2NH + TeF_6 \xrightarrow{\text{1 week, RT}} (CH_3)_3SiNHTeF_5 + (CH3)_3SiF \qquad (27)$$

$$(CH_3)_3SiNHTeF_5 + HF \xrightarrow{\text{RT}} TeF_5NH_2 + (CH_3)_3SiF \qquad (28)$$

This preparation was modified for several reasons: 1) The material must be rigorously anhydrous as it is moisture-sensitive and to exclude side-reactions with moisture-sensitive solvents and reagents, such as BrF_5 and XeF_2, respectively, and 2) the multinuclear magnetic resonance studies of this ligand (see **Results and Discussion**) required the preparation of the ^{15}N enriched compound. In the original preparation of $((CH_3)_3Si)_2NH$ by Sauer[59] (equation (26)), an excess of

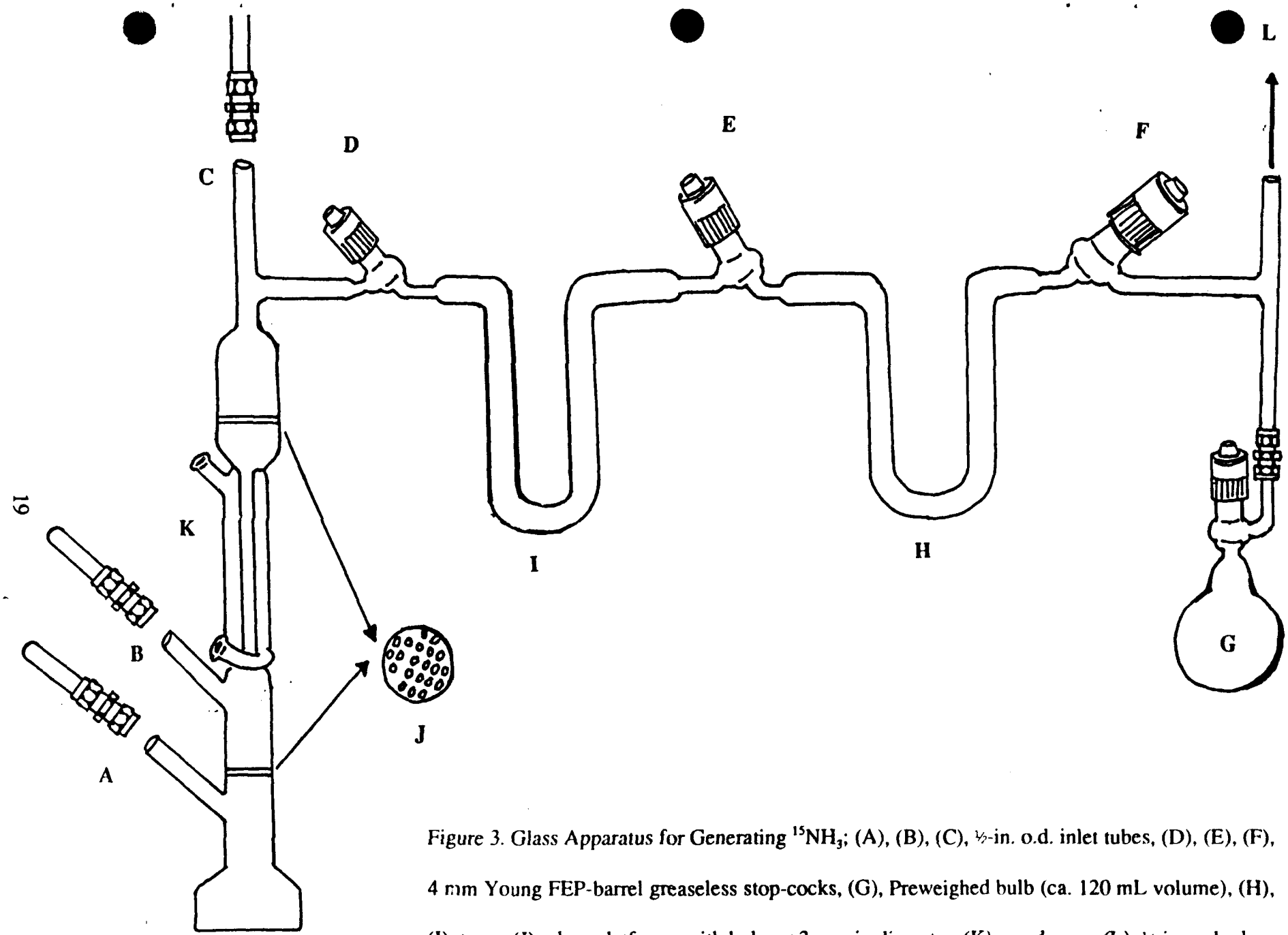

Figure 3. Glass Apparatus for Generating $^{15}NH_3$; (A), (B), (C), ½-in. o.d. inlet tubes, (D), (E), (F), 4 mm Young FEP-barrel greaseless stop-cocks, (G), Preweighed bulb (ca. 120 mL volume), (H), (I), traps, (J), glass platforms with holes < 3 mm in diameter, (K), condenser, (L), ¼-in. o.d. glass tube for attachment to glass vacuum line with Swagelok ¼-in. Teflon union.

NH_3 gas was bubbled through a refluxing $(CH_3)_2SiCl$ solution in diethyl ether. This step was modified to utilise all the ^{15}N enriched compound by carrying out the reaction in a closed system (*vide infra*).

Preparation of 99% ^{15}N Enriched NH_3. The synthesis of anhydrous NH_3 was carried out according to equation (29).[29]

$$NH_4Cl + xs\ KOH \xrightarrow{H_2O} KCl + NH_3\ (g) \qquad (29)$$

In a typical reaction, the glass apparatus depicted in Figure (3) was attached to a glass vacuum line at (L) and dried by pumping dynamically overnight. With a positive pressure of dry nitrogen gas to prevent contamination, the ½-in. Teflon Swagelok connectors were opened at (A), (B) and (C). The chambers at (B) and (C) were filled with KOH pellets (BDH); 13.47 g and 24.39 g, respectively. Distilled water (10 mL) and 1.20829 g (22.1810 mmol) of 99 % ^{15}N enriched NH_4Cl (MSD isotopes) were added through the inlet tube (A). With the Swagelok unions reattached, the aqueous solution was cooled to -78 °C and pumped dynamically while the glass tubes at (A), (B) and (C) were flame sealed. The pressure in the vessel was increased to 450 Torr with dry N_2 gas. The aqueous solution was warmed until reflux began, with trap (I) at -196 °C and stopcock (E) closed. After sufficient heating, the reflux sustained itself and the KOH pellets began to dissolve into the refluxing solution. The dry ammonia was collected as a white solid in trap (I). This was continued until the KOH at (C), which acts as a drying agent, began to show surface wetting. Stopcock (D) was then closed and trap (I), still at -196 °C, evacuated. With stopcock (E) open and (F) closed, the contents of trap (I) (-78 °C) was sublimed into trap (H) (-196 °C) under static vacuum. The dry preweighed bulb (G) was cooled to -196 °C and the contents of trap (H) were condensed into the bulb by warming the trap slowly to ambient temperature. A total of 0.39489

g of 99 % enriched ^{15}N ammonia was recovered (yield, 98.83 %).

Preparation of 99% ^{15}N Enriched $[(CH_3)_3Si]_2NH$. As noted previously, a modification of Sauer's preparation[59] was used to conserve $^{15}NH_3$. A stoichiometric reaction was carried out as in equation (30). Since natural abundance $((CH_3)_3Si)_2NH$ is available commercially (Aldrich), this procedure was only of interest for making the ^{15}N enriched compound. However, all syntheses were first optimized using natural abundance samples.

$$3\ {}^{15}NH_3 + 2\ (CH_3)_3SiCl \xrightarrow[7\ days,\ RT]{Freon\text{-}114} ((CH_3)_3Si)_2{}^{15}NH + 2\ {}^{15}NH_4{}^{+}Cl^{-}\ (s) \qquad (30)$$

A stoichiometric amount of $(CH_3)_3SiCl$ (1.61444 g, 14.86 mmol) was vacuum distilled from its storage container into a preweighed graduated vessel outfitted with a Teflon stopcock (J. Young) through a glass Y-piece. The weighed amount of $(CH_3)_3SiCl$ was then condensed into side (A) of an H-vessel at -196 °C (Figure (4)). Freon-114 (16.2861 g) was distilled onto the $(CH_3)_3SiCl$ and warmed to room temperature to give a clear colorless solution. The solution was cooled to -196 °C and 0.39489 g of $^{15}NH_3$ was sublimed into the vessel and the contents were slowly warmed, whereupon a white precipitate formed as the solvent began to liquify (m.p. Freon-114, -94 °C). After stirring for 7 days at room temperature, side (C) was cooled to -40 °C and the contents of side (A) were filtered through the medium porosity sintered glass frit (B), giving a white precipitate of $^{15}NH_4{}^{+}Cl^{-}$ (side (A)) and a clear solution (side (C)). The precipitate was washed three times by repeatedly back-distilling solvent to side (A) (-60 °C) from side (C) (-40 °C) and repeating the filtration as above. The bulk of the solvent was then condensed back into side (A). The middle stopcock was closed and the $((CH_3)_3Si)_2{}^{15}NH$ was purified by fractionation

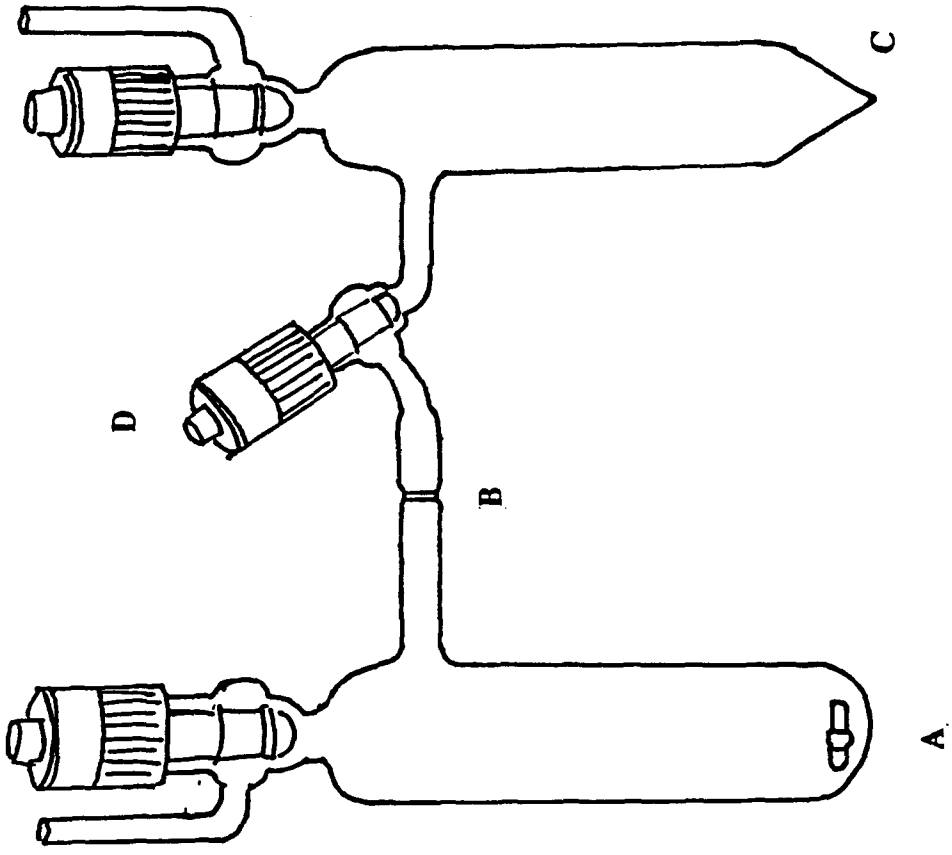

Figure 4. Glass H-vessel for Preparation of $((CH_3)_3Si)_2{}^{15}NH$; (A), (C), (D), see text, (B), medium porosity sintered-glass frit.

through two glass traps, the first at -40 °C to trap $((CH_3)_3Si)_2{}^{15}NH$ and the second at -196 °C to trap unreacted $(CH_3)_3SiCl$ and Freon-114. Pure $((CH_3)_3)_2Si{}^{15}NH$ (1.03452 g, 6.3710 mmol; yield, 87.2%) was collected in the -40 °C trap, as shown by ^1H NMR ($\delta(^1H)$ = -0.61 ppm (CH_3), $^2J(^{29}Si\text{-}^1H)$ = 6.6 Hz, $^3J(^{15}N\text{-}^1H)$ = 1.0 Hz, $^4J(^1H\text{-}^1H)$ = 0.2 Hz; $\delta(^1H)$ = 0.52 ppm (N-H), $^1J(^1H\text{-}^{15}N)$ = 53.1 Hz). The ^{19}F NMR spectrum did not contain a resonance due to residual Freon-114.

Preparation of 99% ^{15}N Enriched F_5TeNH_2. The $((CH_3)_3Si)_2{}^{15}NH$ was condensed at -196 °C into a 40 mL 304 stainless steel Whitey cylinder equipped with a 314 stainless steel Whitey ORM 2 valve via a glass Y-piece. It was necessary, whenever cooling the steel cylinder, to have a constant flow of air aimed directly at the portion where the valve threads into the cylinder to prevent leakage. On the metal line, TeF_6 (10.12 mmol) was condensed into the metal cylinder (at -196 °C), which was then warmed to room temperature and agitated on a mechanical shaker for 1 week. After cooling to -45 °C, excess TeF_6 and $(CH_3)_3SiF$ were pumped off under rough vacuum into a soda lime trap. The mixture was periodically warmed to 35 °C under static vacuum to free any occluded volatiles and upon cooling to -45 °C pumping was resumed. These steps were repeated until no vapor pressure could be detected in the cylinder at -45°C (at this temperature, the vapor pressure of TeF_6 is 511 Torr[61] and that of $(CH_3)_3SiF$ is 37 Torr[62]). The enriched compound $TeF_5{}^{15}NHSi(CH_3)_3$ was not isolated; rather, hydrogen fluoride (0.25748 g, 12.87 mmol) was condensed onto the $TeF_5{}^{15}NHSi(CH_3)_3$ (-196 °C), and then warmed to room temperature. The cylinder and contents were agitated for one day manually every 4 hours. Excess HF (v.p., 59 Torr[63]) and $(CH_3)_3SiF$ (v.p., 50 Torr[62]) were pumped at -40 °C into a soda lime trap with intermittent warming under static vacuum as above until no volatiles were detected at -40 °C. The product was sublimed from the cylinder at 40 °C into a ¼-in. FEP tube equipped with

a Kel-F valve and connector (-196 °C). The product was a white powder (0.74705 g; yield, 48.9 % based on moles of $((CH_3)_3Si)_2{}^{15}NH$), which vitrifies upon standing at room temperature in an inert atmosphere.

The stainless steel cylinder used to prepare F_5TeNH_2 was used in the preparation of $TeF_5NHSi(CH_3)_3$. The procedure suggested by Seppelt[64] for cleaning the cylinder between successive runs was modified. The vessel was rinsed with aqueous NaOH to remove any nonmetal oxides, followed by concentrated sulfuric acid, then distilled water and acetone prior to drying under dynaminc vacuum. Bis(trimethylsilyl)amine (Aldrich) was purified by vacuum distillation and 1.79946 g (11.149 mmol) of the purified compound was condensed into the 40 mL stainless steel cylinder at -196 °c followed by TeF_6 (14.428 mmol). The vessel was shaken mechanically at room temperature for 1 week. The volatiles were removed at -45 °C and the contents were purified by trap to trap distillation using a glass dual trap apparatus (-30 °C and -196 °C). The -30°C trap contained pure $TeF_5NHSi(CH_3)_3$ as determined by ^{19}F NMR in a sealed 5 mm glass tube ($CFCl_3$ solvent) at room temperature ($\delta(^{19}F_{ax})$ = -33.2 ppm, $\delta(^{19}F_{eq})$ = -37.5 ppm, $^2J(^{19}F_{ax}\text{-}^{19}F_{eq})$ = 174 Hz, $^1J(^{19}F_{eq}\text{-}^{125}Te)$ = 3464 Hz, $^1J(^{19}F_{ax}\text{-}^{125}Te)$ = 3250 Hz, $^1J(^{19}F_{eq}\text{-}^{123}Te)$ = 2873 Hz).

Preparation of $TeF_5NH_3{}^+AsF_6{}^-$. The hexafluoroarsenate salt of the conjugate acid of F_5TeNH_2 was prepared by the reaction of excess AsF_5 with a solution of F_5TeNH_2 or $F_5Te^{15}NH_2$ in anhydrous HF at -78 °C. Preparations with the ^{15}N enriched material were performed on an NMR scale in 4 mm or 9 mm o.d. FEP NMR sample tubes. In a typical reaction, 1.1873 g (4.9758 mmol) of F_5TeNH_2 was placed in a ½-in. FEP tube equipped with a stainless steel valve. Hydrogen fluoride (4 mL) was distilled into the vessel at -196 °C followed by warming to -78

°C to give a colorless solution. Arsenic pentafluoride (6.102 mmol) was then condensed onto the solution at -196 °C. A white solid resulted upon warming to -78 °C, dissolving to give a clear solution at -55 °C. The sample was pumped at -78 and at -40 °C through a soda lime trap until the resulting white solid gave no vapor pressure at -40 °C.

Crystal Growth for X-ray Crystal Structure Determination of $F_5TeNH_3^+AsF_6^-$. Approximately 0.08 g of $F_5TeNH_3^+AsF_6^-$ was transferred to a 30 cm long, ¼-in. o.d. FEP tube equipped with a Kel-F valve in the dry box. Aproximately 1 mL of anhydrous HF was distilled into the tube at -196 °C. A colorless solution resulted upon warming to -60 °C in a dewar containing acetone with sufficient dry ice added to give the desired temperature. The temperature was decreased slowly by adding pieces of dry ice, reaching -68 °C over a period of 2 hours. A bath was made of acetone cooled with approximately 2.5 inches of solid dry ice on the bottom in a dewar. The FEP tube was placed in this dewar with the end just above the layer of dry ice on the bottom and left overnight. With the FEP tube at -78 °C, the HF was pumped into a soda lime trap. The colorless rod-like needles were removed in the dry box by cutting the FEP tube at room temperature and picking the crystals off the walls of the FEP tube with an iridium stylus. The crystals were placed in 0.2, 0.3, and 0.4 mm Lindemann glass capillaries, sealed, and stored at -10 °C prior to mounting on the diffractometer. Many of the crystals were twinned, but a single crystal was found and used for the collection of this data set. This crystal had dimensions 0.3 x 0.35 x 0.1 mm.

Purification of Hydrogen Cyanide, HC≡N. Hydrogen cyanide was prepared according to the method of King and Nixon[65] as shown in equation (31) by the dropwise addition addition of H_2O to a mixture of KCN (Merck) and P_4O_{10} (British Drug House).

$$3\ KCN + 3\ H_2O + P_2O_5 \longrightarrow 3\ K_3PO_4 + 3\ HC{\equiv}N \qquad (31)$$

Details of the apparatus used are given in reference (48). Dry HC≡N was stored in a 25 mL glass storage vessel with a Teflon stopcock (J. Young). The compound was transferred by vacuum distillation from this vessel as needed.

Preparation of NMR Samples

Preparation of $F_5TeN(H)$-$Xe^+AsF_6^-$ in HF Solvent for NMR Spectroscopy. In a typical preparation, $F_5Te^{15}NH_2$ (0.04885 g, 0.2039 mmol) was sublimed into a 4 mm o.d. FEP tube and Kel-F valve assembly. This was done by warming the $F_5Te^{15}NH_2$ to ca. 55 °C and cooling the FEP tube to -196 °C and subliming the white solid through a glass Y-piece under static vacuum. The FEP tube was cooled to -196 °C in a dry box and $XeF^+AsF_6^-$ (0.06910 g, 0.2037 mmol) was added. The sample was then warmed to -78 °C and transferred to a metal vacuum line. Hydrogen fluoride (0.4 mL) was distilled into the tube at -196 °C. An intense yellow solution was observed as the reaction proceeded at -32 °C. The tube was then frozen at -196 °C and heat sealed under vacuum. The same synthesis was carried out in a 9 mm FEP tube using 0.15425 g (0.64379 mmol) of $F_5Te^{15}NH_2$ and 0.2278 g (0.6716 mmol) of $XeF^+AsF_6^-$ with 2.1 mL of HF solvent. Similar syntheses were also carried out using natural abundance F_5TeNH_2.

Preparation of HC≡N-Xe-$N(H)TeF_5^+$ in HF Solvent for NMR Spectroscopy. In a typical preparation, F_5TeNH_2 (0.03993 g, 0.1573 mmol) and $XeF^+AsF_6^-$ (0.05360 g, 0.1580 mmol) were combined at -196 °C in a 4 mm FEP tube and Kel-F valve assembly in the cold well of the dry box. The tube was warmed to -78 °C and attached to a metal vacuum line. Hydrogen fluoride (0.4 mL) was distilled into the tube at -196 °C. Warming to -25 °C resulted in a colorless solution.

After 20 to 30 minutes at this temperature, the solution turned intense yellow. Hydrogen cyanide (0.00713 g, 0.264 mmol) was condensed into the tube at -196 °C through a glass Y-piece. The sample was heat-sealed under vacuum at -196 °C. Liquification of the solvent at -78 °C resulted in the disappearance of the yellow color with the formation of a white precipitate. The solution was colorless above the precipitate.

Preparation of $F_5TeN(H)$-$Xe^+AsF_6^-$ in BrF_5 Solvent for NMR Spectroscopy. A typical sample was prepared by combining XeF_2 (0.03562 g, 0.2104 mmol) and $F_5Te^{15}NH_3^+AsF_6^-$ (0.07221 g, 0.1681 mmol) in a 4 mm FEP tube and Kel-F valve assembly at -196 °C in a dry box. The tube was transferred at -78 °C to a metal vacuum line. Bromine pentafluoride (0.4 mL) was then distilled into the tube at -196 °C. A mauve solid resulted. The sample was heat sealed at -196 °C. Warming to -55 °C resulted in dissolution of the XeF_2 and simultaneous disappearance of the mauve color. The solution slowly turned from colorless to pale yellow at this temperature. A similar sample was prepared in a 9mm FEP tube using 0.1005 g (0.5936 mmol) of XeF_2, 0.24532 g (0.5711 mmol) of $F_5Te^{15}NH_3^+AsF_6^-$ and 2.1 mL of BrF_5 solvent. Similar syntheses were carried out using natural abundance $F_5TeNH_3^+AsF_6^-$.

Attempted Preparation of $F_5TeN(H)$-Xe··F··Xe-$F^+AsF_6^-$ in BrF_5 Solvent for NMR Spectroscopy. A sample of natural abundance $F_5TeNH_3^+AsF_6^-$ (0.02471 g, 0.05760 mmol) and XeF_2 (0.01966 g, 0.1161 mmol) was prepared (1:2 molar ratio) in an attempt to generate the fluorine bridged species $F_5TeN(H)$-Xe··F··Xe-F^+. Sample preparation was similar to that used to generate $F_5TeN(H)$-$Xe^+AsF_6^-$ in BrF_5 solvent.

Preparation of $CF_3C(O\text{-}XeF)NH_2^+AsF_6^-$ in BrF_5 Solvent for NMR Spectroscopy. In a dry box, $CF_3C(OH)NH_2^+AsF_6^-$ (0.01668 g, 0.05504 mmol) was transferred to a 4 mm FEP tube

and Kel-F valve assembly. The tube was cooled to -196 °C in the cold well of the dry box and XeF_2 (0.00985 g, 0.05818 mmol) was then added. The tube was transferred out of the dry box and warmed to -78 °C and attached to a metal vacuum line where BrF_5 (0.4 mL) was distilled into the tube at -196 °C. The tube was then heat sealed under vacuum at this temperature. A colorless solution resulted on warming to -58 °C. A 9 mm sample was prepared using 0.13406 g (0.44250 mmol) of $CF_3C(OH)NH_2^+AsF_6^-$ and 0.0840 g (0.496 mmol) of XeF_2 in 2.1 mL of BrF_5 solvent.

NMR Instrumentation

Nuclear magnetic resonance samples were prepared in 4 mm or 9 mm o.d. FEP tubes, heat-sealed at one end and flared (SAE 45°) at the other. The tubes were equipped with Kel-F valves.[48] After reagents and solvents were transferred into the FEP sample tubes, they were heat-sealed off under vacuum at -196 °C and stored at this temperature until NMR spectra could be run. The 9 mm and 4 mm tubes were placed into standard 10 mm and 5 mm Wilmad medium-wall glass NMR tubes, respectively. Multinuclear magnetic resonance spectra were recorded using a Bruker AM-500 500 MHz spectrometer equipped with a 11.745 T cryomagnet. Fluorine-19 and ^1H spectra were recorded using a 5 mm $^1H/^{19}F$ probe. Carbon-13 spectra were recorded using a 5 mm $^1H/^{13}C$ probe. The spectra of other nuclei (^{15}N, ^{129}Xe and ^{125}Te) were recorded using a 10 mm VSP probe broad-banded over the range 50.698 to 139.051 MHz. The acquisition parameters for the NMR spectra are given in Table 2. Samples were referenced externally at 24 °C with respect to the neat liquid references given in the table. A positive chemical shift denotes a resonance occurring to high frequency of the reference compound.

Table 2. Acquisition Parameters for NMR Spectra.

Acquisition Parameter	^{129}Xe	^{15}N	^{125}Te	^{1}H	^{19}F	^{13}C
Reference Standard (23 °C, neat)	$XeOF_4$	CH_3NO_2	$Te(Me)_2$	TMS	$CFCl_3$	TMS
Resonance Frequency (MHz)	139.051	50.698	157.795	500.000	470.599	125.760
Data Point Resolution (Hz/pt)	3.052 - 6.104	0.763 - 3.052	1.526	0.610	0.488 - 1.526	3.052
Spectral Width (KHz)	50 - 100	25	25 - 50	10	2 - 50	50
Memory Size (Kb)	16 - 64	16 - 32	32 - 64	32 64	16 -	32
Pulse Width (μs)	18.00	15.00	10.00	5.0	1.0	2.50
Line Broadening (Hz)	10 - 20	0 - 10	3 - 10	0 - -2.5	0 - 6	4
Number of Scans	1500 - 21000	100 - 600	7000 - 15500	200 - 1500	500 - 5000	11000
Receiver Delay (s)	0	10 - 120	0	0	0	0.5

RESULTS AND DISCUSSION

Part 1: The Ligand Properties of Aminotellurium Pentafluoride Towards Xenon(II) Fluorides

Introduction. In this work, a study involving the preparation of the tellurium analog to the cation $F_5S\text{-}N(H)\text{-}Xe^+$, namely $F_5Te\text{-}N(H)\text{-}Xe^+$, has been carried out to expand the known chemistry of xenon-nitrogen bonds, particularly xenon(II) bonded to a sp^3 hybridized nitrogen. The route to the cation does not involve solvolysis as in the sulfur system because the tellurium analog of the ligand, namely $F_3Te{\equiv}N$, does not exist. However, aminotellurium pentafluoride has been synthesized.[58,64] The compound F_5TeNH_2 exhibits acidic character, consistent with the existence of the room temperature stable salt, $Cs^+TeF_5NH^-$, which is obtained according to equation (32).[58]

$$Me_3SiNHTeF_5 + CsF \xrightarrow{CH_2Cl_2} Me_3SiF + Cs^+TeF_5NH^- \qquad (32)$$

An attempt to isolate of the monochloro-derivative, $ClNHTeF_5$, was not successful but Cl_2NTeF_5 has been isolated as an explosive liquid at -78 °C by the reaction of ClF and $Me_3SiNHTeF_5$ in $CFCl_3$ followed by purification by low temperature trap to trap distillation (-78 and -196 °C).[64] The existence of these derivatives suggests that the TeF_5N- group will be resistant to oxidation by the XeF^+ cation. The ligand TeF_5NH_2 is considered to be less basic than the sulfur analog[58] on the basis of the relative stabilities of their adducts with BF_3. The latter is stable at room temperature whereas the former decomposes with loss of BF_3 at -60 °C. Aminotellurium pentafluoride does possess substantial basic character, as proven by the existence of a room temperature stable adduct with AsF_5.[58]

The protonated species $F_5TeNH_3^+$ was not studied prior to this work. It was isolated as

the hexafluoroarsenate salt by combining F_5TeNH_2 and a 20 mole % excess of AsF_5 (equation (33)) in HF solvent at -40 °C and subsequent removal of HF and excess AsF_5 at this temperature.

$$F_5TeNH_2 + AsF_5 \xrightarrow{HF} F_5TeNH_3^+AsF_6^- \qquad (33)$$

A thorough investigation in solution was possible because each element in the cation $F_5TeNH_3^+$ has at least one nuclide which is suitable for observation by NMR spectroscopy, namely the spin-½ nuclides ^{125}Te, ^{19}F, ^{1}H and ^{15}N and the spin-1 nuclide ^{14}N. The NMR spectra of all spin-½ nuclei above were recorded for a full characterization of the salt, in both HF and BrF_5 solvents. The electric field gradient (efg) at nitrogen was sufficient to cause quadrupolar broadening of the resonances, and scalar couplings to nitrogen were not observed. To resolve these couplings, 99% ^{15}N enriched $F_5TeNH_3^+AsF_6^-$ was prepared.

The cation $F_5TeN(H)\text{-}Xe^+$ was generated in solution by two methods. Stoichiometric amounts of F_5TeNH_2 and $XeF^+AsF_6^-$ were combined in anhydrous HF solvent and warmed to -35 to -30 °C to effect reaction (equation (34)), as indicated by a yellow solution.

$$F_5TeNH_2 + XeF^+AsF_6^- \longrightarrow F_5TeN(H)\text{-}Xe^+AsF_6^- + HF \qquad (34)$$

The cation was also generated by combining stoichiometric amounts of $F_5TeNH_3^+AsF_6^-$ and XeF_2 in BrF_5 solvent and warming to -60 to -50 °C (equation (35)) giving a yellow solution and a colorless phase.

$$F_5TeNH_3^+AsF_6^- + XeF_2 \longrightarrow F_5TeN(H)\text{-}Xe^+AsF_6^- + 2\,HF \qquad (35)$$

As in $TeF_5NH_3^+AsF_6^-$, every element in the $TeF_5N(H)\text{-}Xe^+$ cation possesses at least one

nuclide which is suitable for observation by NMR spectroscopy, namely, the spin-½ nuclei ^{129}Xe, ^{125}Te, ^{19}F, ^{1}H and ^{15}N and the spin-1 nucleus ^{14}N. Nitrogen-15 enrichment was necessary to see couplings to nitrogen due to the fast relaxation of the ^{14}N nucleus in natural abundance the $F_5TeN(H)\text{-}Xe^+$ cation.

Attempts to combine F_5TeNH_2 with $XeF^+AsF_6^-$ in BrF_5 resulted in rapid oxidative fluorination of aminotellurium pentafluoride to TeF_6 at -50 °C. The salt $F_5TeNH_3^+AsF_6^-$ was more resistant to attack; partial fluorination occurred at -50 °C with little further reaction after decomposition of $F_5TeN(H)\text{-}Xe^+$ upon warming to -44 °C.

Characterization of the $F_5TeNH_3^+$ Cation. The NMR spectra of all spin-½ nuclei, namely ^{19}F, ^{125}Te, ^{15}N and ^{1}H, were run, in both BrF_5 and HF solvents. Table 3 lists the NMR parameters for the salt $F_5TeNH_3^+AsF_6^-$. The ^{19}F NMR spectra of F_5TeNH_2 (-50 °C) and $F_5TeNH_3^+AsF_6^-$ (-44.4 °C) in BrF_5 solvent are shown in Figures 5 and 6. Second order effects are observed in the former, due to the close proximity of the $^{19}F_{ax}$ and $^{19}F_{eq}$ resonances (AB_4 pattern). The latter exhibits a first order AX_4 pattern [$^1J(^{19}F_{eq}\text{-}^{19}F_{ax})$ = 162 Hz]. Protonation results in a high-frequency shift of the equatorial fluorine resonance by 7.7 ppm and the axial fluorines are shielded by 12.8 ppm. This is a common phenomenon for compounds $R\text{-}OXF_5$ (X= S, Se, Te) as the electronegativity of R is varied.[37,66] The variation of the axial fluorine resonance is usually greater. The singlet at -53.2 ppm in both spectra is assigned and to results from TeF_6, resulting from oxidative fluorination of the ligand by the solvent. The broad singlet at -52.0 ppm is tentatively assigned to BrF_3 [$\delta(^{19}F)$ = -20 to -40 ppm for neat BrF_3], the expected reduction product. Broadening of this resonance may result from exchange with AsF_6^- (equation(36)).

$$BrF_3 + AsF_6^- \rightleftharpoons BrF_4^- + AsF_5 \qquad (36)$$

Table 3. NMR Chemical Shifts and Spin-Spin Coupling Constants for the Salt $TeF_5NH_3^+AsF_6^-$ [a]

	Chemical Shifts (ppm)[b]	T (°C)
$\delta(^{19}F)$[c]	-56.3 (-55.6), F_{ax} -37.6 (-30.2), F_{eq}	(-44)
$\delta(^{15}N)$	-317.1 (-318.0)	-40 (-45)
$\delta(^{125}Te)$	588	-45
$\delta(^{1}H)$	(7.4)	(-53)

Coupling Constants (Hz)

$^2J(^{19}F_{ax}\text{-}^{19}F_{eq})$	(162)	$^2J(^{1}H\text{-}^{125}Te)$	25 (24)
$^1J(^{19}F_{eq}\text{-}^{125}Te)$	3651 (3698)	$^1J(^{15}N\text{-}^{125}Te)$	48
$^1J(^{19}F_{ax}\text{-}^{125}Te)$	3801	$^1J(^{15}N\text{-}^{1}H)$	76 (76)
$^1J(^{19}F_{eq}\text{-}^{123}Te)$	3024		

[a] All spectra were recorded using samples containing 99 atom % ^{15}N enriched $TeF_5NH_3^+AsF_6^-$. [b] The values in parentheses have been measured in BrF_5 solvent. [c] All ^{19}F spectra displayed a broad resonance at ca. 68 ppm arising from the partially quadrupole-collapsed $^1J(^{75}As\text{-}^{19}F)$ of the octahedral AsF_6^- anion. This resonance was saddle-shaped in HF solvent, but completely collapsed into a broad hump in BrF_5.

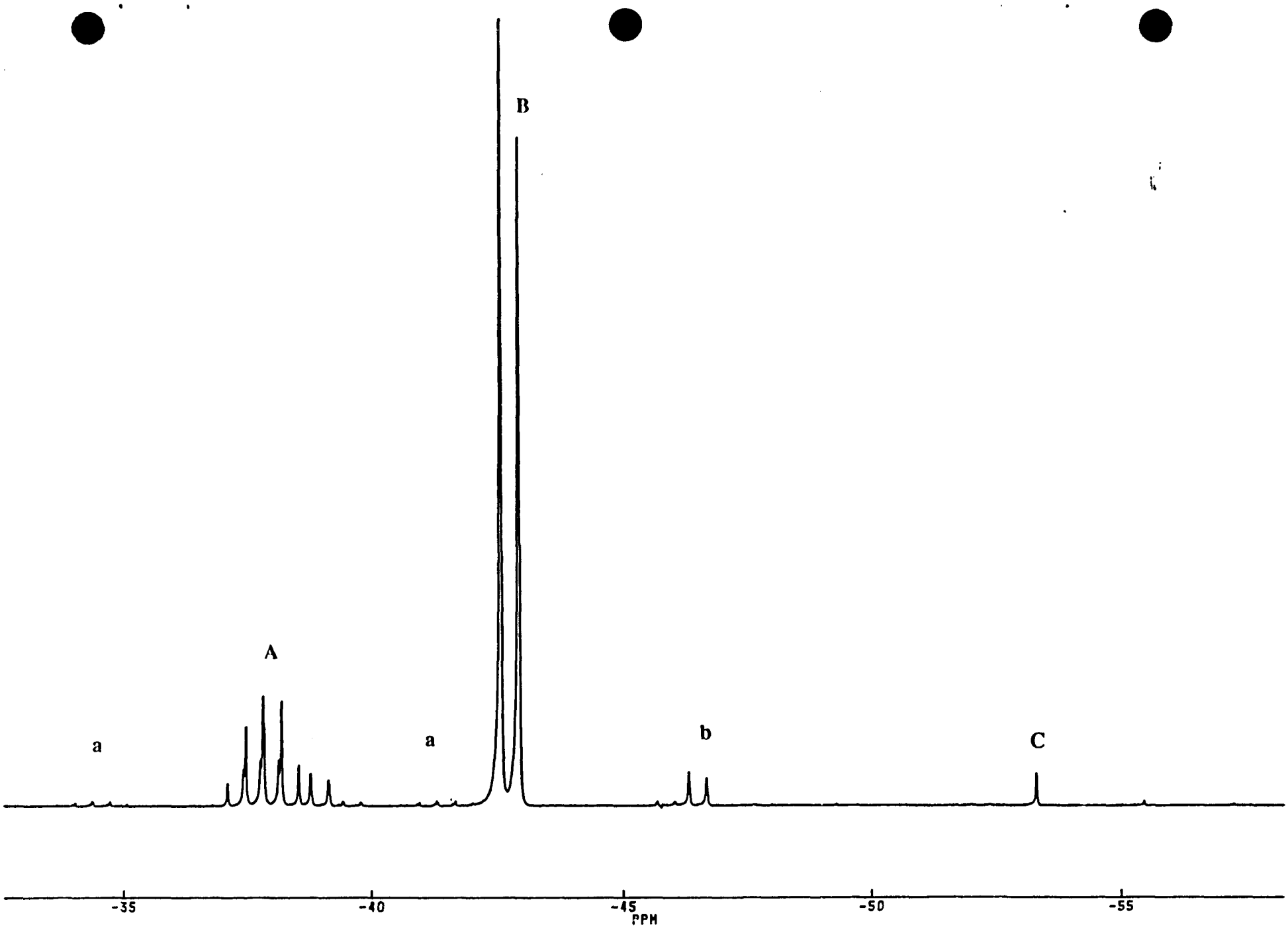

Figure 5. ^{19}F NMR of F_5TeNH_2 in BrF_5 at -50 °C; (A), (B), AB_4 pattern due to F-on-Te(VI), (a), (b), ^{125}Te satellites, (C), TeF_6 resonance.

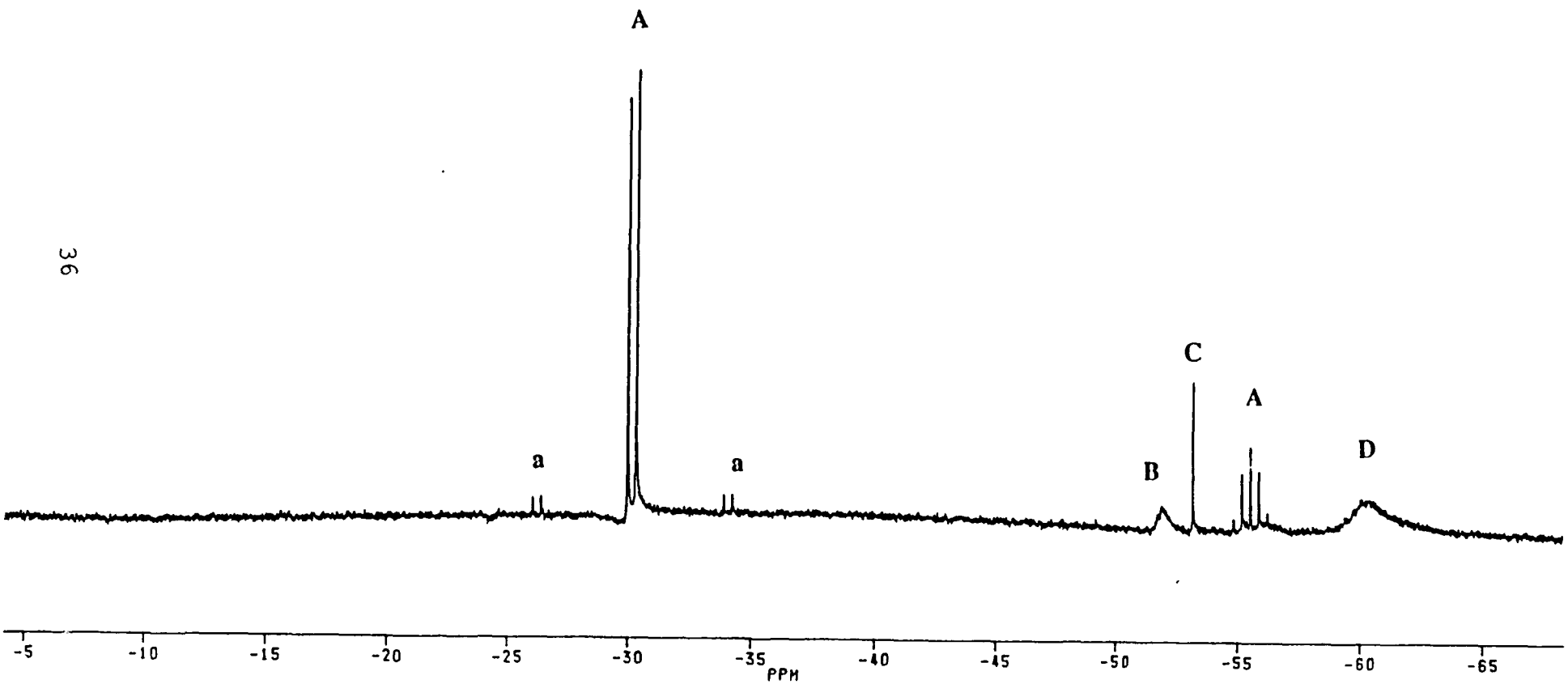

Figure 6. ^{19}F NMR of $F_5TeNH_3^+AsF_6^-$ in BrF_5 at -44.4 °C; (A), AX_4 pattern due to F-on-Te(VI), (a), ^{125}Te satellites, (B), tentatively assigned to BrF_3, (C), TeF_6, (D) AsF_6^-.

The ^{125}Te spectrum of 99 % ^{15}N enriched $TeF_5NH_3^+AsF_6^-$ in HF solution at -45.0 °C shows couplings of tellurium to all other elements in the cation (Figure 7). The ^{125}Te resonance (588 ppm) is split into a quintet from the coupling $^1J(^{125}Te\text{-}^{19}F_{eq})$, 3651 Hz and further splitting to a doublet of quintets is due to $^1J(^{125}Te\text{-}^{19}F_{ax})$, 3801 Hz. Each line is further split into a doublet of quartets from the couplings $^1J(^{125}Te\text{-}^{15}N)$, 48 Hz and $^2J(^{125}Te\text{-}^1H)$, 25 Hz.

The presence of well-defined quartets in the ^{15}N spectra due to $^1J(^{15}N\text{-}^1H)$, 76 Hz demonstrate that $F_5TeNH_3^+$ does not undergo exchange with the solvents (equation (37)).

$$TeF_5NH_3^+ + A \rightleftharpoons TeF_5NH_2 + AH^+ \qquad (A = HF \text{ or } BrF_5) \qquad (37)$$

Tellurium satellites due to $^1J(^{125}Te\text{-}^{15}N)$, 48 Hz, are resolved in the ^{15}N NMR spectrum $\delta(^{15}N$ = -317.1 ppm) of 99 % ^{15}N enriched $F_5TeNH_3^+AsF_6^-$ in HF at -40 °C (Figure 8). The ^1H NMR spectrum (Figure (9)) of $F_5Te^{15}NH_3^+AsF_6^-$ in BrF_5 solvent at -53 °C corroborates this lack of exchange broadening as a doublet with tellurium satellites is resolved.

Structure of the $F_5TeN(H)\text{-}Xe^+$ Cation in Solution. Characterization of $TeF_5N(H)\text{-}Xe^+$ was performed by recording the spectra of all pertinent spin-½ nuclides (Table 4). Spin-spin couplings to nitrogen were quadrupole collapsed due to the asymmetric environment and subsequently large electric field gradient (efg) of the sp^3 hybridized trigonal pyramidal nitrogen (Structure I). Thus 99 % ^{15}N enriched F_5TeNH_2 and $F_5TeNH_3^+AsF_6^-$ were synthesized (see EXPERIMENTAL). Nitrogen-15 enrichment was also necessary in prior studies of the *imidodisulfurylfluoride derivatives* of xenon(II),[41,43,45] where the low symmetry of the trigonal planar geometry of the $-N(SO_2F)_2$ group also results in a large efg at the ^{14}N nucleus.

The ^{129}Xe spectra of natural abundance $F_5TeN(H)\text{-}Xe^+$ in BrF_5 (-48.3 °C) and HF (-45.0 °C) solvents consist of singlets at -2903 and -2840 ppm, respectively (Figures 9 and 10). A study

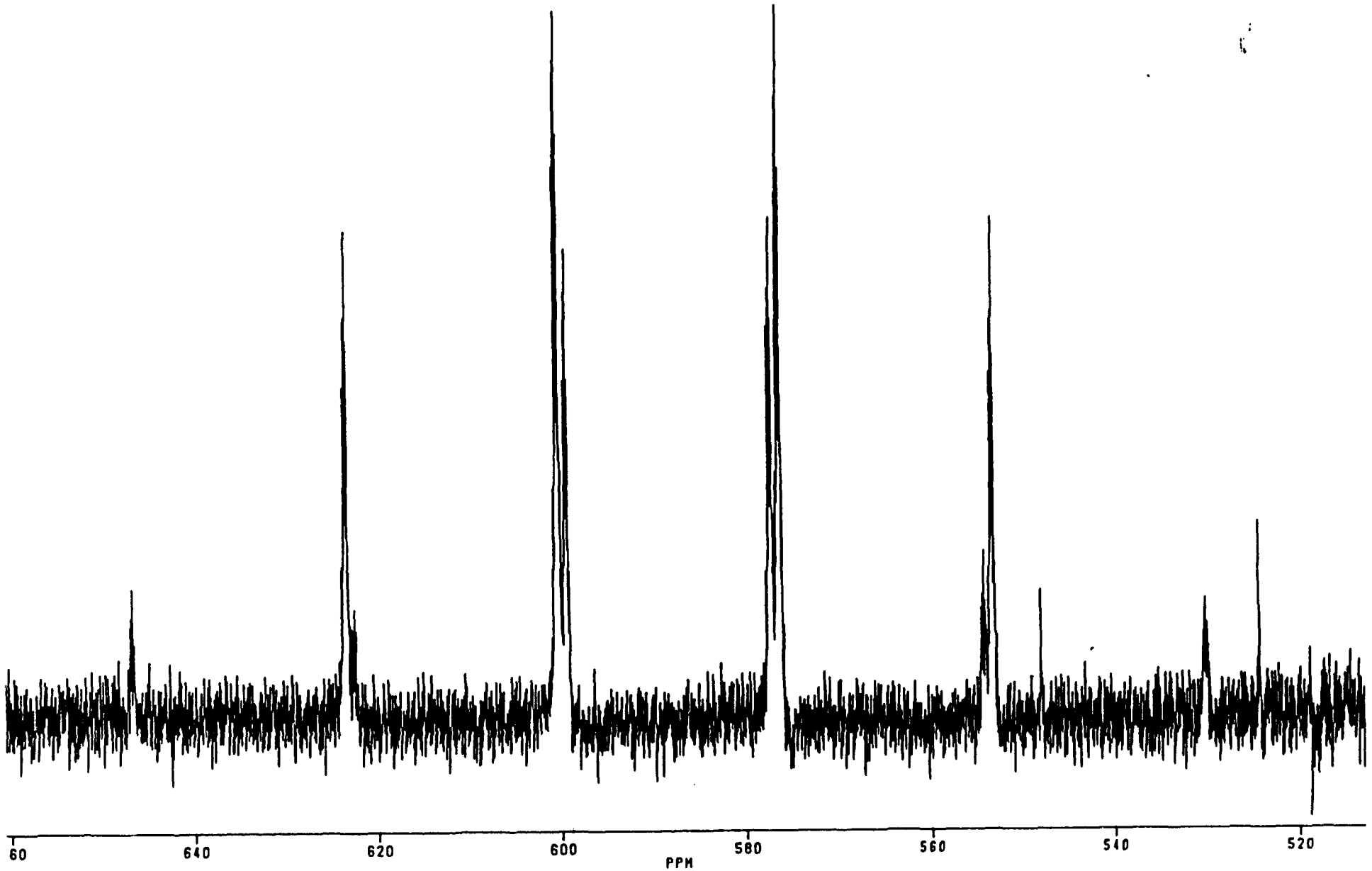

Figure 7. ^{125}Te NMR of 99% [redacted]$e^{15}NH_3^+AsF_6^-$ in HF at -45 °C.

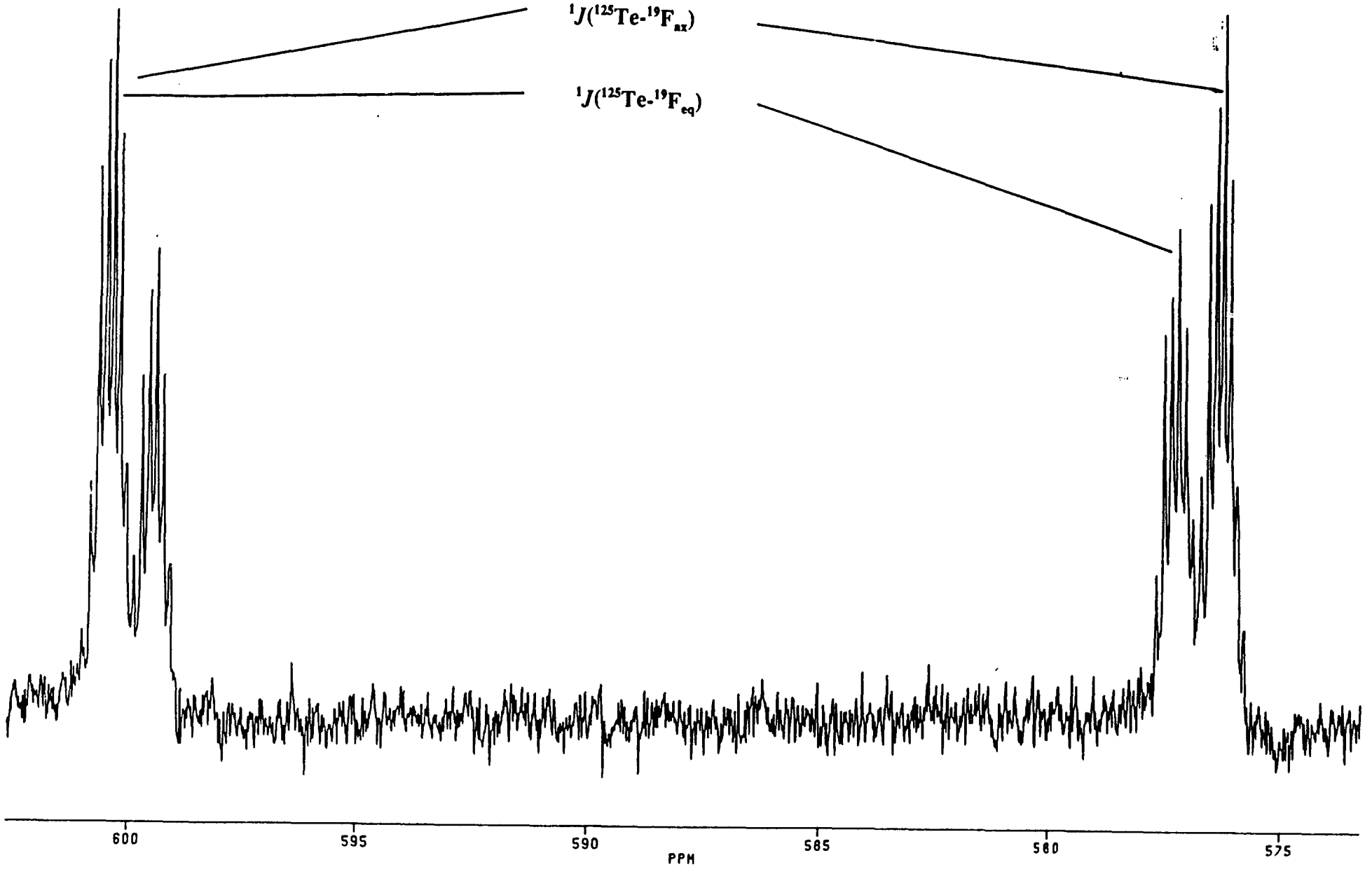

Figure 7. ^{125}Te NMR of 99% $F_5Te^{15}NH_3^+AsF_6^-$ in HF at -45 °C.

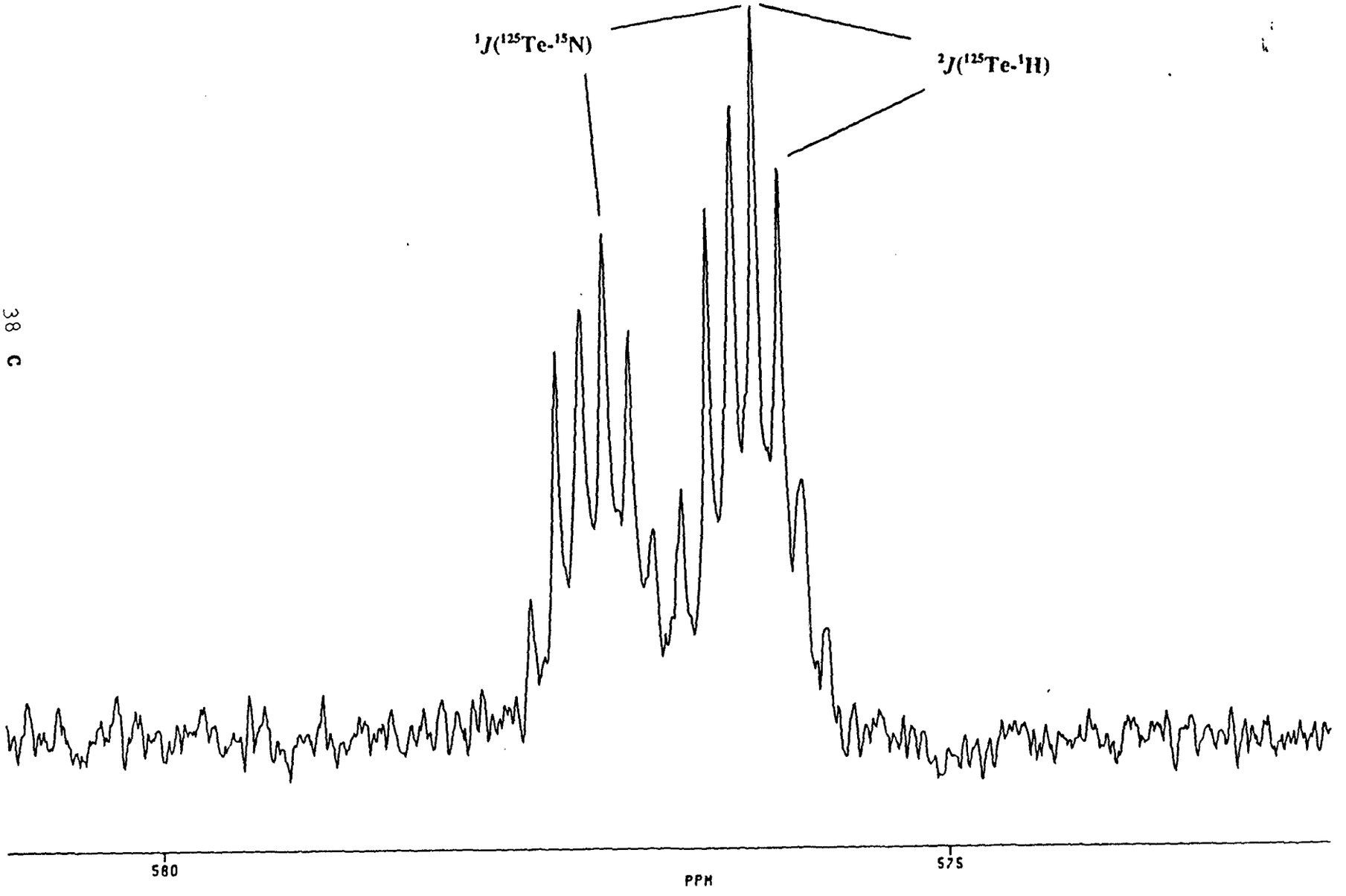

Figure 7. ^{125}Te NMR of 99[redacted]$_5Te^{15}NH_3^+AsF_6^-$ in HF at -45 °C.

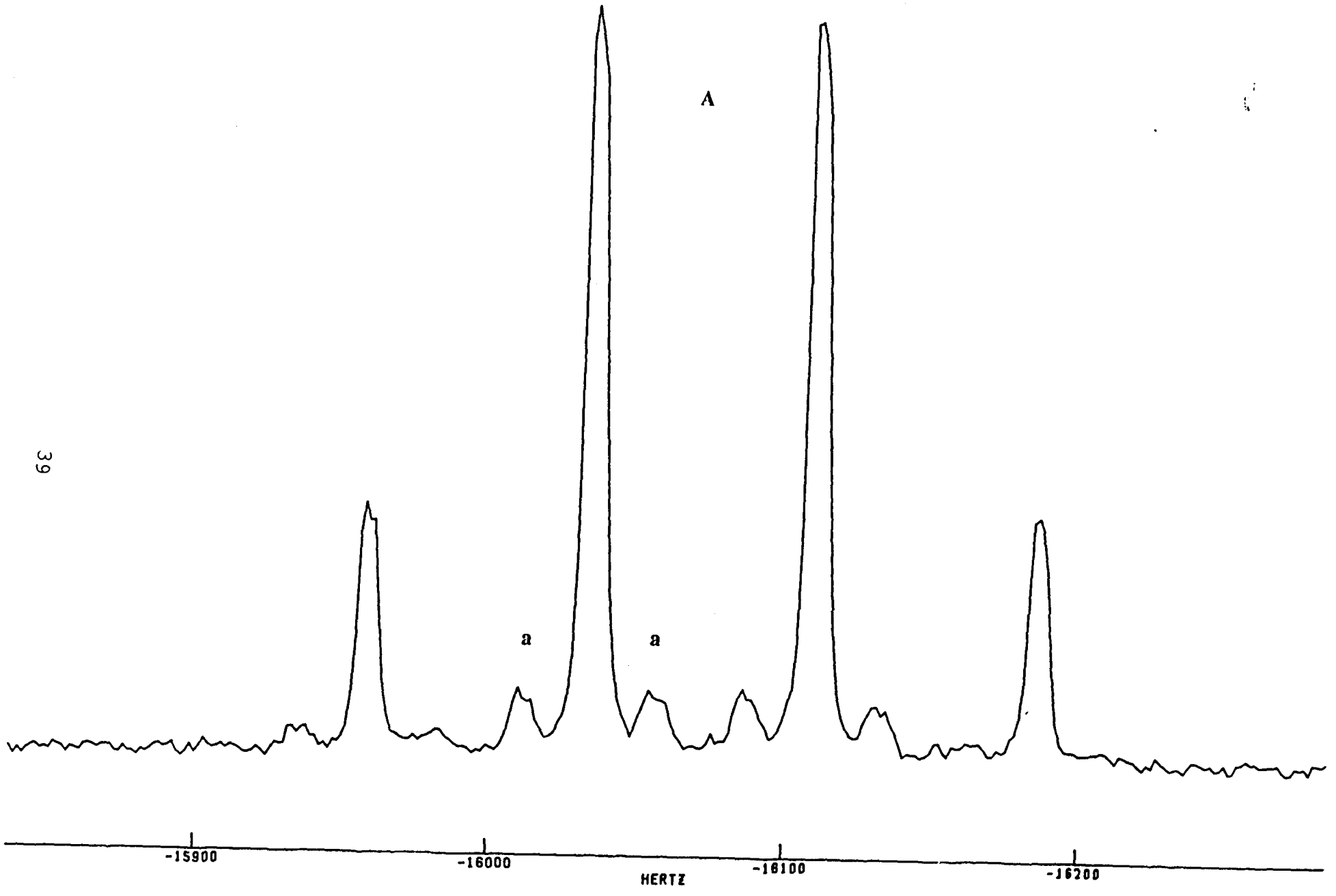

Figure 8. ^{15}N NMR of $F_5Te^{15}NH_3^+AsF_6^-$ in HF at -40 °C; (A), quartet due to one-bond coupling to protons, (a), ^{125}Te satellites.

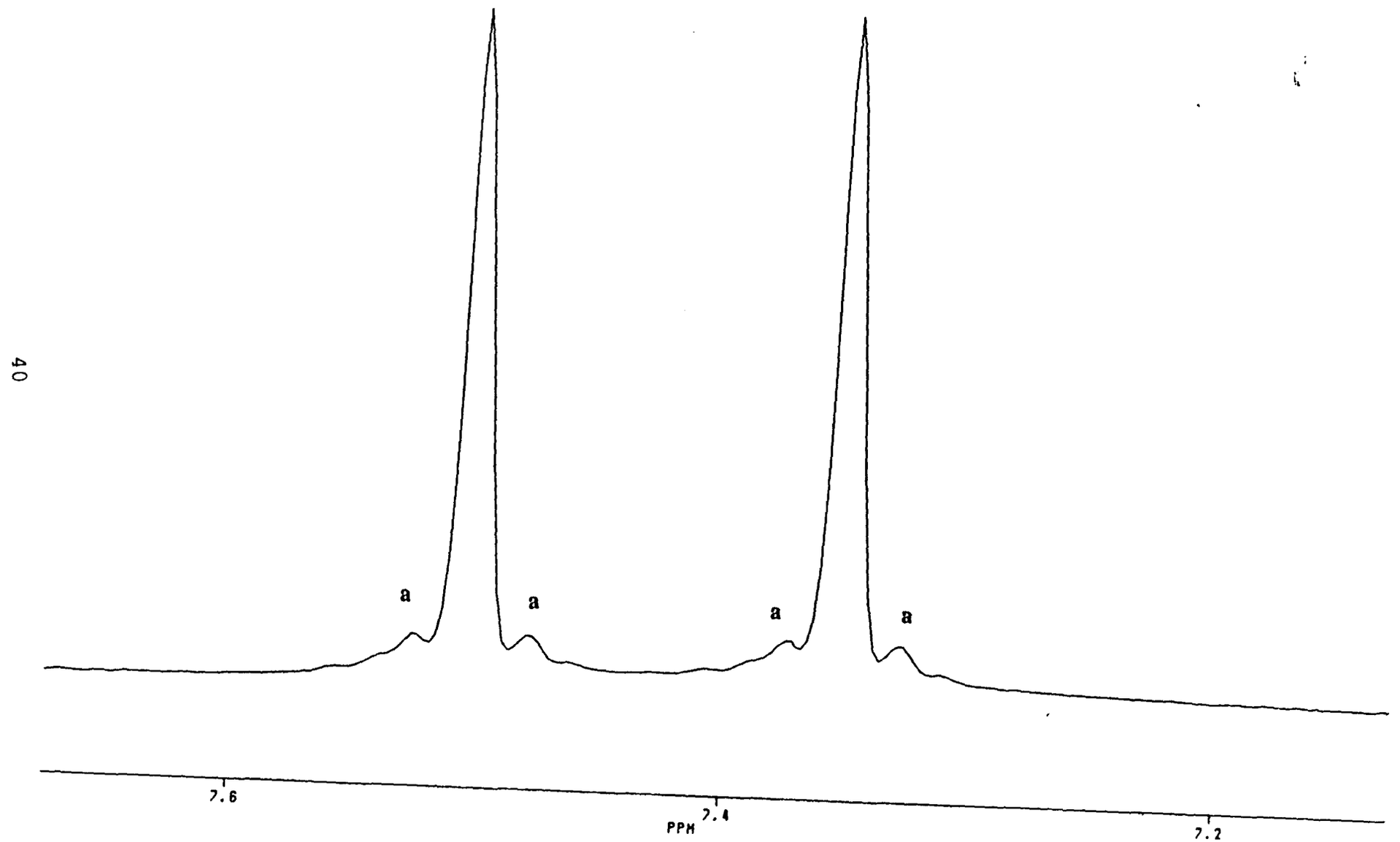

Figure 9. ^{1}H NMR of $F_5Te^{15}NH_3^+AsF_6^-$ in BrF_5 at -53 °C; (a) ^{125}Te satellites.

Table 4. NMR Chemical Shifts and Spin-Spin Coupling Constants for $TeF_5N(H)$-$Xe^+AsF_6^-$ [a]

	Chemical Shifts (ppm)[b]	T (°C)
$\delta(^{129}Xe)$	-2840 (-2902)	-45.0 (-45.0)
$\delta(^{19}F)$[c]	-51.6[d] (-51.9), F_{ax}	-31.2 (-44.0)
	-43.4[d] (-43.2), F_{eq}	
$\delta(^{15}N)$	-268.0 (-266.3)	-40.0 (-45.0)
$\delta(^{125}Te)$	(580)	-45.0 (-50.0)
$\delta(^{1}H)$	(6.90)	-40.0 (-56.0)

Coupling Constants (Hz)

$^1J(^{129}Xe$-$^{15}N)$	138 (142)	$^1J(^{19}F_{eq}$-$^{125}Te)$	3767[d] (3767)
$^1J(^{15}N$-$^{1}H)$	62 (62)	$^1J(^{19}F_{ax}$-$^{19}F_{eq})$	166 (166)

[a] Unless indicated otherwise, all spectra were recorded using samples containing 99% ^{15}N enriched $F_5TeN(H)$-Xe^+. [b] The values in parentheses have been measured in BrF_5 solvent. [c] All ^{19}F spectra displayed a broad resonance at ca. -68 ppm arising from the partially quadrupole-collapsed $^1J(^{75}As$-$^{19}F)$ of the octahedral AsF_6^- anion. This resonance was saddle-shaped in HF solvent, but completely collapsed into a broad resonance in BrF_5 solvent. [d] Spectra recorded with samples containing unenriched $F_5TeN(H)$-Xe^+.

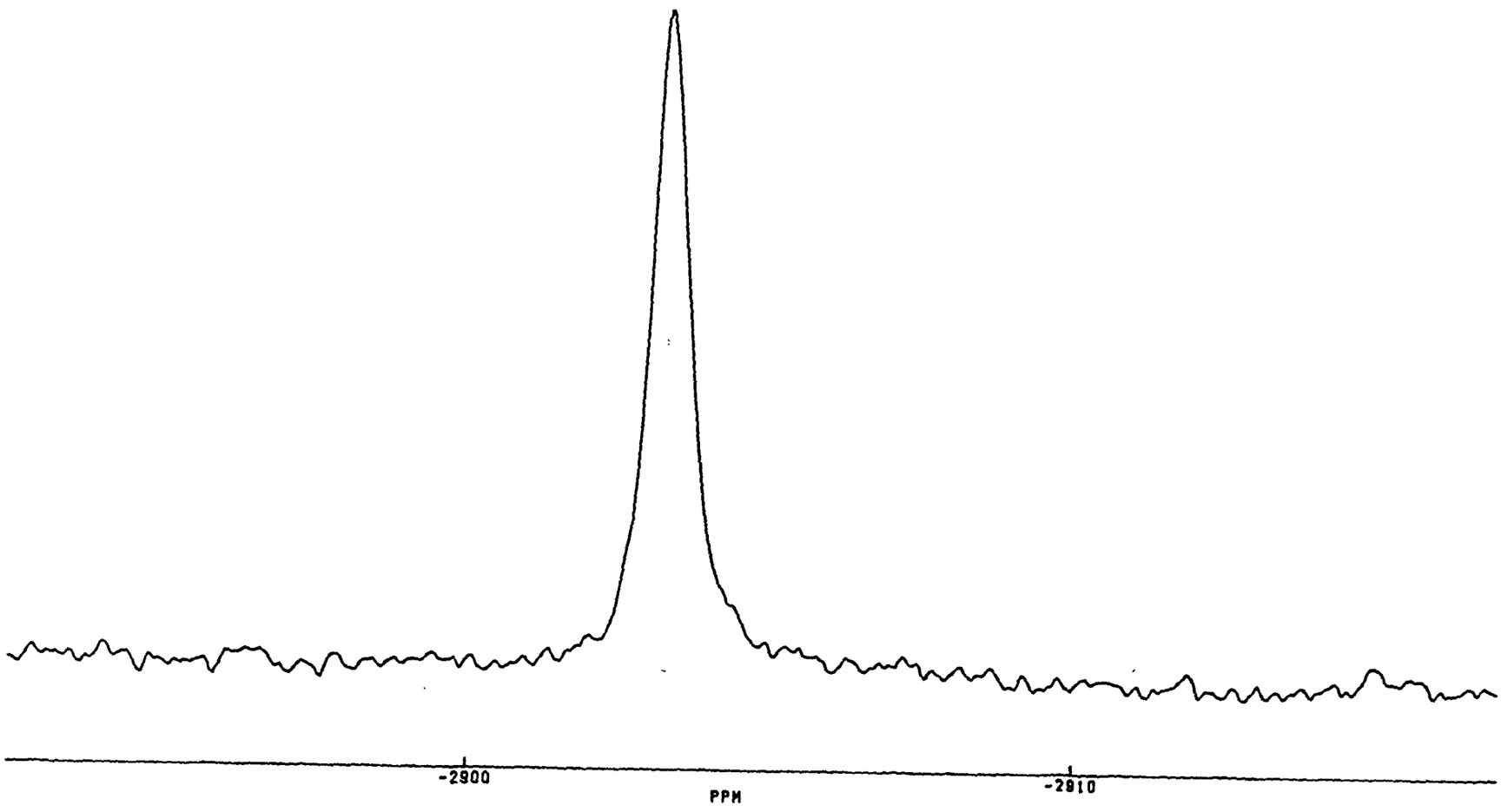

Figure 10. ^{129}Xe NMR of Natural Abundance $F_5TeN(H)\text{-}Xe^+$ in BrF_5 at -48.3 °C.

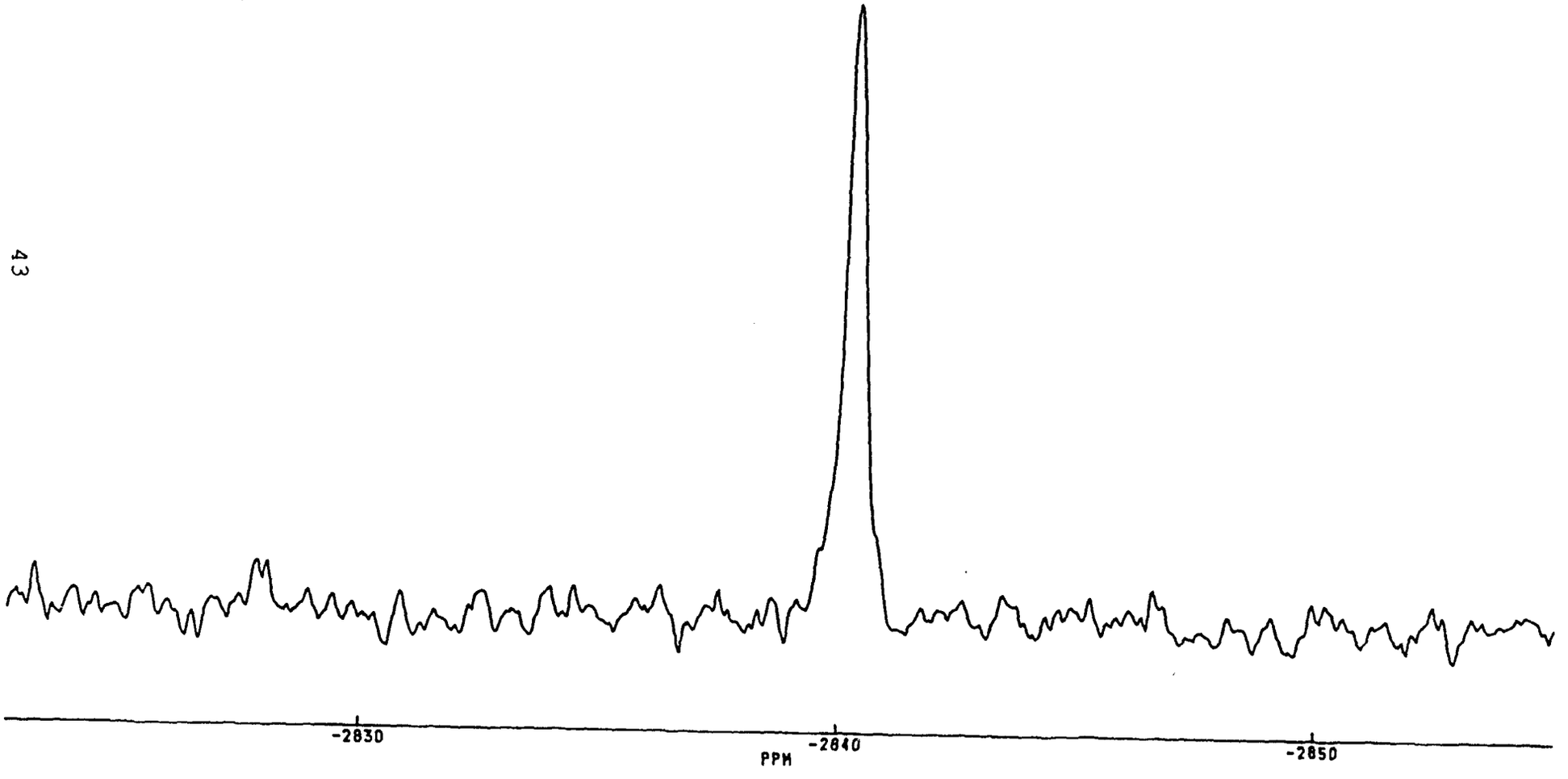

Figure 11. ^{129}Xe NMR of Natural Abundance $F_5TeN(H)\text{-}Xe^+$ in HF at -45.0 °C.

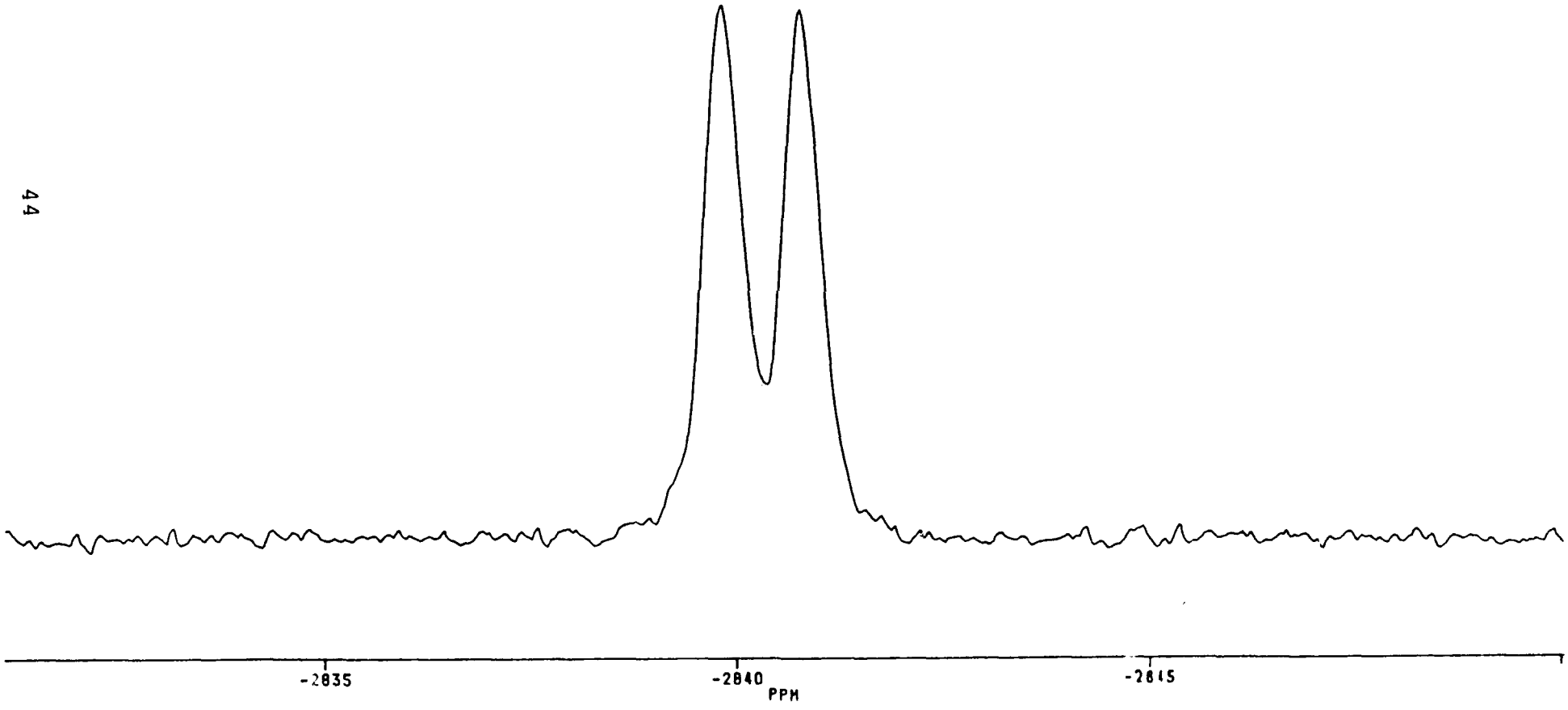

Figure 12. ^{129}Xe NMR 99% $F_5Te^{15}N(H)$-Xe^+ in HF at -45 °C.

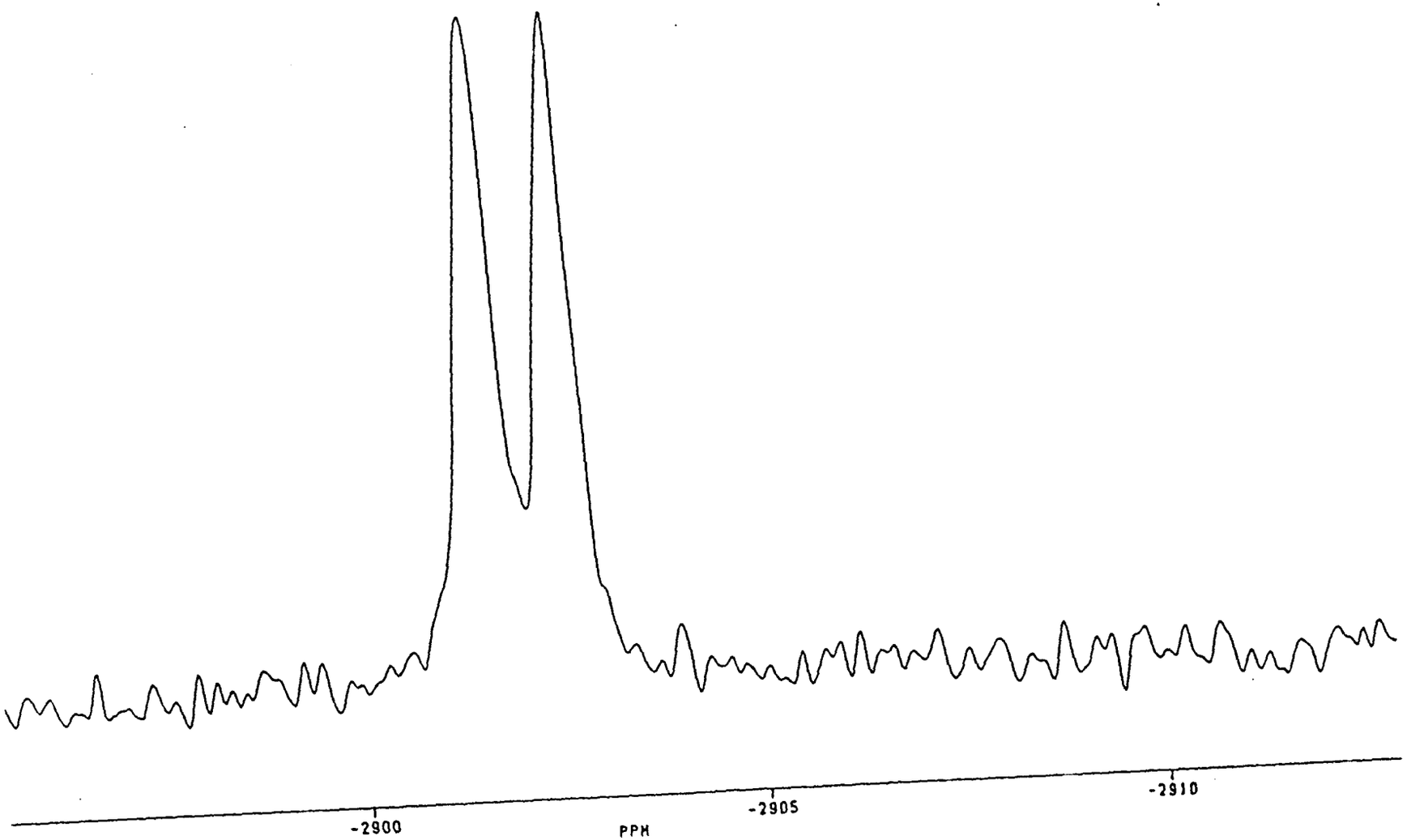

Figure 13. ^{129}Xe NMR 99% $F_5Te^{15}N(H)\text{-}Xe^+$ in BrF_5 at -45 °C.

of the ^{129}Xe chemical shifts of XeF_2 in HF and BrF_5 reveals a large solvent dependence.[67] Nitrogen-15 enrichment was necessary to see the one-bond xenon-nitrogen coupling. The ^{129}Xe spectra of $F_5Te^{15}N(H)\text{-}Xe^+$ in HF at -45 °C (Figure 12) and BrF_5 at -45.0 °C (Figure 13) revealed doublets arising from the one-bond scalar coupling to ^{15}N [$^1J(^{15}N\text{-}^{129}Xe) = 62$ Hz]. The magnitude of $^1K(^{15}N\text{-}Xe)$ is comparable to directly bonded Xe-N couplings of other xenon(II) compounds. Table 5 shows the Xe-N reduced coupling constants of known derivatives of xenon(II) containing xenon-nitrogen bonds and the ^{129}Xe chemical shifts. Both of these parameters correlate with the formal hyridization at nitrogen. The magnitude of the reduced couplings in general decrease with formal hybridization at nitrogen in the order $sp > sp^2 > sp^3$. This trend reflects a significant contribution of the Fermi contact mechanism, which is proportional to the s-electron densities at the nuclei involved. The s-character in the hybrid orbital at nitrogen should be proportional to the s-electron density at the nucleus. The nitrogen in the cation $F_5TeN(H)\text{-}Xe^+$ is sp^3 hybridized, yielding one of the smallest Xe-N reduced coupling constants known ($0.398 \times 10^{22}\ T^2J^{-1}$).

The electronegativity of nitrogen decreases with decreasing s-character of the hybrid valence orbitals (i.e., $sp < sp^2 < sp^3$),[68] resulting in increased electron donation to xenon, and therefore increased shielding of the ^{129}Xe resonance. The nitrogen atom in the cation $TeF_5N(H)\text{-}Xe^+$ is formally sp^3 hybridized and the ^{129}Xe resonance in BrF_5 solvent is the most shielded in the series of Xe(II)-N species to date.

Failure to observe two- and three-bond couplings in the ^{129}Xe NMR spectrum is attributed to relaxation arising from chemical shift anisotropy (CSA). This effect is significant for ^{129}Xe NMR because of the large chemical shift range and is proportional to the square of the field

Table 5. Correlation of Xe(II)-N Reduced Coupling Constants and ^{129}Xe Chemical With Formal Hybridization on Nitrogen[a]

Species	Hybridization at Nitrogen	$^1K(Xe\text{-}N)$ $10^{22}NA^{-2}m^{-3}$	$\delta(^{129}Xe)$ ppm	T, °C
$HCN\text{-}XeF^+$	sp	1.381[b]	-1555 (-1570)	-10 (-58)
$RCN\text{-}XeF^+$	sp	1.297 - 1.393	-1541 to -1721	-10 to -50
$F_3SN\text{-}XeF^+$	sp	1.435	(-1661)	(-60)
$s\text{-}C_3F_3N_2N\text{-}XeF^+$	sp	1.013	-1808 (-1863)	-5 (-50)
$C_5F_5N\text{-}XeF^+$	sp^2	0.983	-1872 (-1922)	-30 (-30)
$4\text{-}CF_3C_5F_4N\text{-}XeF^+$	sp^2	0.991	-1803 (-1853)	-15 (-50)
$(FO_2S)_2N\text{-}Xe^+$	sp^2	0.270[b]	-1943 (SbF_5)	25
$(FO_2S)_2N\text{-}Xe\text{-}F$	sp^2	0.913[c]	-2009	-40
$F_4S{=}N\text{-}Xe^+$	sp^2	-	-2672	-20
$F_5S\text{-}N(H)\text{-}Xe^+$	sp^3	-	-2886	-20
$F_5Te\text{-}N(H)\text{-}Xe^+$	sp^3	0.398[b]	-2841 (-2903)	-45 (-50)

[a] Unless otherwise indicated, values were determined in HF and in BrF_5 (in parentheses) solvent; $^1K(Xe\text{-}N) = [4\pi^2\ ^1J(^{129}Xe\text{-}^{14/15}N)]/[h\gamma(^{14/15}N)\gamma(^{129}Xe)]$

[b] Recorded for the ^{15}N enriched cation.

[c] Measured in SO_2ClF solvent.

strength.

The xenon-nitrogen bond is corroborated by the ^{15}N NMR spectrum of the 99% enriched $F_5TeN(H)\text{-}Xe^+$ cation in HF at -40 °C (Figure 14), which consists of a doublet at -268.0 ppm arising from the one-bond scalar coupling $^1J(^{15}N\text{-}^1H)$, 62 Hz. Each peak of the doublet is flanked by a satellite doublet arising from the one-bond scalar coupling $^1J(^{15}N\text{-}^{129}Xe)$, 138 Hz (nat. abundance of ^{129}Xe is 26.44 %). The inner satellite peaks are obscured by the natural line width of the ^{15}N resonance. The quality of the ^{15}N NMR spectrum at -45 °C in BrF_5 was not sufficient to see the ^{129}Xe satellites. However, the one-bond coupling arising from $^1J(^{15}N\text{-}^1H)$, 62 Hz and the chemical shift the ^{15}N chemical shift (-266.3 ppm) are indicative of the cation $F_5TeN(H)\text{-}Xe^+$. The magnitude of the one-bond coupling can be used to confirm the hybridization at nitrogen using an empirical relationship between the s-character of the N-H bond and $^1J(^{15}N\text{-}^1H)$. This relationship assumes that the coupling is dominated by the Fermi contact term. Using equation (39), the % s character of the N-H bond in $TeF_5N(H)\text{-}Xe^+$ was calculated to be 21%

$$\% \text{ s} = 0.430[^1J(^1H\text{-}^{15}N)] - 6.0 \qquad (39)$$

which approximates an sp^3 hybridized NH orbital. The theoretical % s characters for sp^2 and sp^3 hybridized nitrogen are 33.3 and 25.0 %, respectively.

The ^1H resonance for the 99% ^{15}N enriched cation $TeF_5N(H)\text{-}Xe^+$ in BrF_5 solvent at -56.0 °C (Figure 15) consists of a doublet at 6.90 ppm arising from the one-bond coupling $^1J(^1H\text{-}^{15}N)$, 62 Hz. There is evidence of ^{125}Te satellites which have not yet been resolved. The ^{125}Te satellites have been resolved for natural abundance $F_5TeN(H)\text{-}Xe^+$ in BrF_5 (Figure 19) at -55.5 °C

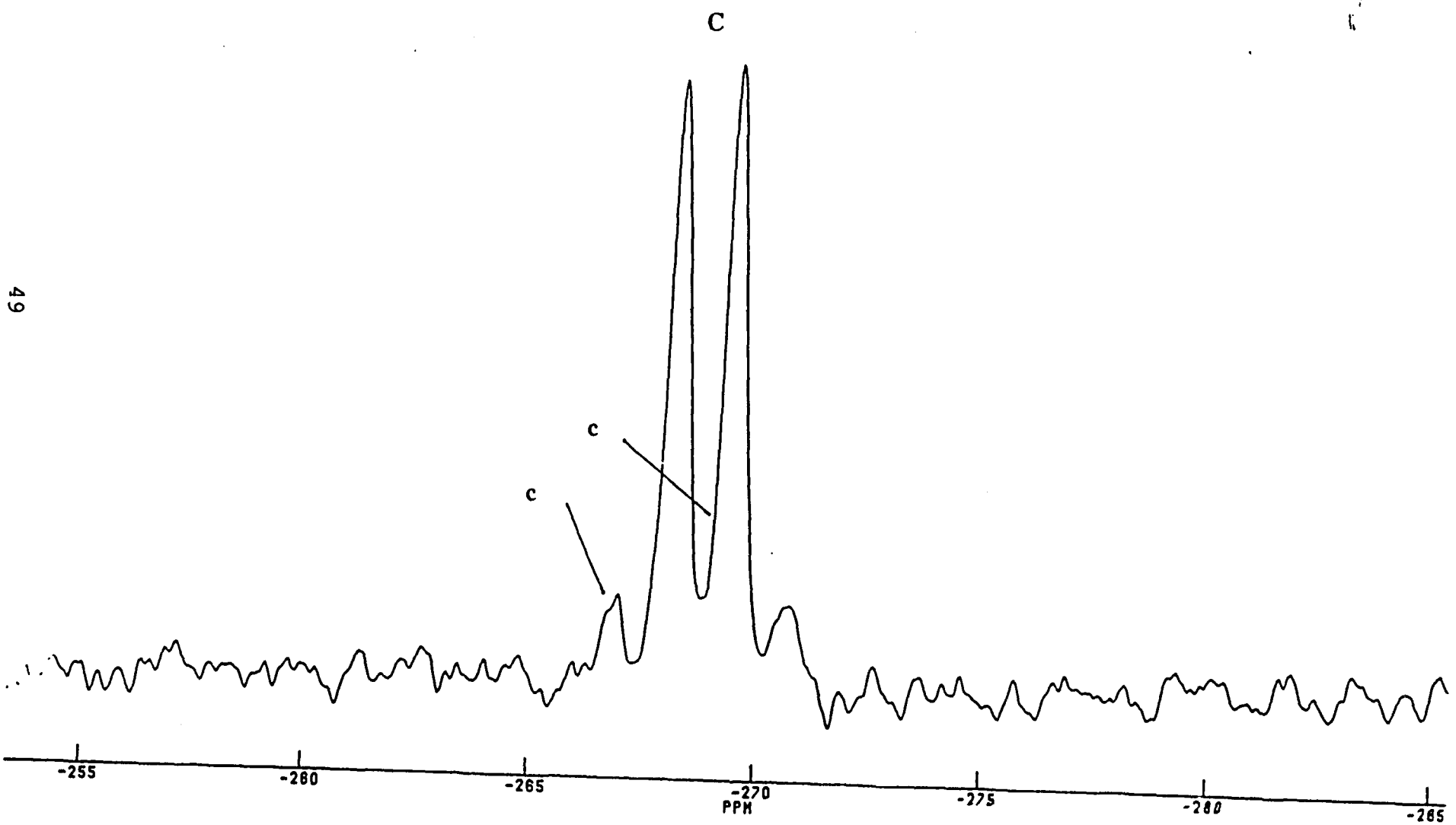

Figure 14. ^{15}N NMR of 99% $F_5Te^{15}N(H)$-Xe^+ in HF at -40 °C; (C), doublet due to one-bond coupling between hydrogen and nitrogen, (c), ^{129}Xe satellites.

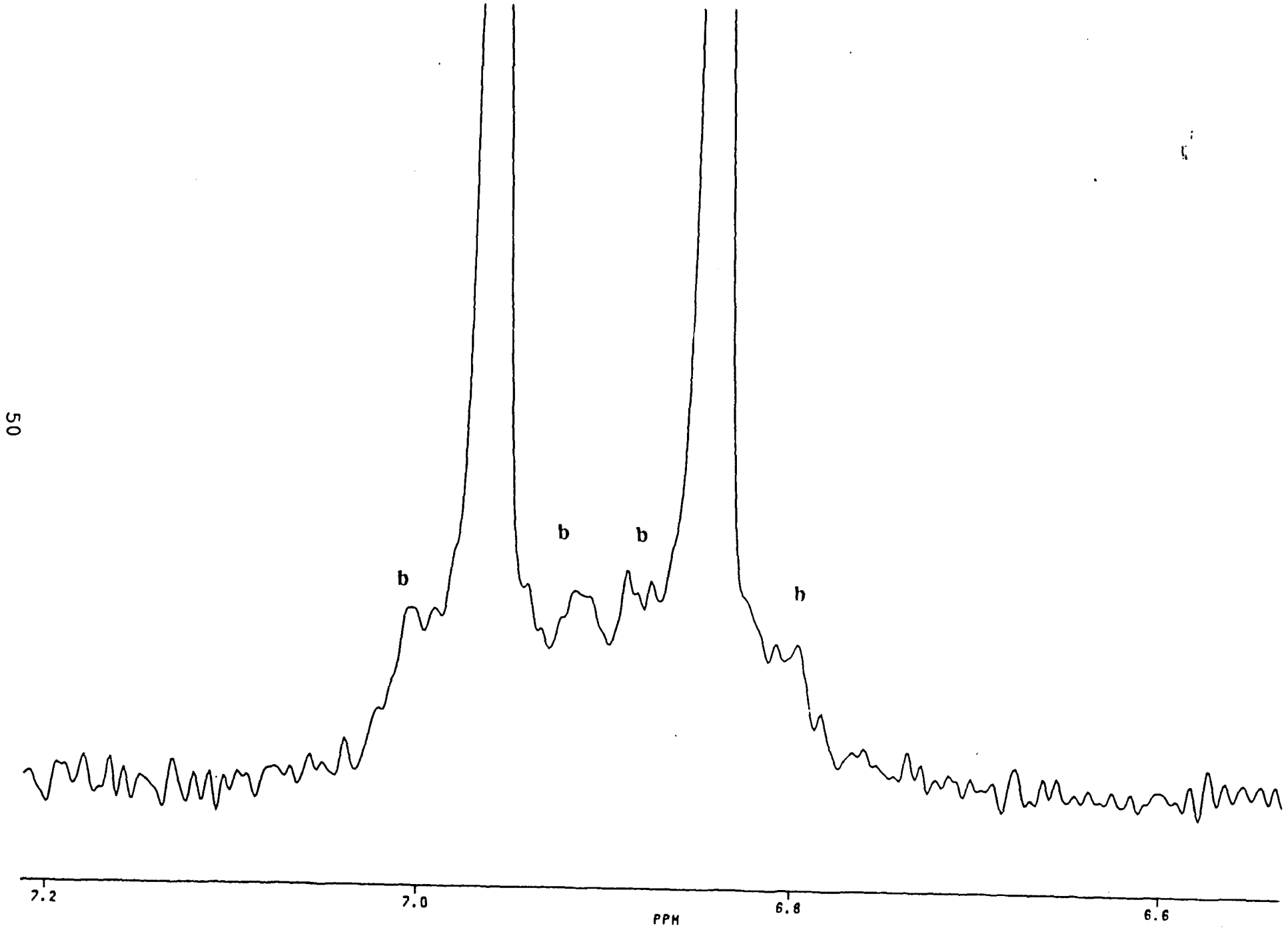

Figure 15. ^{1}H NMR of 99% $F_5Te^{15}N(H)\text{-}Xe^{+}$ in BrF_5 at -56 °C; doublet due to one-bond hydrogen-nitrogen coupling, (b) unresolved ^{125}Te satellites.

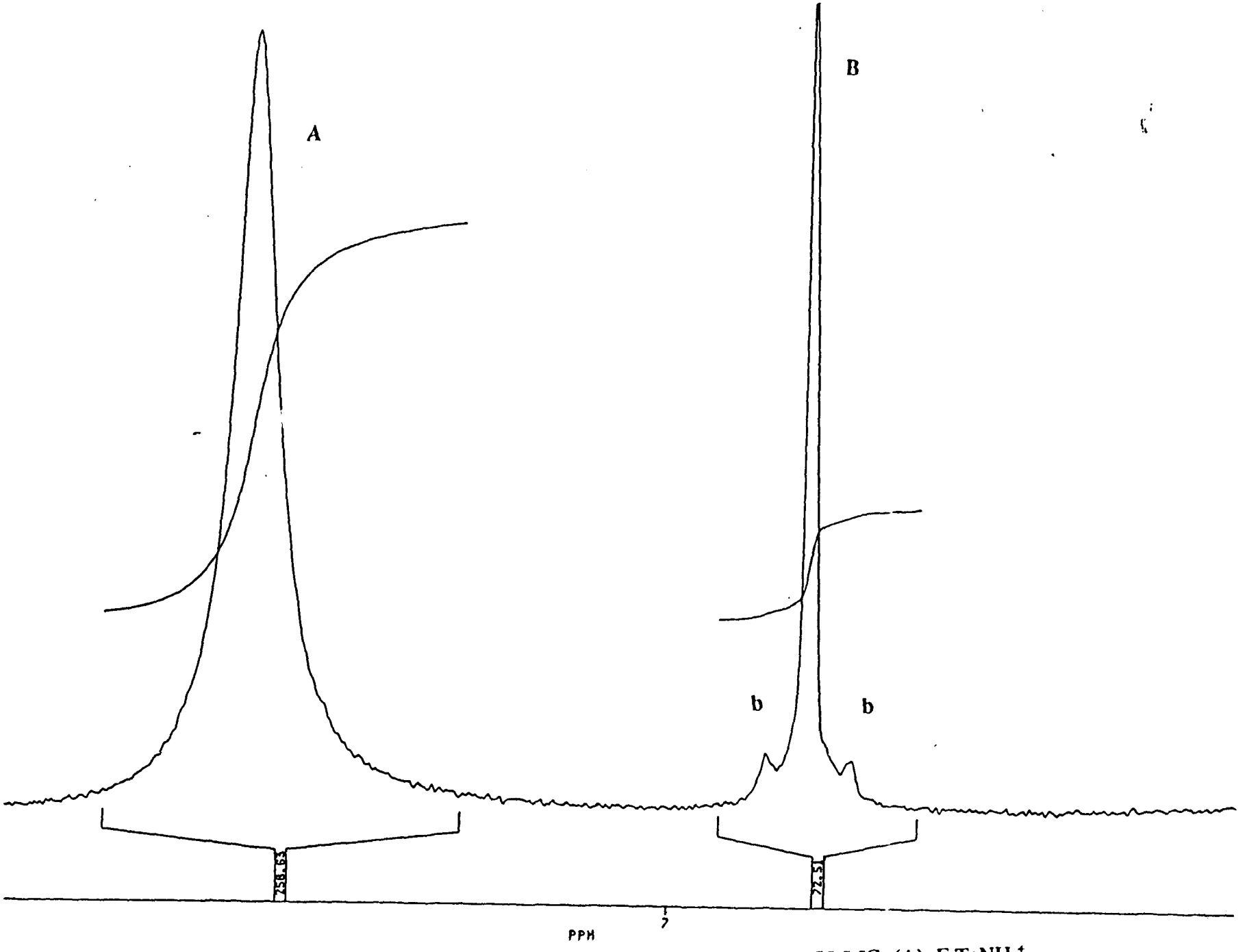

Figure 16. ^{1}H NMR of Natural Abundance $F_5TeN(H)\text{-}Xe^{+}$ in BrF_5 at -55.5 °C; (A), $F_5TeNH_3^{+}$, (B), $F_5TeN(H)\text{-}Xe^{+}$, (b) ^{125}Te satellites.

[$^2J(^1H\text{-}^{125}Te)$, 46 Hz].

The ^{19}F NMR spectra in HF (Figure 17) at -31.2 °C and BrF_5 (Figure 18) at -44.0 °C show equilibrium mixtures of $F_5TeNH_3^+$ (see Table 3 for NMR parameters) and $F_5TeN(H)\text{-}Xe^+$. Both of these species show first order AX_4 subspectra of the F_5Te- group. The axial fluorine resonance gives a quintet at -51.6 ppm in HF (-51.9 ppm in BrF_5) arising from the two-bond scalar coupling to the four equatorial fluorines [$^2J(^{19}F_{ax}\text{-}^{19}F_{eq})$, 166 Hz]. The equatorial fluorine resonance is at -43.4 ppm in HF (-43.2 ppm in BrF_5). Of the four possible couplings to ^{125}Te, only $^1J(^{19}F_{eq}\text{-}^{125}Te)$, 3767 Hz (in HF and BrF_5) has been resolved. As expected HF as solvent reduces the equilibrium amount of the $F_5TeN(H)\text{-}Xe^+$ cation (see equations (1) and (2)), as seen by inspection of the relative intensities of the F_{eq} resonances in the two solvents. The presence of HF and XeF_2 were confirmed by ^1H and ^{129}Xe NMR. The broad resonance at ca. -68 ppm in the ^{19}F NMR spectra in HF solvent arises from the octahedral AsF_6^- anion. The $^1J(^{75}As\text{-}^{19}F)$ coupling is partially quadrupole collapsed (I= 3/2 for ^{75}As) in HF solvent, giving a saddle-shaped resonance. In BrF_5 solvent, which is more viscous, the quadrupolar ^{75}As nucleus relaxes faster so that the $^1J(^{75}As\text{-}^{19}F)$ coupling is collapsed into a single broad line ($W_{1/2}$, 946 Hz). This resonance is shifted to -64.5 ppm in this solvent. This shift is attributed to exchange with the broad resonance at -51.0 ppm, which is tentatively assigned to BrF_3 (equation (37)). This resonance is seen in the ^{19}F NMR spectrum of $F_5TeNH_3^+AsF_6^-$ in BrF_5 solvent at ca. -50 °C. The intense singlet at -56.5 ppm is TeF_6, the major decomposition product of the $F_5TeN(H)\text{-}Xe^+$ cation. An AB_4 pattern centered at ca. -58 ppm in BrF_5 and at ca. -62 ppm in HF is a decomposition product of $F_5TeN(H)\text{-}Xe^+$. This subspectrum was sufficiently resolved in BrF_5 solvent at -44.0 °C (Figure 21) to obtain estimates of $\delta(^{19}F_{ax})$ and $\delta(^{19}F_{eq})$ by NMR simulation. The "doublet" at -62.6 ppm consists of 11

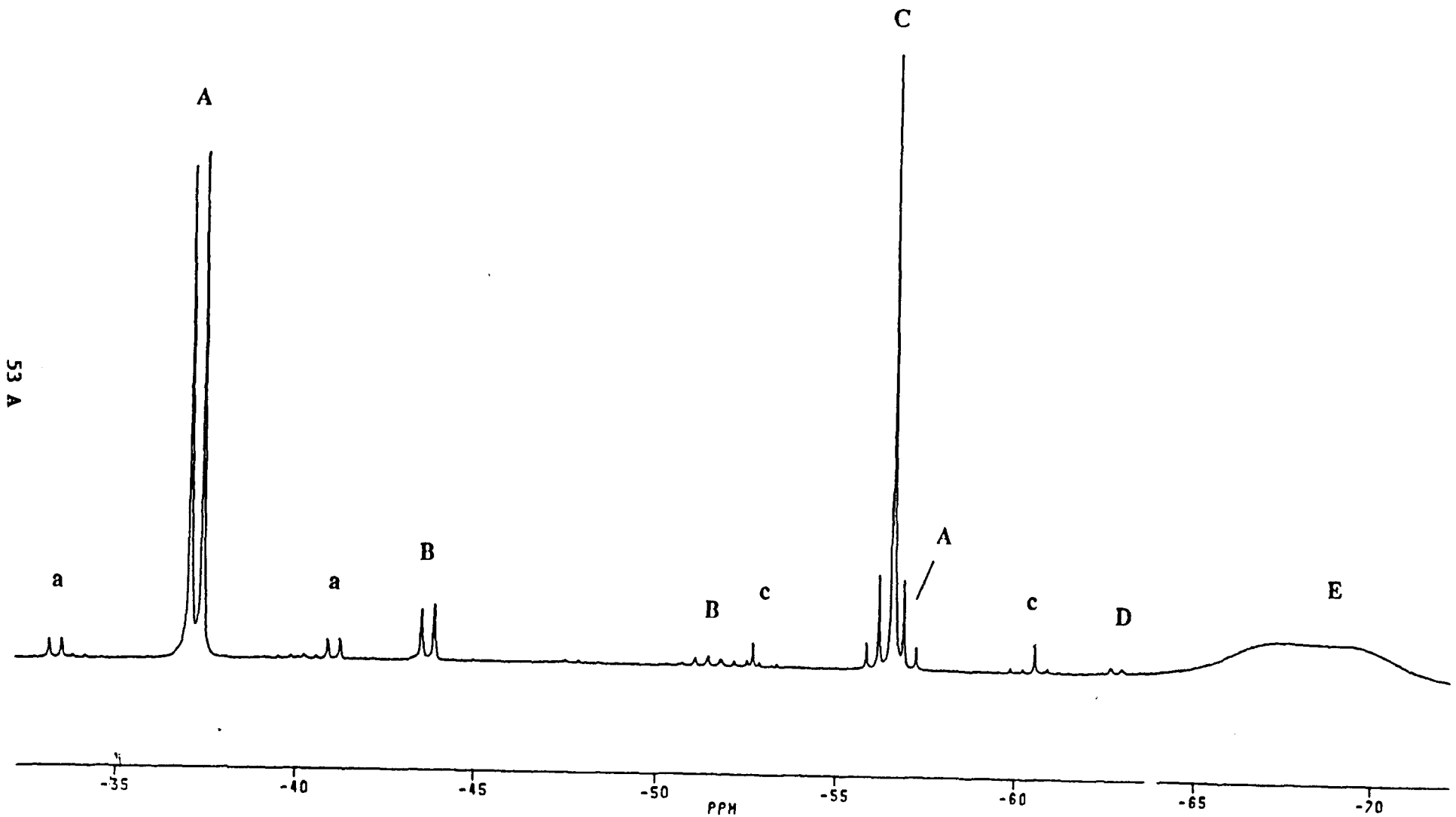

Figure 17. ^{19}F NMR of Equilibrium Mixture of $F_5Te^{15}N(H)\text{-}Xe^+$ and $F_5Te^{15}NH_3^+$ and Decomposition Products of $F_5Te^{15}N(H)\text{-}Xe^+$ in HF at -31.2 °C; (A), AX_4 *pattern of* $F_5Te^{15}NH_3^+$, (a), ^{125}Te satellites, (B), AX_4 pattern of $F_5Te^{15}N(H)\text{-}Xe^+$, (C), TeF_6, (c), ^{125}Te satellites, (D), AB_4 pattern of a principal decomposition product (not yet assigned), (E), AsF_6^-.

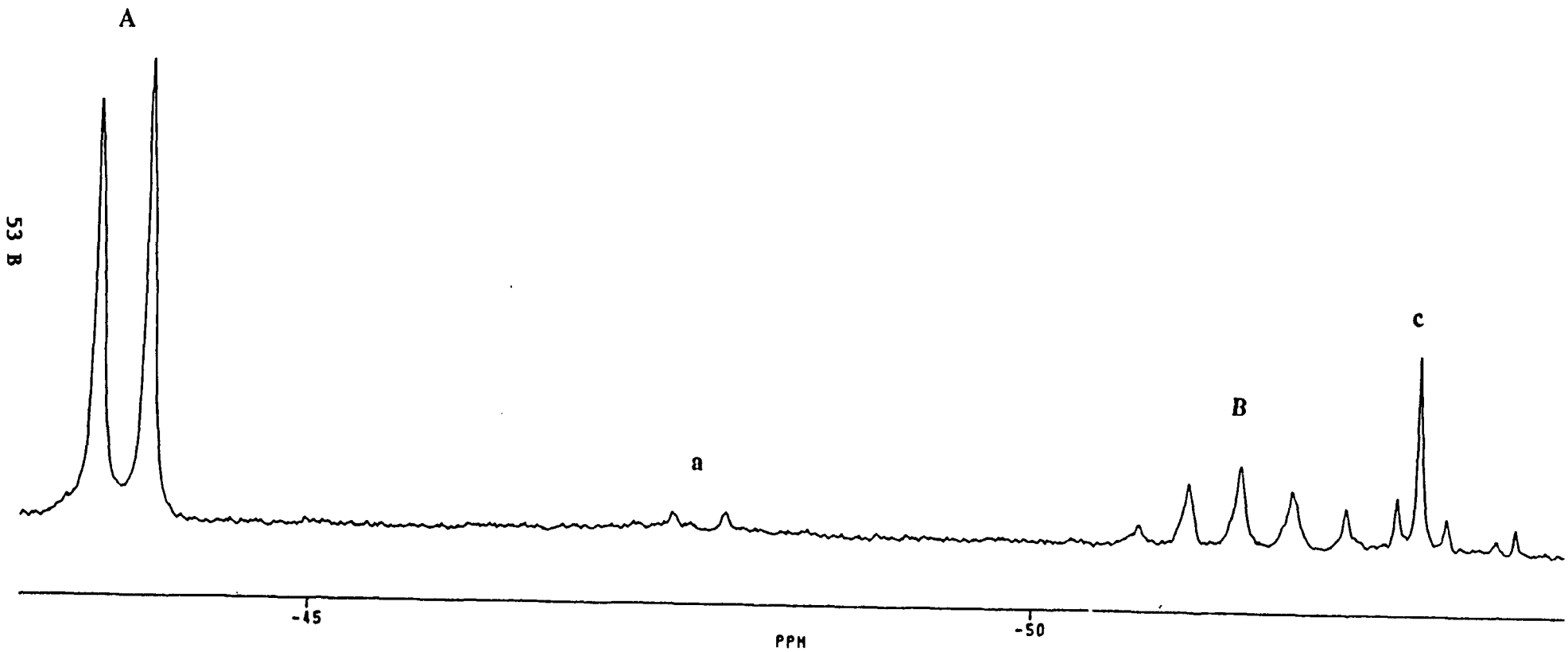

Figure 17. ^{19}F NMR of Equilibrium Mixture of $F_5Te^{15}N(H)\text{-}Xe^+$ and $F_5Te^{15}NH_3^+$ and Decomposition Products of $F_5Te^{15}N(H)\text{-}Xe^+$ in HF at -31.2 °C; (A), AX_4 pattern of $F_5Te^{15}NH_3^+$, (a), ^{125}Te satellites, (B), AX_4 pattern of $F_5Te^{15}N(H)\text{-}Xe^+$, (C), TeF_6, (c), ^{125}Te satellites, (D), AB_4 pattern of a principal decomposition product (not yet assigned), (E), AsF_6^-.

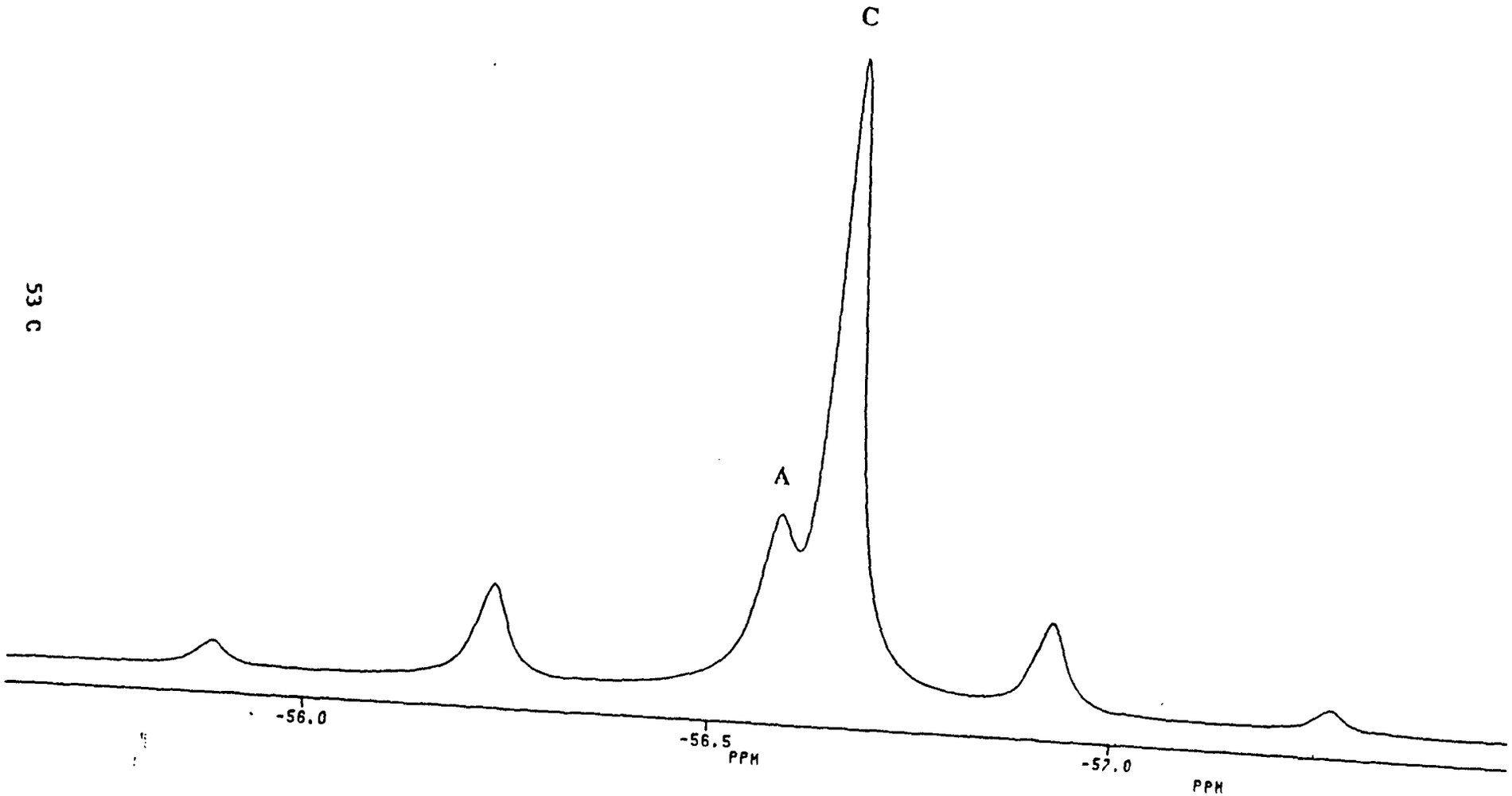

53 C

Figure 17. ^{19}F NMR of Equilibrium Mixture of $F_5Te^{15}N(H)\text{-}Xe^+$ and $F_5Te^{15}NH_3^+$ and Decomposition Products of $F_5Te^{15}N(H)\text{-}Xe^+$ in HF at -31.2 °C; (A), AX_4 pattern of $F_5Te^{15}NH_3^+$, (a), ^{125}Te satellites, (B), AX_4 pattern of $F_5Te^{15}N(H)\text{-}Xe^+$, (C), TeF_6, (c), ^{125}Te satellites, (D), AB_4 pattern of a principal decomposition product (not yet assigned), (E), AsF_6^-.

Figure 18. ^{19}F NMR of Equilibrium Mixture of $F_5Te^5N(H)\text{-}Xe^1$ and $F_5Te^5NH_2^1$ and Decomposition Products of $F_5Te^5N(H)\text{-}Xe^1$ in BrF_5 at 34.0 °C; (A), AX_4 pattern of $F_5Te^5NH_2^1$, (a), ^{125}Te satellites, (B), AX_4 pattern of $F_5Te^5N(H)\text{-}Xe^1$, (C), BrF_5, (c), ^{125}Te satellites, (D), tentatively assigned to BrF_3, (E), AB_4 pattern of a principal decomposition product (not yet assigned), (F), AsF_6^-.

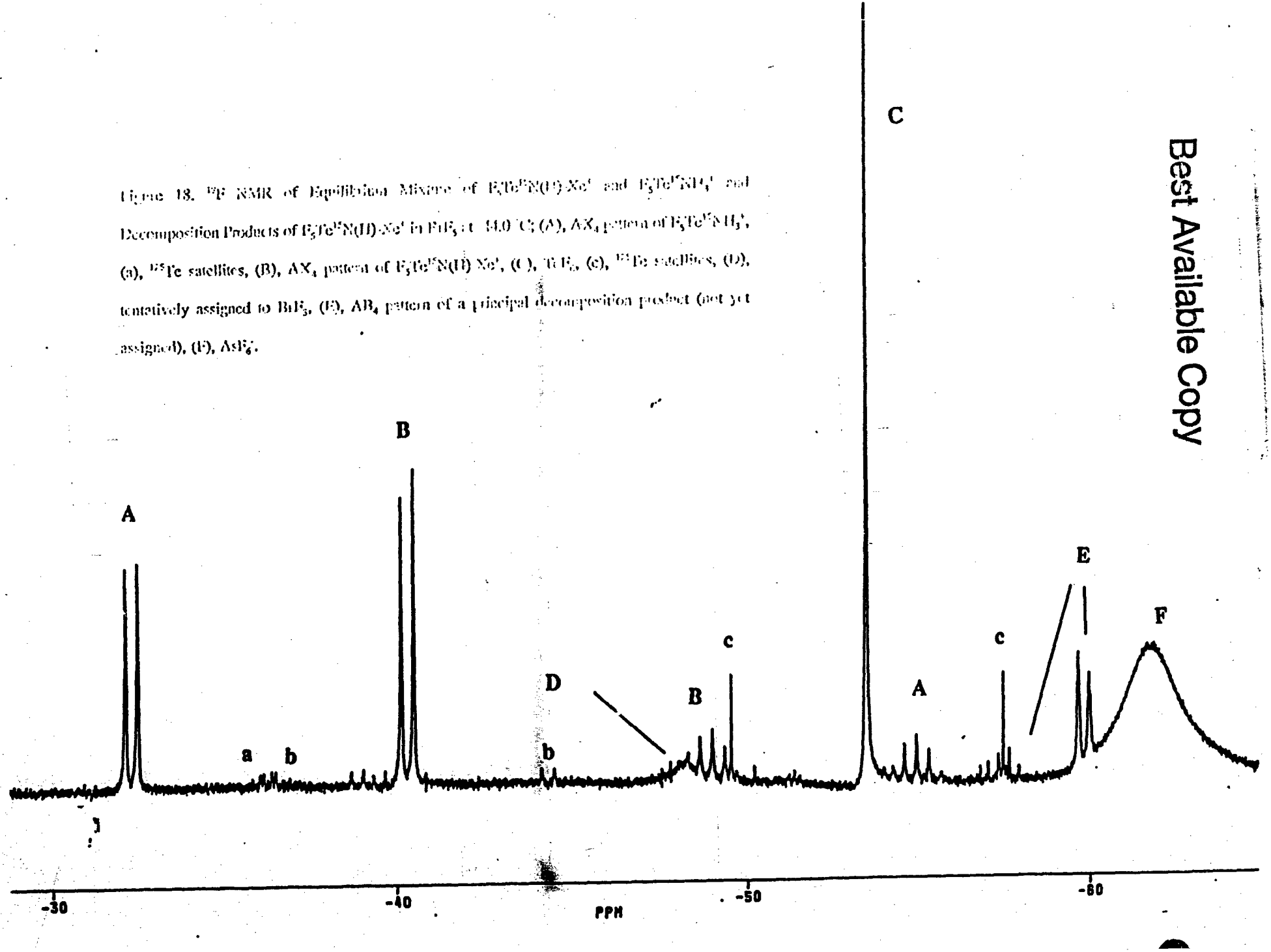

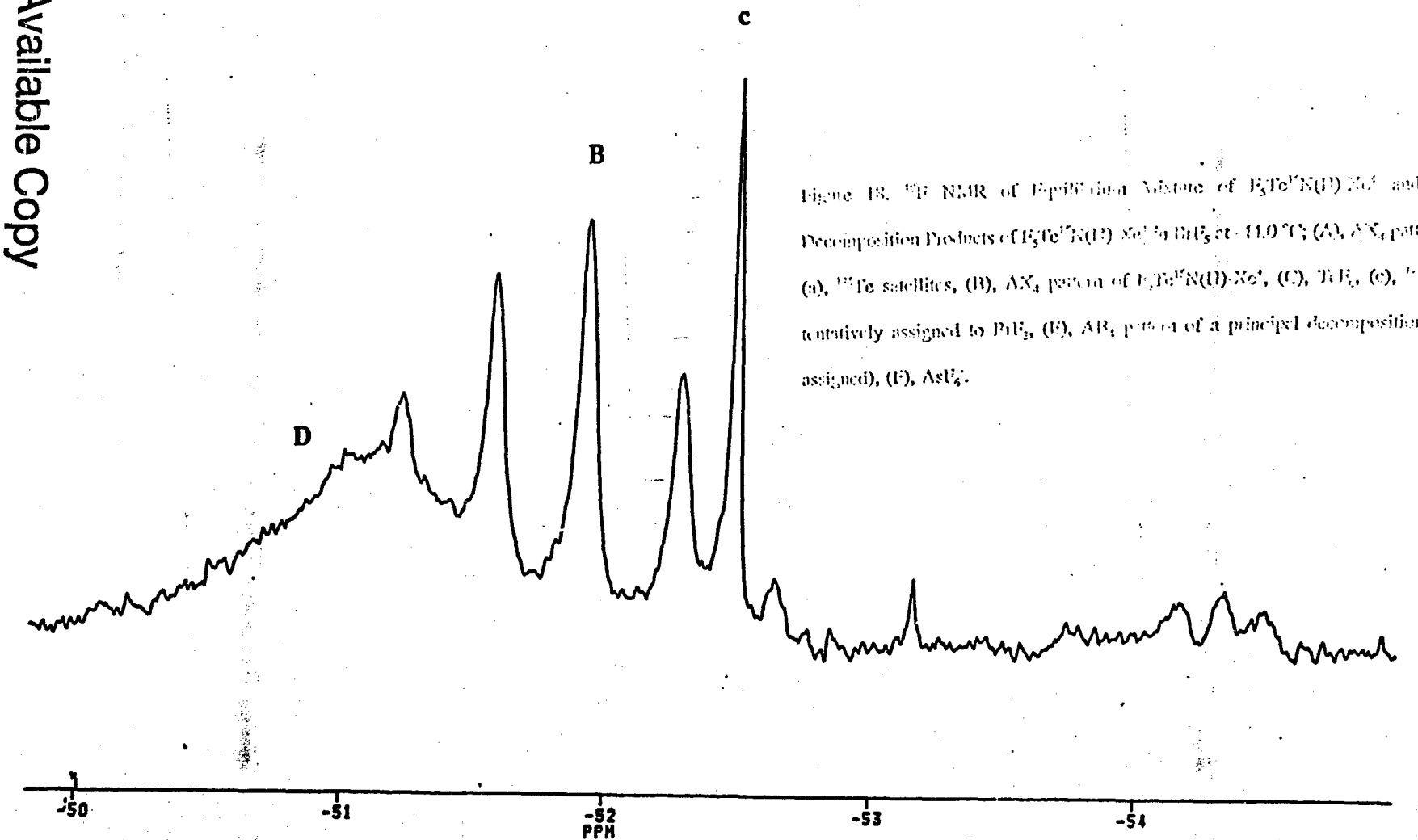

Figure 18. ^{19}F NMR of Equilibration Mixture of $F_5Fe^{IV}N(H)Xe^+$ and $F_5Fe^{IV}NH_4^+$ and Decomposition Products of $F_5Fe^{IV}N(H)Xe^+Sb_2F_{11}^-$ at -11.0 °C; (A), AX_4 pattern of $F_5Fe^{IV}NH_4^+$, (a), ^{57}Fe satellites, (B), AX_4 pattern of $F_5Fe^{IV}N(H)$-Xe^+, (C), TiF_6, (c), ^{57}Fe satellites, (D), tentatively assigned to PtF_5, (E), AB_4 pattern of a principal decomposition product (not yet assigned), (F), AsF_6^-.

Figure 18. ^{19}F NMR of Equilibrium Mixture of $F_5Te^{15}N(H)Xe^+$ and $F_5Te^{15}NH_3^+$ and Decomposition Products of $F_5Te^{15}N(H)Xe^+$ in BrF_5 at -45.0 °C; (A), AX_4 pattern of $F_5Te^{15}NH_3^+$, (a), ^{125}Te satellites, (C), AX_4 pattern of $F_5Te^{15}N(H)$-Xe^+, [illegible], (c), ^{125}Te satellites, [illegible], tentatively assigned to BrF_x, (E), AB_4 pattern of a principal decomposition product (not yet assigned), (F), AsF_6^-.

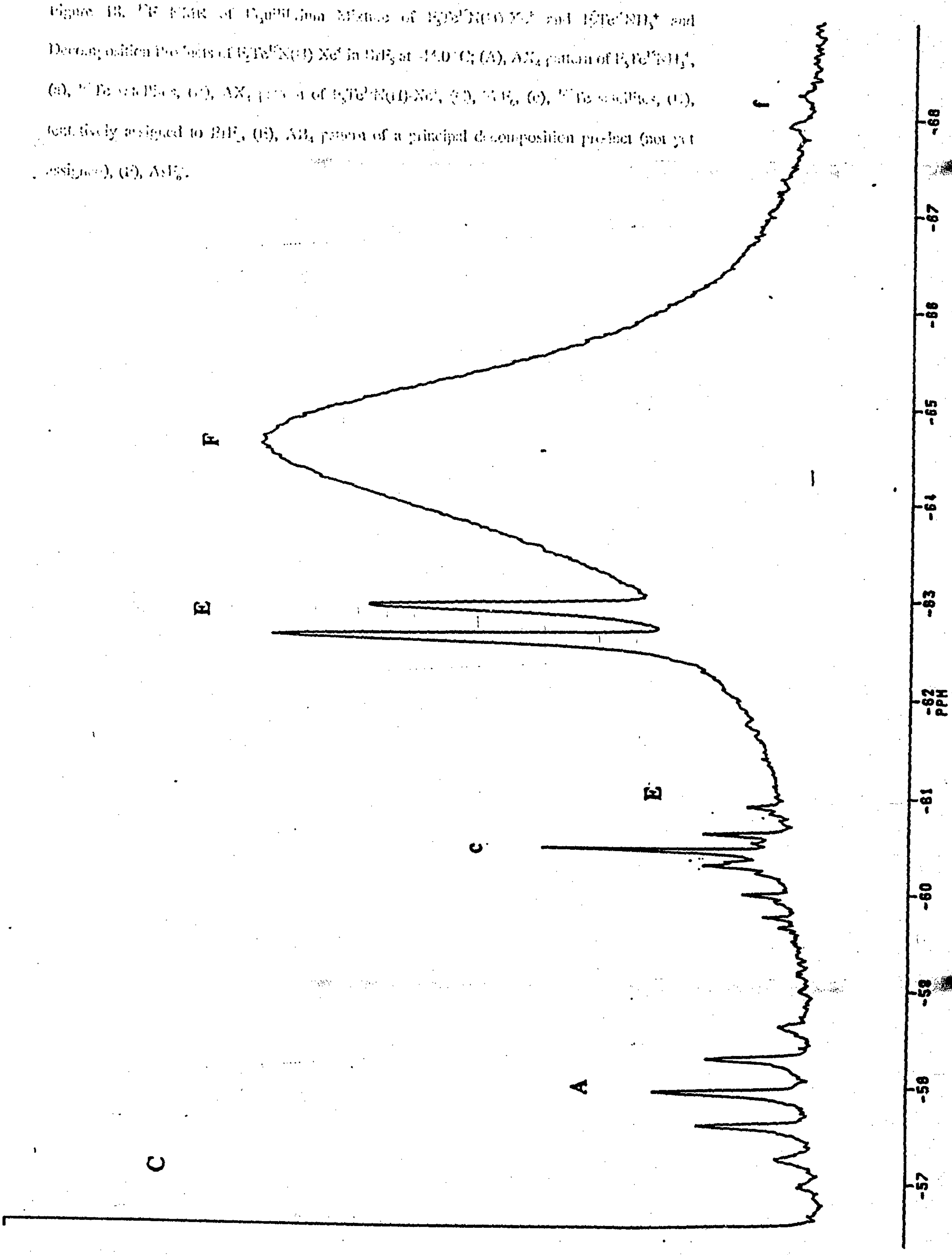

Best Available Copy

lines which were not resolved. From the NMR simulation, the subspectrum parameters were found to be $\delta(^{19}F_{ax})$, -57.3 ppm, $\delta(^{19}F_{eq})$, -59.6 ppm and $^{2}J(^{19}F_{ax}\text{-}^{19}F_{eq})$, 149 Hz. The AB_4 pattern may be due to the dimer TeF_5-N(H)-N(H)-TeF_5, resulting from dimerization of $TeF_5NH\cdot$ radicals formed in the decomposition of the $F_5TeN(H)\text{-}Xe^+$ cation, analogous to the decomposition of $FXeN(SO_2F)_2$ according to equation (40).[42]

$$2\ F\text{-}XeN(SO_2F)_2 \longrightarrow XeF_2 + Xe + [N(SO_2F)_2]_2 \qquad (40)$$

Decomposition of $TeF_5NH\text{-}Xe^+$ in Solution. Tellurium hexafluoride, N_2 gas, Xe gas and HF are the principal decomposition products of the cation $TeF_5N(H)\text{-}Xe^+$. Nitrogen gas was observed as a singlet at ca. -74 ppm in ^{15}N NMR samples in HF and BrF_5. Tellurium hexafluoride was observed by ^{19}F and ^{125}Te NMR. Xenon gas was seen at -5231 ppm in BrF_5 at -57.3 °C and at -5306 ppm in HF at -37.0 °C.

The compound TeF_5NF_2 (Structure II) was observed as an intermediate to the decomposition of $TeF_5N(H)\text{-}Xe^+$ in BrF_5 solvent. The terminal F-on-N resonance, F_t (Figure 19) occurs at 64.2 ppm as a doublet of quintets with ^{125}Te satellites, arising from the couplings $^{1}J(^{19}F_t\text{-}^{15}N)$, 180 Hz, $^{3}J(^{19}F_t\text{-}^{19}F_{eq})$, 15 Hz and $^{2}J(^{19}F_t\text{-}^{125}Te)$, 1025 Hz. The ^{15}N NMR spectrum (Figure 20) of TeF_5NF_2 ($\delta(^{15}N)$, -11.1 ppm) is a triplet of quintets due to the couplings $^{1}J(^{15}N\text{-}^{19}F_t)$, 165 Hz and $^{2}J(^{15}N\text{-}^{19}F_{eq})$, 11 Hz. Difluoroaminotellurium pentafluoride decomposes at -44.4 °C in BrF_5 solvent but is stable for at least 10 h at -58°C. A speculation on the decomposition cannot be made until the presence or absence of F_5TeNF_2 in HF solvent has been established. The dimer $TeF_5N(H)\text{-}N(H)TeF_5$ necessitates radical formation, which may be checked by ESR.

In BrF_5 solvent, the following decomposition is speculated (equation (41) - (44)).

$F_5TeN\text{-}Xe^+\cdots F\text{-}AsF_5^- \longrightarrow F_5TeNHF + Xe + AsF_5$ (41)

$F_5TeNHF + \frac{1}{2} BrF_5 \longrightarrow F_5TeNF_2 + \frac{1}{2} BrF_3 + HF$ (42)

$F_5TeNF_2 + AsF_5 \longrightarrow TeF_6 + F\text{-}N{=}N\text{-}F$ (cis and trans) (43)

$F\text{-}N{=}N\text{-}F \longrightarrow N_2 + N_2F_4 + NF_3$ .... (44)

Difluoramino compounds are thermally unstable and the Lewis acid AsF_5 is known to lower the kinetic barrier by catalysis for decomposition. The catalysis of $ClNF_2$ by AsF_5 at -78 °C results in Cl_2, N_2, NF_3 and several minor amounts of N-F compounds.[69]

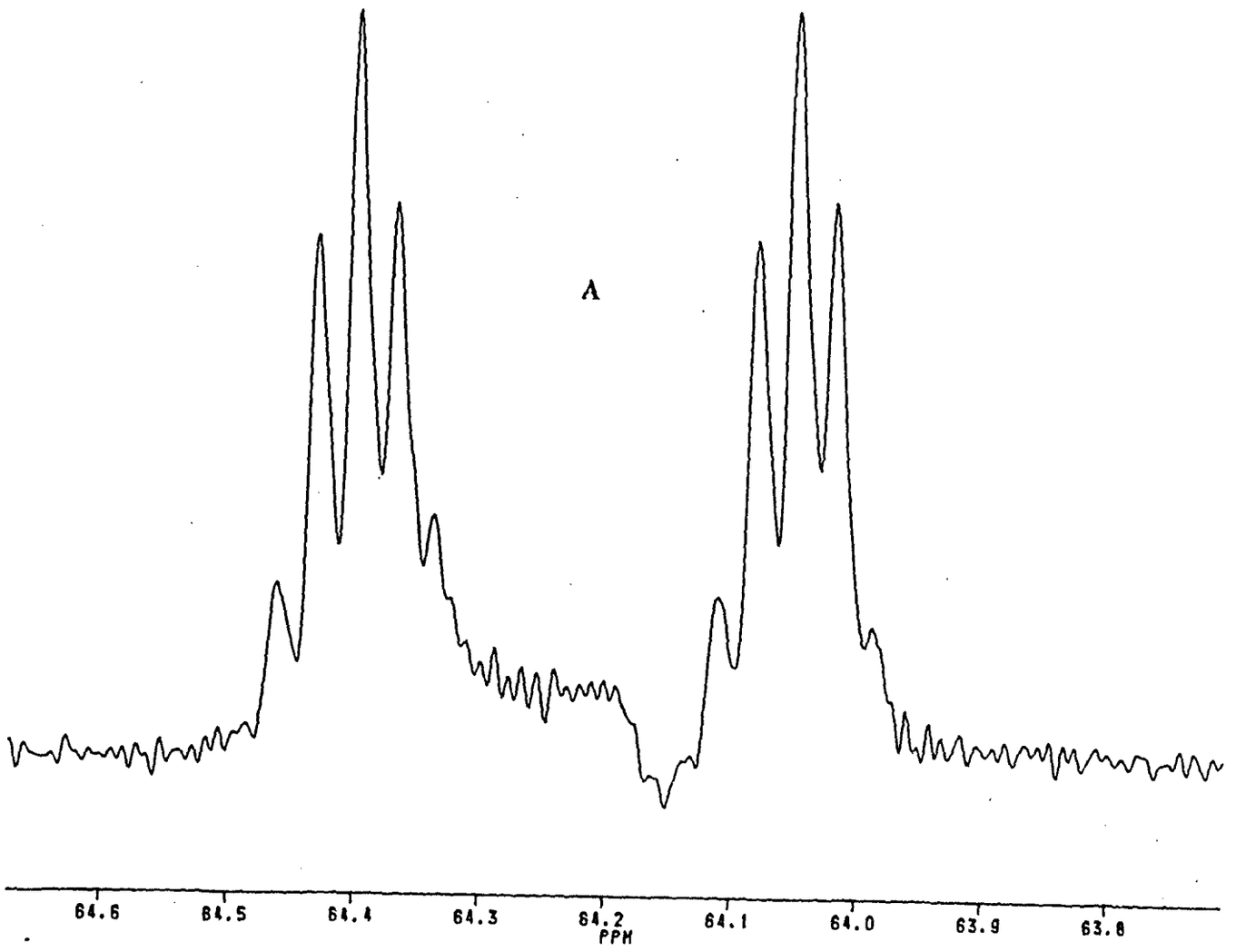

Figure 19. ^{19}F NMR of 99% $F_2{}^{15}NTeF_5$ in BrF_5 at -44.4 °C; (A) doublet of quintets, (a) ^{125}Te satellites.

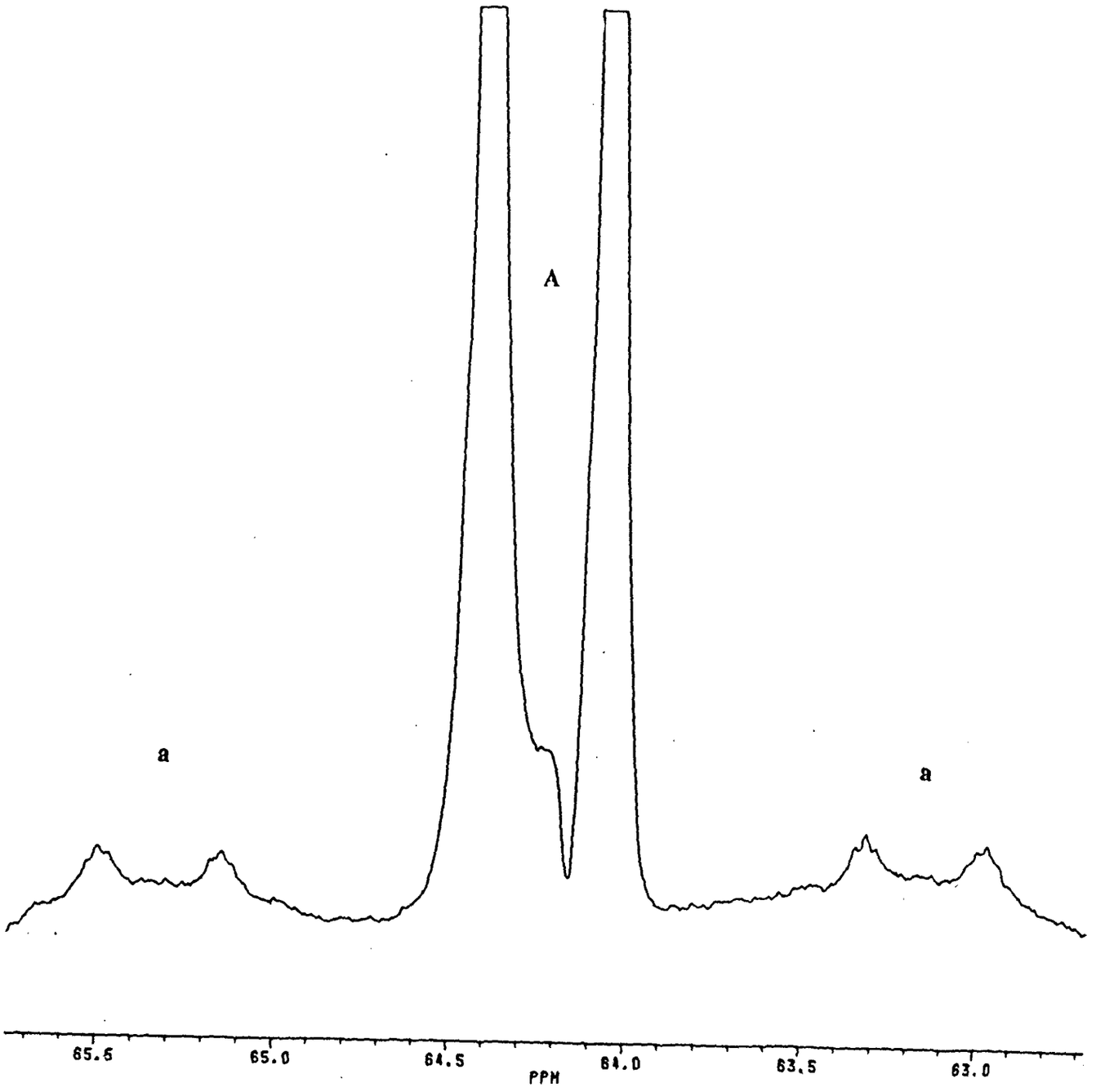

Figure 19. ^{19}F NMR of 99% $F_2{}^{15}NTeF_5$ in BrF_5 at -44.4 °C; (A) doublet of quintets, (a) ^{125}Te satellites.

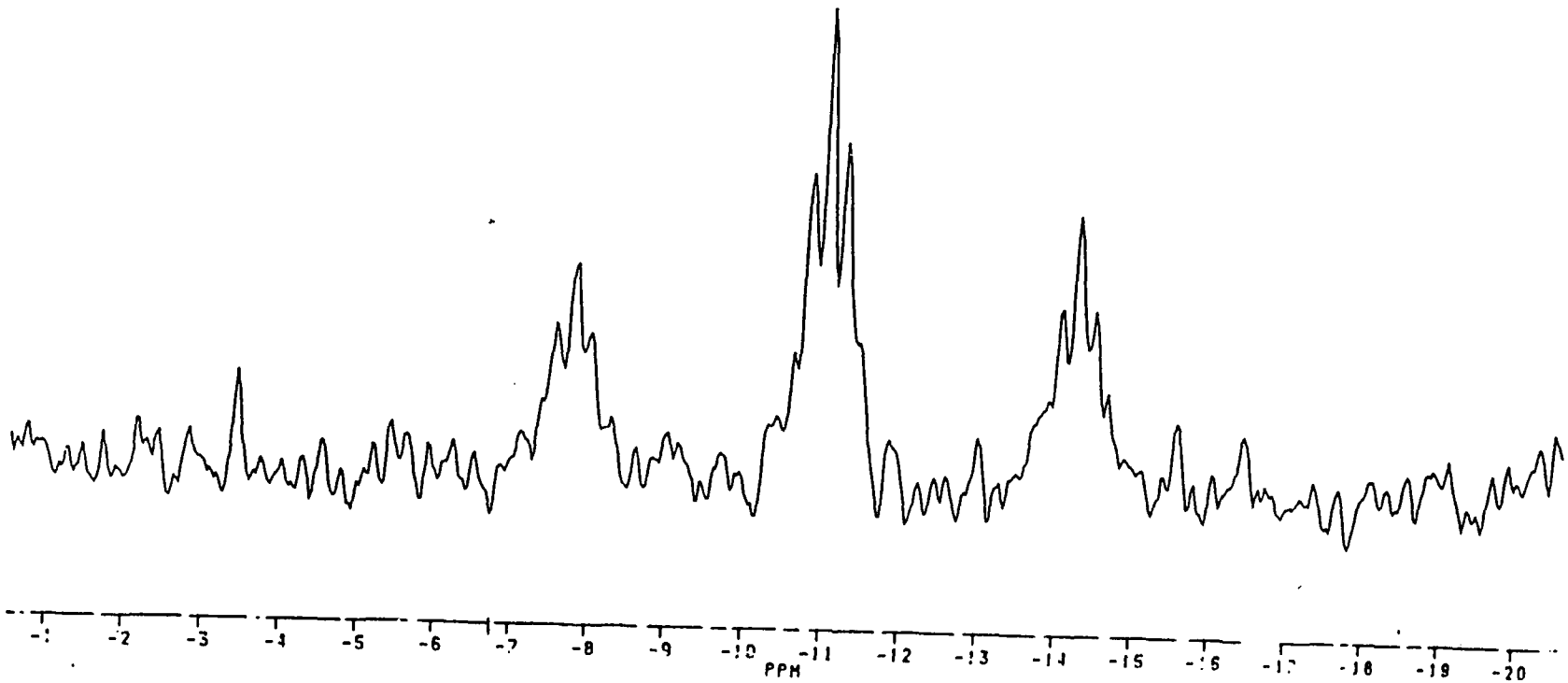

Figure 20. ^{15}N NMR of 99% $F_2{}^{15}NTeF_5$ in BrF_5 at -58 °C.

Investigation of the Lewis Acid Properties of the $F_5TeNH\text{-}Xe^+$ Cation.

Reaction of $TeF_5N(H)\text{-}Xe^+$ and XeF_2 in Solution.

The salt $TeF_5NH_3^+AsF_6^-$ and XeF_2 were combined in a 1:2 mole ratio in BrF_5 solvent at -55 °C in an attempt to synthesize the fluorine bridged species $F_5TeN(H)\text{-}Xe\cdot\cdot F\cdot\cdot Xe\text{-}F^+$ by reaction of a stoichiometric amoint of XeF_2 and $TeF_5NH\text{-}Xe^+$ (Equation (45)).

$$XeF_2 + F_5TeNH\text{-}Xe^+ \longrightarrow F\text{-}Xe\cdot\cdot F\cdot\cdot Xe\text{-}N(H)\text{-}TeF_5^+ \qquad (45)$$

Characterization by ^1H and ^{19}F NMR spectroscopy at -55 °C showed typical resonances for the $F_5TeN(H)\text{-}Xe^+$ cation and excess XeF_2, indicating no reaction.

Reaction of $HC\equiv N$ with $F_5TeN(H)\text{-}Xe^+$ in HF Solution. The cation $F_5TeN(H)\text{-}Xe^+$ was generated as above (equation (35)). A stoichiometric amount of $HC\equiv N$ was added, producing a colorless solution and white precipitate at -78 °C (equation (46))

$$F_5TeN(H)\text{-}Xe^+ + HC\equiv N \longrightarrow HC\equiv N\text{-}Xe\text{-}N(H)TeF_5^+ \qquad (46)$$

The ^{19}F NMR spectrum at -31.0 °C (Figure 21) shows that $F_5TeN(H)\text{-}Xe^+$ reacts quantatively as indicated by the disappearance of the F_{ax} resonance at -51.6 ppm and the appearance of a F_{ax} resonance at -56.5 ppm, corresponding to a 4.95 ppm complexation shift of this resonance upon adduct formation. The F_{eq} resonance is shifted to low frequency by 1.4 ppm. Unreacted $TeF_5NH_3^+$ is also present, as shown by the F_{ax} and F_{eq} resonances at -56.4 and -37.0 ppm, respectively. The ^1H NMR spectrum at -31.0 °C (Figure 22) shows a resonance at 6.1 ppm which has a doublet of satellites attributable to $^3J(^1H\text{-}^{129}Xe)$ = 24.4 Hz. Hydrogen cyanide is protonated in anhydrous HF solution; the proton-on-carbon resonance is at $\delta(^1H)$ = 4.5 ppm. The $F_5TeNH_3^+$ resonance is obscured by the HF solvent resonance in the ^1H NMR spectrum.

Figure 21. ^{19}F NMR of HCN and $TeF_5N(H)Xe^+AsF_6^-$ in HF at -31.0 °C; (A), $F_5TeNH_3^+$ equatorial resonance, (a), ^{125}Te satellites, (a'), ^{123}Te satellites, (B), $F_5TeN(H)$-Xe-NCH^+ equatorial fluorine resonance, (b), ^{125}Te satellites, (C), TeF_6, (D), $F_5TeNH_3^+$ axial fluorine resonance, (E), $F_5TeN(H)$-Xe-NCH^+ axial fluorine resonance, (F), AsF_6^-.

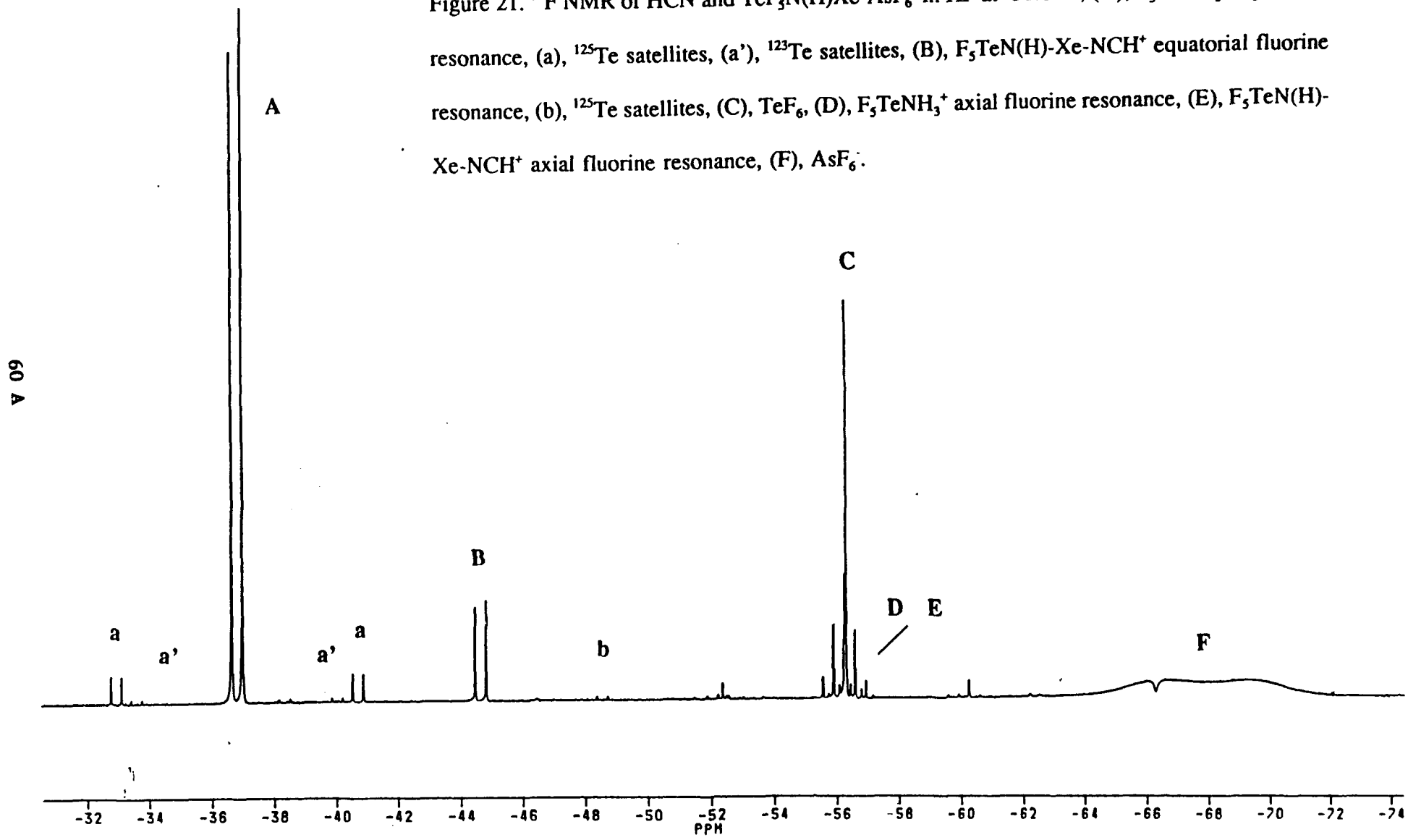

Figure 21. ^{19}F NMR of HCN and $TeF_5N(H)Xe^+AsF_6^-$ in HF at -31.0 °C; (A), $F_5TeNH_3^+$ equatorial resonance, (a), ^{125}Te satellites, (a'), ^{123}Te satellites, (B), $F_5TeN(H)$-Xe-NCH^+ equatorial fluorine resonance, (b), ^{125}Te satellites, (C), TeF_6, (D), $F_5TeNH_3^+$ axial fluorine resonance, (E), $F_5TeN(H)$-Xe-NCH^+ axial fluorine resonance, (F), AsF_6^-.

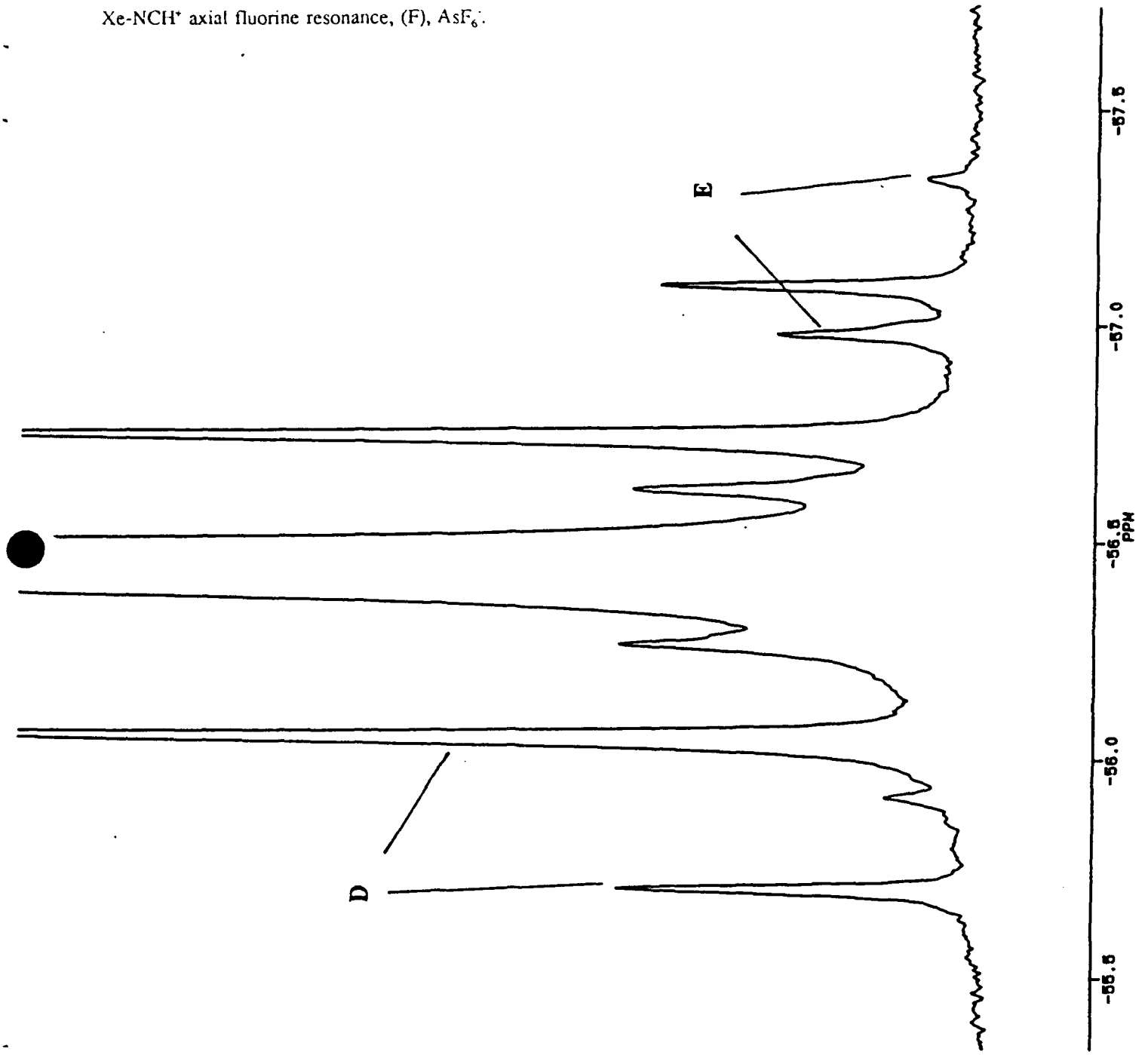

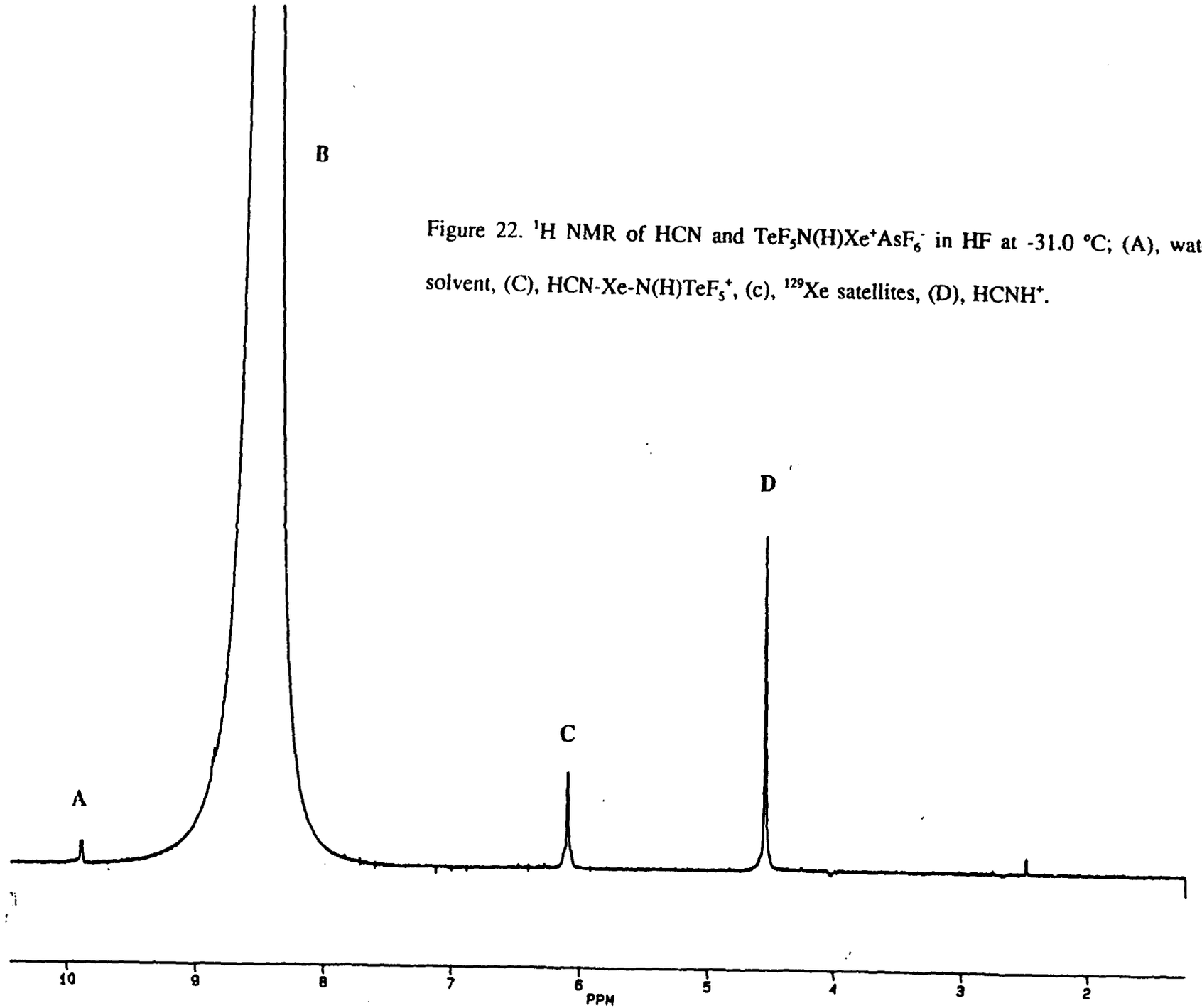

Figure 22. ^{1}H NMR of HCN and $TeF_5N(H)Xe^{+}AsF_6^{-}$ in HF at -31.0 °C; (A), water, (B) HF solvent, (C), HCN-Xe-$N(H)TeF_5^{+}$, (c), ^{129}Xe satellites, (D), $HCNH^{+}$.

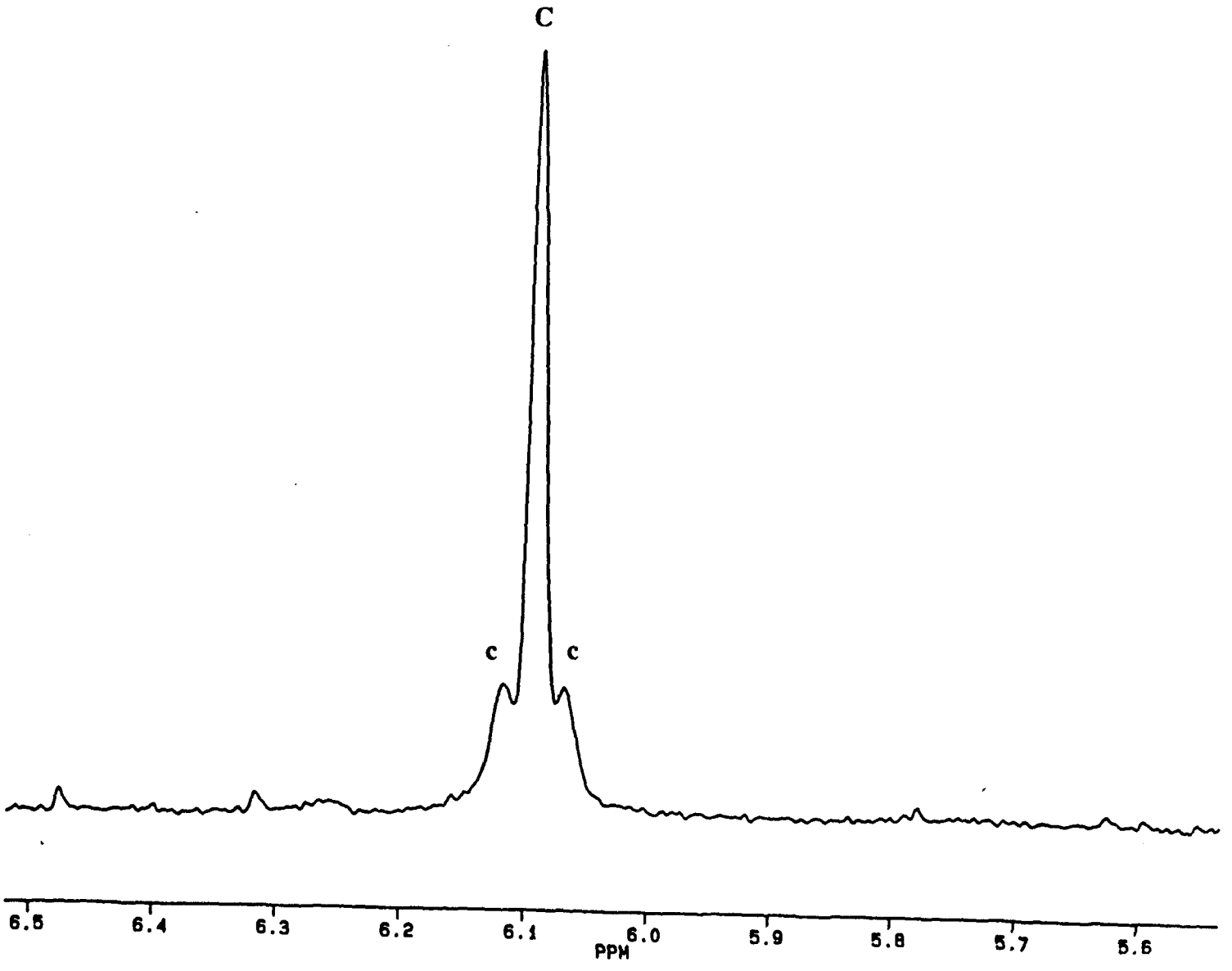

Figure 22. ^{1}H NMR of HCN and $TeF_5N(H)Xe^{+}AsF_6^{-}$ in HF at -31.0 °C; (A), water, (B) HF solvent, (C), HCN-Xe-N(H)TeF_5^{+}, (c), ^{129}Xe satellites, (D), $HCNH^{+}$.

Crystal Structure Determination of $TeF_5NH_3^+AsF_6^-$. The crystal structure of the salt $F_5TeNH_3^+AsF_6^-$ was solved with the assumption that it would provide complementary data for the structure of the salt $F_5TeN(H)\text{-}Xe^+AsF_6^-$. A mixture of orange and white crystals ($F_5TeNH_3^+AsF_6^-$) have been obtained from the reaction of TeF_5NH_2 and $XeF^+AsF_6^-$ at -36 °C in HF solvent. The orange crystals, which are believed to be $F_5TeN(H)\text{-}Xe^+AsF_6^-$, are stable at -30 °C under dynamic vaccum. No change in physical appearance was noted at room temperature under static vacuum. Further pumping at -30 °C resulted in decomposition to an orange powder. This indicated that solvent molecules may be present in the crystal. An attempt at determinating the crystal structure was postponed until a cold table, currently under construction, was available. This would enable one to mount the crystals in capillaries at low temperature (-78 to -30 °C).

Crystal Data. The compound $As_2F_{11}TeNH_3$ (f_w = 428.53 g mol^{-1}), crystallizes in the monoclinic system, space group $P2_1$; a = 4.8221(8), b = 17.010(2), c = 4.9564(9) Å; β = 94.46(1)°; D_{calcd} = 3.511 g cm^{-3} for Z = 2. Ag(K_α) radiation (λ = 0.56087 Å, μ(Ag K_α) = 41.6 cm^{-1}) was used.

Solution and Refinement of the Structure. The XPREP program was used for determining the correct cell and space group and first confirmed the original cell and that the lattice was monoclinic primitive. The two space groups which were consistent with the systematic absences were the chiral $P2_1$ (4) and the non-centrosymmetric $P2_1/m$ (11) space groups. The structure was solved by Dr. H.P. Mercier in both space groups.

The structure was first solved in the space group $P2_1/m$. The solution was obtained by direct methods which located the positions of the Te and As atoms. The Te was located on the

mirror plane and the As on the inversion center. The full matrix least-squares refinement of the positions and isotropic thermal parameters of the Te and As atoms gave a conventional agreement index R (= Σ |F_o| - |F_c| / Σ |F_o|) of 0.21. The resulting difference Fourier synthesis revealed the positions of atoms bonded to the Te and As atoms. Around the Te, two atoms were located on the miror plane, while two others were positioned on general positions; there was however no difference in the bond lengths which could allow the distinction of the N atom from the F atoms. Around the As, all the atoms were located on general positions. Refinement of positional and isotropic temperature parameters for all atoms (the N atom being assigned a F scattering factor) converged at R = 0.14, but there was still no difference in bond lengths, or in thermal parameters among the F bonded to the Te atom. This was suggesting that the N atom was positionally disordered around the Te.

The structure was also solved by direct methods in the $P2_1$ space group which this time located the positions of the two heavy atoms on general positions. The two atoms were first assigned Te scattering factors and the y value of one of them was fixed to define the origin. The full matrix least-squares refinement of the positions and isotropic thermal parameters of the Te atoms gave an agreement index R of 0.22. The resulting difference Fourier revealed the general positions of twelve atoms bonded to these tellurium atoms. However, there was still no real difference in the environment of the two heavy atoms which could allow distinction between the As and the Te atoms. Consequently, the positions and isotropic thermal parameters of all atoms (the heavy atoms being assigned a tellurium scattering factor, the lighter ones, a fluorine scattering factor) were refined, and this resulted in a drop of the residual R to 0.102. At this stage, it was possible to distinguish some differences in the stereochemistry about the two heavy

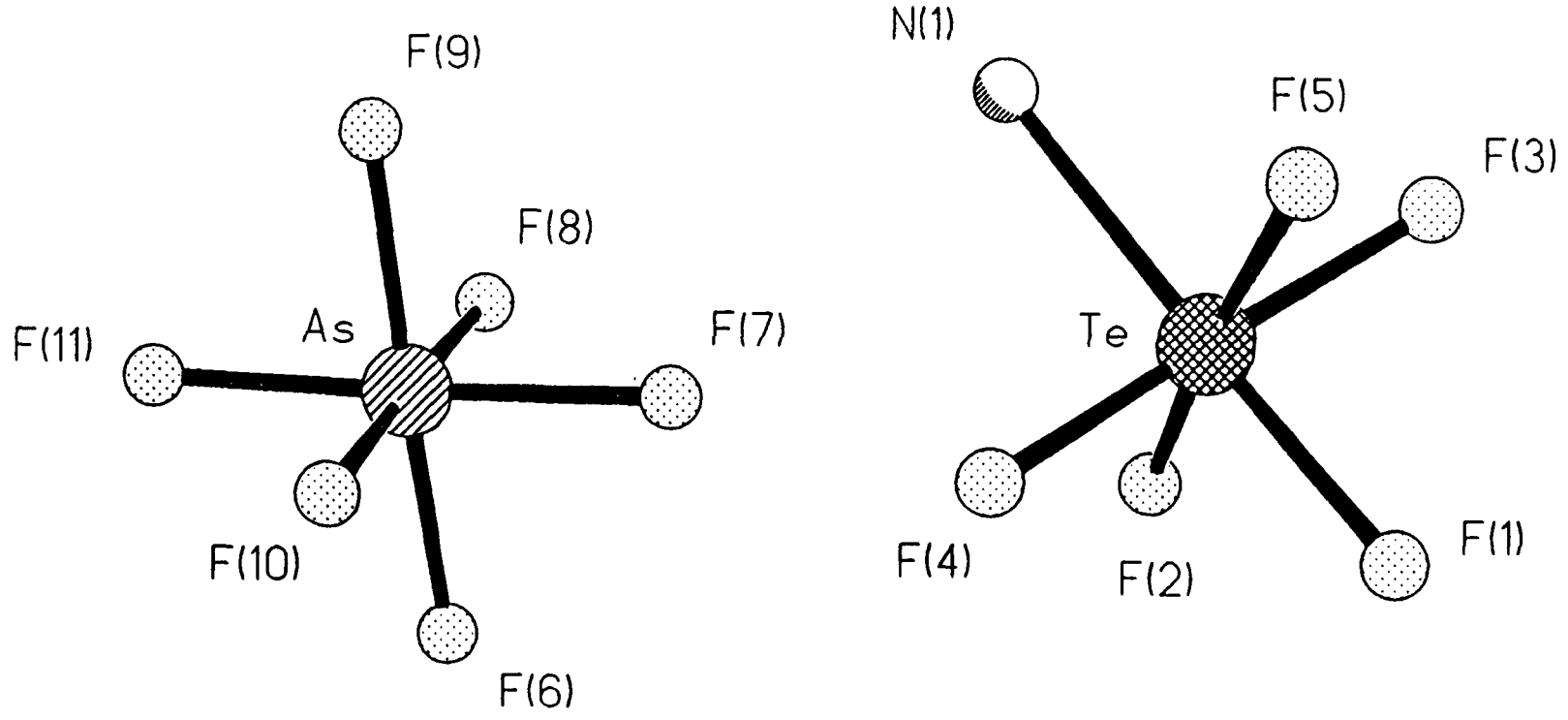

Figure 23. Partially Solved Crystal Structure of $F_5TeNH_3^+AsF_6^-$

atoms. One of them showed shorter "Te"-F bond lengths and was consequently assigned to the As atom. The other one showed one longer Te-"F" bond length (1.91 Å), indicating that the fluorine atom was in fact the missing nitrogen atom. Scattering factors for As and N were introduced and resulted in a residual R = 0.083. An improvement of the structure was achieved by introducing anisotropic thermal parameters for the two heavy atoms (R = 0.066).

Complete structure solution awaits an analytical absorption correction of the data using the program DIFABS. The structure as determined without absorption correction is shown in Figure (23).

Part 2: The Formation of a Lewis Acid-Base Adduct between $CF_3C(O)NH_2$ and XeF^+

Introduction. The first ionization potential of $CF_3C(O)NH_2$ (10.77 eV)[70] suggests that it will withstand oxidative attack by the XeF^+ cation. The potential of this ligand as a Lewis base has not been evaluated by reacting it with typical Lewis acids such as BF_3 or AsF_5 but amides in general coordinate to Lewis acids to form adducts through the carbonyl oxygen[71] as shown in equation (46) as opposed to the amide nitrogen.[71,72]

R-C(O)NR'(R") + M ———> R-C(O-M)NR'R" (M = Lewis acid) (46)

Adduct formation with other Lewis acids is occurs at oxygen as illustrated in the bulk of examples involving main group and transition metal Lewis acid centers.[72-81] The inactivity of the amido nitrogen is attributed to partial (p-p)π bonding between the carbonyl carbon and the lone pair on nitrogen which occupies an orbital with p character. The expected hybridization at nitrogen is sp^2, and this is corroborated by the observed planar geometry of the nitrogen center in acetamide and formamide[82] and the hindered rotation about the C-N bond in $CFH_2C(O)NH_2$,

$CF_2HC(O)NH_2$ and $CF_3C(O)NH_2$ on the ^{19}F NMR time scale.[83,84]

It was not certain whether the ligand $CF_3C(O)NH_2$ would behave as a nitrogen or an oxygen donor towards the cation XeF^+, although the majority of Lewis acids coordinate via the carbonyl oxygen. In the following study it was found that a xenon-oxygen bond was formed.

The cation $CF_3C(O\text{-}XeF)NH_2^+$ was generated in solution by combining stoichiometric amounts of XeF_2 and $CF_3C(OH)NH_2^+AsF_6^-$ at -60 to -55 °C in BrF_5 solvent (equation (47)) giving a colorless solution.

$$CF_3C(OH)NH_2^+AsF_6^- + XeF_2 \longrightarrow CF_3C(O\text{-}XeF)NH_2^+AsF_6^- + HF \qquad (47)$$

Structure of the $CF_3C(OH)NH_2^+$ Cation in Solution. The salt $CF_3C(OH)NH_2^+AsF_6^-$ was prepared by combining $CF_3C(O)NH_2$ and a 30 mole % excess of AsF_5 in HF solvent at -50 °C (equation (48)).

$$CF_3C(O)NH_2 + AsF_5 \longrightarrow CF_3C(OH)NH_2^+AsF_6^- \qquad (48)$$

The salt was isolated as a white powder by removal of the solvent and excess AsF_5 at -50 °C, and was found to slowly decompose over one month at room temperature under anhydrous conditions. The salt was characterized by ^{13}C, ^1H and ^{19}F NMR spectroscopy in BrF_5 solvent (Table 6). Gillespie and Birchall[71,85] have studied selected amides in fluorosulfuric acid by low-temperature ^1H NMR spectroscopy. Protonation occurred exclusively at oxygen. The proton-on-oxygen resonance occcurs at ca. 10 ppm and is seen only when exchange broadening is minimized at low temperature (-70 to -80 °C) and in highly acidic media. The ^1H NMR spectrum of $CF_3C(OH)NH_2^+AsF_6^-$ in BrF_5 solution at -55.4 °C (Figure 24) shows a resonance at $\delta(^1H)$ = 11.6 ppm, characteristic of the protonated carbonyl group (Structure III). The two broad peaks

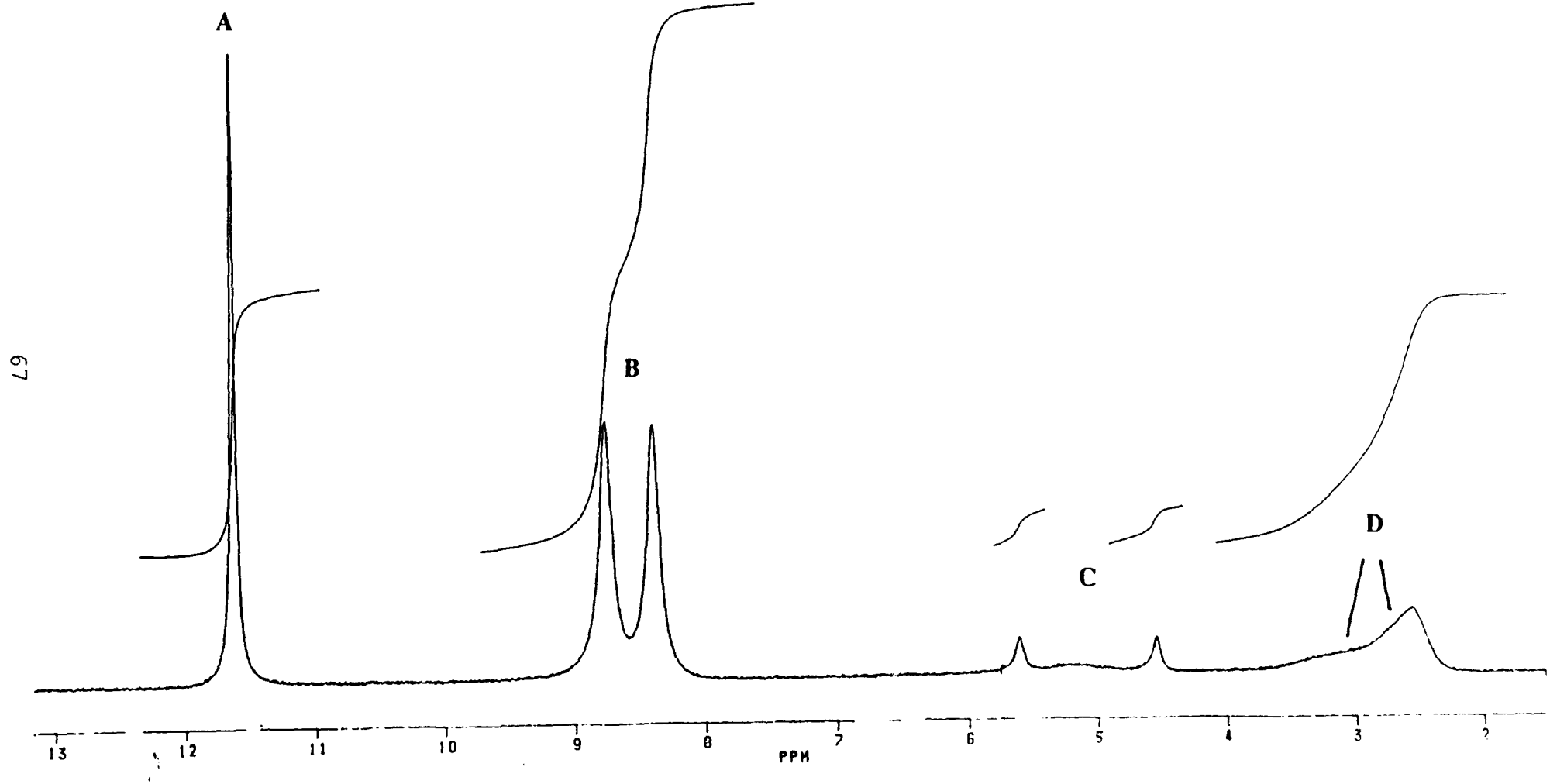

Figure 24. ^1H NMR of $CF_3C(OH)NH_2^+AsF_6^-$ in BrF_5 solution at -55.4 °C; (A), protonated carbonyl group, (B), protons on nitrogen, (C) HF, assumed to br a residue from the protonation of $CF_3C(O)NH_2$ in HF / AsF_5, (D), unidentified resonances.

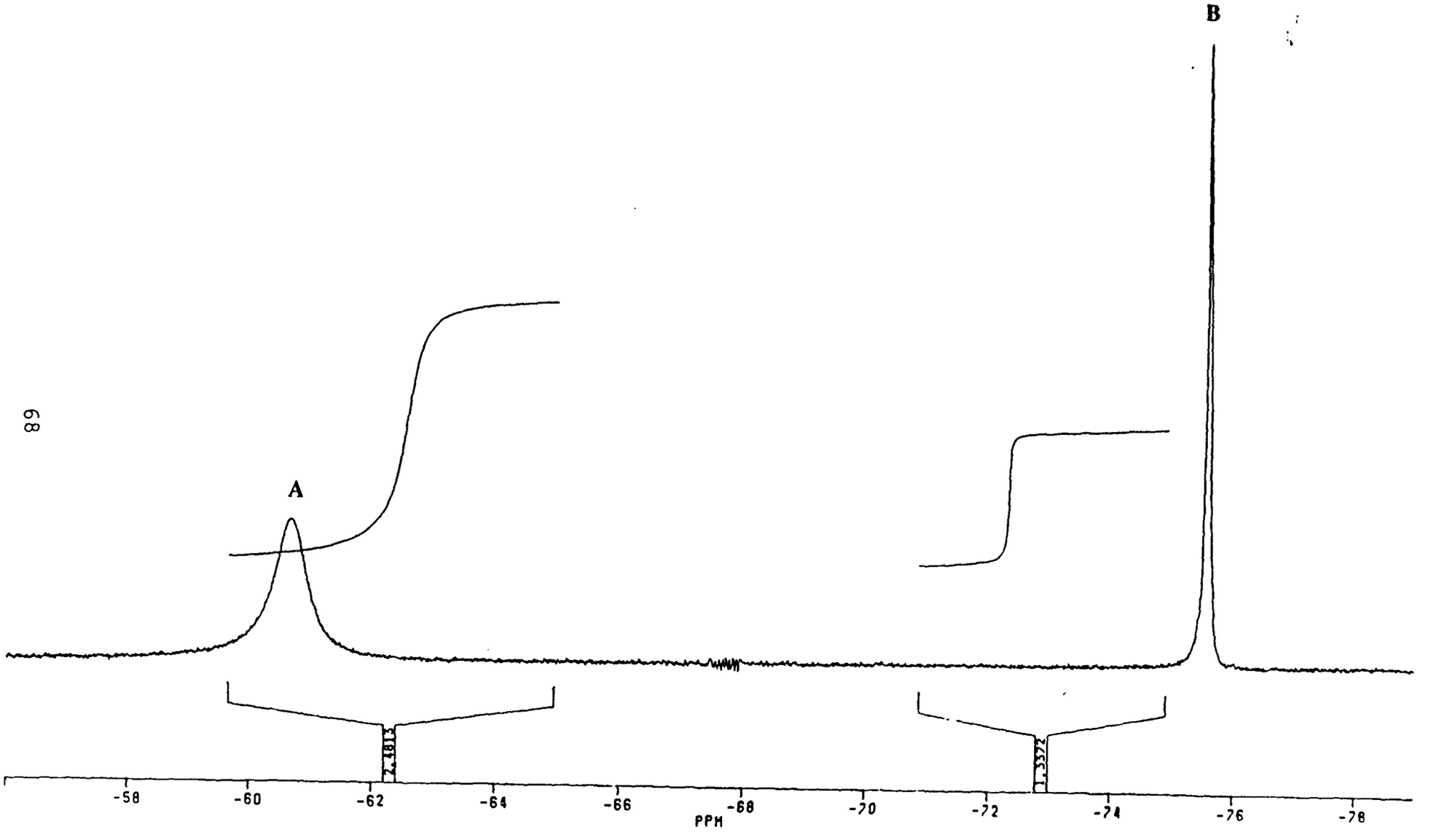

Figure 25. ^{19}F NMR spectrum of $CF_3C(OH)NH_2^+AsF_6^-$ in BrF_5 solvent at -54.0 °C; (A), AsF_6^-, (B), CF_3 resonance. The integration ratio is 2 (A : B).

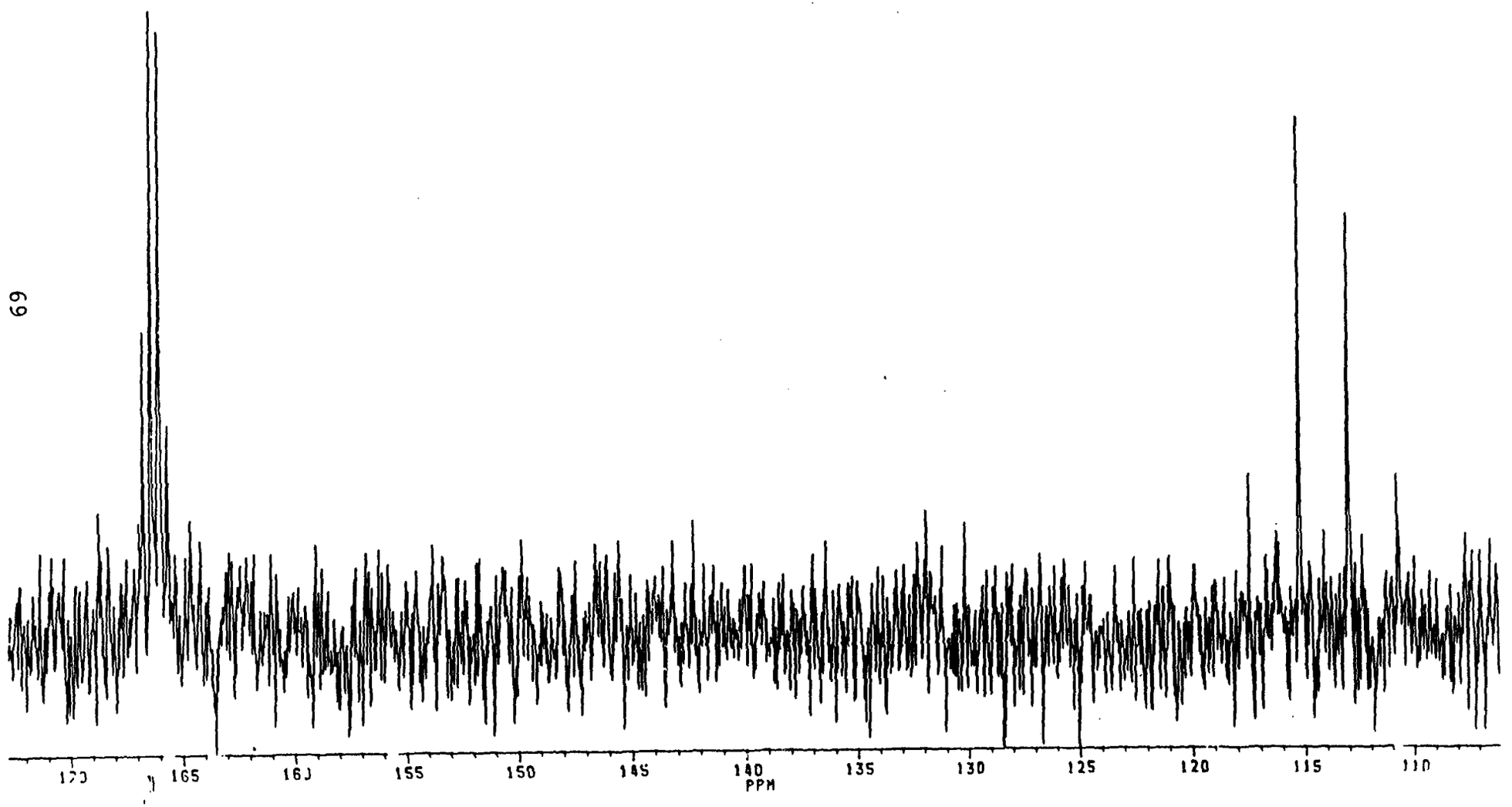

Figure 26. ^{11}H decoupled ^{13}C NMR spectrum at -56.2 °C in BrF_5; (A), carbonyl group, quartet due to two-bond couipling to fluorines, (B), CF_3 resonance.

at 8.8 and 8.4 ppm have equal integrated intensities and are attributed to the protons on nitrogen. Similar resonances at 8.24 and 8.36 ppm are seen in the spectrum of acetamide in fluorosulfuric acid at -80 °C. Hindered rotation arising from C-N double bond character in protonated amides results in the observation of two separate resonances at low temperature for the protons bonded to the trigonal planar nitrogen; one *cis* and one *trans* to the carbonyl group. It is not possible to discern which of the protons on nitrogen peaks corresponds to which proton.

The ^{19}F NMR spectrum of $CF_3C(OH)NH_2^+AsF_6^-$ in BrF_5 solvent at -54.0 °C (Figure 25) consists of a singlet at -75.6 ppm, which is typical for the $CF_3(C=O)$- linkage, and a broad resonance at -60.7 ppm assigned to the octahedral AsF_6^- anion. The $-CF_3$ and AsF_6^- resonances integrate in the ratio 1:2 as expected. The ^1H decoupled ^{13}C NMR spectrum at -56.2 °C (Figure 26) showed two quartets at $\delta(^{13}C)$ = 114.0 ppm (CF_3) and 166.2 ppm (C=O). These are typical ^{13}C chemical shifts for these environments. The magnitude of the one-bond coupling constant $^1J(^{13}C\text{-}^{19}F)$ =284 Hz, which is typical for a fluorine bonded to an sp^3 hybridized carbon. A negative signis assumed. The two-bond coupling, $^2J(^{13}C\text{-}^{19}F)$, is 46 Hz.

Characterization of the Adduct Cation $CF_3C(O\text{-}XeF)NH_2^+$ in Solution. Characterization in solution was carried out by ^1H, ^{19}F and ^{129}Xe NMR spectroscopy (Table 7). The peaks at 11.6 and at 8.8 and 8.4 ppm in the ^1H NMR spectrum at -55.4 °C (Figure 27) correspond to the cation $CF_3C(OH)NH_2^+$. New resonances at 7.88 and 7.71 ppm integrate with relative intensities 1:1 and are assigned to the adduct cation $CF_3C(O\text{-}XeF)NH_2^+$. The presence of two sets of H-on-N peaks and one H-on-O indicates an equilibrium between the two species, with formation of a xenon-oxygen bond.

Table 6. Chemical Shifts and Spin-Spin Coupling Constants for the Salt $CF_3C(OH)NH_2^+AsF_6^-$ in BrF_5 Solvent.

Chemical Shift (ppm)[a]		T (°c)
$\delta(^{19}F)$[b]	-75.6	-54.0
$\delta(^{13}C)$[c]	166.2 (C=O), q 114.0 (CF_3), q	-56.2
$\delta(^{1}H)$	11.6 (-O-H$^+$), s 8.8 (N-H), s 8.4 (N-H'), s	-55.4
	Coupling Constants (Hz)	
$^{1}J(^{13}C-^{19}F)$	-284 (CF_3)	
$^{2}J(^{13}C-^{19}F)$	46 (C=O)	

[a] Samples were referenced externally at 24 °C with respect to the neat liquid references $CFCl_3$ (^{19}F) and $(CH_3)_4Si$ (^{1}H and ^{13}C). A positive chemical shift denotes a resonance occurring to high frequency of the reference compound. The symbols s and q denote singlet and quartet multiplicities. [b] The ^{19}F spectrum displayed a broad redonance at ca. -61 ppm arising from the partially quadrupole-collapsed $^{1}J(^{75}As-^{19}F)$ of the octahedral AsF_6^- anion. [c] ^{1}H decoupled.

Table 7. Chemical Shifts and Spin-Spin Coupling Constants for the Adduct Cation $CF_3C(O\text{-}XeF)NH_2^+$ in BrF_5 Solvent.

	Chemical Shift (ppm)[a]	T (°C)
$\delta(^{129}Xe)$	-1578, d[b]	-53.0
$\delta(^{19}F)$[c]	-74.4 (CF_3), s -183.1 (F-on-Xe), s[d]	-54.0
$\delta(^{1}H)$[e]	7.88 (N-H) 7.71 (N-H')	-55.4

[a] The symbols s and d denote singlet and doublet multiplicity patterns. [b] The doublet splitting is attributed to $^1J(^{129}Xe\text{-}^{19}F)$ = 5991 Hz. Xenon difluoride is present, $\delta(^{129}Xe)$ = -1572 ppm; $^1J(^{129}Xe\text{-}^{19}F)$ = 5651 Hz. [c] The ^{19}F spectrum displayed a broad resonance at ca. -61 ppm arising from the partially quadrupole-collapsed $^1J(^{75}As\text{-}^{19}F)$ of the octahedral AsF_6^- anion. [d] The resonance at $\delta(^{19}F)$ = -183.1 ppm has a doublet of xenon satellites, attributable to the coupling $^1J(^{19}F\text{-}^{129}Xe)$ = 6012 Hz. Hydrogen fluoride is present ($\delta(^{19}F)$ = -193 ppm); the doublet is resolved ($^1J(^{119}F\text{-}^{1}H)$ = 534 Hz. [e] The protons on nitrogen which are cis and trans to the carbonyl group cannot be assigned to individual peaks. Hydrogen fluoride is present; $\delta(^1H)$ = 5.2 ppm, $^1J(^1H\text{-}^{19}F)$ = 530 Hz.

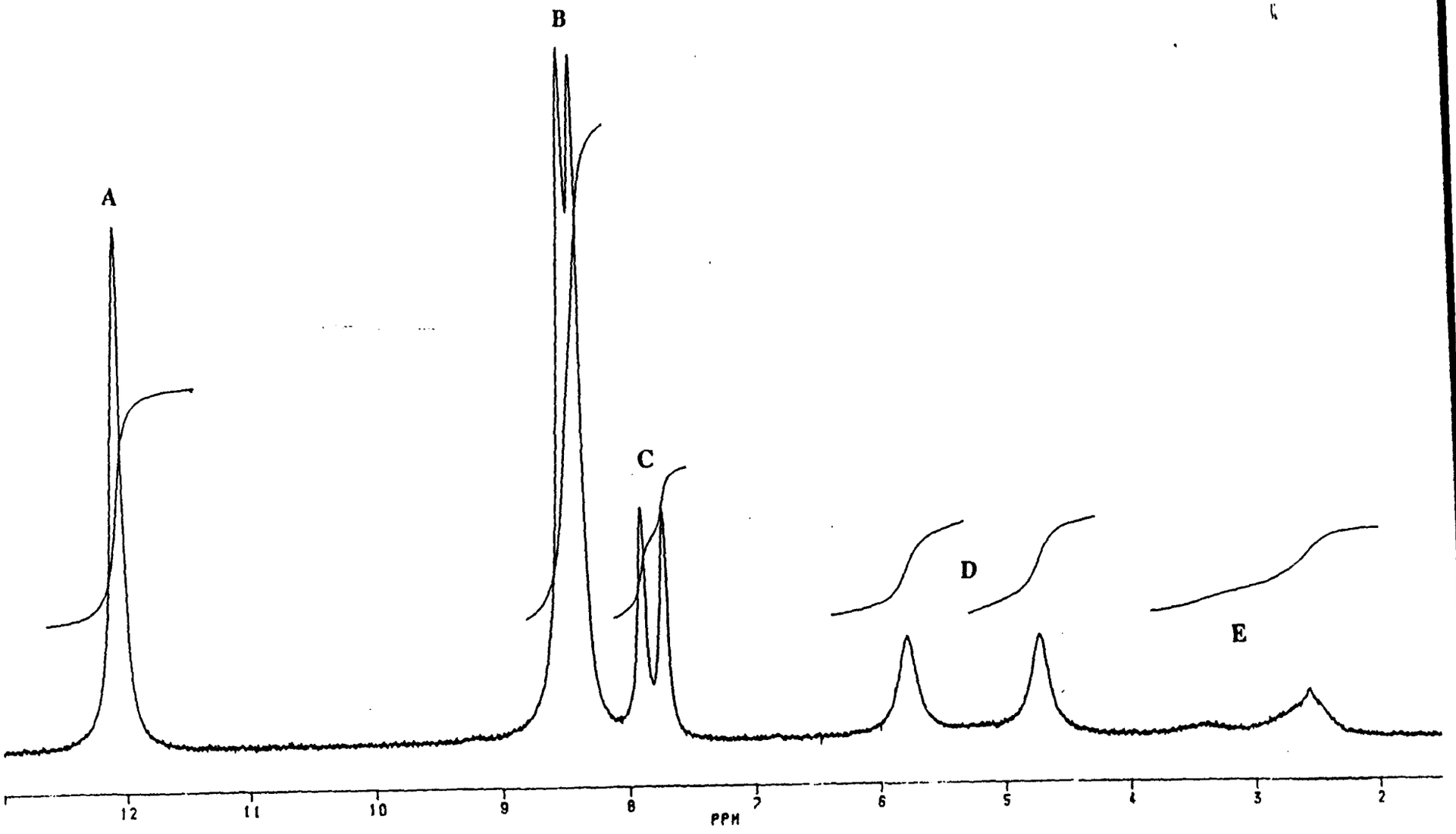

Figure 27. ^1H NMR spectrum at -55.4 °C in BrF_5; (A), protonated carbonyl group, (B), H-on-N in $CF_3C(OH)NH_2^+$, (C), H-on-N in $CF_3C(O\text{-}XeF)NH_2^+$, (D), HF, (E), unidentified resonances.

Figure 28. ^{19}F NMR spectrum at -54 °C in BrF_5; (A), AsF_6^-, (B), CF_3 in adduct, (C), CF_3 in $CF_3C(OH)NH_2^+$, (D), F-on-Xe(II) for $CF_3C(O\text{-}XeF)NH_2^+$, (d), ^{129}Xe satellites, (E), XeF_2, (e), ^{129}Xe satellites, (F), HF.

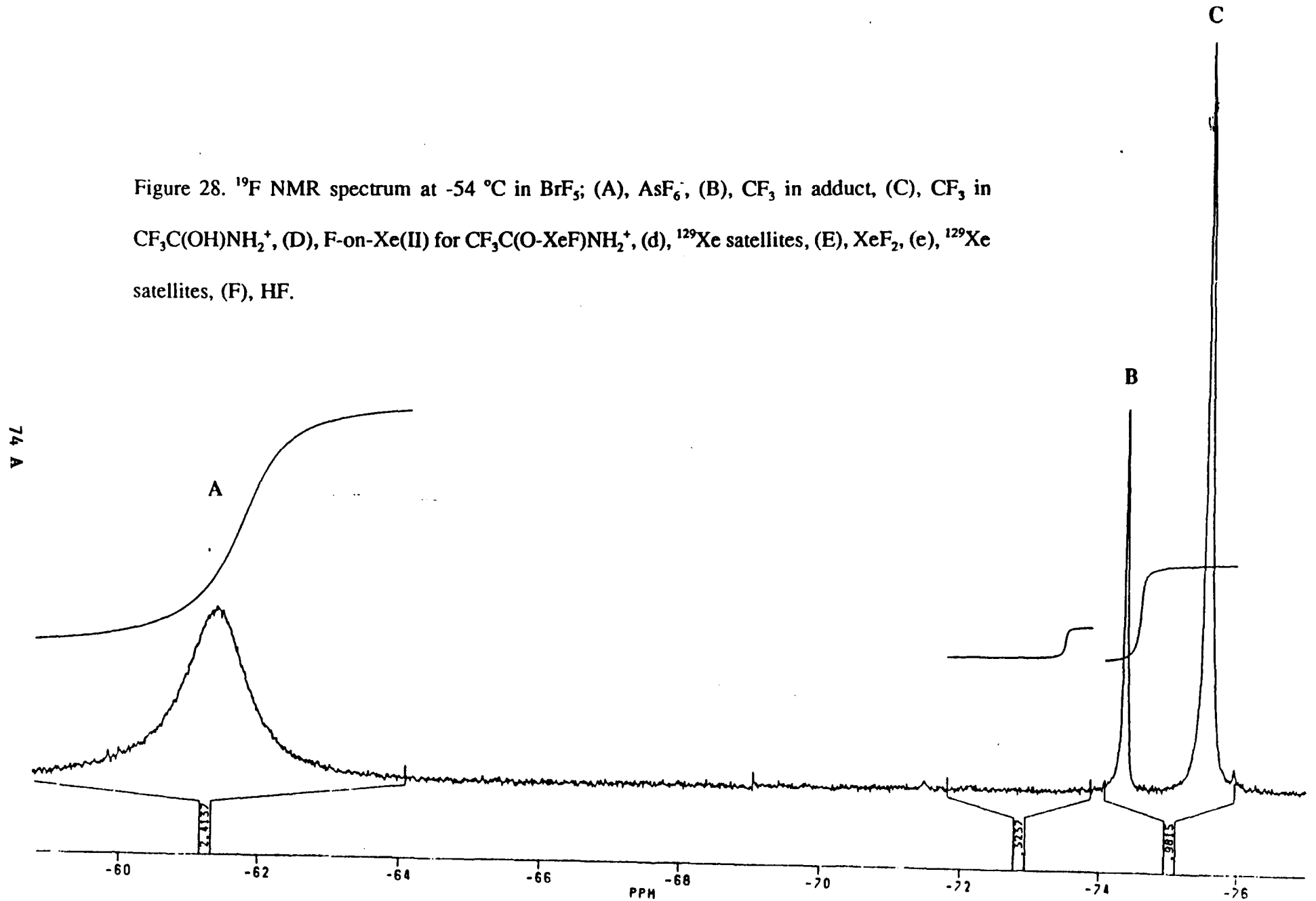

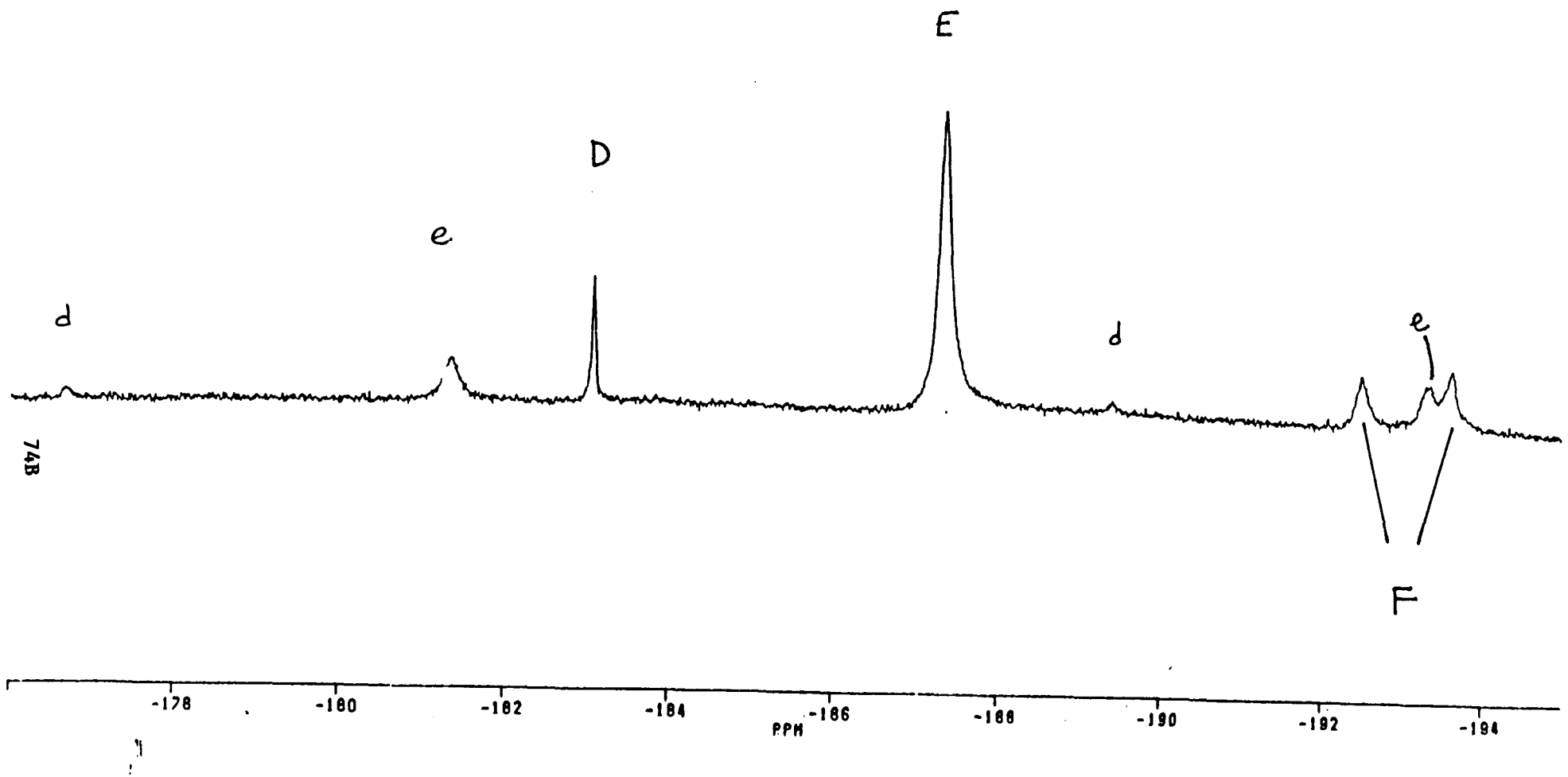

Figure 28. ^{19}F NMR spectrum at -54 °C in BrF_5; (A), AsF_6^-, (B), CF_3 in adduct, (C), CF_3 in $CF_3C(OH)NH_2^+$, (D), F-on-Xe(II) for $CF_3C(O\text{-}XeF)NH_2^+$, (d), ^{129}Xe satellites, (E), XeF_2, (e), ^{129}Xe satellites, (F), HF.

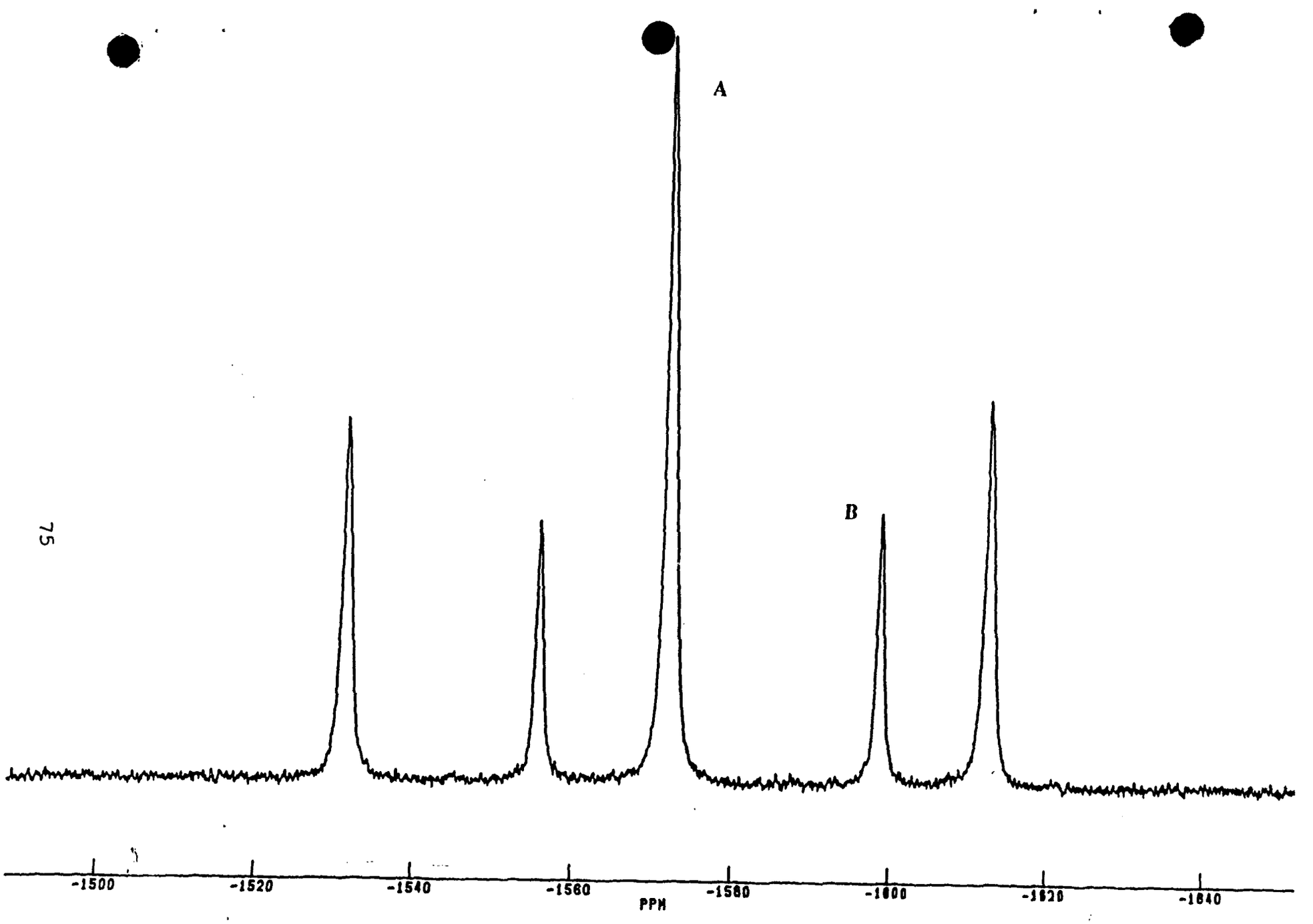

Figure 29. ^{129}Xe NMR spectrum at -53 °C in BrF_5; (A), XeF_2, (B), $CF_3C(O\text{-}XeF)NH_2^+$

The presence of singlets attributable to $-CF_3$ groups at $\delta(^{19}F)$ = -75.6 ppm ($CF_3C(OH)NH_2^+$) and -74.4 ppm ($CF_3C(O\text{-}XeF)NH_2^+$) in the ^{19}F NMR spectrum at -54.0 °C (Figure 27) indicate an equilibrium between $CF_3C(OH)NH_2^+$ and $CF_3C(OXeF)NH_2^+$ (equation (49)).

$$CF_3C(OH)NH_2^+ + XeF_2 \rightleftharpoons CF_3C(OXeF)NH_2^+ + HF \qquad (49)$$

From integration of these peaks the ratio $[CF_3C(O\text{-}XeF)NH_2^+]/[CF_3C(OH)NH_2^+]$ = 0.33. A value of 0.35 is obtained from integration of the protons on nitrogen in the ^1H NMR spectrum. The singlet at -183.1 ppm in the ^{19}F spectrum has xenon satellites corresponding to $^1J(^{19}F\text{-}^{129}Xe)$, 6012 Hz whereas ^{19}F resonance resonance at -187.3 ppm, also accompanied by ^{129}Xe satellites [$^1J(^{19}F\text{-}^{129}Xe)$ = 5649 Hz], is assigned to XeF_2. The ^{19}F NMR resonance assigned to HF at -192.9 ppm displayed doublet fine structure, which can be assigned to $^1J(^{19}F\text{-}^1H)$, 534 Hz.

The ^{129}Xe spectrum at -53.0 °C (Figure 29) displays the resonances of XeF_2, $\delta(^{129}Xe$ = -1572 ppm which is a triplet arising from the one-bond coupling $^1J(^{19}F\text{-}^{129}Xe)$ = 5651 Hz] and the $CF_3C(O\text{-}XeF)NH_2^+$ cation at $\delta(^{129}Xe)$ = -1578 ppm, which is a doublet arising from the one-bond coupling $^1J(^{19}F\text{-}^{129}Xe)$ = 5651 Hz. The magnitude of $^1J(^{19}F\text{-}^{129}Xe)$ for the cation is less than in the XeF^+ cationin SbF_5 solvent at 25 °C[x] $^1J(^{19}F\text{-}^{129}Xe)$, indicating decreased covalent character of the Xe-F bond on adduct formation. This has been observed in the recently published adduct cation $(CF_3)_2S{=}O\text{-}XeF^+$, for which $^1J(^{19}F\text{-}^{129}Xe)$ = 6343 Hz.[39]

FUTURE WORK

Decomposition of the Cation $F_5TeN(H)\text{-}Xe^+$. The principle decomposition pathway of the $F_5TeN(H)Xe^+$ cation must be determined in both HF and BrF_5 solvents. The presence or absence of F_5TeNF_2 must be confirmed in HF solvent. The spectra in HF have been run at ca. -32 °C.

Difluoraminotellurium pentafluoride decomposes at -44 °C in BrF_5, so a lower temperature may be necessary to observe F_5TeNF_2 in HF solvent. The ^{19}F NMR spectrum in BrF_5 solvent must also be run at ca. -60 °C, at which temperature F_5TeNF_2 is stable for at least 10 hours, to locate the F-on-Te(VI) resonances. The unidentified AB_4 pattern centered at ca. -58 ppm in the ^{19}F NMR spectra in BrF_5 solvent (-62 ppm in HF) may be due to $F_5TeN(H)$-$N(H)TeF_5$. A doublet at 8.8 ppm in the ^1H NMR spectrum of ^{15}N enriched $F_5TeN(H)$-$Xe^+AsF_6^-$ in BrF_5 at -56.0 °C (Figure 30) has a coupling constant of 85 Hz. In the ^1H NMR spectrum of natural abundance ^{15}N $F_5TeN(H)$-$Xe^+AsF_6^-$, the resonance is a singlet. Thus the coupling is assigned to $^1J(^{15}N$-$^1H)$. This resonance may be assigned to the dimer $F_5TeN(H)$-$N(H)TeF_5$ by recording the ^{19}F and ^1H NMR spectra of a fresh sample of $F_5TeNH_3^+AsF_6^-$ and XeF_2 in BrF_5. The simultaneous evolution with time of the ^{19}F and ^1H resonances may be integrated relative to the fluorine and proton resonances of the cation $F_5TeNH_3^+$. Evolution of the peaks at the same rate will provide evidence that they are in the same molecule. Definitive evidence requires the observation of spin-spin coupling $^3J(^{19}F$-$^1H)$, which will probably not be resolved. Nitrogen-15 NMR may provide the necessary spin-spin coupling information.

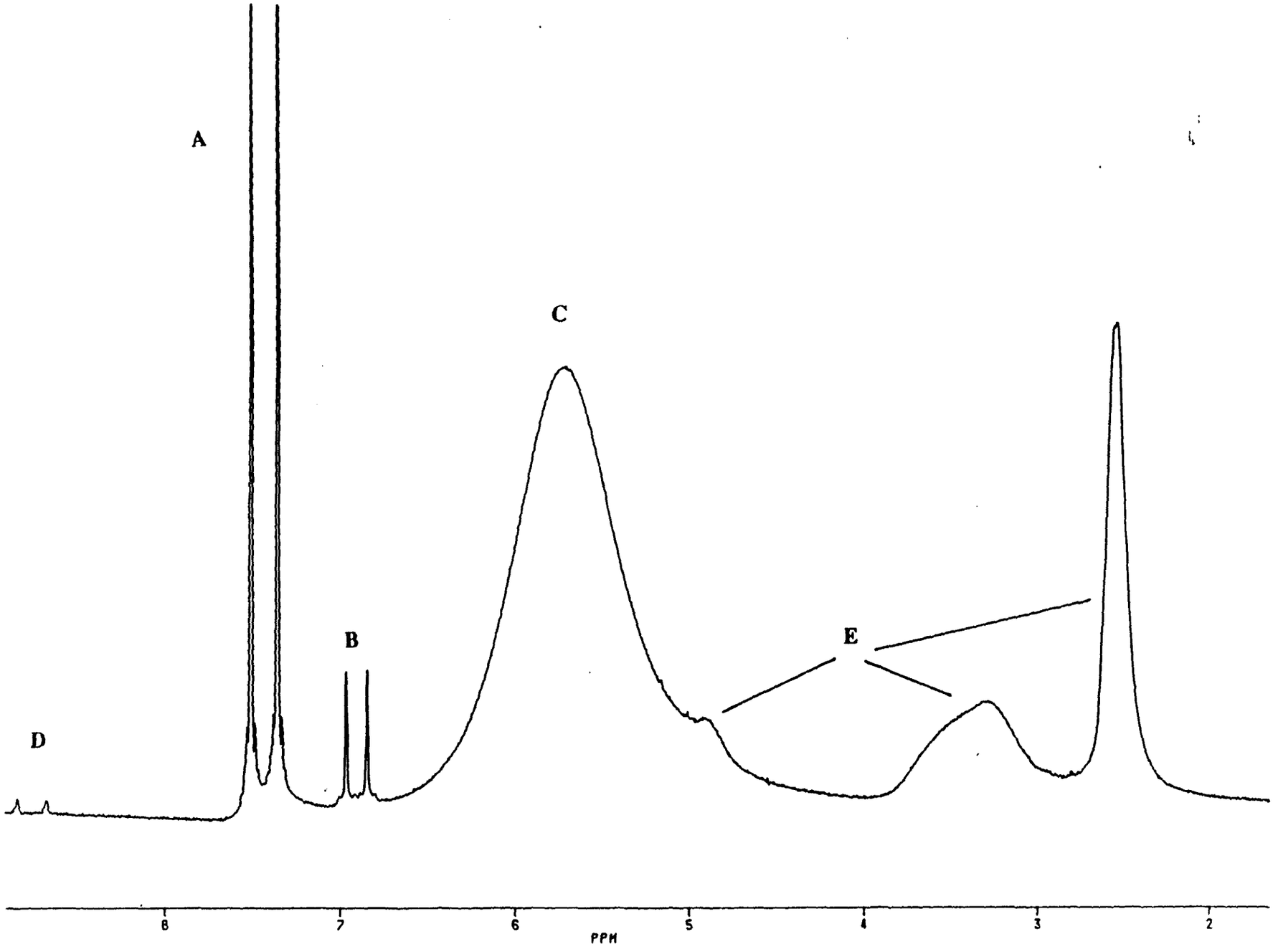

Figure (30). ^{1}H NMR of 99% $F_5Te^{15}NH_3^+AsF_6^-$ in BrF_5 at -53 °C.

Crystal Structure of $F_5TeN(H)$-$Xe^+AsF_6^-$. An attempt will be made to mount, in quartz capillaries, the thermally unstable orange crystals isolated from HF solution which are attributed to $F_5TeN(H)$-$Xe^+AsF_6^-$. This will be done using a cold table cooled to -196 °C (presently under construction) in the dry box. If successful, this will be the first crystal structure of a molecule containing a Xe(II)-N(sp^3) bond. Comparison of bond lengths with those in the structure of $F_5TeNH_3^+AsF_6^-$ will provide information about bonding changes upon formation of the Xe(II)-N bond. Orange crystals believed to be $F_5SN(H)$-$Xe^+AsF_6^-$ isolated by Dr. J.C.P. Sanders behave similarly to those isolated in the present system. The structural similarities of the two systems warrant an attempt at solving this structure as well.

Fluoroamines and Fluoroammonium Salts as Precursors to Xe(II)-N(sp^3) Bonded Species. A direct analog to F_5TeNH_2 is fluoramine, FNH_2, whose 1st ionization potential (11.62 eV)[86] suggests that it will be resistent to oxidation by Xe(II), at least at low temperature. Fluoramine is thermally unstable, decomposing with melting at -103 °C (equation (50)).[87]

$$3\ H_2NF \longrightarrow NH_4F{\cdot}nHF + N_2 \qquad (50)$$

Thermal stability is gained by forming fluorammonium salts by solvolysis of isopropylfluorocarbamate[88] in HF[89] (equations (51) and (52)).

$$(CH_3)_2CHOC(O)NH_2 \xrightarrow[H_2O,\ 0\ °C]{F_2\ /\ N_2} (CH_3)_2CHOC(O)NHF + HF \qquad (51)$$

$$(CH_3)_2CHOC(O)NHF + 3\ HF \xrightarrow{HF,\ RT} NH_3F^+HF_2^-{\cdot}nHF + CO_2 + (CH_3)_2CHF \qquad (52)$$

The salts $NH_3F^+MF_6^-$ (M = As, Sb), which decompose above -30 and -20 °C, are isolated according to equations (53) and (54).

$$NH_3F^+HF_2^-\cdot nHF + MF_5 \xrightarrow{\text{RT, in HF}} NH_3F^+MF_6^- + (n+1)\,HF \quad (53)$$

$$NH_3F^+MF_6^- + HF \xrightarrow[\text{vacuum}]{\text{-30 °C}} NH_3F^+MF_6^- \quad (54)$$

Combination of the salt $NH_3F^+MF_6^-$ with a stoichiometric amount of XeF_2 in BrF_5 solvent at low temperature may result in the synthesis of the novel cation, $FN(H)\text{-}Xe^+$ (equation (55)).

$$XeF_2 + NH_3F^+MF_6^- \xrightarrow[\text{-60 °C}]{BrF_5} FN(H)\text{-}Xe^+AsF_6^- + 2\,HF \quad (55)$$

Difluoramine, HNF_2, may be resistant to oxidative attack by xenon(II) as indicated by its 1st IP (12.38 eV).[86] Difluoramine forms an adduct with BF_3 which decomposes reversibly above -56 °C.[90] The BF_3 adduct with F_5TeNH_2 decomposes reversibly at -60 °C.[58] The Lewis basicities suggests that HNF_2 is sufficiently basic to form a covalent bond to xenon(II). Difluoramine tends to explode when frozen at -196 °C (m.p., -116 ± 3 °C), but not at -142 °C. It can be transferred in a glass apparatus (b.p., -23.6 °C). Reaction (56) represents a potential route to Xe(II)-N(sp^3) bonded species.

$$HNF_2 + XeF^+AsF_6^- \xrightarrow[\text{-80 (-60 °C)}]{HF\ (BrF_5)} F_2N\text{-}Xe^+AsF_6^- + HF \quad (56)$$

Difluoramine is synthesized by direct fluorination of urea[91] or by the hydrolysis of $(CH_3)_2CHOC(O)NF_2$ in 25% sulfuric acid at 70 °C.[92] Difluorammonium hexafluoroarsenate, $F_2NH_2^+AsF_6^-$, is prepared according to equation (57), followed by removal of excess HF at -78

to 0 °C under vacuum.

$$HNF_2 + AsF_5 \xrightarrow[-78\ °C]{HF} F_2NH_2^+AsF_6^- \quad (57)$$

The compounds CF_3NH_2 and CF_3OH are unstable with respect to intramolecular HF elimination above -30 °C (equations (58) and (59)) because of the acidic hydrogens in the β

$$CF_3NH_2 \xrightarrow{-HF} CF_2{=}NH \quad (58)$$

$$CF_3OH \xrightarrow{-HF} CF_2{=}O \quad (59)$$

position to the fluorines on carbon.[92] Combination of these species with an equimolar amount of $XeF^+AsF_6^-$ in HF or BrF_5 solution (equations (60) and (61)) may form the cations $CF_3N(H)\text{-}Xe^+$ and $CF_3O\text{-}Xe^+$.

$$CF_3OH + XeF^+AsF_6^- \xrightarrow[-80\ (-60\ °C)]{HF\ (BrF_5)} CF_3\text{-}O\text{-}Xe^+AsF_6 + HF \quad (60)$$

$$CF_3NH_2 + XeF^+AsF_6^- \xrightarrow[-80\ (-60\ °C)]{HF\ (BrF_5)} CF_3\text{-}N(H)\text{-}Xe^+AsF_6^- + HF \quad (61)$$

The hydrogen on nitrogen in the cation $CF_3\text{-}N(H)\text{-}Xe^+$ leaves open the possibility for HF elimination as in CF_3NH_2 (equation (62)).

$$CF_3\text{-}N(H)\text{-}Xe^+ \xrightarrow{-HF} CF_2{=}N\text{-}Xe^+ \quad (62)$$

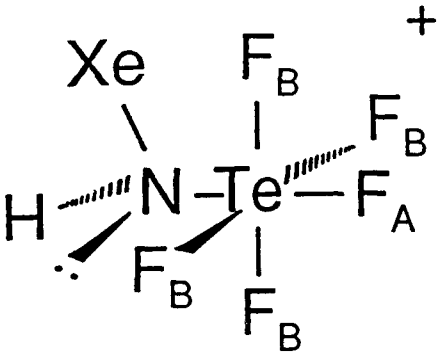

I

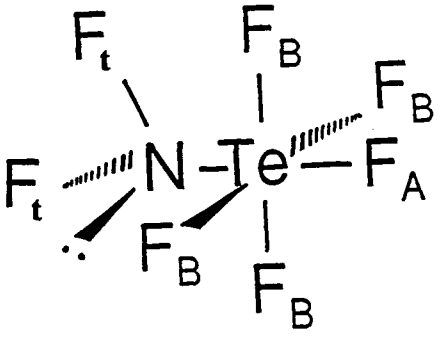

II

Fig. A

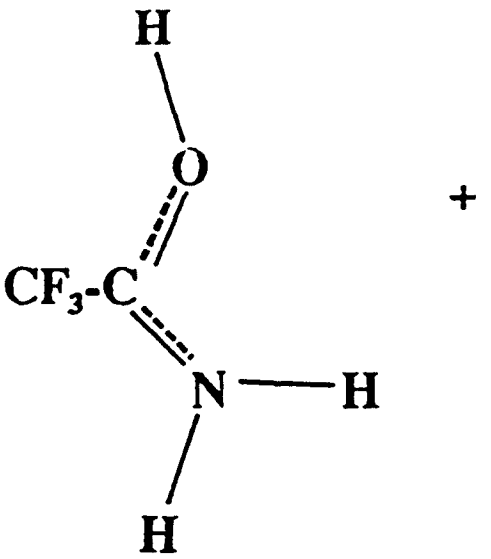

III

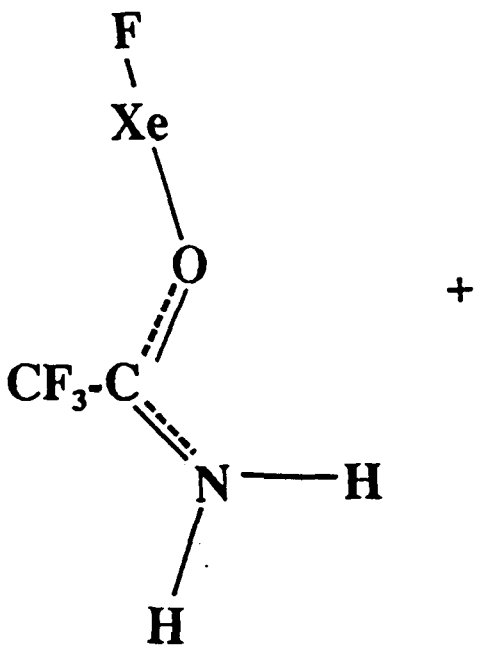

IV

Fig. B

REFERENCES

1. H. Moissan, Bull. Soc. Chim., 13, 973 (1895).
2. D.M. Yost and A.L. Kaye, J. Am. Chem. Soc., 55, 3890 (1933).
3. G.N. Lewis, J. Am. Chem. Soc., 38, 762 (1916).
4. W. Kossel, An. Phys. (Leipzig), 49, 229 (1916).
5. N. Bartlett and D.H. Lohmann, Proc. Chem. Soc., 115 (1962).
6. N. Bartlett and D.H. Lohmann, J. Chem. Soc., 5253 (1962).
7. R. Hoppe, W. Dahne, H. Mattauch and K.M. Rodder, Angew. Chem. 74, 903 (1962).
8. H.H. Claassen, H. Selig and J.G. Malm, J. Am. Chem. Soc., 84, 3593 (1962).
9. E.E. Weaver, B. Weinstock and C.P. Knop, J. Am. Chem. Soc., 85, 111 (1963).
10. D.F. Smith, J. Am. Chem. Soc., 85, 816 (1963).
11. D.F. Smith, Science, 140, 899 (1963).
12. J.L. Huston, J. Phys. Chem., 71, 3339 (1967).
13. R.J. Gillespie and G.J. Schrobilgen, J. Chem. Soc., Chem. Commun., 595 (1977).
14. J.H. Holloway, In " Noble-Gas Chemistry", Methuen & Co.: Bungay, Suffolk, 1968.
15. H.H. Claassen, In " The Noble Gases", D.C. Heath and Company: Boston, 1966.
16. H.H. Hyman, In " Noble-Gas Compounds", The University of Chicago: Chicago, 1963.

17. H. Selig and J.H. Holloway, In "Topics in Current Chemistry", F.L. Boschke, Ed.; Springer-Verlag: New York, 1984, pp. 33-90.

18. N. Bartlett, Inorg. Chem., 12, 1717 (1973).

19. V.M. McRae, R.D. Peacock and D.R. Russell, J. Chem. Soc., Chem. Commun., 62 (1969).

20. J. Burgess, J. Inorg. Nucl. Chem., Suppl., 183 (1976).

21. N. Bartlett, M. Wechsberg, F.O. Sladky, P.A. Bulliner, G.R. Jones and R.D. Burbank, J. Chem. Soc., Chem. Commun., 703 (1969).

22. M. Wechsberg, P.A. Bulliner, F.O Sladky, R. Mews and N. Bartlett, Inorg. Chem., 11, 3063 (1972).

23. M. Eisenberg and D.D. DesMarteau, Inorg. Chem., 6, 29 (1970).

24. J.I. Musher, J. Am. Chem. Soc., 90, 7371 (1968).

22. N. Bartlett, M. Wechsberg, G.R. Jones and R.D. Burbank, Inorg. Chem., 11, 1124 (1972).

25. R.G. Syvret and G.J. Schrobilgen, Inorg. Chem., 28, 1564 (1989).

26. M. Eisenberg and D.D. DesMarteau, Inorg. Chem., 11, 1901 (1972).

27. K. Seppelt, Angew. Chem. Int. Ed. Engl., 11, 723 (1972).

28. K. Seppelt, Chem. Ber., 106, 57 (1973).

29. F.O. Sladky, Angew. Chem. Int. Ed. Engl., 8, 373 (1969).

30. F.O. Sladky, Angew. Chem. Int. Ed. Engl., 8, 523 (1969).

31. F.O. Sladky, Monatsch. Chem., 101, 1559 (1970).

32. F.O. Sladky, Monatsch. Chem., 101, 1571 (1970).

33. D. Lentz and K. Seppelt, Angew. Chem. Int. Ed. Engl., 15, 66 (1976).

34. D. Lentz and K. Seppelt, Angew. Chem. Int. Ed. Engl., 17, 356 (1978).

35. E. Jacob, D. Lentz, K. Seppelt and A. Simon, Z. Anorg. Allg. Chem., 472, 7 (1981).

36. G.A. Schumacher and G.J. Schrobilgen, Inorg. Chem., 23, 2923 (1984).

37. K. Seppelt, Angew. Chem. Int. Ed. Engl., 21, 877 (1982).

38. D. Lentz and K. Seppelt, Angew. Chem. Int. Ed. Engl., 18, 66 (1979).

39. R. Minkwitz and W. Molsbeck, Z. Anorg. Allg. Chem., 612, 35 (1992).

40. R.D. LeBlond and D.D. DesMarteau, J. Chem. Soc., Chem. Commun., 555 (1974).

41. J.F. Sawyer, G.J. Schrobligen and S.J. Sutherland, Inorg. Chem., 21, 11 (1982).

42. D.D. DesMarteau, R.D. LeBlond, S.F. Hossain and D. Nothe, J. Am. Chem. Soc., 103, 7734 (1981).

43. G.A. Schumacher and G. J. Schrobilgen, Inorg. Chem., 22, 2178 (1983).

44. J. Foropoulos and D.D. DesMarteau, J. Am. Chem. Soc., 104, 4260 (1982).

45. R. Faggiani, D.K. Kennepohl, C.J.L. Lock, and G.J. Schrobilgen, Inorg. Chem., 25, 563 (1986).

46. G.J. Schrobilgen, In "Synthetic Fluorine Chemistry"; G.A. Olah, R.D. Chambers and G.K.S. Prakash, Eds.; Wiley, New York, 1992.

47. D.D. DesMarteau, J. Am. Chem. Soc., 100, 6270 (1978).

48. A.A.A. Emara, PhD. Thesis, McMaster University, Hamilton, Ontario, Canada (1991).

49. V.H. Dibeler and S.K. Liston, J. Chem. Phys., 48, 4765 (1968).

50. G.J. Schrobilgen, J. Chem. Soc., Chem. Commun., 1506 (1988).

51. A.A.A. Emara and G.J. Schrobilgen, J. Chem. Soc., Chem. Commun., 1644 (1987).

52. A.A.A. Emara and G.J. Schrobilgen, J. Chem. Soc., Chem. Commun., 257 (1988).

53. C.R. Brundle, M.B. Robin and N.A. Keubler, J. Am. Chem. Soc., 94, 1466 (1972).

54. D.B. Beach, W.L. Jolly, R. Mews and A. Waterfeld, Inorg. Chem., 23, 4080 (1984).

55. G.J. Schrobilgen, unpublished results.

56. J.G. Malm and C.L. Chernick, Inorg. Synth., 8, 254 (1966).

57. C.J. Hoffman, Inorg. Synth., 4, 150 (1953).

58. K. Seppelt, Inorg. Chem., 12, 2837 (1973).

59. R.O. Sauer and R.H. Hasek, J. Am. Chem. Soc., 66, 1706 (1944).

60. F. Feher, J. Cremer and W. Tromm, Z. Anorg. Alig. Chem., 287,175 (1956).

61. D.M. Yost and W.H. Claussen, J. Am. Chem. Soc., 55, 885 (1933).

62. H.S. Booth and J.F. Suttle, J. Am. Chem. Soc., 2658 (1946).

63. R.L. Jarry and W.J. Davis, J. Phys. Chem., 57, 600 (1953).

64. H. Hartl, P. Huppmann, D. Lentz and K. Seppelt, Inorg. Chem.,22,2183 (1983).

65. C.M. King and E.R. Nixon, J. Chem. Phys., 48, 1685 (1968).

66. K. Seppelt, Z. Anorg. Allg. Chem., 339, 65 (1973).

67. G.J. Schrobilgen, J.H. Holloway, P. Granger and C. Brevard, Inorg. Chem., 17, 980 (1978).

68. J.E. Huheey, In "Inorganic Chemistry, Principles of Structure and Reactivity", Harper & Row: New York (1978) Chapter 4.

69. K.O. Christe, W.W. Wilson, C.J.Schack and R.D. Wilson, Inorg. Chem., 24, 303 (1985).

70. U.H. Mölder, I.A. Koppel, R.J. Pikver and J.J. Tapver, Organic Reactivity, 25, 255 (1988).

71. T. Birchall and R.J. Gillespie, Can. J. Chem., 41, 2642 (1963).

72. S.J. Kuhn and J.S. McIntyre, Can. J. Chem., 43, 995 (1965).

73. A.J. Carty, Can. J. Chem., 44, 1881 (1966).

74. P.A. Temussi and F. Quadrifoglio, J. Chem. Soc., Chem. Commun., 844 (1968).

75. N.A. Matwiyoff and W.G. Movius, J. Am. Chem. Soc., 89, 6077 (1967).

76. W.H. Knoth, J.C. Sauer, D.C. England, W.R. Hertler and E.L. Muetterties, J. Am. Chem. Soc., 86, 3973 (1964).

77. W. Gerrard, M.F. Lappert, H. Pyszora and J.W. Wallis, J. Chem. Soc., 2144 (1960).

78. N.A. Matwiyoff, Inorg. Chem., 5, 788 (1966).

79. W.R. Hertler and E.L. Meutterties, Inorg. Chem., 5, 160 (1966).

80. D.S. Dyer and R.O.Ragsdale, Inorg. Chem., 6, 8 (1967).

81. W.G. Movius and N.A. Matwiyoff, Inorg. Chem., 6, 847 (1967).

82. T. Ottersen, Acta. Chem. Scand., A 29, 939 (1975).

83. M.H. Pendlebury and L.Phillips, Org. Magn. Res., 4, 529 (1972).

84. H. Akiyama, F. Yamauchi and K. Ouchi, J. Chem. Soc. (B), 1014 (1971).

85. T. Birchall and R.J. Gillespie, Can. J. Chem., 41, 148 (1963).

86. H. Baumgärtel, H.-W. Jochims, E. Rühl, H. Bock, R. Dammel, J. Minkwitz and R. Nass, Inorg. Chem., 28, 943 (1989).

87. R. Minkwitz and R. Nass, Z. Naturforsch., 43b, 1478 (1988).

88. V. Grakauskas and K. Baum, J. Am. Chem. Soc., 91, 1679 (1969).

89. R. Minkwitz, A. Liedtke and R. Nass, J. Fluorine Chem., 35, 307 (1986).

90. A.D. Craig, Inorg. Chem., 3, 1628 (1964).

91. E.A. Lawton and J.Q. Weber, J. Chem. Soc., 4755 (1969).

92. G. Klöter and K. Seppelt, J. Am. Chem. Soc., 101, 347 (1979).

PART IV

NEW DERIVATIVES OF XENON (IV)

The chemistry of xenon(IV) has been limited to XeF_4, $XeOF_2$ and $Xe(OTeF_5)_4$. In attempts to prepare the $OTeF_5$ and mixed $F/OTeF_5$ analogs of novel XeF_5^- anion previously characterized in the course of the previous contract work (see Final Technical Report No. PL-TR-91-3108, July 1, 1991) according to equations (1) and (2), the novel neutral species $O{=}XeF(OTeF_5)$ and $O{=}Xe(OTeF_5)_2$ were identified and characterized in solution by ^{129}Xe NMR spectroscopy (Figures 1 and 2 and Table 1). The ^{129}Xe NMR spectrum of $O{=}XeF_2$ has also been obtained for the first time (Figure 3). All these species are probably solvated with CH_3CN and their most likely structures are depicted in Figure 4.

$$Xe(OTeF_5)_4 + OTeF_5^- \xrightarrow[-40\ ^\circ C]{CH_3CN} Xe(OTeF_5)_5^- \qquad (1)$$

$$Xe(OTeF_5)_4 + nF^- \xrightarrow[-40\ ^\circ C]{CH_3CN} XeF_n(OTeF_5)_{5-n}^- + nOTeF_5^- \qquad (2)$$

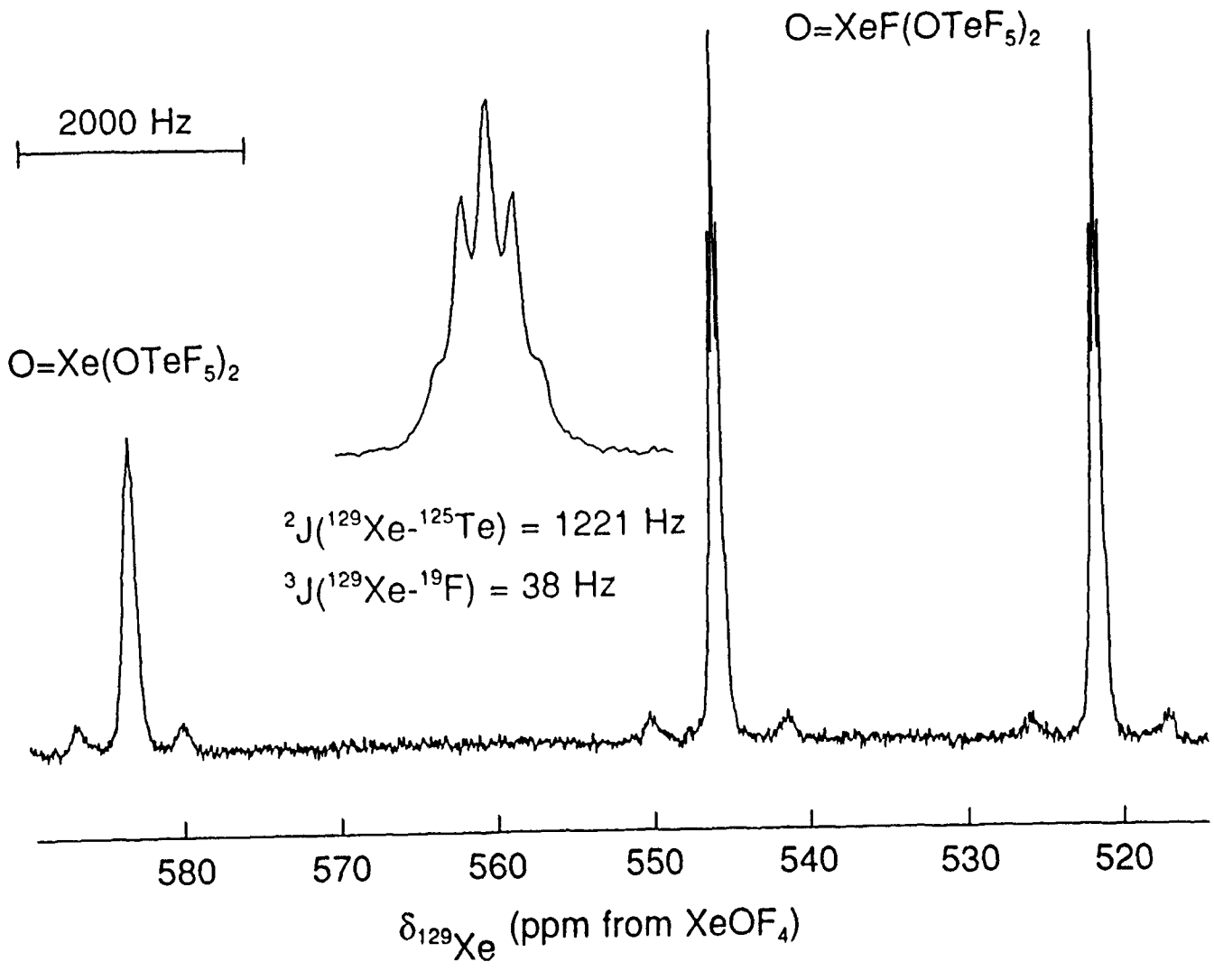

Figure 1. The ^{129}Xe NMR spectrum (139.051 MHz) at -42 °C showing the reaction products of $Xe(OTeF_5)_4$ with $2N(CH_3)_4^+F^-$ in CH_3CN.

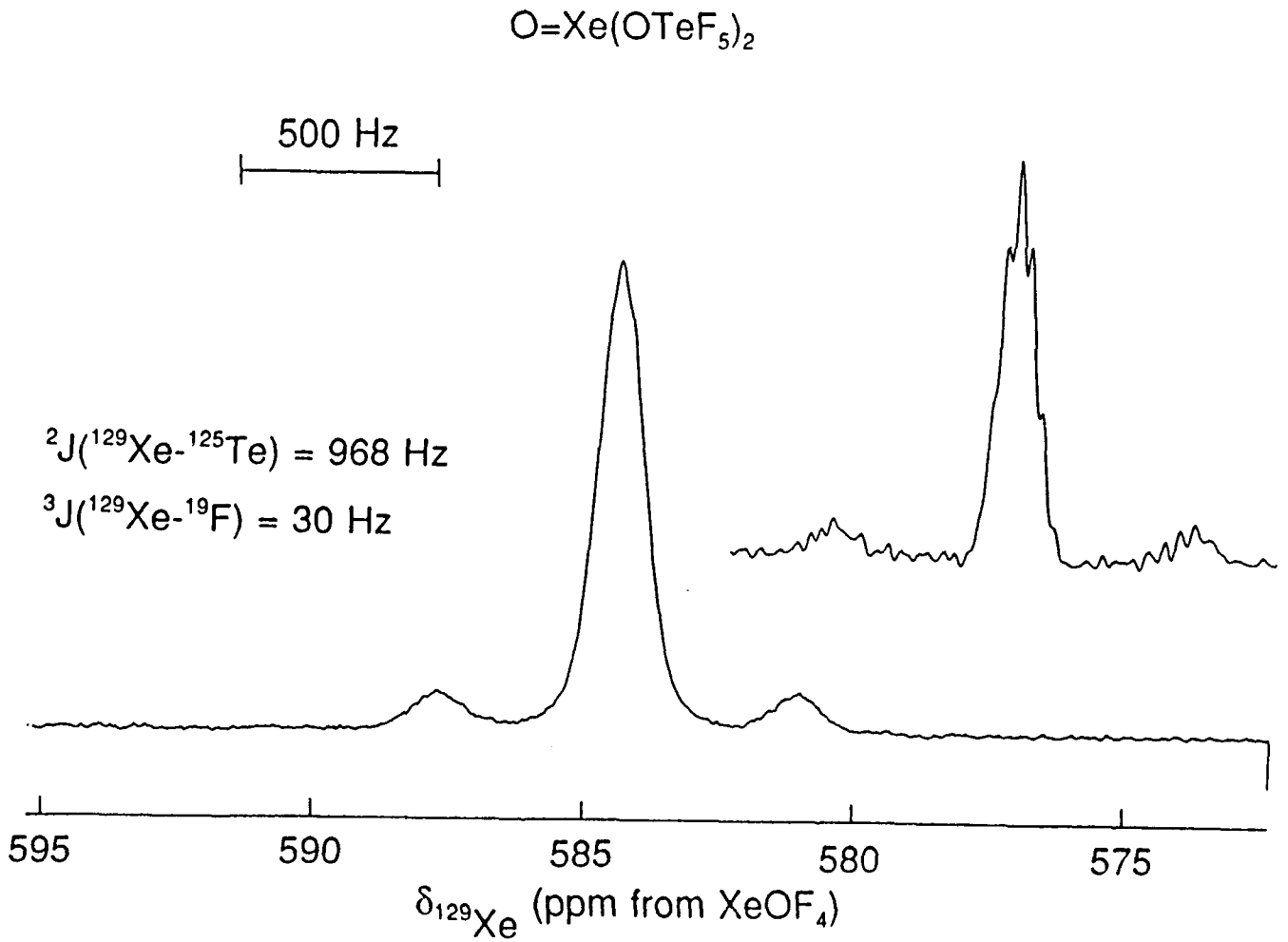

Figure 2. The ^{129}Xe NMR spectrum (139.051 MHz) at -42 °C showing the reaction products of $Xe(OTeF_5)_4$ with $2N(CH_3)_4^+OTeF_5^-$ in CH_3CN.

Table 1. NMR DATA FOR XeF_4 AND $O{=}XeF_n(OTeF_5)_{2-n}$ (n = 0 - 2)

Species	$\delta(^{19}F)$	$\delta(^{129}Xe)$	$^1J(^{129}Xe\text{-}^{19}F)$, Hz	$^2J(^{129}Xe\text{-}^{125}Te)$, Hz
XeF_4	-20.1	335.3	3913	-
$O{=}XeF_2$	-45.2	283.5	3554	-
$O{=}XeF(OTeF_5)$	-27.2	533.6	3374	1221
$O{=}Xe(OTeF_5)_2$	-	583.3	-	968

Recorded in CH_3CN at -40 °C.

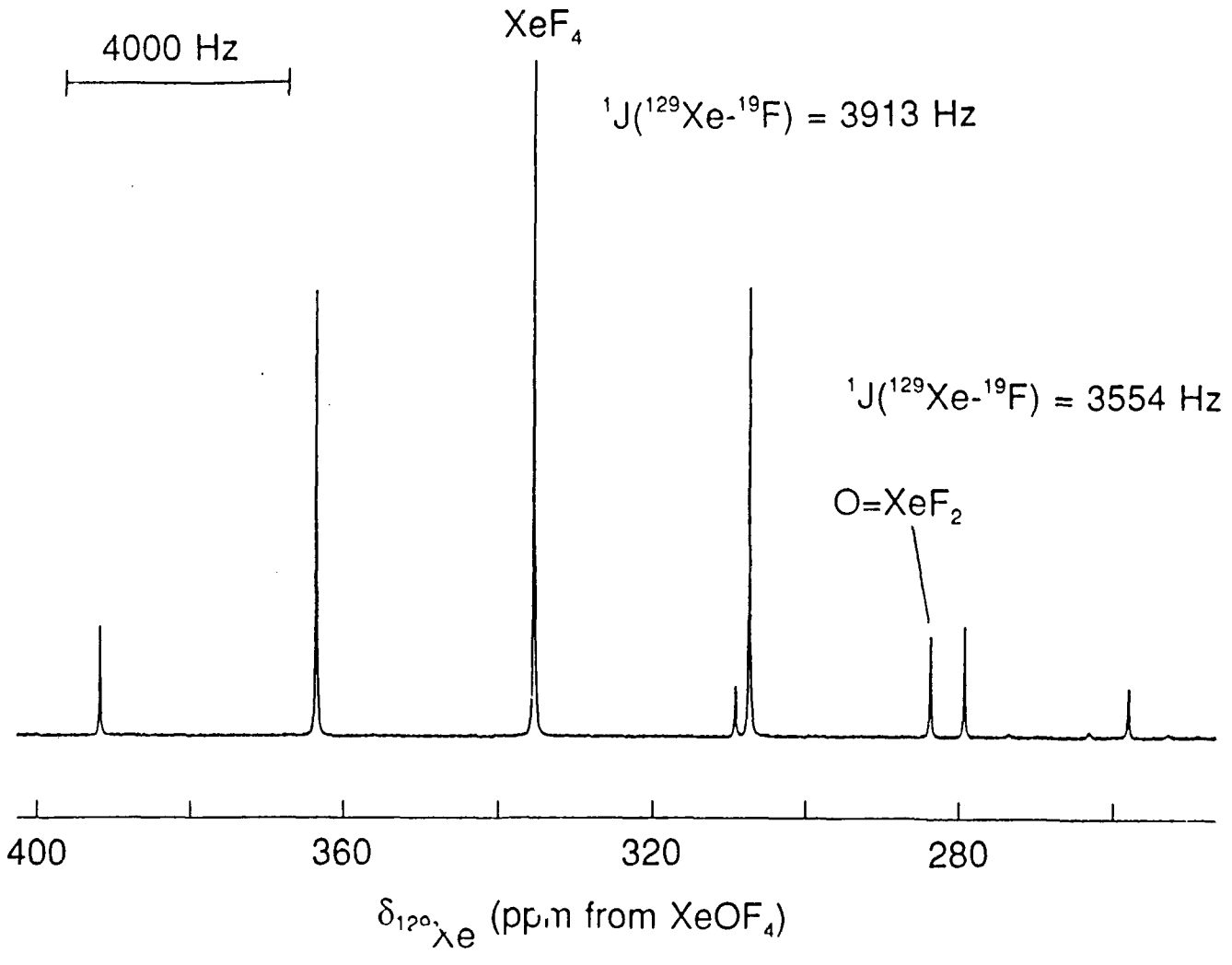

Figure 3. The ^{129}Xe NMR spectrum (139.051 MHz) at -42 °C showing the reaction products of XeF_4 + $Xe(OTeF_5)_4$ with $2N(CH_3)_4^+F^-$ in CH_3CN.

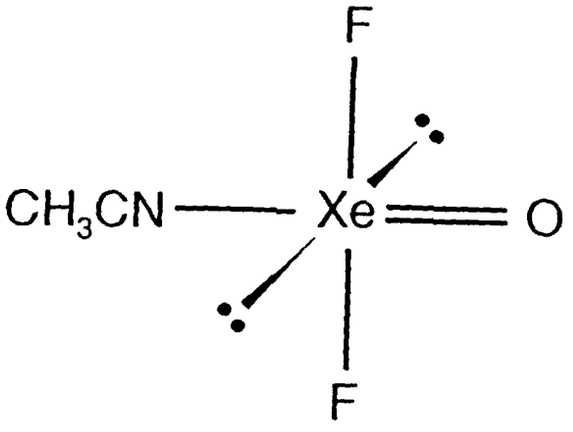

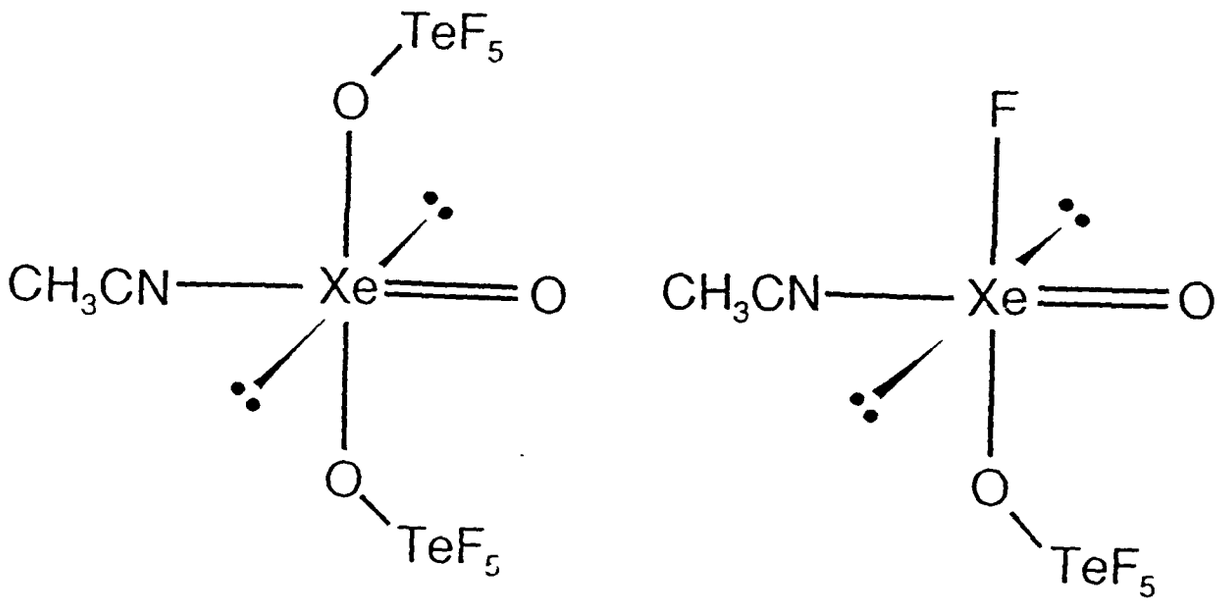

Figure 4.

$O{=}XeF_2$ was initially observed as one of the products in the reaction of $N(CH_3)_4^+F^-$ with $Xe(OTeF_5)_4$ in CH_3CN at -42 °C and was characterized by ^{129}Xe and ^{19}F NMR spectroscopy for the first time. A solution of $XeOF_2$ in CH_3CN was prepared by the reaction of XeF_4 with ^{17}O-enriched water (35.4%, ^{16}O; 21.9%, ^{17}O; 42.77%, ^{18}O) dissolved in CH_3CN at -45 °C according to equation (3)

$$XeF_4 + H_2O \xrightarrow[-45\ ^\circ C]{CH_3CN} O{=}XeF_2 + 2HF \qquad (3)$$

The ^{19}F NMR spectrum has been obtained (Figure 5). The spectrum shows two singlets with accompanying ^{129}Xe satellites: the weaker resonance [δ = -20.1 ppm; $^1J(^{19}F\text{-}^{129}Xe)$ = 3910 Hz] is assigned to the excess XeF_4 used in the reaction; the more intense resonance [δ = -48.6 ppm; $^1J(^{19}F\text{-}^{129}Xe)$ = 3448 Hz] is assigned to $O{=}XeF_2$. This assignment was further corroborated by the observation that both the central line and the satellites of the resonance displayed a small "doublet" splitting corresponding to the secondary isotope shift between $^{16}O{=}XeF_2$ and $^{18}O{=}XeF_2$ (Figure 6). This is the first time that a two-bond isotope effect has been observed for a xenon compound [$^2\Delta^{19}F(^{18,16}O)$ = -0.014 ppm]. The resulting solution is bright yellow in color. The sample was immediately placed in the NMR probe which had been precooled to -45 °C. The ^{129}Xe NMR spectrum at -45 °C showed a triplet [δ = 240.1 ppm; $^1J(^{129}Xe\text{-}^{19}F)$ = 3448 Hz]. The ^{17}O NMR spectrum of the same sample shows three resonances: an intense broad resonance at $\delta(^{17}O)$ = 209 ppm, assigned to $XeOF_2$; a weak broad resonance at $\delta(^{17}O)$ = 3.4 ppm which may arise from H_3O^+; and a very sharp singlet at $\delta(^{17}O)$ = 77.7 ppm. The latter results from the decomposition of $XeOF_2$ in CH_3CN at -45 °C. Xenon oxodifluoride is known to decompose according to equation (4)

$$XeOF_2 \longrightarrow XeF_2 + \tfrac{1}{2}O_2 \qquad (5)$$

and may be acting as a source of singlet oxygen, $^1O_2$. In the CH_3CN sample, singlet oxygen could react with CH_3CN to give a cyanate or fulminate according to equations (6) and (7).

$$CH_3C{\equiv}N + XeOF_2 \longrightarrow CH_3OCN + XeF_2 \quad (6)$$

$$CH_3C{\equiv}N + XeOF_2 \longrightarrow CH_3CNO + XeF_2 \quad (7)$$

It is one of these species which is thought to give rise to the sharp singlet at 77.7 ppm.

In relation to this work, attempts have also been made to characterize the little studied $XeOF_3^-$ anion in solution as its $N(C_2H_5)_4^+$ salt for the first time. Owing to the low thermal stability of $O{=}XeF_2$, the preparation of this new salt was attempted in an NMR tube according to equation (8).

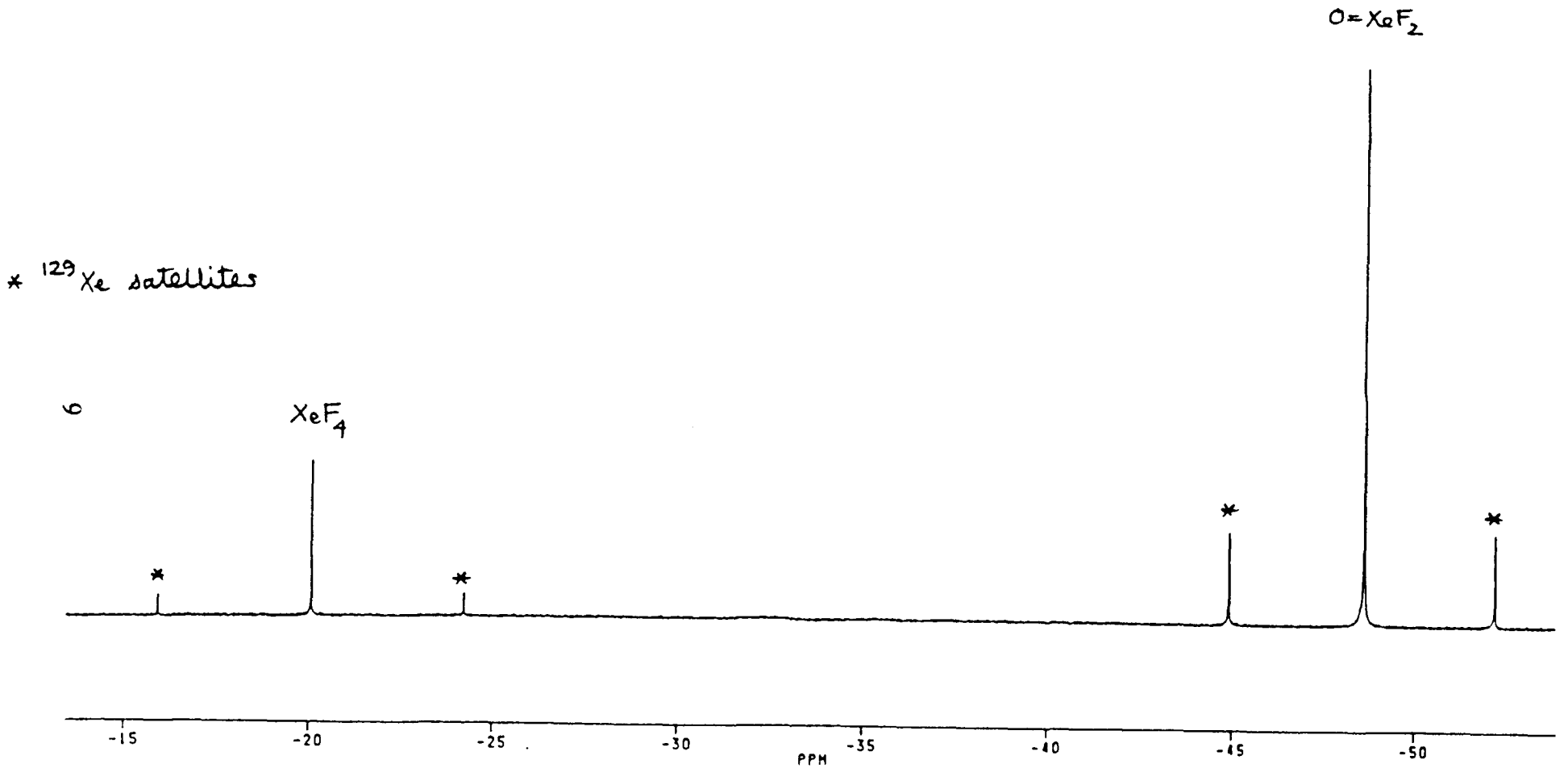

Figure 5. The ^{19}F NMR spectrum (470.599 Mhz) of the reaction of XeF_4 with $H_2{}^{16,17,18}O$ in CH_3CN at -45 °C.

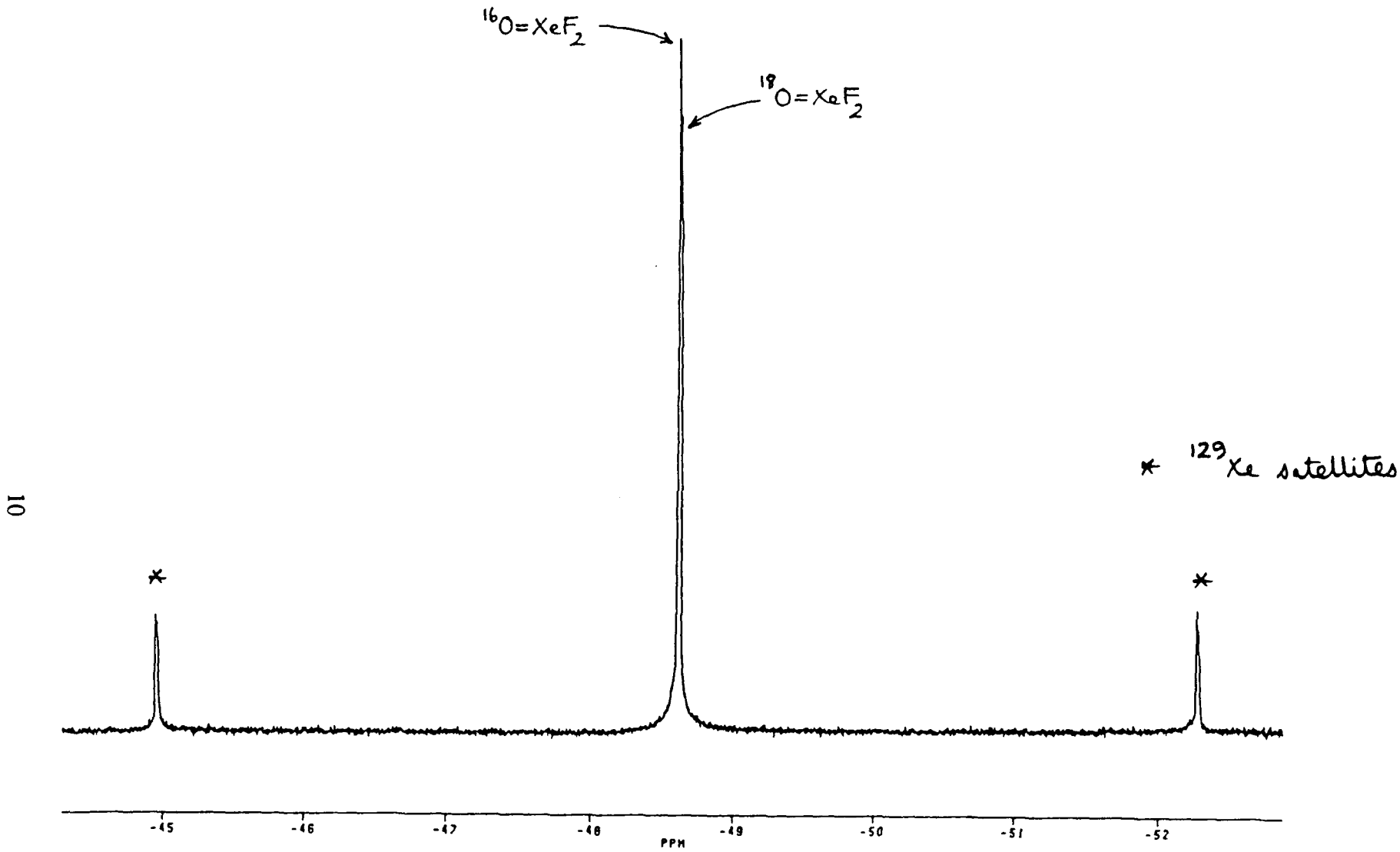

Figure 6. The ^{19}F NMR spectrum (470.599 Mhz) of the reaction of XeF_4 with $H_2{}^{16,17,18}O$ in CH_3CN at -45 °C. Expansion of the $Xe^{16}OF_2$ and $Xe^{18}OF_2$ resonances.

$$XeF_4 + H_2O + N(C_2H_5)_4^+F(HF)_n^- \xrightarrow[-45\ ^\circ C]{CH_3CN} N(C_2H_5)_4^+XeOF_3^- + (n+2)HF \quad (8)$$

The ^{129}Xe and ^{19}F NMR spectra of the sample did not reveal any resonances attributable to the $XeOF_3^-$ anion; only signals due to $O{=}XeF_2$ and excess XeF_4 could be located. In view of this, it seems that $O{=}XeF_2$ is a rather poor F^- acceptor and that the $XeOF_3^-$ anion can only be observed in the absence of HF. Interestingly, the ^{19}F resonance of $O{=}XeF_2$ was sharp and displayed well resolved ^{129}Xe satellites, while that of XeF_4 was severely broadened (Figure 7) thereby suggesting that the latter was in exchange with the HF_2^- present in the solution (equation 9).

$$XeF_4 + HF_2^- \rightleftharpoons XeF_5^- + HF \quad (9)$$

This observation suggests that either $O{=}XeF_2$ forms a strong adduct with CH_3CN from which HF_2^- cannot displace the CH_3CN or, contrary to expectation, XeF_4 is a stronger fluoro-acid than $O{=}XeF_2$.

PART V

TECHNETIUM(VII) DIOXOTRIFLUORIDE, TcO_2F_3; SYNTHESIS, X-RAY STRUCTURE DETERMINATION AND RAMAN SPECTRUM

Technitium (VII) Dioxotriflouride, TcO_2F_3: Synthesis, X-ray Structure Determination, and Raman Spectrum

Helene P.A. Mercier and Gary J. Schrobilgen

Department of Chemistry, McMaster University, Hamilton, Ontario L8S 4M1, Canada

The synthesis of TcO_2F_3, which is reported for the first time, was accomplished by the reaction of XeF_6 and Tc_2O_7 in a 3:1 molar ratio in anhydrous HF solution. Technitium (VII) dioxotriflouride is yellow (mp 200 ± 1 °C) and crystallized in the triclinic system, space group $P\bar{1}$, with a = 7.774 (3) Å, b = 7.797 (1) Å, c = 11.602 (3) Å, α = 89.41 (2)°, β = 88.63 (3)°, Υ = 84.32 (2)°, V = 699.6 (3) Å^3, D_{calc} = 3.551 g cm^{-3} for Z = 8 from HF solutions containing excess XeF_6. The structure consists of open chains of flourine bridged TcO_2F_4 units in which the bridge flourines (F_b) are trans to the oxygens and the light atoms surrounding technitium form near-undistorted octahedra in which the technitium atoms are displaced toward the oxygen atom in the [F_b,F_b,O,O] plane: terminal Tc–F, 1.834 (7) Å; bridging Tc——F, 2.080 (5) Å; Tc–O, 1.646 (9) Å; Tc——F——Tc, 148.8 (3)°. The Raman spectrum of the polymeric *cis*-TcO_2F_4 unit has been assigned under C_{2v} point symmetry and exhibits only weak vibrational coupling in the unit cell.